6-2020

Investigation of Finite Temperature and Continuum Effects on Nuclear Excitations

Herlik Wibowo
Western Michigan University, herlikw@gmail.com

INVESTIGATION OF FINITE TEMPERATURE AND CONTINUUM EFFECTS ON NUCLEAR EXCITATIONS

by

Herlik Wibowo

A dissertation submitted to the Graduate College
in partial fulfillment of the requirements
for the degree of Doctor of Philosophy
Physics
Western Michigan University
June 2020

Doctoral Committee:

Elena Litvinova, Ph.D., Chair
Dean Halderson, Ph.D.
Michael Famiano, Ph.D.
Morten Hjorth-Jensen, Ph.D.

INVESTIGATION OF FINITE TEMPERATURE AND CONTINUUM EFFECTS ON NUCLEAR EXCITATIONS

Herlik Wibowo, Ph.D.

Western Michigan University, 2020

The low-energy nuclear response at finite-temperature significantly affects the radiative neutron capture reaction rates of the r-process nucleosynthesis. In order to address this topic, the first part of this study focuses on the response of compound nuclei or nuclei at finite temperature. The thermal nuclear response satisfies the Bethe-Salpeter equation (BSE) with the static and dynamical kernels of different origins. While the origin of the static kernel is the nearly instantaneous nucleon-meson interaction, the dynamical kernel is induced by the coupling between nucleons and phonons. The presence of singularities in the dynamical kernel makes the BSE unsolvable, however, a time projection technique known for the zero-temperature case allows for constructing a hierarchy of feasible approximations. In this study a temperature-dependent projection operator on the subspace of the imaginary time was found to generalize the method to finite temperatures. The method named the finite-temperature relativistic time blocking approximation (FT-RTBA), is implemented numerically to calculate the multipole responses of medium-mass and heavy nuclei. This study reveals common phenomena that occur for all thermal multipole responses: the disappearance of the high-frequency collective motion at very high temperature and arising prominent low-energy strength of thermal origin.

The inclusion of pairing correlations and continuum effects is essential for an accurate microscopic description of the nuclear response of the exotic nuclei far from the valley of

beta-stability and close to the drip-lines. Therefore, the second part of this study aims to extend the current zero-temperature nuclear response theory, which is based on the contact effective interactions between nucleons and takes into account the pairing correlations within the framework of the BCS approximation and exact coupling to the continuum. This extension involves the application of the time-blocking approximation in the coordinate space representation to incorporate the coupling between nucleons and phonons, which is the leading-order mechanism of the fragmentation of the nuclear multipole responses at both low- and high-frequency domains.

ACKNOWLEDGMENTS

I want to thank Dr. Elena Litvinova for her time, effort, support, and, especially, patience in guiding and supervising my Ph.D. research for four years. I came to you as a graduate student with limited background in theoretical nuclear physics and computational physics. I am indebted to you for triggering my scientific curiosity, teaching me about the subjects, and pushing me to my true potential. Thank you for sharing your own experiences in pursuing a career in academia! I have learned a lot from a role model for the past four years.

I would like to appreciate my committee members: Dr. Dean Halderson, Dr. Michael Famiano, and Dr. Morten Hjorth-Jensen, for their valuable time to read and assess my dissertation work. All of their feedback, comments, and insights during my oral dissertation defense are gratefully acknowledged.

It is my pleasure to acknowledge the constructive discussions with my colleagues at Western Michigan University (WMU) Nuclear Theory Group, namely Dr. Caroline Robin, Dr. Jian Li, Dr. Yinu Zhang, and Irina Egorova, throughout my academic years. I am especially indebted to Dr. Yinu Zhang, a current research associate in our group, for being an enthusiastic reader, and his valuable comments and insights on drafts of this dissertation.

Being a Ph.D. student in a foreign country far away from family can be tough. Having some supportive fellow graduate students within the Department of Physics is a blessing. I especially want to thank Dr. Masoud Shabani-Nezhad Navrood, who was a fantastic officemate, and Dr. Jagjit Kaur, who helped me with some basic knowledge about computer cluster. I am also grateful for being a part of the Fulbright family at WMU, where I have met and built a friendship with many talented individuals worldwide. I want to appreciate

Dr. Michelle Metro-Roland, our Fulbright Student Advisor, for her continuous support, hospitality, and guidance during my study at WMU.

Special thanks to Mom for her constant love, prayer, patience, and encouragement! I am blessed to be raised by a strong and independent woman from whom I learn the meaning of hard work to achieve success. I want to thank my brother for his moral support and advice.

Finally, I want to express my gratitude to the American Indonesian Exchange Foundation (AMINEF), who awarded me a Fulbright Indonesia Presidential Scholarship PhD Grant 2014-2017. This grant has allowed me not just to pursue my doctoral degree in the US, but also to introduce myself to international communities and friends, where I have learned to embrace diversity among us and shared the cultural value of Indonesia. The continuation of my doctoral study would not have been possible without the financial supports from the College of Arts and Sciences, the Graduate College, and the Department of Physics. I am very grateful for their never-ending support and hospitality during my study at WMU.

Herlik Wibowo

TABLE OF CONTENTS

Acknowledgments **ii**

List of Tables **vii**

List of Figures **viii**

1 Introduction **1**

2 Nuclear Mean Field at Finite Temperature **10**

2.1 Grand Canonical Ensemble 11

2.2 Finite-temperature Relativistic Mean-field Theory 12

2.3 Solution of the Finite-temperature RMF Equations 20

3 Finite-temperature Relativistic Time Blocking Approximation **22**

3.1 Finite-temperature Response Function 22

3.2 The Temperature-dependent Mass Operator and Interaction Amplitude . . . 29

3.3 Time Blocking Approximation in Imaginary-time Formalism 31

3.4 Correlated Particle-hole Propagator 36

3.5 Strength Function and Transition Density 46

4 Numerical Results **50**

4.1 Numerical Details 50

4.2 Thermal Mean-field Calculations for Compound Nuclei 52

4.3 Isovector Dipole Resonance in ^{48}Ca, ^{68}Ni, and ^{100,120,132}Sn 53

4.4 Isoscalar Monopole and Quadrupole Resonances in ^{68}Ni 64

5 Nuclear Mean Field with Point Couplings and Pairing Correlations **67**

5.1 Relativistic Mean-field Theory of Point Coupling 67

5.1.1 DD-PC1 Force 68

5.1.2 Treatment of the Coulomb Interaction in the Coordinate-channel Representation . . . 77
5.2 The BCS Theory . . . 79
5.2.1 The BCS Wave Function . . . 79
5.2.2 The BCS Equations . . . 81
5.2.3 The Matrix Elements of One-body Operators . . . 83

6 Continuum Relativistic Quasiparticle Random Phase Approximation 85
6.1 The Quasiparticle Random Phase Approximation (QRPA) Equations . . . 86
6.2 The Particle-hole Response Function Formalism for Continuum Relativistic QRPA . . . 89
6.3 Pairing Interactions and Particle-particle Channels . . . 99
6.4 Strength Function . . . 101

7 Further Developments: The Inclusion of PVC Effects in the CRQRPA 105
7.1 Extraction of the Phonon Transition Densities . . . 106
7.2 Numerical Verification of the QRPA Normalization Condition . . . 107

8 Conclusions and Outlook 109

References 111

Appendices 122

A Summation Over the Matsubara Frequencies 122

B Imaginary-time Projection Operator for Particle-hole Channel 125

C Derivation of Finite-temperature Free Response Function 131

D PC-F1 Force 143

E Time-reversal Transformation 162

F Some Useful Formulas From The Quantum Theory of Angular Momentum 164
F.1 Clebsch-Gordan Coefficients . . . 164
F.2 3-j Symbol and the Wigner-Eckart Theorem . . . 166
F.3 Spin Angular Tensor Operator . . . 167

G Reduced Matrix Elements of the Particle-hole Free Response Function in the Continuum Relativistic QRPA **172**

List of Tables

4.1 Widths of the giant dipole resonance in ^{120}Sn calculated by fitting the FT-RRPA and FT-RTBA strengths with the Lorentz distribution within the energy interval $0 \leq E \leq 25$ MeV. 59

4.2 Major contributions of neutron (n) and proton (p) ph and $\widetilde{\text{ph}}$ configurations to the strongest dipole states below 10 MeV in ^{68}Ni calculated within FT-RTBA for various temperatures. 62

5.1 The density-dependent coupling constants in the DD-PC1 parameterization . 71

5.2 The effective interactions $v_{cc'}(r)$ for the DD-PC1 parameterization. 76

5.3 The Coulomb interactions $v^C_{cc'}(r, r')$ for each channel. 78

6.1 The list of channels c_F and their corresponding effective charges e_{cc_F}. 102

7.1 Comparison between the isovector dipole (IVD) strengths $S^{(\text{IVD})}(\omega)$ and $S^{(\text{IVD})}_{\text{ref}}(\omega)$ at the poles $\omega = \Omega_\nu$ for ^{16}O nucleus computed with the smearing parameter $\Delta = 200$ keV. 106

D.1 The set of coupling constants in the PC-F1 parameterization 144

D.2 The list of channels $c = (D,\ S,\ L,\ J,\ M, T)$. 158

D.3 The effective interactions $v_c(r)$ for each channel. 160

List of Figures

3.1 Diagrammatic representation of the energy-dependent mass operator Σ^e for (a) $\sigma = +1$ and (b) $\sigma = -1$ in the particle-vibration coupling model. 26

3.2 Diagrammatic representation of the Bethe-Salpeter equation for the correlated propagator $\mathscr{R}^e$ given by Eq. (3.44). 29

3.3 Diagrammatic representation of the g^4 terms (a) $\widetilde{\mathscr{R}}^0\mathscr{U}^e\widetilde{\mathscr{R}}^0\mathscr{U}^e\widetilde{\mathscr{R}}^0$ and (b) $\widetilde{\mathscr{R}}^0\mathscr{U}^e\widetilde{\mathscr{R}}^0\Sigma^e\widetilde{\mathscr{G}}^{-1}\widetilde{\mathscr{R}}^0$, which are included in the infinite sum (3.79). 35

3.4 Diagrammatic representation of the imaginary-time ordered g^4 terms (a) $\widetilde{\mathscr{D}}\mathscr{U}^e\widetilde{\mathscr{D}}\mathscr{U}^e\widetilde{\mathscr{R}}^0$ and (b) $\widetilde{\mathscr{D}}\mathscr{U}^e\widetilde{\mathscr{D}}\Sigma^e\widetilde{\mathscr{G}}^{-1}\widetilde{\mathscr{R}}^0$. 35

4.1 The energies of the thermally excited nuclei ^{48}Ca, ^{68}Ni and ^{100,132}Sn as functions of temperature. 53

4.2 Electric dipole spectral density in ^{48}Ca and ^{68}Ni nuclei calculated within FT-RRPA (left panels) and FT-RTBA (right panels) at various temperatures. . 55

4.3 Same as in Fig. 4.2 but for ^{100,120,132}Sn nuclei with the smearing parameter $\Delta = 200$ keV. 56

4.4 Emergence of thermally unblocked states below and above the Fermi energy ε_F. 57

4.5 The role of the exponential factor 57

4.6 Width and energy-weighted sum rule (EWSR) of the giant dipole resonance. 58

4.7 The temperature evolution of the low-energy dipole spectral density in ^{68}Ni calculated within FT-RTBA with the smearing parameter $\Delta = 20$ keV. . . . 61

4.8 The evolution of the proton and neutron transition densities for the most prominent peaks below 10 MeV in ^{68}Ni and ^{100}Sn within FT-RTBA. 61

4.9 The isoscalar monopole response in ^{68}Ni as a function of temperature calculated within FT-RRPA (top panel) and FT-RTBA (bottom panel) with the smearing parameter $\Delta = 500$ keV. 65

4.10 The isoscalar quadrupole response in ^{68}Ni as a function of temperature calculated within FT-RRPA (top panel) and FT-RTBA (bottom panel) with the smearing parameter $\Delta = 500$ keV. 65

5.1 Diagrammatic representation of finite-range interactions and their corresponding approximate point-coupling interactions. 68

A.1 Integration contours C and C' in the complex ξ'-plane. 123

Chapter 1

Introduction

The atomic nucleus plays a significant role in our understanding of the fundamental forces of nature and the emergent phenomena that occur at various scales of physics [1]. It serves as a 'laboratory' for testing the standard model of particle physics via the weak interaction processes, searching the new physics beyond the standard model, and studying the breaking of fundamental symmetries. Besides its importance to particle physics, the electromagnetic interaction between an atomic nucleus and electrons, and between atoms gives rise to the complex structures of materials studied in condensed matter physics. Remarkably, the knowledge about the nuclear structure, decays, and nuclear reactions have paved the way for our understanding of the origin of elements via nucleosynthesis processes, the evolution of stars, neutron stars, and the cataclysmic events, such as supernovas and neutron star mergers.

Nuclear structure research aims to construct a comprehensive and unified framework that describes all properties of nuclei, nucleonic matter, and interactions between nuclei [2]. In the nuclear physics research, the choice of nuclear degrees of freedom depends on the energy of the experimental probe. A high-energy probe resolves quark and gluon degrees of freedom, whereas the more relevant constituents at low energies are protons and neutrons (collectively called nucleons). The description of nuclei with nucleonic degrees of freedom requires detailed knowledge of nucleon-nucleon (NN) interaction. The bare NN interaction can be considered as an emergent interaction of quantum chromodynamics (QCD), which is the underlying theory of quark-gluon dynamics. Although it is a challenging task to derive the bare NN force directly from QCD, the analytical structure of bare NN force still can be studied and formulated based on the known symmetry constraints (e.g., translational, rotational, isospin, parity, time-reversal, and charge), both low- and high-energy NN scattering experiments, and the meson theory. Some of the semi-phenomenological potentials that arise from these considerations are the Hamada-Johnston potential [3], Reid hard-core and soft-core

potentials [4], the Bonn potential [5], the Argonne potential [6, 7], the Paris potential [8], and the Nijmegen potential [9, 10, 11]. Alternatively, the nuclear force can also be studied using the chiral perturbation theory [12] and lattice QCD calculation [13, 14, 15]. For a concise review on the bare NN interaction, see Ref. [16]. While the bare NN interaction can be used to describe the very light nuclei via ab initio calculations (e.g., Green's Function Monte Carlo (GFMC) [17, 18] and coupled-cluster [19, 20] methods), it has to be promoted to effective NN interaction when dealing with the medium-mass and heavy nuclei. The reasons are two-fold. First, the bare NN interaction contains either hard- or soft-repulsive core at the short distance, making it too strong to be applied in the many-body methods. Second, the nucleons do not feel the bare NN interaction inside the nucleus, which means that the bare NN interaction is significantly modified in the presence of many nucleons. One way to circumvent the strong repulsive core problem of the nuclear force is to use the effective interaction obtained from the Brueckner G-matrix theory [21]. In this method, instead of the bare nuclear force, one uses the so-called G-matrix, which takes into account the effects of multiple scattering in nuclear medium and Pauli principle, to perform the nuclear structure calculations. The G-matrix can be obtained by solving the Bethe-Goldstone equation. The other way is to adopt the phenomenological effective NN potentials which contain fitting parameters adjusted to the experimental data for nuclear matter and finite nuclei. The examples of these forces are Skyrme forces [22, 23, 24, 25, 26] and Gogny force [27, 28]. The Skyrme and Gogny density-dependent forces respectively have been used in the Hartree-Fock (HF) [29] and Hartree-Fock-Bogoliubov (HFB) [30] calculations for spherical nuclei with great success. The density-dependent Hartree-Fock (DDHF) models of Skyrme [29] and Gogny [30] are the examples of the mean-field calculations based on the non-relativistic energy density functional.

It has been known that the Fermi energies of the nucleons in nuclei are small compared to the rest mass, making the relativistic effects seemingly unimportant for the low-energy nuclear structure calculations. However, the relativistic version of the mean-field calculations recently gains recognition for several reasons. First, the spin-orbit interaction finds its natural explanation in terms of the scalar field S and vector field V in the relativistic mean-field (RMF) theory [31, 32, 33]. In the RMF theory, nucleons are depicted as Dirac particles moving independently in the average fields, which consist of the scalar field S and vector field V. In the relativistic meson-exchange theory, the attractive scalar field S and repulsive vector field V are derived mostly from an exchange of mesons with Lorentz scalar and vector character, respectively. In nuclear physics, their typical values are $S \approx -400$ MeV and $V \approx 350$ MeV. While the addition of these two fields gives the potential depth of roughly -50 MeV and, thus, allows the non-relativistic kinematics, the subtraction of the scalar field

S from the vector field V leads to the strong spin-orbit interaction between nucleons. Second, the scalar density decreases as the small components of the Dirac spinors become important. As the source of the attractive field S, its reduction reduces the attraction leading to the stability of the nuclear system: the relativistic saturation mechanism [31, 32, 33]. In the non-relativistic DDHF calculations for Skyrme and Gogny forces, this saturation is taken care of by the strongly repulsive density-dependent terms. Third, the pseudo-spin symmetry in nuclei can be explained as an immediate consequence of the nearly equal magnitude, but with opposite signs, of the attractive scalar and repulsive vector fields [32, 34]. In the relativistic meson-exchange theory, an additional density dependence originates from either non-linear self-interactions between mesons or the density-dependent coupling constants. In the relativistic point-coupling theory, one derives the covariant energy density functional from the point-coupling effective interactions [35, 36, 37, 38], where the additional density dependence can be introduced either by the density-dependent coupling constants or by point-couplings of higher order. For a recent review on the types of the meson-exchange and point-coupling effective interactions, the interested reader can refer to Ref. [39] and references therein.

In order to describe the ground state properties of the open-shell nuclei, the relativistic mean-field theory has to be extended to include pairing correlations. The pairing correlations can be included in the relativistic mean-field theory via the constant gap approximation [31, 40]. However, since the experimental value of the gap parameter is taken from the odd-even mass difference, this approximation fails when one deals with the exotic nuclei far from the valley of beta-stability and close to the drip-lines. To gain a consistent relativistic treatment of pairing correlations, Kucharek and Ring [31, 41] derived the relativistic extension of the HFB (RHFB) theory: Dirac-Hartree-Fock-Bogoliubov (DHFB) equations. It was shown how the pairing field originates from one-meson exchange potentials. However, applications in nuclear matter demonstrated that an attempt to use the same force in the pp- and ph-channel resulted in the strong ω-repulsion at short distances leading to a large pairing gap. Therefore, a proper force for pp-channel is needed. Some forces, e.g., contact force [42], Bonn potential [43], and Gogny forces [44, 45], have been used for the interaction in the pp-channel.

A giant resonance (GR) in an atomic nucleus is a broad resonance in the photo-absorption or particle (electron, proton, etc.) scattering cross section observed typically in the energy range between 10 and 30 MeV [46]. It is associated with predominantly vibrational motion, originates from collective excitations of nucleons and exhausts a major part of the sum rule. It can be characterized by three important parameters: centroid energy E, width Γ, and integral strength S. Isoscalar giant monopole resonance (ISGMR), also known as

breathing mode, occurs when a nucleus vibrates without changing its shape. The centroid energy of this compression mode is directly related to the finite-nucleus incompressibility K_A. Isoscalar giant quadrupole resonance (ISGQR) takes place when in-phase oscillations of protons and neutrons cause the nucleus to change its shape back and forth according to a cycle: spherical-prolate-spherical-oblate-spherical. The most studied isovector giant dipole resonance (IVGDR) originates from the oscillations of protons against neutrons in the dipole pattern. In the microscopic description, the ground-state GR (GR at zero temperature) can be viewed as a result of the correlated multiparticle-multihole (npnh) excitations. The total width of the GR comes from Landau damping, spreading, and escape widths. The Landau damping width is caused by the coupling between correlated 1p1h excitations and uncorrelated ones, which have energies close to the excitation energy. The spreading width comes from the coupling of the correlated 1p1h excitations to 2p2h, 3p3h, and higher-order configurations. Lastly, the escape width originates from the coupling of the correlated npnh excitations to the continuum.

The relativistic mean-field theories mentioned so far mostly focused on the ground-state properties of the nuclei all over the periodic table. To describe the excited states, one derives the time-dependent relativistic mean-field (TDRMF) equations using the time-dependent variational principle. The TDRMF equations have been applied to describe giant resonances in nuclei [47, 48, 49]. A huge computational effort and the breaking of rotational symmetries become the drawbacks of these TDRMF calculations [50]. In the limit of small amplitudes, one derives relativistic random phase approximation (RRPA) [51] from the TDRMF equations. A realistic RRPA calculation can be performed by taking into account: (1) the non-linear meson self-interaction terms [51, 52] and (2) antiparticle-hole configurations in addition to the usual particle-hole configurations [51]. The latter is necessary to ensure the current conservation and the decoupling of the spurious state [53]. The RRPA has been applied to the calculation of monopole and dipole compression modes in nuclei [54], and isoscalar and isovector giant resonances in spherical nuclei [55]. The natural extension of the RRPA to include pairing correlations is relativistic quasiparticle random phase approximation (RQRPA). Analogous to the RRPA, the RQRPA is the small-amplitude limit of the time-dependent relativistic Hartree-Bogoliubov (TDRHB) equations [56]. The RHB+RQRPA approach has been applied, for instance, in the calculations of multipole responses of ^{22}O nucleus, where NL3 parametrization has been used for RMF Lagrangian and Gogny D1S finite-range interaction for the pp-channel. The same approach has been employed to investigate the evolution of low-lying isovector dipole strength in Tin isotopes and $N = 82$ isotones [56].

The strength distribution of the giant resonances can be obtained either by diagonalizing

the R(Q)RPA equations or by solving the Bethe-Salpeter equation (BSE) for the response function on an appropriate basis. There are some different methods to handle the continuum states: the truncated harmonic oscillator basis [57], the Wood-Saxon basis with the box-discretized continuum [58], and the exact Green's function [59, 60, 61, 62]. However, to reproduce the escape width of the giant resonances, one has to address the excitations to continuum states, for which the most elegant way is to solve the BSE in the coordinate space representation using the exact Green's function method. Shlomo and Bertsch [63] pioneered this exact treatment of the single-particle continuum states for non-relativistic RPA. Their work was generalized to open-shell nuclei, where pairing correlations were included by means of the BCS approximation, by Kamerdzhiev et al. [64] and by Hagino and Sagawa [65]. Matsuo [66] took a different approach to address pairing correlations by starting with the time-dependent HFB formalism in the coordinate space representation from the beginning and deriving the continuum quasiparticle response function using single-quasiparticle Green's functions defined in the static HFB basis. In the framework of relativistic point-coupling theory, Daoutidis and Ring employed the relativistic single-particle Green's function for the exact treatment of the continuum states and derived the continuum RRPA [59]. They extended their work to include the pairing correlations using the BCS approximation and derived the continuum relativistic QRPA [60]. The relativistic single-particle Green's function technique has been also used by Yang, Cao, and Ma to obtain the continuum relativistic QRPA in the framework of the relativistic meson-exchange theory [61, 62].

As mentioned before, to reproduce the spreading width of the GR and, hence, to obtain an accurate description of the nuclear response, one needs to go beyond the R(Q)RPA. The leading mechanism of the spreading width is known to be the particle-phonon, or particle-vibration, coupling (PVC), however, the inclusion of the PVC requires quite a non-trivial quantum-field-theoretical (QFT) effort. Time blocking approximation was initially introduced in Ref. [67] as a non-perturbative approach to the nuclear response beyond RPA. It utilizes a time projection technique within the Green's function formalism to decouple the configurations of the lowest complexity beyond 1p1h, such as 1p1h$\otimes$phonon (particle-hole pair coupled to a phonon), from the higher-order ones. As a result, the time projection reduces the Bethe-Salpeter equation to a one-frequency variable equation. The method was applied systematically in nuclear structure calculations as an extension of the Landau-Migdal theory for non-superfluid nuclear systems [68] and later generalized for superfluid ones [69, 70]. It has been supplemented by the subtraction procedure to avoid double counting of the particle-vibration coupling in the frameworks based on phenomenological mean fields or effective energy density functionals [70, 71]. Since then the time blocking approximation is used consistently in non-relativistic [72, 73, 74, 75, 76] and relativistic

[77, 78, 79, 80, 81, 82, 83] nuclear structure calculations. The method has been improved systematically to include time-reversed PVC loops as complex ground state correlations [68, 69, 83] and higher-order configurations [84]. At zero temperature the inclusion of the PVC effects in the time blocking approximation leads to a consistent refinement of the calculated spectra in both neutral [79, 80, 85, 86, 87, 88, 89, 90, 91, 92, 93, 94] and charge-exchange [81, 82, 83, 95, 96, 97] channels, as compared to the (Q)RPA approaches, due to the spreading effects[1].

The isovector giant dipole resonance in highly excited nuclei is mainly observed in heavy-ion fusion reactions [46, 99]. In the Steinwedel-Jensen hydrodynamical model, the IVGDR can be understood as a coherent oscillation of protons against neutrons in the dipole pattern. The general features of the IVGDR built on the excited states can be summarized as follows [99]: (i) The energy-weighted sum rule (EWSR) is independent of temperature T and spin angular momentum J; (ii) The centroid energy can be parameterized as $E_{GDR} = 18A^{-1/3} + 25A^{-1/6}$ MeV and is independent of temperature T and spin angular momentum J; (iii) The width grows with temperature T and spin angular momentum J.[2]

The temperature dependence of the high-energy part of the GDR above the neutron emission threshold was extensively studied experimentally in the past [100, 101, 102, 103, 104, 105], see also a relatively recent review [106]. In later studies of the dipole response of both ground and excited states of nuclear systems, a concentration of electric dipole strength has been observed in the low-energy region [85], being most prominent in neutron-rich nuclei. The distribution of E1 strength below the GDR region is usually classified as pygmy dipole resonance (PDR), which, according to the Steinwedel-Jensen hydrodynamical model, originates from the coherent oscillation of the neutron excess against the isospin-saturated core. Some microscopic models also favor for a collective nature of the PDR which forms at a sufficient amount of the excess neutrons [107, 108]. There are two important physical aspects related to the study of the PDR. First, the structure of the PDR can significantly enhance the neutron-capture reaction rates of rapid neutron-capture nucleosynthesis (or r-process) [86, 87, 109, 110, 111], which is responsible for the formation of chemical elements heavier than iron [112]. Second, the PDR can be related to the isovector components of effective nuclear interactions and to the equation of state (EOS) of nuclear matter [107, 108]. The total PDR strength can provide an experimental constraint on the neutron skin thickness

[1]This paragraph is reprinted from Ref. [98], in accordance with with American Physical Society (APS) copyright policies (`https://journals.aps.org/copyrightFAQ.html`)

[2]This paragraph is reprinted from Ref. [98], in accordance with with American Physical Society (APS) copyright policies (`https://journals.aps.org/copyrightFAQ.html`)

and, in turn, on the symmetry energy of the EOS, which is a key ingredient to study dense astrophysical objects, such as neutron stars [85][3].

An accurate theoretical description of response of compound nuclei, or nuclei at finite temperature, is an arduous task. In the past, the multipole response of hot nuclei has been studied theoretically within several frameworks, such as finite-temperature random-phase approximation (FT-RPA) using schematic models [113, 114, 115, 116, 117, 118] or FT-RPA with separable forces for deformed rotating nuclei [119, 120]. Approaches beyond FT-RPA include spreading mechanisms and are represented by the finite-temperature nuclear field theory (NFT), which takes into account the coupling between nucleons and low-lying vibrational modes [121, 122], the collision-integral approach [123, 124], and the quasiparticle-phonon model (QPM), which operates by the phonon-phonon coupling, formulated as thermofield dynamics [125]. On the other hand, phenomenological treatment of thermal shape fluctuations and of the particle evaporation have enabled a good description of the overall temperature evolution of the GDR [126, 127, 128, 129, 130][4].

The finite-temperature Hartree-Fock-Bogoliubov (FTHFB) equations were derived in [131] and applied for solving the two-level model in [113]. The finite-temperature quasiparticle random phase approximation (FT-QRPA) equations were derived based on FTHFB theory and solved for a schematic model to calculate the GDR response of hot spherical nuclei [132]. Shortly after that, the formalism was applied successfully to hot rotating nuclei in [133]. The continuum FT-RPA [134] and FT-QRPA [135, 136] were successfully applied to various calculations of dipole and quadrupole response of medium-mass nuclei. Later it was realized that thermal continuum effects may play the major role in explaining the enhancement of the low-energy dipole strength [137] observed in experiments [138, 139, 140]. More recently, realistic self-consistent approaches in the framework of the relativistic FT-RPA [141] and non-relativistic Skyrme FT-QRPA [142] became available for systematic studies of atomic nuclei across the nuclear chart[5].

In the first part of this Ph.D. work we focus on building a novel self-consistent microscopic approach to the finite-temperature nuclear response which (i) is based on the high-quality, effective meson-exchange interaction, (ii) takes into account spreading mechanism microscopically, self-consistently and in a parameter-free manner, (iii) is numerically stable and executable, and (iv) allows for systematic studies of both low- and high-

[3]This paragraph is reprinted from Ref. [98], in accordance with with American Physical Society (APS) copyright policies (`https://journals.aps.org/copyrightFAQ.html`)

[4]This paragraph is reprinted from Ref. [98], in accordance with with American Physical Society (APS) copyright policies (`https://journals.aps.org/copyrightFAQ.html`)

[5]This paragraph is reprinted from Ref. [98], in accordance with with American Physical Society (APS) copyright policies (`https://journals.aps.org/copyrightFAQ.html`)

energy excitations and deexcitations of compound nuclei in a wide range of mass and temperatures. For this purpose, we generalize the response theory developed since the late 2000s [77, 78, 79, 80] in the relativistic framework of quantum hadrodynamics for the case of zero temperature. This approach is based on the covariant energy density functional with the meson-nucleon interaction [31, 143] and applies the Green's function formalism and the time blocking approximation [67] for the time-dependent part of the nucleon-nucleon interaction in the correlated medium. In the second part of this Ph.D. work, we attempt to extend the zero-temperature nuclear response theory [60], which is based on the effective point-coupling interaction [38], and takes into account pairing correlations within the framework of the BCS approximation, PVC, and exact coupling to the continuum [59]. This extension utilizes the time blocking approximation [70] to incorporate the particle-vibration coupling as a microscopic mechanism to describe the spreading width of the nuclear multipole spectra in both low- and high-energy domains.

This Ph.D. work is organized into two main parts, the first of which deals with the construction of the finite-temperature nuclear response theory, and the second focuses on the extension of the zero-temperature nuclear response theory. The first part of the present work consists of three chapters. Chapter 2 provides an overview of the nuclear mean field at finite temperature. Starting with the grand-canonical ensemble in Section 1.1, we review the zero-temperature relativistic mean-field (RMF) theory of finite range in detail and generalize it for finite temperature in Section 1.2. We discuss the solution of the finite-temperature RMF equations with an emphasis on the iterative numerical procedure to solve the equations. We dedicate Chapter 3 to give a great detailed account of the essential steps to construct the finite-temperature relativistic time-blocking approximation (FT-RTBA). Section 3.1 discusses the Matsubara Green's function formalism to determine the finite-temperature response function and, in turn, the finite-temperature strength function. The essential steps to construct the energy-dependent mass operator and the dynamical induced interaction is highlighted in Section 3.2. We introduce the concept of the time-blocking approximation in the imaginary-time formalism in Section 3.3 and employ it in Section 3.4 to derive the particle-vibration coupling amplitude. The extraction of transition densities is discussed in Section 3.5. In Chapter 4, we describe details of the numerical implementation of the FT-RTBA and discuss the results of the calculations. The second part of the present work consists of three chapters as well. In Chapter 5, we briefly overview the zero-temperature RMF theory of point-coupling and the BCS approximation. The main goal is to introduce the particle-hole interaction in the coordinate-channel representation. In Chapter 6, we take a different approach than the one done in Ref. [144] to derive the continuum relativistic quasiparticle random phase approximation (CRQRPA). In Chapter 7, we briefly discuss the

crucial steps to incorporate the PVC effects in the CRQRPA. The conclusions and outlook are presented in Chapter 8.

Chapter 2

Nuclear Mean Field at Finite Temperature

Hot nuclei (highly excited compound nuclei) are the product of the fusion between a target of heavy atomic nuclei and a heavy-ion projectile, which takes place for a long time in the heavy-ion reactions. During this intermediate state, the mean field of the system gets established soon, and the thermalization process of the excitation energy occurs among all the single-particle degrees of freedom. Since the system achieves the thermal equilibrium in a short time ($\approx 10^{-22}$ s), which is less than the typical time it takes to decay by particle and γ-ray emissions ($\approx 10^{-19} - 10^{-9}$ s), one can apply the concept of equilibrium statistical mechanics to describe the compound nucleus in its intermediate state.

To define the nuclear temperature T, one employs the microcanonical ensemble's definition of temperature [99]

$$T = \left(\frac{1}{\rho} \frac{\partial \rho}{\partial E^*} \right)^{-1}, \tag{2.1}$$

where E^* is the excitation energy, and the density of levels $\rho(A, E^*)$ is given as

$$\rho(A, E^*) \approx \frac{e^{2\sqrt{aE^*}}}{\sqrt{48}E^*}, \tag{2.2}$$

according to the Bethe's Fermi gas formula. Here, the level density parameter $a \approx A/k$ MeV^{-1}, $k = 8 - 12$ MeV, and A is the mass number [46]. Inserting (2.2) into (2.1) yields

$$\frac{1}{T} = \sqrt{\frac{a}{E^*}} - \frac{1}{E^*}, \tag{2.3}$$

where, for high excitation energy, the first term dominates leading to an approximate relation $E^* \approx aT^2$.

2.1 Grand Canonical Ensemble

The grand canonical ensemble represents all possible microstates of an open system which allows the exchange of particles as well as energy with a reservoir. For these possible microstates in equilibrium with the reservoir at a fixed temperature T and chemical potential μ, the grand potential [131, 132, 145]

$$\Omega = E - TS - \mu N \tag{2.4}$$

is minimal. Introducing a positive definite density operator $\hat{\rho}$, which is Hermitian ($\hat{\rho}^\dagger = \hat{\rho}$) and has a unit trace ($\mathrm{Tr}\,\hat{\rho} = 1$), one can express the average energy E, the average particle number N, and the average entropy S as

$$\begin{aligned} E &= \mathrm{Tr}(\hat{\rho}\hat{H}), & (2.5)\\ N &= \mathrm{Tr}(\hat{\rho}\hat{N}), & (2.6)\\ S &= -k\,\mathrm{Tr}(\hat{\rho}\ln\hat{\rho}), & (2.7) \end{aligned}$$

where k is the Boltzmann's constant. Here the symbol Tr represents a summation of all diagonal elements of the matrix or matrices under the operation, and the summation includes all possible numbers of particles of all kinds and all possible states of these particles. From the last three equations and the constraint $\mathrm{Tr}\,\hat{\rho} = 1$, the minimization of the grand potential Ω leads to the solution of the density operator $\hat{\rho}$ of the form

$$\begin{aligned} \hat{\rho} &= Z^{-1}e^{-(\hat{H}-\mu\hat{N})/kT}, & (2.8)\\ Z &= \mathrm{Tr}\left[e^{-(\hat{H}-\mu\hat{N})/kT}\right], & (2.9) \end{aligned}$$

where Z is the grand partition function. The thermal average of an operator $\hat{O}$ then can be defined as

$$\langle\hat{O}\rangle = \mathrm{Tr}(\hat{\rho}\hat{O}) = Z^{-1}\,\mathrm{Tr}\left[e^{-(\hat{H}-\mu\hat{N})/kT}\hat{O}\right]. \tag{2.10}$$

Given the grand partition function Z, several thermodynamic quantities can be determined as follows [145]:

$$\begin{aligned} \Omega &= -kT\ln Z = -PV, & (2.11)\\ E &= -\left.\frac{\partial\ln Z}{\partial\beta}\right|_{z,V}, & (2.12)\\ N &= z\left.\frac{\partial\ln Z}{\partial z}\right|_{\beta,V}, & (2.13) \end{aligned}$$

where $z = e^{\mu/kT}$ is the fugacity and $\beta = 1/kT$. For the rest of this chapter, we take the value of the Boltzmann's constant $k = 1$.

2.2 Finite-temperature Relativistic Mean-field Theory

We start with a relativistic covariant Lagrangian density $\mathscr{L}$ given by [31, 39, 146]

$$\mathscr{L} = \mathscr{L}_{\text{nucleons}} + \mathscr{L}_{\text{mesons}} + \mathscr{L}_{\text{interactions}}. \tag{2.14}$$

The free nucleons are described by the Lagrangian density

$$\mathscr{L}_{\text{nucleons}} = \overline{\Psi}(x)(i\gamma^{\mu}\partial_{\mu} - M)\Psi(x), \tag{2.15}$$

where M is the mass of the nucleon, $\Psi(x) \equiv \Psi(\mathbf{r}, t)$ is the nucleonic field, and the Einstein summation convention is implied. The Greek indices, such as $\mu = \{0, 1, 2, 3\}$, represent the components in Minkowski space, where 0 indicates the time-like component and the other denote the space-like components. The interactions between nucleons are mediated by mesons and photon. The mesons are categorized according to their angular momentum J, isospin T, and parity P quantum numbers. Attractive interaction is provided by the isoscalar scalar σ-meson with the quantum numbers $J = 0$, $T = 0$, and $P = +1$. The ω-meson is an isoscalar vector meson ($J = 1$, $T = 0$, and $P = -1$) which causes repulsive interaction. The isospin dependence of the nuclear force is the result of the exchange of the isovector vector ρ-meson with the quantum numbers $J = 1$, $T = 1$, and $P = -1$. The photon is responsible for the electromagnetic interaction between nucleons. The Lagrangian density $\mathscr{L}_{\text{mesons}}$ is then given by

$$\begin{aligned} \mathscr{L}_{\text{mesons}} &= \frac{1}{2}\left(\partial^{\mu}\sigma\partial_{\mu}\sigma - m_{\sigma}^{2}\sigma^{2}\right) - \frac{1}{2}\left(\frac{1}{2}\Omega_{\mu\nu}\Omega^{\mu\nu} - m_{\omega}^{2}\omega_{\mu}\omega^{\mu}\right) \\ &- \frac{1}{2}\left(\frac{1}{2}\vec{R}_{\mu\nu}\vec{R}^{\mu\nu} - m_{\rho}^{2}\vec{\rho}_{\mu}\vec{\rho}^{\,\mu}\right) - \frac{1}{4}F^{\mu\nu}F_{\mu\nu}, \end{aligned} \tag{2.16}$$

where m_{σ}, m_{ω}, and m_{ρ} are the meson masses, the arrow denote isovectors, and the field tensors are defined as

$$\Omega^{\mu\nu} = \partial^{\mu}\omega^{\nu} - \partial^{\nu}\omega^{\mu}, \tag{2.17}$$

$$\vec{R}^{\mu\nu} = \partial^{\mu}\vec{\rho}^{\,\nu} - \partial^{\nu}\vec{\rho}^{\,\mu}, \tag{2.18}$$

$$F^{\mu\nu} = \partial^{\mu}A^{\nu} - \partial^{\nu}A^{\mu}. \tag{2.19}$$

Here $\sigma(x)$, $\omega^\mu(x)$, and $\vec{\rho}^{\,\mu}(x)$ are the meson fields, and $A^\mu(x)$ is the photon field. The interactions are described by the Lagrangian density

$$\mathscr{L}_{\text{interactions}} = -\overline{\Psi}\Gamma_\sigma\sigma\Psi - \overline{\Psi}\Gamma^\mu_\omega\omega_\mu\Psi - \overline{\Psi}\vec{\Gamma}^\mu_\rho\vec{\rho}_\mu\Psi - \overline{\Psi}\Gamma^\mu_e A_\mu\Psi - U(\sigma), \tag{2.20}$$

where the vertices Γ_σ, Γ^μ_ω, $\vec{\Gamma}^\mu_\rho$, and Γ^μ_e takes the form

$$\Gamma_\sigma = g_\sigma, \quad \Gamma^\mu_\omega = g_\omega\gamma^\mu, \quad \vec{\Gamma}^\mu_\rho = g_\rho\gamma^\mu\vec{\tau}, \quad \Gamma^\mu_e = \frac{1}{2}(1+\tau_3)e\gamma^\mu. \tag{2.21}$$

The quantities g_σ, g_ω, and g_ρ are the corresponding coupling constants for the mesons and e is the unit of electric charge. The non-linear term $U(\sigma)$ describing the self-interaction between the σ-mesons reads [147]

$$U(\sigma) = \frac{1}{3}g_2\sigma^3 + \frac{1}{4}g_3\sigma^4, \tag{2.22}$$

with the additional parameters g_2 and g_3. The presence of this non-linear term is very crucial to reproduce the experimental data on the nuclear matter incompressibility.

From the Euler-Lagrange equation,

$$\frac{\partial}{\partial x^\mu}\left(\frac{\partial\mathscr{L}}{\partial(\partial_\mu\overline{\Psi})}\right) - \frac{\partial\mathscr{L}}{\partial\overline{\Psi}} = 0, \tag{2.23}$$

we obtain the time-dependent Dirac equation for the nucleonic fields:

$$\left[i\gamma_\mu\partial^\mu - M - \Gamma_m\phi_m(\mathbf{r},t)\right]\Psi(\mathbf{r},t) = 0, \tag{2.24}$$

where we have introduced the notations $m = \{\sigma,\ \omega,\ \rho,\ e\}$, $\Gamma_m = \left\{\Gamma_\sigma,\ \Gamma^\mu_\omega,\ \vec{\Gamma}^\mu_\rho,\ \Gamma^\mu_e\right\}$, and $\phi_m = \{\sigma,\ \omega^\mu,\ \vec{\rho}^{\,\mu},\ A^\mu\}$. The corresponding Euler-Lagrange equation for the meson and electromagnetic fields results in

$$(\Box + m_\sigma^2)\sigma(\mathbf{r},t) = -\overline{\Psi}(\mathbf{r},t)\Gamma_\sigma\Psi(\mathbf{r},t) - \frac{dU(\sigma)}{d\sigma}, \tag{2.25}$$

$$(\Box + m_\omega^2)\omega^\mu(\mathbf{r},t) = \overline{\Psi}(\mathbf{r},t)\Gamma^\mu_\omega\Psi(\mathbf{r},t), \tag{2.26}$$

$$(\Box + m_\rho^2)\vec{\rho}^{\,\mu}(\mathbf{r},t) = \overline{\Psi}(\mathbf{r},t)\vec{\Gamma}^\mu_\rho\Psi(\mathbf{r},t), \tag{2.27}$$

$$\Box A^\mu(\mathbf{r},t) = \overline{\Psi}(\mathbf{r},t)\Gamma^\mu_e\Psi(\mathbf{r},t), \tag{2.28}$$

where the d'Alembertian operator $\Box$ is defined as

$$\Box := \partial_\mu\partial^\mu = \frac{\partial^2}{\partial t^2} - \nabla^2, \tag{2.29}$$

and we have imposed the Lorenz gauge conditions:

$$\partial_\mu \omega^\mu(\mathbf{r},t) = 0, \qquad \partial_\mu \vec{\rho}^{\,\mu}(\mathbf{r},t) = 0, \qquad \text{and} \qquad \partial_\mu A^\mu(\mathbf{r},t) = 0. \tag{2.30}$$

It is not a trivial task to obtain the exact solution of the time-dependent self-consistent field equations (2.24)-(2.28). One then introduces the **relativistic mean-field (RMF) approximation** to replace the meson field and electromagnetic field operators by their expectation values in the nuclear ground state. As a result, the nucleons behave as non-interacting particles moving in the classical meson and electromagnetic fields. The nucleonic fields $\Psi(\mathbf{r},t)$ can be expanded in terms of single-particle spinors $\psi_k(\mathbf{r},t)$,

$$\Psi(\mathbf{r},t) = \sum_k \psi_k(\mathbf{r},t)\hat{a}_k \qquad \text{and} \qquad \Psi^\dagger(\mathbf{r},t) = \sum_k \psi_k^\dagger(\mathbf{r},t)\hat{a}_k^\dagger, \tag{2.31}$$

where the role of the operator $\hat{a}_k^\dagger$ ($\hat{a}_k$) is to create (annihilate) a fermion in a state k. The operator $\hat{a}_k$ and its Hermitian conjugate $\hat{a}_k^\dagger$ satisfy the fermion anti-commutation rules:

$$\{\hat{a}_k, \hat{a}_{k'}^\dagger\} = \delta_{kk'}; \qquad \{\hat{a}_k, \hat{a}_{k'}\} = \{\hat{a}_k^\dagger, \hat{a}_{k'}^\dagger\} = 0, \tag{2.32}$$

where $\{\hat{A}, \hat{B}\} \equiv \hat{A}\hat{B} + \hat{B}\hat{A}$. In the **no-sea approximation** [148], the set of states k consists of the occupied states $|h\rangle$ below Fermi level, unoccupied states $|p\rangle$ above Fermi level, and the unoccupied states $|\alpha\rangle$ in the Dirac sea with negative energies. At zero temperature, the nuclear ground state $|\Phi\rangle$ can be constructed as

$$|\Phi\rangle = \prod_k \hat{a}_k^\dagger |0\rangle \tag{2.33}$$

and it is normalized according to $\langle\Phi|\Phi\rangle = 1$. Given the normalized nuclear ground state $|\Phi\rangle$, the single-particle density matrix $\rho_{k\ell}$ takes the form

$$\rho_{k\ell} = \langle\Phi|\hat{a}_\ell^\dagger \hat{a}_k|\Phi\rangle. \tag{2.34}$$

The Hamiltonian operator $\hat{H}$ can be derived from the Lagrangian density $\mathscr{L}$ via

$$\hat{H} = \int d^3\mathbf{r} \left[\frac{\partial \mathscr{L}}{\partial(\partial_0 q)}(\partial_0 q) - \mathscr{L} \right], \tag{2.35}$$

where $q = \{\Psi, \sigma, \omega^\mu, \vec{\rho}^{\,\mu}, A^\mu\}$. Inserting Eqs. (2.14)-(2.20) into Eq. (2.35), we obtain the

Hamiltonian operator:

$$\begin{aligned}
\hat{H} &= \int d^3\mathbf{r}\Psi^\dagger \left\{\boldsymbol{\alpha}\cdot\mathbf{p} + \beta\left(M+\Gamma_m\phi_m\right)\right\}\Psi \\
&+ \frac{1}{2}\int d^3\mathbf{r}\left[\dot{\sigma}^2 + (\nabla\sigma)^2 + m_\sigma^2\sigma^2\right] \\
&- \frac{1}{2}\int d^3\mathbf{r}\left[\dot{\omega}^\mu\dot{\omega}_\mu + (\boldsymbol{\nabla}\omega^\mu)\cdot(\boldsymbol{\nabla}\omega_\mu) + m_\omega^2\omega^\mu\omega_\mu\right] \\
&- \frac{1}{2}\int d^3\mathbf{r}\left[\dot{\vec{\rho}}^\mu\dot{\vec{\rho}}_\mu + (\boldsymbol{\nabla}\vec{\rho}^\mu)\cdot(\boldsymbol{\nabla}\vec{\rho}_\mu) + m_\rho^2\vec{\rho}^\mu\vec{\rho}_\mu\right] \\
&- \frac{1}{2}\int d^3\mathbf{r}\left[\dot{A}^\mu\dot{A}_\mu + (\boldsymbol{\nabla}A^\mu)\cdot(\boldsymbol{\nabla}A_\mu)\right] + \int d^3\mathbf{r}\, U(\sigma), \qquad (2.36)
\end{aligned}$$

where $\beta = \gamma^0$ and $\boldsymbol{\alpha} = \beta\boldsymbol{\gamma}$.

Applying the expansion (2.31) to Hamiltonian operator (2.36), we obtain

$$\begin{aligned}
\hat{H} &= \int d^3\mathbf{r}\sum_{\ell k}\psi_\ell^\dagger(\mathbf{r},t)\left\{\boldsymbol{\alpha}\cdot\mathbf{p} + \beta\left(M+\Gamma_m\phi_m\right)\right\}\psi_k(\mathbf{r},t)\hat{a}_\ell^\dagger\hat{a}_k \\
&+ \frac{1}{2}\int d^3\mathbf{r}\left[\dot{\sigma}^2 + (\nabla\sigma)^2 + m_\sigma^2\sigma^2\right] \\
&- \frac{1}{2}\int d^3\mathbf{r}\left[\dot{\omega}^\mu\dot{\omega}_\mu + (\boldsymbol{\nabla}\omega^\mu)\cdot(\boldsymbol{\nabla}\omega_\mu) + m_\omega^2\omega^\mu\omega_\mu\right] \\
&- \frac{1}{2}\int d^3\mathbf{r}\left[\dot{\vec{\rho}}^\mu\dot{\vec{\rho}}_\mu + (\boldsymbol{\nabla}\vec{\rho}^\mu)\cdot(\boldsymbol{\nabla}\vec{\rho}_\mu) + m_\rho^2\vec{\rho}^\mu\vec{\rho}_\mu\right] \\
&- \frac{1}{2}\int d^3\mathbf{r}\left[\dot{A}^\mu\dot{A}_\mu + (\boldsymbol{\nabla}A^\mu)\cdot(\boldsymbol{\nabla}A_\mu)\right] + \int d^3\mathbf{r}\, U(\sigma). \qquad (2.37)
\end{aligned}$$

Using the mean-field approximation for the meson and electromagnetic fields:

$$\langle\Phi|\phi_m|\Phi\rangle \approx \phi_m\underbrace{\langle\Phi|\Phi\rangle}_{=1} = \phi_m, \qquad (2.38)$$

$$\langle\Phi|\phi_m\hat{a}_{k'}^\dagger\hat{a}_k|\Phi\rangle \approx \phi_m\langle\Phi|\hat{a}_{k'}^\dagger\hat{a}_k|\Phi\rangle = \phi_m\rho_{kk'}, \qquad (2.39)$$

we obtain the corresponding covariant energy density functional (CEDF):

$$\begin{aligned}
E_{\mathrm{RMF}}[\hat{\rho},\phi] &= \langle\Phi|\hat{H}|\Phi\rangle \\
&= \mathrm{Tr}\left[(\boldsymbol{\alpha}\cdot\mathbf{p} + \beta M + \beta\Gamma_m\phi_m)\hat{\rho}\right] \\
&+ \frac{1}{2}\int d^3\mathbf{r}\left[\dot{\sigma}^2 + (\nabla\sigma)^2 + m_\sigma^2\sigma^2\right] \\
&- \frac{1}{2}\int d^3\mathbf{r}\left[\dot{\omega}^\mu\dot{\omega}_\mu + (\boldsymbol{\nabla}\omega^\mu)\cdot(\boldsymbol{\nabla}\omega_\mu) + m_\omega^2\omega^\mu\omega_\mu\right]
\end{aligned}$$

$$
\begin{aligned}
&- \frac{1}{2}\int d^3\mathbf{r}\left[\dot{\vec{\rho}}^{\mu}\dot{\vec{\rho}}_{\mu} + (\boldsymbol{\nabla}\vec{\rho}^{\mu})\cdot(\boldsymbol{\nabla}\vec{\rho}_{\mu}) + m_{\rho}^2\vec{\rho}^{\mu}\vec{\rho}_{\mu}\right] \\
&- \frac{1}{2}\int d^3\mathbf{r}\left[\dot{A}^{\mu}\dot{A}_{\mu} + (\boldsymbol{\nabla}A^{\mu})\cdot(\boldsymbol{\nabla}A_{\mu})\right] + \int d^3\mathbf{r}\, U(\sigma), \qquad (2.40)
\end{aligned}
$$

where the trace symbol Tr here represents a sum over Dirac indices and an integral in the coordinate space. In the static approximation, we assume the meson and electromagnetic fields being time-independent, and the single-particle spinor $\psi_k(\mathbf{r},t)$ takes the form:

$$
\psi_k(\mathbf{r},t) = \varphi_k(\mathbf{r})e^{-i\varepsilon_k t}, \qquad (2.41)
$$

where ε_k is the single-particle energy of the state k. Applying the static approximation to the time-dependent Dirac equation (2.24), we obtain the time-independent Dirac equation of the form:

$$
\hat{h}^D\varphi_k(\mathbf{r}) \;=\; \varepsilon_k\varphi_k(\mathbf{r}). \qquad (2.42)
$$

Here the Dirac Hamiltonian $\hat{h}^D$ is

$$
\hat{h}^D = \boldsymbol{\alpha}\cdot\mathbf{p} + \beta\left[M + \widetilde{\Sigma}(\mathbf{r})\right], \qquad (2.43)
$$

where $\widetilde{\Sigma}(\mathbf{r})$ is the static RMF mass operator (self-energy):

$$
\widetilde{\Sigma}(\mathbf{r}) = \sum_m \Gamma_m\phi_m(\mathbf{r}). \qquad (2.44)
$$

Furthermore we assume: (1) the time-reversal symmetry of RMF, so that the current densities are equal to zero and, therefore, the space-like components of the meson and electromagnetic fields, i.e., $\omega^j(\mathbf{r})$, $\vec{\rho}^{\,j}(\mathbf{r})$, and $A^j(\mathbf{r})$, vanish; (2) the isospin τ_3 is a good quantum number, so that only the third component ρ_3^0 of $\vec{\rho}^{\,0}$ survives. Under these assumptions, the static RMF mass operator consists of the scalar $\widetilde{\Sigma}_s(\mathbf{r})$ and the vector time-like $\widetilde{\Sigma}^0(\mathbf{r})$ components, viz.

$$
\begin{aligned}
\widetilde{\Sigma}_s(\mathbf{r}) &= g_\sigma\sigma(\mathbf{r}), \qquad (2.45)\\
\widetilde{\Sigma}^0(\mathbf{r}) &= \beta\left[g_\omega\omega^0(\mathbf{r}) + \frac{1}{2}(1+\tau_3)eA^0(\mathbf{r}) + g_\rho\tau_3\rho_3^0(\mathbf{r})\right]. \qquad (2.46)
\end{aligned}
$$

The Dirac Hamiltonian $\hat{h}^D$ then becomes

$$
\hat{h}^D = \boldsymbol{\alpha}\cdot\mathbf{p} + \beta(M + S(\mathbf{r})) + V(\mathbf{r}), \qquad (2.47)
$$

where the scalar potential $S(\mathbf{r})$ and the vector potential $V(\mathbf{r})$ are

$$\begin{aligned} S(\mathbf{r}) &= g_\sigma \sigma(\mathbf{r}), & (2.48)\\ V(\mathbf{r}) &= g_\omega \omega^0(\mathbf{r}) + \frac{1}{2}(1+\tau_3) e A^0(\mathbf{r}) + g_\rho \tau_3 \rho_3^0(\mathbf{r}). & (2.49) \end{aligned}$$

The scalar potential $S(\mathbf{r})$ contributes to the effective Dirac mass

$$M^* = M + S(\mathbf{r}). \tag{2.50}$$

Applying the RMF and static approximations to the field equations (2.25)-(2.28), one finds that the non-vanishing meson and electromagnetic fields satisfy the following equations:

$$\begin{aligned} \left(-\nabla^2 + m_\sigma^2\right) \sigma(\mathbf{r}) &= -g_\sigma \rho_s(\mathbf{r}) - \frac{dU(\sigma)}{d\sigma}, & (2.51)\\ \left(-\nabla^2 + m_\omega^2\right) \omega^0(\mathbf{r}) &= g_\omega \rho_v(\mathbf{r}), & (2.52)\\ \left(-\nabla^2 + m_\rho^2\right) \rho_3^0(\mathbf{r}) &= g_\rho \rho_3(\mathbf{r}), & (2.53)\\ -\nabla^2 A^0(\mathbf{r}) &= e\rho_c(\mathbf{r}), & (2.54) \end{aligned}$$

where the time-dependent counterparts of the scalar $\rho_s(\mathbf{r},t)$, baryon $\rho_v(\mathbf{r},t)$, isovector $\rho_3(\mathbf{r},t)$, and charge $\rho_c(\mathbf{r},t)$ densities are given as

$$\begin{aligned} \rho_s(\mathbf{r},t) &= \sum_{k\ell} \rho_{\ell k} \overline{\varphi}_k(\mathbf{r}) \varphi_\ell(\mathbf{r}) e^{i(\varepsilon_k - \varepsilon_\ell)t}, & (2.55)\\ \rho_v(\mathbf{r},t) &= \sum_{k\ell} \rho_{\ell k} \varphi_k^\dagger(\mathbf{r}) \varphi_\ell(\mathbf{r}) e^{i(\varepsilon_k - \varepsilon_\ell)t}, & (2.56)\\ \rho_3(\mathbf{r},t) &= \sum_{k\ell} \rho_{\ell k} \varphi_k^\dagger(\mathbf{r}) \tau_3 \varphi_\ell(\mathbf{r}) e^{i(\varepsilon_k - \varepsilon_\ell)t}, & (2.57)\\ \rho_c(\mathbf{r},t) &= \sum_{k\ell} \rho_{\ell k} \varphi_k^\dagger(\mathbf{r}) \frac{1}{2}\left(1+\tau_3\right) \varphi_\ell(\mathbf{r}) e^{i(\varepsilon_k - \varepsilon_\ell)t}. & (2.58) \end{aligned}$$

At zero temperature, the single-particle density matrix $\rho_{\ell k}$ satisfies

$$\rho_{\ell k} = \rho_k \delta_{k\ell} \begin{cases} 1, & \text{for states } |h\rangle \text{ below the Fermi level,} \\ 0, & \text{otherwise.} \end{cases} \tag{2.59}$$

The densities (2.55)-(2.58) then reduce to the static densities

$$\rho_s(\mathbf{r}) = \sum_{k=1}^{A} \overline{\varphi}_k(\mathbf{r}) \varphi_k(\mathbf{r}), \tag{2.60}$$

$$\rho_v(\mathbf{r}) = \sum_{k=1}^{A} \varphi_k^\dagger(\mathbf{r})\varphi_k(\mathbf{r}), \tag{2.61}$$

$$\rho_3(\mathbf{r}) = \sum_{k=1}^{A} \varphi_k^\dagger(\mathbf{r})\tau_3\varphi_k(\mathbf{r}), \tag{2.62}$$

$$\rho_c(\mathbf{r}) = \sum_{k=1}^{A} \varphi_k^\dagger(\mathbf{r})\frac{1}{2}(1+\tau_3)\varphi_k(\mathbf{r}). \tag{2.63}$$

Accordingly, the CEDF (2.40) now becomes

$$\begin{aligned} E_{\rm RMF}[\hat{\rho},\phi] &= {\rm Tr}\left[\hat{h}^D\hat{\rho}\right] + \frac{1}{2}\int d^3\mathbf{r}\left[(\nabla\sigma(\mathbf{r}))^2 + m_\sigma^2\sigma^2(\mathbf{r})\right] \\ &- \frac{1}{2}\int d^3\mathbf{r}\left[(\boldsymbol{\nabla}\omega^0(\mathbf{r}))\cdot(\boldsymbol{\nabla}\omega_0(\mathbf{r})) + m_\omega^2\omega^0(\mathbf{r})\omega_0(\mathbf{r})\right] \\ &- \frac{1}{2}\int d^3\mathbf{r}\left[(\boldsymbol{\nabla}\rho_3^0(\mathbf{r}))\cdot(\boldsymbol{\nabla}\rho_{30}(\mathbf{r})) + m_\rho^2\rho_3^0\rho_{30}\right] \\ &- \frac{1}{2}\int d^3\mathbf{r}\,(\boldsymbol{\nabla}A^0(\mathbf{r}))\cdot(\boldsymbol{\nabla}A_0(\mathbf{r})) + \int d^3\mathbf{r}\,U(\sigma(\mathbf{r})). \end{aligned} \tag{2.64}$$

To establish the finite-temperature generalization of the RMF theory, we make use of the general procedures discussed in section 2.1. We first construct the grand potential Ω, where the CEDF now plays a role of the average energy E. Minimization of the grand potential Ω results in the single-particle density operator

$$\hat{\rho} = \mathscr{Z}^{-1}e^{-(\hat{h}^D-\mu\hat{\mathscr{N}})/T}, \tag{2.65}$$

where the grand partition function $\mathscr{Z}$ is now given by

$$\mathscr{Z} = {\rm Tr}\left[e^{-(\hat{h}^D-\mu\hat{\mathscr{N}})/T}\right]. \tag{2.66}$$

At finite temperature, the single-particle density matrix $\rho_{k\ell}$ is

$$\rho_{k\ell} = {\rm Tr}\left(\hat{\rho}\hat{a}_\ell^\dagger\hat{a}_k\right) = \langle\hat{a}_\ell^\dagger\hat{a}_k\rangle = \delta_{k\ell}\langle\hat{a}_k^\dagger\hat{a}_k\rangle, \tag{2.67}$$

where we have used the definition of the thermal average of an operator given by Eq. (2.10). In the Dirac basis (2.42), the static Dirac Hamiltonian $\hat{h}^D$ can be written as

$$\hat{h}^D = \sum_k \varepsilon_k\hat{a}_k^\dagger\hat{a}_k, \tag{2.68}$$

while the total particle number operator $\hat{\mathscr{N}}$ is

$$\hat{\mathscr{N}} = \sum_k \hat{a}_k^\dagger \hat{a}_k. \tag{2.69}$$

After inserting the two last equations into Eq. (2.66), the grand partition function $\mathscr{Z}$ takes the form

$$\mathscr{Z} = \prod_k \left[1 + z e^{-\varepsilon_k/T}\right] \tag{2.70}$$

and, using Eq. (2.13), the mean value of the operator $\hat{\mathscr{N}}$ is

$$\mathscr{N} = \sum_k \langle \hat{a}_k^\dagger \hat{a}_k \rangle = \sum_k n_k, \tag{2.71}$$

where the Fermi-Dirac occupation number n_k of the state k reads:

$$n_k(T) = n(\varepsilon_k, T) = \frac{1}{1 + e^{(\varepsilon_k - \mu)/T}}. \tag{2.72}$$

The Fermi-Dirac occupation number $n_k(T)$ satisfies the constraint

$$\sum_k n_k(T) = A, \tag{2.73}$$

where A is the total number of nucleons. From Eq. (2.71), the single-particle density matrix $\rho_{k\ell}$ at finite temperature now reads:

$$\rho_{k\ell} = \delta_{k\ell} n_k, \tag{2.74}$$

and the densities (2.55)-(2.58) reduce to the following set:

$$\rho_s(\mathbf{r}) = \sum_k n_k \overline{\varphi}_k(\mathbf{r}) \varphi_k(\mathbf{r}), \tag{2.75}$$

$$\rho_v(\mathbf{r}) = \sum_k n_k \varphi_k^\dagger(\mathbf{r}) \varphi_k(\mathbf{r}), \tag{2.76}$$

$$\rho_3(\mathbf{r}) = \sum_k n_k \varphi_k^\dagger(\mathbf{r}) \tau_3 \varphi_k(\mathbf{r}), \tag{2.77}$$

$$\rho_c(\mathbf{r}) = \sum_k n_k \varphi_k^\dagger(\mathbf{r}) \frac{1}{2}(1 + \tau_3) \varphi_k(\mathbf{r}). \tag{2.78}$$

In summary, the finite-temperature RMF (FT-RMF) equations comprise the time-independent Dirac equation (2.42), with Dirac Hamiltonian $\hat{h}^D$ is given by Eq. (2.47),

and the field equations (2.51)-(2.54) for the meson and electromagnetic fields, if the meson-nucleon system is in thermal equilibrium. The scalar and vector potentials are given by Eqs. (2.48) and (2.49), respectively, and the finite-temperature densities are given by the formulas (2.75)-(2.78), where the Fermi-Dirac occupation number $n_k(T)$ is given by Eq. (2.72).

2.3 Solution of the Finite-temperature RMF Equations

In the present work, we deal with spherical nuclei, which implies that the total angular momentum is a good quantum number. For the spherically-symmetric nuclear system, the set of quantum numbers $k = \{(k), m_k\}$, where $(k) = \{n_k, j_k, \pi_k, \tau_k\}$, specifies the Dirac spinor $\varphi_k(\mathbf{r})$. Here the set of quantum numbers k consists of radial quantum number n_k, total angular momentum quantum number j_k and its z-component m_k, the parity π_k and the isospin τ_k. The Dirac spinor $\varphi_k(\mathbf{r}, s, t)$ takes the form [77]

$$\varphi_k(\mathbf{r}, s, t) = \begin{bmatrix} f_{(k)}(r)\Omega_{\ell_k j_k m_k}(\theta, \varphi, s) \\ ig_{(k)}(r)\Omega_{\tilde{\ell}_k j_k m_k}(\theta, \varphi, s) \end{bmatrix} \chi_{\tau_k}(t), \tag{2.79}$$

where we have included spin s and isospin t coordinates. The quantum numbers ℓ_k and $\tilde{\ell}_k$ are the orbital angular momentum of large and small components, respectively. Their relations to the total angular momentum j_k and parity π_k are given by

$$\begin{aligned} &\ell_k = j_k + \tfrac{1}{2}, \quad \tilde{\ell}_k = j_k - \tfrac{1}{2}, \quad \text{for} \quad \pi_k = (-1)^{\ell_k} = (-1)^{j_k + \frac{1}{2}}; \\ &\ell_k = j_k - \tfrac{1}{2}, \quad \tilde{\ell}_k = j_k + \tfrac{1}{2}, \quad \text{for} \quad \pi_k = (-1)^{\ell_k} = (-1)^{j_k - \frac{1}{2}}. \end{aligned} \tag{2.80}$$

The functions $f_{(k)}(r)$ and $g_{(k)}(r)$ represent the radial wave functions of large and small components, respectively, and the spin-angular part $\Omega_{\ell j m}(\theta, \varphi, s)$ is defined as

$$\Omega_{\ell j m}(\theta, \varphi, s) = \sum_{m_s m_\ell} \langle \ell m_\ell \tfrac{1}{2} m_s | j m \rangle Y_{\ell m_\ell}(\theta, \varphi) \chi_{m_s}(s). \tag{2.81}$$

Inserting Eq. (2.79) into Eq. (2.42), we obtain two coupled radial equations

$$\frac{dF_{(k)}(r)}{dr} + \frac{\kappa_k}{r} F_{(k)}(r) - \{\varepsilon_k + M - [V(r) - S(r)]\} G_{(k)}(r) = 0, \tag{2.82}$$

$$\frac{dG_{(k)}(r)}{dr} - \frac{\kappa_k}{r} G_{(k)}(r) + \{\varepsilon_k - M - [V(r) + S(r)]\} F_{(k)}(r) = 0, \tag{2.83}$$

where the new radial wave functions $F_{(k)}(r)$ and $G_{(k)}(r)$ are defined as

$$f_{(k)}(r) = \frac{F_{(k)}(r)}{r} \quad \text{and} \quad g_{(k)}(r) = \frac{G_{(k)}(r)}{r}, \tag{2.84}$$

and the new quantum number κ_k takes the values $\kappa_k = \mp(j_k + \frac{1}{2})$ for $j_k = \ell_k \pm \frac{1}{2}$. Introducing the radial Dirac Hamiltonian operator

$$\hat{h}^D_{(k)}(r) \equiv \begin{pmatrix} M + V(r) + S(r) & -\frac{d}{dr} + \frac{\kappa_k}{r} \\ \frac{d}{dr} + \frac{\kappa_k}{r} & -M + V(r) - S(r) \end{pmatrix}, \tag{2.85}$$

the coupled radial equations (2.82) and (2.83) can be written concisely as

$$\hat{h}^D_{(k)}(r) \begin{pmatrix} F_{(k)}(r) \\ G_{(k)}(r) \end{pmatrix} = \varepsilon_k \begin{pmatrix} F_{(k)}(r) \\ G_{(k)}(r) \end{pmatrix}. \tag{2.86}$$

The FT-RMF equations are non-linear coupled equations, so that it is impossible to obtain the analytical solutions. One then employs an iteration method to solve these coupled equations self-consistently. The iteration procedure can be summarized as follows:

(1) For the initial iteration, the meson fields $\sigma(\mathbf{r})$, $\omega^0(\mathbf{r})$, and $\rho^0_3(\mathbf{r})$ take the form of the Woods-Saxon potential, and the photon field $A^0(\mathbf{r})$ takes the form of the Coulomb potential generated by Z protons. The radial Dirac Hamiltonian $\hat{h}^D(r)$ is diagonalized using the spherical harmonic oscillator basis to obtain the radial wave functions $F_{(k)}(r)$ and $G_{(k)}(r)$, and the single-particle energy ε_k of the state k. The corresponding Dirac spinor $\varphi_k(\mathbf{r}, s, t)$ is constructed from Eqs. (2.79) and (2.84).

(2) For every single-particle energy ε_k and specific temperature T, the occupation number $n_k(T)$ can be computed according to Eq. (2.72), and the chemical potential μ can be determined by solving Eq. (2.73).

(3) From Eqs. (2.75)-(2.78), the densities $\rho_s(\mathbf{r})$, $\rho_v(\mathbf{r})$, $\rho_3(\mathbf{r})$, and $\rho_c(\mathbf{r})$ can be computed using the values of the occupation numbers $n_k(T)$ and the Dirac spinors $\varphi_k(\mathbf{r}, s, t)$.

(4) The obtained densities $\rho_s(\mathbf{r})$, $\rho_v(\mathbf{r})$, $\rho_3(\mathbf{r})$, and $\rho_c(\mathbf{r})$ now serve as inputs for the field equations (2.51)-(2.54). The new meson fields $\sigma(\mathbf{r})$, $\omega^0(\mathbf{r})$, and $\rho^0_3(\mathbf{r})$, and photon field $A^0(\mathbf{r})$ can be determined by solving these field equations.

(5) The new fields $\sigma(\mathbf{r})$, $\omega^0(\mathbf{r})$, $\rho^0_3(\mathbf{r})$, and $A^0(\mathbf{r})$ are inserted into the radial Dirac Hamiltonian $\hat{h}^D(r)$, and all procedures of the iteration are repeated until the condition of convergence is achieved.

Chapter 3

Finite-temperature Relativistic Time Blocking Approximation

3.1 Finite-temperature Response Function

A nuclear excitation under a short-duration weak perturbation induced by an external field $\hat{V}^0$ is described in terms of the strength function. At zero temperature, the strength function $S(\omega)$ is defined as [68]

$$S(\omega) = \sum_{n>0} \left[|\langle n|\hat{V}^{0\dagger}|0\rangle|^2 \delta(\omega - \omega_n) - |\langle n|\hat{V}^0|0\rangle|^2 \delta(\omega + \omega_n) \right], \tag{3.1}$$

where $\omega_n = E_n - E_0$ is the excitation energy with respect to the ground state energy E_0. Here the states $|n\rangle$ and energies E_n are the exact eigenstates and eigenvalues of the many-body Hamiltonian $\hat{H}$ specified by a set of quantum numbers n. An external field $\hat{V}^0$ is a one-body operator of the form:

$$\hat{V}^0 = \sum_{k_1 k_2} V^0_{k_1 k_2} \hat{a}^\dagger_{k_1} \hat{a}_{k_2}, \tag{3.2}$$

which gives rise to the transition between the ground state $|0\rangle$ and excited state $|n\rangle$ with the corresponding transition density $\rho^{n0}_{k_1 k_2}$ defined as

$$\rho^{n0}_{k_1 k_2} = \langle n|\hat{a}^\dagger_{k_1} \hat{a}_{k_2}|0\rangle. \tag{3.3}$$

Using Eqs. (3.2) and (3.3) together with one definition of the delta function:

$$\delta(x) = \lim_{\Delta \to +0} \frac{1}{\pi} \frac{\Delta}{x^2 + \Delta^2}, \tag{3.4}$$

the strength function $S(\omega)$ can be expressed in terms of the response function $R(\omega)$, defined as $(\eta \to +0)$ [68]

$$R_{k_1k_2,k_3k_4}(\omega) = \sum_{n>0} \left(\frac{\rho^{n0*}_{k_2k_1} \rho^{n0}_{k_4k_3}}{\omega + \omega_n + i\eta} - \frac{\rho^{n0}_{k_1k_2} \rho^{n0*}_{k_3k_4}}{\omega - \omega_n + i\eta} \right), \tag{3.5}$$

via:

$$S(\omega) = \frac{1}{\pi} \lim_{\Delta \to +0} \mathrm{Im}\Pi(\omega + i\Delta), \tag{3.6}$$

where the polarizability $\Pi(\omega + i\Delta)$ is defined as the double convolution of the full response function $R(\omega)$ with the external field $\hat{V}^0$:

$$\Pi(\omega) = \sum_{k_1k_2k_3k_4} V^{0*}_{k_2k_1} R_{k_1k_2,k_3k_4}(\omega) V^0_{k_4k_3}. \tag{3.7}$$

Here the finite imaginary part Δ of the energy variable is the smearing parameter, which accounts for the finite experimental resolution and missing microscopic effects.

At finite temperature, the strength function $\widetilde{S}(E)$ is defined as

$$\widetilde{S}(E) = \sum_{if} p_i |\langle f|\hat{V}^{0\dagger}|i\rangle|^2 \delta(E - E_f + E_i) \equiv S_+(E), \tag{3.8}$$

where f represents the set of final states and i denotes the possible initial states distributed with the probabilities:

$$p_i = \frac{e^{-E_i/T}}{\sum_j e^{-E_j/T}}. \tag{3.9}$$

The absorption strength function $S_+(E)$ is given by definition (3.8), whereas the emission strength function $S_-(E)$ can be determined via the principle of detailed balance. The emission strength function $S_-(E)$ takes the form

$$S_-(E) = \sum_{if} p_i |\langle f|\hat{V}^0|i\rangle|^2 \delta(E + E_f - E_i) = e^{-\beta E} S_+(E), \tag{3.10}$$

so that the strength function $\widetilde{S}(E)$ becomes

$$\begin{aligned} \widetilde{S}(E) &= \frac{1}{1 - e^{-E/T}} \left[S_+(E) - S_-(E) \right] \\ \widetilde{S}(E) &= \frac{1}{1 - e^{-E/T}} \sum_{if} p_i \left[|\langle f|\hat{V}^{0\dagger}|i\rangle|^2 \delta(E - E_f + E_i) - |\langle f|\hat{V}^0|i\rangle|^2 \delta(E + E_f - E_i) \right]. \end{aligned} \tag{3.11}$$

With the aid of Eq. (3.2) and the definition (3.4) of delta function, the finite-temperature strength function $\widetilde{S}(E)$ can be expressed as

$$\widetilde{S}(E) = \frac{1}{1-e^{-E/T}} S(E), \tag{3.12}$$

$$S(E) = \lim_{\Delta\to+0} \frac{1}{\pi} \mathrm{Im} \sum_{k_1k_2k_3k_4} V^{0*}_{k_2k_1} \mathscr{R}_{k_1k_2,k_3k_4}(E+i\Delta) V^0_{k_4k_3}, \tag{3.13}$$

where we have defined the finite-temperature response function $\mathscr{R}_{k_1k_2,k_3k_4}(E)$ as ($\delta \to +0$)

$$\mathscr{R}_{k_1k_2,k_3k_4}(E) = \sum_{if} p_i \left\{ \frac{\langle f|\hat{a}^\dagger_{k_4}\hat{a}_{k_3}|i\rangle\langle i|\hat{a}^\dagger_{k_1}\hat{a}_{k_2}|f\rangle}{E+E_f-E_i+i\delta} - \frac{\langle f|\hat{a}^\dagger_{k_1}\hat{a}_{k_2}|i\rangle\langle i|\hat{a}^\dagger_{k_4}\hat{a}_{k_3}|f\rangle}{E-E_f+E_i+i\delta} \right\}. \tag{3.14}$$

In analogy to the case of zero temperature [68], the finite-temperature response function $\mathscr{R}_{k_1k_2,k_3k_4}(\omega_n)$ in the spectral representation, defined as

$$\mathscr{R}_{k_1k_2,k_3k_4}(\omega_n) := T\sum_\ell \mathscr{R}_{k_1k_2,k_3k_4}(\omega_n,\varepsilon_\ell), \tag{3.15}$$

is the solution of the Bethe-Salpeter equation in the particle-hole (ph) channel:

$$\begin{aligned} \mathscr{R}_{k_1k_2,k_3k_4}(\omega_n,\varepsilon_\ell) &= -\mathscr{G}_{k_3k_1}(\omega_n+\varepsilon_\ell)\mathscr{G}_{k_2k_4}(\varepsilon_\ell) \\ &+ \sum_{k_5k_6k_7k_8} \mathscr{G}_{k_5k_1}(\omega_n+\varepsilon_\ell)\mathscr{G}_{k_2k_6}(\varepsilon_\ell) \\ &\times T\sum_{\ell'} \mathscr{U}_{k_5k_6,k_7k_8}(\omega_n,\varepsilon_\ell,\varepsilon_{\ell'})\mathscr{R}_{k_7k_8,k_3k_4}(\omega_n,\varepsilon_{\ell'}), \end{aligned} \tag{3.16}$$

where $\mathscr{G}$ is the exact one-body Matsubara Green's function [149, 150, 151] and $\mathscr{U}$ is the nucleon-nucleon interaction amplitude. Here, each subscript k represents all single-particle quantum numbers. The Matsubara frequencies ω_n, ε_ℓ, and $\varepsilon_{\ell'}$ are discrete and defined as [149, 150, 151]

$$\omega_n = 2n\pi T, \qquad \varepsilon_\ell = (2\ell+1)\pi T, \qquad \text{and} \qquad \varepsilon_{\ell'} = (2\ell'+1)\pi T, \tag{3.17}$$

where n, ℓ, and ℓ' are integer. The interaction amplitude is given in terms of the mass operator Σ as

$$\mathscr{U}_{k_1k_2,k_3k_4} = \frac{\delta\Sigma_{k_3k_4}}{\delta\mathscr{G}_{k_1k_2}}. \tag{3.18}$$

The mass operator Σ and the exact one-body temperature Green's function $\mathscr{G}$ are related

by the Dyson equation:

$$\mathscr{G}_{k_1k_2}(\varepsilon_\ell) = \mathscr{G}^0_{k_1k_2}(\varepsilon_\ell) + \sum_{k_3k_4} \mathscr{G}^0_{k_1k_3}(\varepsilon_\ell)\Sigma_{k_3k_4}(\varepsilon_\ell)\mathscr{G}_{k_4k_2}(\varepsilon_\ell), \tag{3.19}$$

where $\mathscr{G}^0$ is the unperturbed one-body temperature Green's function. According to the general equation of motion (EOM) framework [152, 153, 154], the mass operator Σ can be decomposed into the energy-independent part $\widetilde{\Sigma}$, which can be approximated by the static RMF mass operator (2.44), and the energy-dependent part Σ^e, viz.,

$$\Sigma_{k_3k_4}(\varepsilon_\ell) = \widetilde{\Sigma}_{k_3k_4} + \Sigma^e_{k_3k_4}(\varepsilon_\ell). \tag{3.20}$$

To eliminate the unperturbed one-body Matsubara Green's function $\mathscr{G}^0$ from Eq. (3.19), one introduces the thermal mean-field Green's function $\widetilde{\mathscr{G}}$ which satisfies the Dyson equation:

$$\widetilde{\mathscr{G}}_{k_1k_2}(\varepsilon_\ell) = \mathscr{G}^0_{k_1k_2}(\varepsilon_\ell) + \sum_{k_3k_4} \mathscr{G}^0_{k_1k_3}(\varepsilon_\ell)\widetilde{\Sigma}_{k_3k_4}\widetilde{\mathscr{G}}_{k_4k_2}(\varepsilon_\ell). \tag{3.21}$$

In the operator form, Eq. (3.21) can be arranged to give

$$\widetilde{\Sigma} = (\mathscr{G}^0)^{-1} - \widetilde{\mathscr{G}}^{-1}. \tag{3.22}$$

Inserting Eqs. (3.20) and (3.22) into Eq. (3.19), we obtain the Dyson equation:

$$\mathscr{G} = \widetilde{\mathscr{G}} + \widetilde{\mathscr{G}}\Sigma^e\mathscr{G} \tag{3.23}$$

or

$$\mathscr{G}_{k_1k_2}(\varepsilon_\ell) = \widetilde{\mathscr{G}}_{k_1k_2}(\varepsilon_\ell) + \sum_{k_3k_4} \widetilde{\mathscr{G}}_{k_1k_3}(\varepsilon_\ell)\Sigma^e_{k_3k_4}(\varepsilon_\ell)\mathscr{G}_{k_4k_2}(\varepsilon_\ell). \tag{3.24}$$

In the spectral representation, the thermal mean-field Green's function is defined as [150]

$$\widetilde{\mathscr{G}}_{k_1k_2}(\varepsilon_\ell) = \delta_{k_1k_2}\widetilde{\mathscr{G}}_{k_1}(\varepsilon_\ell), \qquad \widetilde{\mathscr{G}}_{k_1}(\varepsilon_\ell) = \frac{1}{i\varepsilon_\ell - \varepsilon_{k_1} + \mu}. \tag{3.25}$$

The mass operator Σ^e describes the coupling between ph configuration and more complex ones. In this work, we employ the particle-vibration coupling (PVC) model to approximate the mass operator Σ^e. At zero temperature, the analytical form of the leading-order mass

operator Σ^e is given by [68, 155]

$$\Sigma^e_{k_1k_2}(\varepsilon) = \sum_{k_3,m} \frac{g^{m(\sigma_{k_3})*}_{k_1k_3} g^{m(\sigma_{k_3})}_{k_2k_3}}{\varepsilon - \tilde{\varepsilon}_{k_3} - \sigma_{k_3}(\omega_m - i\delta)}, \quad \delta \to +0, \tag{3.26}$$

where $\tilde{\varepsilon}_k$ denotes the mean-field single-particle energy of state k, and m represents the complete set of phonon quantum numbers with the corresponding phonon frequency ω_m. At zero temperature, σ_k is equal to $+1$ for particle states and -1 for hole states. The diagrammatic representation of the mass operator Σ^e for the two values of σ is given by Figure 3.1. The phonon vertices $g^{m(\sigma_k)}_{k_1k_2}$ are defined as

$$g^{m(\sigma_k)}_{k_1k_2} = \delta_{\sigma_k,+1} g^m_{k_1k_2} + \delta_{\sigma_k,-1} g^{m*}_{k_2k_1}. \tag{3.27}$$

Once the analytical form of the mass operator Σ^e is specified, a solution of the Dyson equation (3.24) can be obtained.

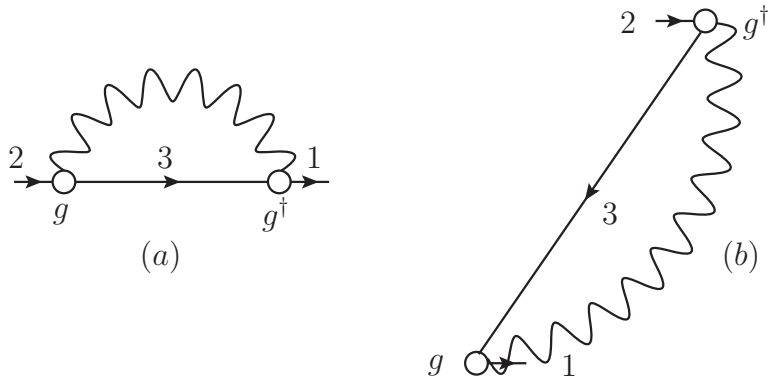

Figure 3.1: Diagrammatic representation of the energy-dependent mass operator Σ^e for (a) $\sigma = +1$ and (b) $\sigma = -1$ in the particle-vibration coupling model. Straight lines correspond to one-fermion propagators and wiggly lines represent the phonon propagators. The empty circles denote the particle-phonon coupling vertices [98].

Similar to the case of the mass operator, the interaction amplitude $\mathscr{U}_{k_1k_2,k_3k_4}(\omega_n, \varepsilon_\ell, \varepsilon_{\ell'})$ consists of the energy-independent part $\widetilde{\mathscr{U}_{k_1k_2,k_3k_4}}$ and the energy-dependent part $\mathscr{U}^e_{k_1k_2,k_3k_4}(\omega_n, \varepsilon_\ell, \varepsilon_{\ell'})$:

$$\mathscr{U}_{k_1k_2,k_3k_4}(\omega_n, \varepsilon_\ell, \varepsilon_{\ell'}) = \widetilde{\mathscr{U}_{k_1k_2,k_3k_4}} + \mathscr{U}^e_{k_1k_2,k_3k_4}(\omega_n, \varepsilon_\ell, \varepsilon_{\ell'}). \tag{3.28}$$

The relation between the mean-field mass operator $\widetilde{\Sigma}$ and the mean-field interaction

amplitude $\widetilde{\mathscr{U}}$ is given by

$$\widetilde{\mathscr{U}}_{k_1k_2,k_3k_4} = \frac{\delta\widetilde{\Sigma}_{k_3k_4}}{\delta\rho_{k_1k_2}}, \tag{3.29}$$

where ρ is the ground state density. At zero temperature, the analytical form of the interaction amplitude U^e is given by [68, 155]

$$U^e_{k_1k_2,k_3k_4}(\omega,\varepsilon,\varepsilon') = \sum_{\sigma,m} \frac{\sigma g^{m(\sigma)*}_{k_3k_1} g^{m(\sigma)}_{k_4k_2}}{\varepsilon - \varepsilon' + \sigma(\omega_m - i\delta)}. \tag{3.30}$$

and satisfy the dynamical consistency condition

$$\Sigma^e_{k_1k_2}(\varepsilon+\omega) - \Sigma^e_{k_1k_2}(\varepsilon) \;=\; \int_{-\infty}^{\infty} \frac{d\varepsilon'}{2\pi i} \sum_{k_3k_4} U^e_{k_2k_1,k_4k_3}(\omega,\varepsilon,\varepsilon') \left[\widetilde{G}_{k_3k_4}(\varepsilon'+\omega) - \widetilde{G}_{k_3k_4}(\varepsilon')\right], \tag{3.31}$$

where $\widetilde{G}$ represents the mean-field Green's function at zero temperature. The construction of the mass operator Σ^e and the interaction amplitude $\mathscr{U}^e$ for the case of finite temperature will be discussed in Section 3.2.

We define the so-called correlated propagator $\mathscr{R}^e(\omega_n,\varepsilon_\ell)$ as a solution of the Bethe-Salpeter equation (BSE) with only the dynamical interaction kernel:

$$\mathscr{R}^e = -\mathscr{G}\mathscr{G} + \mathscr{G}\mathscr{G}\mathscr{U}^e\mathscr{R}^e. \tag{3.32}$$

From Eq. (3.32), the interaction amplitude $\mathscr{U}^e$ can be expressed as

$$\mathscr{U}^e = (\mathscr{R}^e)^{-1} + \mathscr{G}^{-1}\mathscr{G}^{-1}. \tag{3.33}$$

Equation (3.16) can be written as operator equation:

$$\mathscr{R} = -\mathscr{G}\mathscr{G} + \mathscr{G}\mathscr{G}\mathscr{U}\mathscr{R}, \tag{3.34}$$

where the interaction amplitude $\mathscr{U}$ is given by Eq. (3.28). Inserting Eq. (3.33) into Eq. (3.34), we obtain

$$\mathscr{R} = \mathscr{R}^e - \mathscr{R}^e\widetilde{\mathscr{U}}\mathscr{R}. \tag{3.35}$$

Equation (3.35) implies that the full finite-temperature response function $\mathscr{R}$ can be obtained once the analytical form of the function $\mathscr{R}^e$ is determined. To formulate the analytical form

of $\mathscr{R}^e$, we first rewrite the Dyson equation (3.23) as

$$\mathscr{G}^{-1} = \widetilde{\mathscr{G}}^{-1} - \Sigma^e \tag{3.36}$$

and multiply the BSE (3.32) with $\widetilde{\mathscr{G}}\widetilde{\mathscr{G}}\mathscr{G}^{-1}\mathscr{G}^{-1}$ from the left to obtain

$$\mathscr{R}^e = \widetilde{\mathscr{R}}^0 - \widetilde{\mathscr{R}}^0 \mathscr{W}^e \mathscr{R}^e, \tag{3.37}$$

where

$$\begin{aligned}
\widetilde{\mathscr{R}}^0 &= -\widetilde{\mathscr{G}}\widetilde{\mathscr{G}}, && (3.38)\\
\mathscr{W}^e &= W^e - \Sigma^e\Sigma^e, && (3.39)\\
W^e &= \mathscr{U}^e + \widetilde{\mathscr{G}}^{-1}\Sigma^e + \Sigma^e\widetilde{\mathscr{G}}^{-1}. && (3.40)
\end{aligned}$$

In the imaginary-time τ representation, Eqs. (3.37)-(3.40) take the form:

$$\begin{aligned}
\widetilde{\mathscr{R}}^0(12,34) &= -\widetilde{\mathscr{G}}(3,1)\widetilde{\mathscr{G}}(2,4), && (3.41)\\
\mathscr{W}^e(12,34) &= W^e(12,34) - \Sigma^e(3,1)\Sigma^e(2,4), && (3.42)\\
W^e(12,34) &= \mathscr{U}^e(12,34) + \widetilde{\mathscr{G}}^{-1}(3,1)\Sigma^e(2,4) + \Sigma^e(3,1)\widetilde{\mathscr{G}}^{-1}(2,4), && (3.43)\\
\mathscr{R}^e(12,34) &= \widetilde{\mathscr{R}}^0(12,34) - \sum_{5678}^{\tau} \widetilde{\mathscr{R}}^0(12,56)\mathscr{W}^e(56,78)\mathscr{R}^e(78,34) && \\
\mathscr{R}^e(12,34) &= -\widetilde{\mathscr{G}}(3,1)\widetilde{\mathscr{G}}(2,4) + \sum_{5678}^{\tau} \widetilde{\mathscr{G}}(5,1)\widetilde{\mathscr{G}}(2,6)\mathscr{U}^e(56,78)\mathscr{R}^e(78,34) && \\
&+ \sum_{5678}^{\tau} \widetilde{\mathscr{G}}(5,1)\widetilde{\mathscr{G}}(2,6)\widetilde{\mathscr{G}}^{-1}(7,5)\Sigma^e(6,8)\mathscr{R}^e(78,34) && \\
&+ \sum_{5678}^{\tau} \widetilde{\mathscr{G}}(5,1)\widetilde{\mathscr{G}}(2,6)\Sigma^e(7,5)\widetilde{\mathscr{G}}^{-1}(6,8)\mathscr{R}^e(78,34) && \\
&- \sum_{5678}^{\tau} \widetilde{\mathscr{G}}(5,1)\widetilde{\mathscr{G}}(2,6)\Sigma^e(7,5)\Sigma^e(6,8)\mathscr{R}^e(78,34), && (3.44)
\end{aligned}$$

where

$$\sum_{12..}^{\tau} = \sum_{k_1 k_2 \ldots} \int_0^{1/T} d\tau_1 d\tau_2 \cdots . \tag{3.45}$$

Here each number index consists of a set of single-particle quantum numbers k, and imaginary-time τ with interval $0 \leq \tau \leq 1/T$ [149, 150, 151], viz., $1 \coloneqq \{k_1, \tau_1\}$. The corresponding Feynman diagram for Eq. (3.44) is given by Figure 3.2.

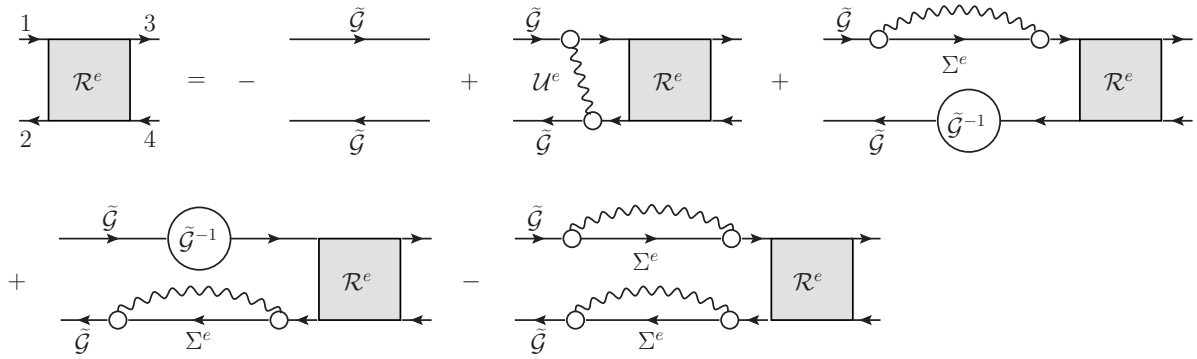

Figure 3.2: Diagrammatic representation of the Bethe-Salpeter equation for the correlated propagator $\mathscr{R}^e$ given by Eq. (3.44) [98].

3.2 The Temperature-dependent Mass Operator and Interaction Amplitude

In this section, we discuss the essential steps to construct the analytical form of the energy-dependent mass operator Σ^e and interaction amplitude $\mathscr{U}^e$ for the case of finite temperature. We start with the definition of the finite-temperature phonon propagator in energy representation [149, 150, 151]:

$$\begin{aligned}\mathscr{D}_m(\varepsilon_\ell - \varepsilon_{\ell'}) &= \frac{2\omega_m}{(i\varepsilon_\ell - i\varepsilon_{\ell'})^2 - \omega_m^2} = \frac{1}{i\varepsilon_\ell - i\varepsilon_{\ell'} - \omega_m} - \frac{1}{i\varepsilon_\ell - i\varepsilon_{\ell'} + \omega_m} \\ &= \sum_{\sigma=\pm 1} \frac{\sigma}{i\varepsilon_{\ell'} - i\varepsilon_\ell - \sigma\omega_m}, \end{aligned} \tag{3.46}$$

where m specifies the complete set of phonon quantum numbers with the corresponding real phonon frequency ω_m. The analytical form of the mass operator $\Sigma^e_{k_1k_2}(\varepsilon_\ell)$ corresponding to the Feynman diagram shown in Figure 3.1 reads

$$\begin{aligned}\Sigma^e_{k_1k_2}(\varepsilon_\ell) &= -T\sum_{k_3,m}\sum_{\ell'} \widetilde{\mathscr{G}}_{k_3}(\varepsilon_{\ell'}) \sum_{\sigma=\pm 1} \frac{\sigma}{i\varepsilon_\ell - i\varepsilon_{\ell'} - \sigma\omega_m} g^{m(\sigma)*}_{k_1k_3} g^{m(\sigma)}_{k_2k_3} \\ &= T\sum_{k_3,m}\sum_{\ell'} \frac{1}{i\varepsilon_{\ell'} - \varepsilon_{k_3} + \mu} \frac{g^m_{k_3k_1} g^{m*}_{k_3k_2}}{i\varepsilon_\ell - i\varepsilon_{\ell'} + \omega_m} \\ &- T\sum_{k_3,m}\sum_{\ell'} \frac{1}{i\varepsilon_{\ell'} - \varepsilon_{k_3} + \mu} \frac{g^{m*}_{k_1k_3} g^m_{k_2k_3}}{i\varepsilon_\ell - i\varepsilon_{\ell'} - \omega_m}, \end{aligned} \tag{3.47}$$

where the phonon vertices $g^{m(\sigma)}$ are defined according to Eq. (3.27). The phonon vertices $g^m_{k_1k_2}$ are, in the leading approximation, related to the effective meson-exchange interaction $\widetilde{\mathscr{U}}$ via

$$g^m_{k_1k_2} = \sum_{k_3k_4} \widetilde{\mathscr{U}}_{k_1k_2,k_3k_4}\rho^m_{k_3k_4}, \tag{3.48}$$

where $\rho^m_{k_3k_4}$ are the transition densities of the phonons. The summation over ℓ' in Eq. (3.47) can be transformed into a contour integral as demonstrated in Appendix A. We then obtain the final expression of the mass operator $\Sigma^e_{k_1k_2}(\varepsilon_\ell)$ of the form:

$$\Sigma^e_{k_1k_2}(\varepsilon_\ell) \;=\; \sum_{k_3,m}\left\{ g^{m*}_{k_1k_3}g^m_{k_2k_3}\frac{N(\omega_m,T)+1-n(\varepsilon_{k_3},T)}{i\varepsilon_\ell-\varepsilon_{k_3}+\mu-\omega_m} + g^m_{k_3k_1}g^{m*}_{k_3k_2}\frac{n(\varepsilon_{k_3},T)+N(\omega_m,T)}{i\varepsilon_\ell-\varepsilon_{k_3}+\mu+\omega_m}\right\}, \tag{3.49}$$

where

$$N(\omega_m,T) = \frac{1}{e^{\omega_m/T}-1} \tag{3.50}$$

is the phonon occupation number with the energy ω_m [149, 150, 151]. At this point, it is instructive to take the limit $T \to 0$ of Eq. (3.49) and compare the result with Eq. (3.26). Before that, it is convenient to rewrite Eq. (3.26) as

$$\Sigma^e_{k_1,k_2}(\varepsilon) = \sum_{\substack{k_3,m\\ \tilde\varepsilon_{k_3}>\varepsilon_F}} \frac{g^{m*}_{k_1k_3}g^m_{k_2k_3}}{\varepsilon-\tilde\varepsilon_{k_3}-\omega_m+i\delta} + \sum_{\substack{k_3,m\\ \tilde\varepsilon_{k_3}\le\varepsilon_F}} \frac{g^m_{k_3k_1}g^{m*}_{k_3k_2}}{\varepsilon-\tilde\varepsilon_{k_3}+\omega_m-i\delta}, \qquad \delta\to+0. \tag{3.51}$$

In the limit $T \to 0$ the phonon occupation number $N(\omega_m,T) \to 0$, the energy difference $\varepsilon_{k_3}-\mu \to \tilde\varepsilon_{k_3}$, and the fermion occupation number $n(\varepsilon_{k_3},T)$ goes to 1 (0) for $\tilde\varepsilon_{k_3} \le \varepsilon_F$ ($\tilde\varepsilon_{k_3} > \varepsilon_F$). Applying this limit to the first term of the right-hand side (RHS) of Eq. (3.49) gives

$$\begin{aligned}
\sum_{k_3,m} g^{m*}_{k_1k_3}g^m_{k_2k_3}\frac{N(\omega_m,T)+1-n(\varepsilon_{k_3},T)}{i\varepsilon_\ell-\varepsilon_{k_3}+\mu-\omega_m} \;&\to\; \sum_{\substack{k_3,m\\ \tilde\varepsilon_{k_3}>\varepsilon_F}} g^{m*}_{k_1k_3}g^m_{k_2k_3}\frac{0+1-0}{\varepsilon-\tilde\varepsilon_{k_3}-\omega_m}\\
&\quad + \sum_{\substack{k_3,m\\ \tilde\varepsilon_{k_3}\le\varepsilon_F}} g^m_{k_2k_3}\underbrace{\frac{0+1-1}{\varepsilon-\tilde\varepsilon_{k_3}-\omega_m}}_{=0}\\
\sum_{k_3,m} g^{m*}_{k_1k_3}g^m_{k_2k_3}\frac{N(\omega_m,T)+1-n(\varepsilon_{k_3},T)}{i\varepsilon_\ell-\varepsilon_{k_3}+\mu-\omega_m} \;&\to\; \sum_{\substack{k_3,m\\ \tilde\varepsilon_{k_3}>\varepsilon_F}} \frac{g^{m*}_{k_1k_3}g^m_{k_2k_3}}{\varepsilon-\tilde\varepsilon_{k_3}-\omega_m},
\end{aligned} \tag{3.52}$$

which is the first term of the RHS of Eq. (3.51). Similarly, it can be shown that the application of the limit $T \to 0$ to the second term of the RHS of Eq. (3.49) gives us the second term of the RHS of Eq. (3.51). Therefore, we have obtained the correct limit $T \to 0$ for the energy-dependent mass operator Σ^e given by (3.49).

The interaction amplitude $\mathscr{U}^e_{k_1k_2,k_3k_4}(\omega_n, \varepsilon_\ell, \varepsilon_{\ell'})$ is specified by the finite-temperature dynamical consistency condition:

$$\Sigma^e_{k_1k_2}(\varepsilon_\ell + \omega_n) - \Sigma^e_{k_1k_2}(\varepsilon_\ell) \;=\; T\sum_{k_3k_4}\sum_{\ell'} \mathscr{U}^e_{k_2k_1,k_4k_3}(\omega_n, \varepsilon_\ell, \varepsilon_{\ell'})[\widetilde{\mathscr{G}}_{k_3k_4}(\varepsilon_{\ell'} + \omega_n) - \widetilde{\mathscr{G}}_{k_3k_4}(\varepsilon_{\ell'})], \tag{3.53}$$

analogous to the zero-temperature case [68, 155]. It can be shown that the interaction amplitude $\mathscr{U}^e_{k_1k_2,k_3k_4}(\omega_n, \varepsilon_\ell, \varepsilon_{\ell'})$, which satisfies the condition (3.53), takes the form:

$$\mathscr{U}^e_{k_1k_2,k_3k_4}(\omega_n, \varepsilon_\ell, \varepsilon_{\ell'}) = \sum_m \frac{g^m_{k_4k_2} g^{m*}_{k_3k_1}}{i\varepsilon_\ell - i\varepsilon_{\ell'} + \omega_m} - \sum_m \frac{g^{m*}_{k_2k_4} g^m_{k_1k_3}}{i\varepsilon_\ell - i\varepsilon_{\ell'} - \omega_m}, \tag{3.54}$$

which has obviously the correct $T \to 0$ limit.

3.3 Time Blocking Approximation in Imaginary-time Formalism

As the equation (3.37) has the singular kernel, it cannot be solved directly in its present form. The time-blocking approximation proposed originally in Ref. [67] for the case of $T = 0$ and adopted for the relativistic framework in Refs. [77, 78] allows for a reduction of the BSE to one-energy variable equation with the interaction kernel where the internal energy variables can be integrated out separately. The main idea of the method is to introduce a time projection operator into the integral part of the BSE for the correlated propagator $\mathscr{R}^e$. This operator acting between the uncorrelated mean-field propagator and the PVC processes in the second term on the right-hand side of Eq. (3.37) brings it to a separable form with respect to its two energy variables, see Ref. [68] for details. The analogous imaginary-time projection operator for the finite temperature case would look as follows:

$$\Theta(12, 34) = \delta_{\sigma_{k_1}, -\sigma_{k_2}} \theta(\sigma_{k_1}\tau_{41})\theta(\sigma_{k_1}\tau_{32}); \tag{3.55}$$

however, it turns out that at $T > 0$ it does not lead to a similar separable function in the kernel of Eq. (3.37).

In order to reach the desired separable form, we found that the imaginary-time projection operator has to be modified as follows:

$$\begin{aligned}\Theta(12,34;T) &= \delta_{\sigma_{k_1},-\sigma_{k_2}}\theta(\sigma_{k_1}\tau_{41})\theta(\sigma_{k_1}\tau_{32})\left[n(\sigma_{k_1}\varepsilon_{k_2},T)\theta(\sigma_{k_1}\tau_{12})\right.\\ &+ \left. n(\sigma_{k_2}\varepsilon_{k_1},T)\theta(\sigma_{k_2}\tau_{12})\right], \end{aligned} \tag{3.56}$$

i.e., it should contain an additional multiplier with the dependence on the diffuse Fermi-Dirac distribution function, which turns to unity in the $T = 0$ limit at the condition $\sigma_{k_1} = -\sigma_{k_2}$.

Using the correct analytical expression of the imaginary-time projection operator $\Theta(12, 34; T)$, we construct an operator $\widetilde{\mathscr{D}}$ of the form:

$$\begin{aligned}\widetilde{\mathscr{D}}(12,34) &= \delta_{\sigma_{k_1},-\sigma_{k_2}}\widetilde{\mathscr{G}}^{\sigma_{k_1}}(3,1)\widetilde{\mathscr{G}}^{\sigma_{k_2}}(2,4)\theta(\sigma_{k_1}\tau_{41})\theta(\sigma_{k_1}\tau_{32})\\ &\times \left[n(\sigma_{k_1}\varepsilon_{k_2},T)\theta(\sigma_{k_1}\tau_{12}) + n(\sigma_{k_2}\varepsilon_{k_1},T)\theta(\sigma_{k_2}\tau_{12})\right], \end{aligned} \tag{3.57}$$

where $\sigma_k = +1(-1)$ for particle (hole). Due to the presence of the Kronecker delta $\delta_{\sigma_{k_1},-\sigma_{k_2}}$, the non-vanishing combinations of $(\sigma_{k_1}, \sigma_{k_2})$ would be $(+1, -1)$ and $(-1, +1)$. A pair of state $\{k_1, k_2\}$ is assigned as a ph (hp) pair if the energy difference $\varepsilon_{k_1} - \varepsilon_{k_2}$ is larger (smaller) than zero. The thermal mean-field Green's function for $\sigma_k = +1$ is defined as [149, 150, 151]

$$\widetilde{\mathscr{G}}^{(+1)}(3,1) = -\delta_{k_1k_3}[1 - n(\varepsilon_{k_1},T)]e^{-(\varepsilon_{k_1}-\mu)\tau_{31}}\theta(\tau_{31}) \tag{3.58}$$

and for $\sigma_k = -1$, it reads [149, 150, 151]:

$$\widetilde{\mathscr{G}}^{(-1)}(3,1) = \delta_{k_1k_3}n(\varepsilon_{k_1},T)e^{-(\varepsilon_{k_1}-\mu)\tau_{31}}\theta(-\tau_{31}). \tag{3.59}$$

In a concise form, the thermal mean-field Green's function is given by

$$\widetilde{\mathscr{G}}^{\sigma_{k_1}}(3,1) = -\sigma_{k_1}\delta_{k_1k_3}n(-\sigma_{k_1}\varepsilon_{k_1},T)e^{-(\varepsilon_{k_1}-\mu)\tau_{31}}\theta(\sigma_{k_1}\tau_{31}). \tag{3.60}$$

For particle-hole channel, Eq. (3.57) gives

$$\widetilde{\mathscr{D}}^{ph}(12,34) = \widetilde{\mathscr{G}}^{(+1)}(3,1)\widetilde{\mathscr{G}}^{(-1)}(2,4)\theta(\tau_{41})\theta(\tau_{32})[n_{k_2}\theta(\tau_{12}) + (1-n_{k_1})\theta(\tau_{21})], \tag{3.61}$$

where we have introduced the shorthand notations:

$$n(\varepsilon_{k_1},T) = \frac{1}{e^{(\varepsilon_{k_1}-\mu)/T}+1} \equiv n_{k_1}, \tag{3.62}$$

$$n(-\varepsilon_{k_1},T) = \frac{1}{e^{-(\varepsilon_{k_1}-\mu)/T}+1} = \frac{e^{(\varepsilon_{k_1}-\mu)/T}}{e^{(\varepsilon_{k_1}-\mu)/T}+1} = 1 - \frac{1}{e^{(\varepsilon_{k_1}-\mu)/T}+1} \equiv 1 - n_{k_1}. \tag{3.63}$$

Inserting Eqs. (3.58) and (3.59) into Eq. (3.61), we obtain

$$\begin{aligned}\widetilde{\mathscr{D}}^{ph}(12,34) &= -\delta_{k_1k_3}\delta_{k_2k_4}(1-n_{k_1})n_{k_2}\theta(\tau_{31})\theta(\tau_{42})\theta(\tau_{41})\theta(\tau_{32}) \\ &\times [n_{k_2}\theta(\tau_{12})+(1-n_{k_1})\theta(\tau_{21})]e^{-[(\varepsilon_{k_1}-\mu)\tau_{31}+(\varepsilon_{k_2}-\mu)\tau_{24}]} \\ &= -\delta_{k_1k_3}\delta_{k_2k_4}(1-n_{k_1})n_{k_2}[n_{k_2}\theta(\tau_{31})\theta(\tau_{42})\theta(\tau_{41})\theta(\tau_{32})\theta(\tau_{12}) \\ &+ (1-n_{k_1})\theta(\tau_{31})\theta(\tau_{42})\theta(\tau_{41})\theta(\tau_{32})\theta(\tau_{21})]e^{-[(\varepsilon_{k_1}-\mu)\tau_{31}+(\varepsilon_{k_2}-\mu)\tau_{24}]}. \quad (3.64)\end{aligned}$$

The terms in the bracket can be evaluated using the identity:

$$\theta(\tau_{13})\theta(\tau_{12})\theta(\tau_{23}) = \theta(\tau_{12})\theta(\tau_{23}). \quad (3.65)$$

Using the identity (3.65), Eq. (3.64) becomes

$$\begin{aligned}\widetilde{\mathscr{D}}^{ph}(12,34) &= -\delta_{k_1k_3}\delta_{k_2k_4}(1-n_{k_1})n_{k_2}[n_{k_2}\theta(\tau_{41})\theta(\tau_{31})\theta(\tau_{12}) \\ &+ (1-n_{k_1})\theta(\tau_{42})\theta(\tau_{32})\theta(\tau_{21})]e^{-[(\varepsilon_{k_1}-\mu)\tau_{31}+(\varepsilon_{k_2}-\mu)\tau_{24}]}. \quad (3.66)\end{aligned}$$

We next introduce the τ-difference variables $\tau_{31} = \tau_3 - \tau_1$, $\tau_{21} = \tau_2 - \tau_1$, and $\tau_{34} = \tau_3 - \tau_4$, so that $\widetilde{\mathscr{D}}^{ph}(12,34) \equiv \widetilde{\mathscr{D}}^{ph}_{k_1k_2,k_3k_4}(\tau_{31},\tau_{21},\tau_{34})$, and transform $\widetilde{\mathscr{D}}^{ph}(12,34)$ into its spectral representation using the Fourier transformation:

$$\begin{aligned}\widetilde{\mathscr{D}}^{ph}_{k_1k_2,k_3k_4}(\omega_n,\varepsilon_\ell,\varepsilon_{\ell'}) &= \int_{-1/T}^{1/T}\int_{-1/T}^{1/T}\int_{-1/T}^{1/T} d\tau_{31}d\tau_{21}d\tau_{34}\widetilde{\mathscr{D}}^{ph}_{k_1k_2,k_3k_4}(\tau_{31},\tau_{21},\tau_{34}) \\ &\times e^{i(\omega_n\tau_{31}+\varepsilon_\ell\tau_{21}+\varepsilon_{\ell'}\tau_{34})}. \quad (3.67)\end{aligned}$$

Inserting Eq. (3.66) into Eq. (3.67), we obtain

$$\widetilde{\mathscr{D}}^{ph}_{k_1k_2,k_3k_4}(\omega_n,\varepsilon_\ell,\varepsilon_{\ell'}) = \delta_{k_1k_3}\delta_{k_2k_4}(i\omega_n-\varepsilon_{k_1}+\varepsilon_{k_2})\widetilde{\mathscr{G}}_{k_1}(\varepsilon_\ell+\omega_n)\widetilde{\mathscr{G}}_{k_2}(\varepsilon_\ell)\widetilde{\mathscr{G}}_{k_3}(\varepsilon_{\ell'}+\omega_n)\widetilde{\mathscr{G}}_{k_4}(\varepsilon_{\ell'}). \quad (3.68)$$

For a more detailed derivation, an interested reader can refer to Appendix B. For hole-particle channel, Eq. (3.57) gives

$$\widetilde{\mathscr{D}}^{hp}(12,34) = \widetilde{\mathscr{G}}^{(-1)}(3,1)\widetilde{\mathscr{G}}^{(+1)}(2,4)\theta(\tau_{14})\theta(\tau_{23})[(1-n_{k_2})\theta(\tau_{21})+n_{k_1}\theta(\tau_{12})]. \quad (3.69)$$

In the spectral representation, operator $\widetilde{\mathscr{D}}^{hp}(12,34)$ takes the form:

$$\widetilde{\mathscr{D}}^{hp}_{k_1k_2,k_3k_4}(\omega_n,\varepsilon_\ell,\varepsilon_{\ell'}) = -\delta_{k_1k_3}\delta_{k_2k_4}(i\omega_n-\varepsilon_{k_1}+\varepsilon_{k_2})\widetilde{\mathscr{G}}_{k_1}(\varepsilon_\ell+\omega_n)\widetilde{\mathscr{G}}_{k_2}(\varepsilon_\ell)\widetilde{\mathscr{G}}_{k_3}(\varepsilon_{\ell'}+\omega_n)\widetilde{\mathscr{G}}_{k_4}(\varepsilon_{\ell'}). \quad (3.70)$$

In the concise form, the time-blocking operator takes the form

$$\begin{aligned}\widetilde{\mathscr{D}}_{k_1k_2,k_3k_4}(\omega_n,\varepsilon_\ell,\varepsilon_{\ell'}) &= \sigma_{k_1}\delta_{\sigma_{k_1},-\sigma_{k_2}}\delta_{k_1k_3}\delta_{k_2k_4}(i\omega_n-\varepsilon_{k_1}+\varepsilon_{k_2})\widetilde{\mathscr{G}}_{k_1}(\varepsilon_\ell+\omega_n)\widetilde{\mathscr{G}}_{k_2}(\varepsilon_\ell)\\ &\times \widetilde{\mathscr{G}}_{k_3}(\varepsilon_{\ell'}+\omega_n)\widetilde{\mathscr{G}}_{k_4}(\varepsilon_{\ell'}).\end{aligned} \tag{3.71}$$

After having defined the $\widetilde{\mathscr{D}}$-operator we are now ready to apply it to the BSE (3.37). We first transform the BSE (3.37) into

$$\mathscr{R}^e=\widetilde{\mathscr{R}}^0-\widetilde{\mathscr{R}}^0\Gamma^e\widetilde{\mathscr{R}}^0, \tag{3.72}$$

where the amplitude Γ^e is defined as

$$\Gamma^e=\mathscr{W}^e-\mathscr{W}^e\widetilde{\mathscr{R}}^0\mathscr{W}^e+\mathscr{W}^e\widetilde{\mathscr{R}}^0\mathscr{W}^e\widetilde{\mathscr{R}}^0\mathscr{W}^e-\cdots=\mathscr{W}^e-\mathscr{W}^e\widetilde{\mathscr{R}}^0\Gamma^e. \tag{3.73}$$

By making the substitutions:

$$\widetilde{\mathscr{R}}^0\to-\widetilde{\mathscr{D}}\qquad\text{and}\qquad\mathscr{W}^e\to\widetilde{\mathscr{W}^e} \tag{3.74}$$

in Eq. (3.73), where $\widetilde{\mathscr{D}}$ is defined by Eq. (3.71), one obtains the new amplitude $\widetilde{\Gamma}^e$, viz.,

$$\widetilde{\Gamma}^e=\widetilde{\mathscr{W}^e}-\widetilde{\mathscr{W}^e}(-\widetilde{\mathscr{D}})\widetilde{\Gamma}^e, \tag{3.75}$$

where

$$\widetilde{\mathscr{W}^e}(12,34)=W^e(12,34)+W^{\rm comp}(12,34). \tag{3.76}$$

Like in the zero-temperature case [68], we omit the term $W^{\rm comp}(12,34)$ because it accounts for a higher-order contribution as compared to W^e of (3.40). Using the new amplitude $\widetilde{\Gamma}^e$, the Bethe-Salpeter equation (3.72) becomes

$$\begin{aligned}\widetilde{\mathscr{R}}^e &= \widetilde{\mathscr{R}}^0-\widetilde{\mathscr{R}}^0\widetilde{\Gamma}^e\widetilde{\mathscr{R}}^0\\ &= \widetilde{\mathscr{R}}^0-\widetilde{\mathscr{R}}^0\widetilde{\mathscr{W}^e}\widetilde{\mathscr{R}}^e\\ &= \widetilde{\mathscr{R}}^0+\widetilde{\mathscr{D}}\widetilde{\mathscr{W}^e}\widetilde{\mathscr{R}}^e\\ \widetilde{\mathscr{R}}^e &= \widetilde{\mathscr{R}}^0+\widetilde{\mathscr{D}}W^e\widetilde{\mathscr{R}}^e,\end{aligned} \tag{3.77}$$

where $\widetilde{\mathscr{R}}^0=-\widetilde{\mathscr{G}}\widetilde{\mathscr{G}}$. In the τ representation, (3.77) can be written as

$$\widetilde{\mathscr{R}}^e(12,34) = -\widetilde{\mathscr{G}}(3,1)\widetilde{\mathscr{G}}(2,4)+\sum_{5678}^{\tau}\widetilde{\mathscr{D}}(12,56)\Big[\mathscr{U}^e(56,78)+\Sigma^e(7,5)\widetilde{\mathscr{G}}^{-1}(6,8)$$

$$+ \quad \widetilde{\mathscr{G}}^{-1}(7,5)\Sigma^e(6,8)\Big]\,\widetilde{\mathscr{R}}^e(78,34). \tag{3.78}$$

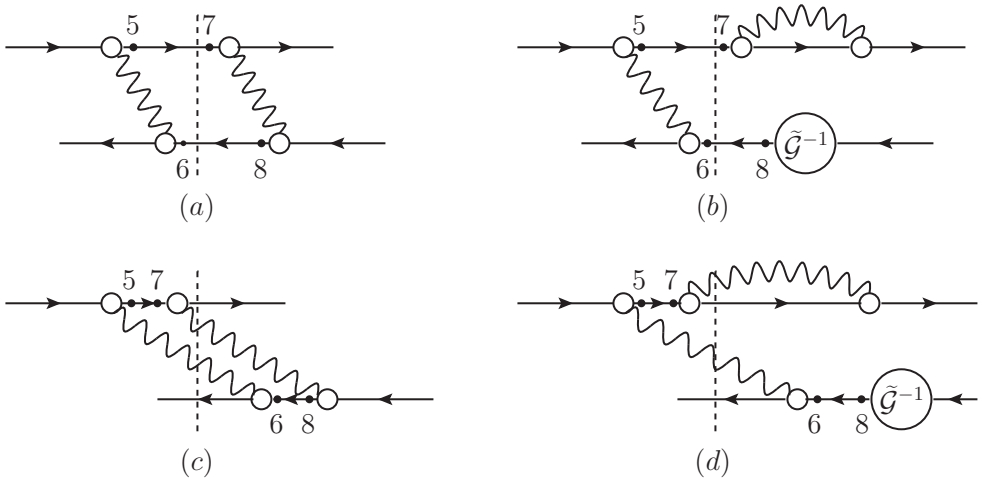

Figure 3.3: Diagrammatic representation of the g^4 terms (a) $\widetilde{\mathscr{R}}^0\mathscr{U}^e\widetilde{\mathscr{R}}^0\mathscr{U}^e\widetilde{\mathscr{R}}^0$ and (b) $\widetilde{\mathscr{R}}^0\mathscr{U}^e\widetilde{\mathscr{R}}^0\Sigma^e\widetilde{\mathscr{G}}^{-1}\widetilde{\mathscr{R}}^0$, which are included in the infinite sum (3.79). The similar fourth-order diagrams for (c) $\widetilde{\mathscr{R}}^0\mathscr{U}^e\widetilde{\mathscr{R}}^0\mathscr{U}^e\widetilde{\mathscr{R}}^0$ and (d) $\widetilde{\mathscr{R}}^0\mathscr{U}^e\widetilde{\mathscr{R}}^0\Sigma^e\widetilde{\mathscr{G}}^{-1}\widetilde{\mathscr{R}}^0$ with the imaginary time τ_6 is later than τ_7. The dashed line denotes the specific imaginary time τ.

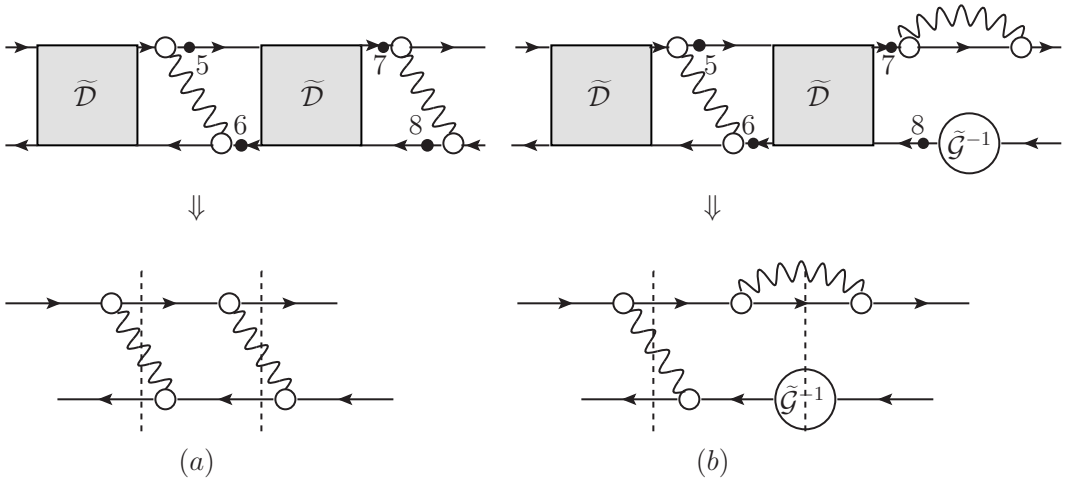

Figure 3.4: Diagrammatic representation of the imaginary-time ordered g^4 terms (a) $\widetilde{\mathscr{D}}\mathscr{U}^e\widetilde{\mathscr{D}}\mathscr{U}^e\widetilde{\mathscr{R}}^0$ and (b) $\widetilde{\mathscr{D}}\mathscr{U}^e\widetilde{\mathscr{D}}\Sigma^e\widetilde{\mathscr{G}}^{-1}\widetilde{\mathscr{R}}^0$. After making the substitution (3.74), the g^4 terms $\widetilde{\mathscr{R}}^0\mathscr{U}^e\widetilde{\mathscr{R}}^0\mathscr{U}^e\widetilde{\mathscr{R}}^0$ and $\widetilde{\mathscr{R}}^0\mathscr{U}^e\widetilde{\mathscr{R}}^0\Sigma^e\widetilde{\mathscr{G}}^{-1}\widetilde{\mathscr{R}}^0$ becomes (a) $\widetilde{\mathscr{D}}\mathscr{U}^e\widetilde{\mathscr{D}}\mathscr{U}^e\widetilde{\mathscr{R}}^0$ and (b) $\widetilde{\mathscr{D}}\mathscr{U}^e\widetilde{\mathscr{D}}\Sigma^e\widetilde{\mathscr{G}}^{-1}\widetilde{\mathscr{R}}^0$. These imaginary-time ordered diagrams now enter the infinite sum (3.81).

Let us now discuss the physical meaning of the $\widetilde{\mathscr{D}}$-operator by taking the operator

$\widetilde{\mathscr{D}}^{ph}(12,34)$ as an example. For this purpose, we first rewrite $\mathscr{R}^e$ of Eq. (3.37) as an infinite sum:

$$\begin{aligned}\mathscr{R}^e &= \widetilde{\mathscr{R}}^0 - \widetilde{\mathscr{R}}^0 \mathscr{W}^e \mathscr{R}^e \\ &= \widetilde{\mathscr{R}}^0 - \widetilde{\mathscr{R}}^0 \mathscr{W}^e \widetilde{\mathscr{R}}^0 + \widetilde{\mathscr{R}}^0 \mathscr{W}^e \widetilde{\mathscr{R}}^0 \mathscr{W}^e \widetilde{\mathscr{R}}^0 - \cdots ,\end{aligned} \tag{3.79}$$

where

$$\mathscr{W}^e = \mathscr{U}^e + \widetilde{\mathscr{G}}^{-1}\Sigma^e + \Sigma^e \widetilde{\mathscr{G}}^{-1} - \Sigma^e \Sigma^e. \tag{3.80}$$

As a matter of illustration, let us consider the terms of $\mathscr{R}^e$ which are fourth-order in g, such as $\widetilde{\mathscr{R}}^0 \mathscr{U}^e \widetilde{\mathscr{R}}^0 \mathscr{U}^e \widetilde{\mathscr{R}}^0$ and $\widetilde{\mathscr{R}}^0 \mathscr{U}^e \widetilde{\mathscr{R}}^0 \Sigma^e \widetilde{\mathscr{G}}^{-1} \widetilde{\mathscr{R}}^0$. The diagrammatic representation of these terms are shown in Figure 3.3 (a) and (b). However, since the intermediate imaginary-time variables τ_i $(i = 5, ..., 8)$ can take any values between 0 and $1/T$, it is possible that the imaginary time τ_6 (τ_5) is later than τ_7 (τ_8), as shown in Figure 3.3 (c) and (d). On the other hand, the correlated propagator $\widetilde{\mathscr{R}}^e$ is given as an infinite sum:

$$\begin{aligned}\widetilde{\mathscr{R}}^e &= \widetilde{\mathscr{R}}^0 + \widetilde{\mathscr{D}} W^e \widetilde{\mathscr{R}}^e \\ &= \widetilde{\mathscr{R}}^0 + \widetilde{\mathscr{D}} W^e \widetilde{\mathscr{R}}^0 + \widetilde{\mathscr{D}} W^e \widetilde{\mathscr{D}} W^e \widetilde{\mathscr{R}}^0 + \cdots ,\end{aligned} \tag{3.81}$$

where

$$W^e = \mathscr{U}^e + \widetilde{\mathscr{G}}^{-1}\Sigma^e + \Sigma^e \widetilde{\mathscr{G}}^{-1}. \tag{3.82}$$

Figure 3.4 shows the fourth-order diagrams for $\widetilde{\mathscr{D}} \mathscr{U}^e \widetilde{\mathscr{D}} \mathscr{U}^e \widetilde{\mathscr{R}}^0$ and $\widetilde{\mathscr{D}} \mathscr{U}^e \widetilde{\mathscr{D}} \Sigma^e \widetilde{\mathscr{G}}^{-1} \widetilde{\mathscr{R}}^0$ as a comparison. The operator $\widetilde{\mathscr{D}}^{ph}(56,78)$ contains the step functions $\theta(\tau_{85})$ and $\theta(\tau_{76})$, which prohibit the imaginary time τ_6 (τ_5) to be later than τ_7 (τ_8), as demonstrated in Figure 3.4 (a) and (b). This unique property of $\widetilde{\mathscr{D}}$-operator hence coins the name of our method, i.e., finite-temperature relativistic time blocking approximation (FT-RTBA). The role of operator $\widetilde{\mathscr{D}}^{ph}(56,78)$ is thus to eliminate the processes with the configuration more complex than 1p1h $\otimes$ phonon ones. As a result, the types of diagram included in Eq. (3.81) are the 1p1h and 1p1h $\otimes$ phonon ones.

3.4 Correlated Particle-hole Propagator

In this section, we derive the Bethe-Salpeter equation (BSE) for the single-frequency correlated ph propagator $\widetilde{\mathscr{R}}^e_{k_1k_2,k_3k_4}(\omega_n)$ from the BSE for the correlated propagator $\widetilde{\mathscr{R}}^e_{k_1k_2,k_3k_4}(\omega_n, \varepsilon_\ell, \varepsilon_{\ell'})$ given by Eq. (3.78). The one-variable correlated propagator $\widetilde{\mathscr{R}}^e_{k_1k_2,k_3k_4}(\omega_n)$ can be obtained from the correlated propagator $\widetilde{\mathscr{R}}^e_{k_1k_2,k_3k_4}(\omega_n, \varepsilon_\ell, \varepsilon_{\ell'})$ by double

summation:

$$\widetilde{\mathscr{R}}^{e}_{k_1k_2,k_3k_4}(\omega_n) = T^2 \sum_{\ell} \sum_{\ell'} \widetilde{\mathscr{R}}^{e}_{k_1k_2,k_3k_4}(\omega_n, \varepsilon_\ell, \varepsilon_{\ell'}). \tag{3.83}$$

The Fourier transform of the correlated propagator $\widetilde{\mathscr{R}}^{e}(12,34)$,

$$\widetilde{\mathscr{R}}^{e}_{k_1k_2,k_3k_4}(\omega_n, \varepsilon_\ell, \varepsilon_{\ell'}) = \frac{1}{8}\int_{-1/T}^{1/T} d\tau_{31} d\tau_{21} d\tau_{34} e^{i(\omega_n\tau_{31}+\varepsilon_\ell\tau_{21}+\varepsilon_{\ell'}\tau_{34})} \widetilde{\mathscr{R}}^{e}(12,34), \tag{3.84}$$

can be decomposed into four integrals:

$$I_1 = -\frac{1}{8}\int_{-1/T}^{1/T} d\tau_{31} d\tau_{21} d\tau_{34} e^{i(\omega_n\tau_{31}+\varepsilon_\ell\tau_{21}+\varepsilon_{\ell'}\tau_{34})} \widetilde{\mathscr{G}}(3,1)\widetilde{\mathscr{G}}(2,4), \tag{3.85}$$

$$\begin{aligned} I_2 &= \frac{1}{8}\sum_{5678}^{\tau}\int_{-1/T}^{1/T} d\tau_{31} d\tau_{21} d\tau_{34} e^{i(\omega_n\tau_{31}+\varepsilon_\ell\tau_{21}+\varepsilon_{\ell'}\tau_{34})} \widetilde{\mathscr{D}}(12,56)\mathscr{U}^{e}(56,78) \\ &\times \widetilde{\mathscr{R}}^{e}(78,34), \end{aligned} \tag{3.86}$$

$$\begin{aligned} I_3 &= \frac{1}{8}\sum_{5678}^{\tau}\int_{-1/T}^{1/T} d\tau_{31} d\tau_{21} d\tau_{34} e^{i(\omega_n\tau_{31}+\varepsilon_\ell\tau_{21}+\varepsilon_{\ell'}\tau_{34})} \widetilde{\mathscr{D}}(12,56)\Sigma^{e}(7,5)\widetilde{\mathscr{G}}^{-1}(6,8) \\ &\times \widetilde{\mathscr{R}}^{e}(78,34), \end{aligned} \tag{3.87}$$

$$\begin{aligned} I_4 &= \frac{1}{8}\sum_{5678}^{\tau}\int_{-1/T}^{1/T} d\tau_{31} d\tau_{21} d\tau_{34} e^{i(\omega_n\tau_{31}+\varepsilon_\ell\tau_{21}+\varepsilon_{\ell'}\tau_{34})} \widetilde{\mathscr{D}}(12,56)\widetilde{\mathscr{G}}^{-1}(7,5)\Sigma^{e}(6,8) \\ &\times \widetilde{\mathscr{R}}^{e}(78,34). \end{aligned} \tag{3.88}$$

The integral I_1 is the Fourier transform of the finite-temperature free response function $\widetilde{\mathscr{R}}^{0}(12,34)$, which is given by

$$\widetilde{\mathscr{R}}^{0}_{k_1k_2,k_3k_4}(\omega_n, \varepsilon_\ell, \varepsilon_{\ell'}) = -\frac{1}{T}\delta_{\ell'\ell}\delta_{k_1k_3}\delta_{k_2k_4}\widetilde{\mathscr{G}}_1(\omega_n+\varepsilon_\ell)\widetilde{\mathscr{G}}_2(\varepsilon_\ell). \tag{3.89}$$

A more detailed derivation of $\widetilde{\mathscr{R}}^{0}_{k_1k_2,k_3k_4}(\omega_n, \varepsilon_\ell, \varepsilon_{\ell'})$ is placed in Appendix C. The integral I_2 can be carried out as follows:

$$\begin{aligned} I_2 &= \frac{1}{8}\sum_{5678}^{\tau}\int_{-1/T}^{1/T} d\tau_{31} e^{i\omega_n\tau_{31}} \int_{-1/T}^{1/T} d\tau_{21} e^{i\varepsilon_\ell\tau_{21}} \int_{-1/T}^{1/T} d\tau_{34} e^{i\varepsilon_{\ell'}\tau_{34}} \\ &\times T^3 \sum_{n_1,\ell_1,\ell'_1} e^{-i(\alpha_{n_1}\tau_{51}+\beta_{\ell_1}\tau_{21}+\gamma_{\ell'_1}\tau_{56})} \widetilde{\mathscr{D}}_{k_1k_2,k_5k_6}(\alpha_{n_1},\beta_{\ell_1},\gamma_{\ell'_1}) \\ &\times T^3 \sum_{n_2,\ell_2,\ell'_2} e^{-i(\alpha_{n_2}\tau_{75}+\beta_{\ell_2}\tau_{65}+\gamma_{\ell'}\tau_{78})} \mathscr{U}^{e}_{k_5k_6,k_7k_8}(\alpha_{n_2},\beta_{\ell_2},\gamma_{\ell'_2}) \end{aligned}$$

$$
\begin{aligned}
&\times \quad T^3 \sum_{n_3,\ell_3,\ell_3'} e^{-i(\alpha_{n_3}\tau_{37}+\beta_{\ell_3}\tau_{87}+\gamma_{\ell_3'}\tau_{34})} \widetilde{\mathscr{R}}^e_{k_7k_8,k_3k_4}(\alpha_{n_3},\beta_{\ell_3},\gamma_{\ell_3'}) \\
&= \quad \frac{1}{8}\sum_{5678}^{\tau}\int_{-1/T}^{1/T} d\tau_{31} e^{i\omega_n\tau_{31}} T^3 \sum_{n_1,\ell_1,\ell_1'} e^{-i(\alpha_{n_1}\tau_{51}+\gamma_{\ell_1'}\tau_{56})} \widetilde{\mathscr{D}}_{k_1k_2,k_5k_6}(\alpha_{n_1},\beta_{\ell_1},\gamma_{\ell_1'}) \\
&\times \quad T^3 \sum_{n_2,\ell_2,\ell_2'} e^{-i(\alpha_{n_2}\tau_{75}+\beta_{\ell_2}\tau_{65}+\gamma_{\ell'}\tau_{78})} \mathscr{U}^e_{k_5k_6,k_7k_8}(\alpha_{n_2},\beta_{\ell_2},\gamma_{\ell_2'}) \\
&\times \quad T^3 \sum_{n_3,\ell_3,\ell_3'} e^{-i(\alpha_{n_3}\tau_{37}+\beta_{\ell_3}\tau_{87})} \widetilde{\mathscr{R}}^e_{k_7k_8,k_3k_4}(\alpha_{n_3},\beta_{\ell_3},\gamma_{\ell_3'}) \underbrace{\int_{-1/T}^{1/T} d\tau_{21} e^{i(\varepsilon_\ell-\beta_{\ell_1})\tau_{21}}}_{=\frac{2}{T}\delta_{\varepsilon_\ell,\beta_{\ell_1}}} \\
&\times \quad \underbrace{\int_{-1/T}^{1/T} d\tau_{34} e^{i(\varepsilon_{\ell'}-\gamma_{\ell_3'})\tau_{34}}}_{=\frac{2}{T}\delta_{\varepsilon_{\ell'},\gamma_{\ell_3'}}} \\
&= \quad \frac{1}{2}\sum_{5678}^{\tau}\int_{-1/T}^{1/T} d\tau_{31} e^{i\omega_n\tau_{31}} T^2 \sum_{n_1,\ell_1'} e^{-i(\alpha_{n_1}\tau_{51}+\gamma_{\ell_1'}\tau_{56})} \widetilde{\mathscr{D}}_{k_1k_2,k_5k_6}(\alpha_{n_1},\varepsilon_\ell,\gamma_{\ell_1'}) \\
&\times \quad T^3 \sum_{n_2,\ell_2,\ell_2'} e^{-i(\alpha_{n_2}\tau_{75}+\beta_{\ell_2}\tau_{65}+\gamma_{\ell'}\tau_{78})} \mathscr{U}^e_{k_5k_6,k_7k_8}(\alpha_{n_2},\beta_{\ell_2},\gamma_{\ell_2'}) \\
&\times \quad T^2 \sum_{n_3,\ell_3} e^{-i(\alpha_{n_3}\tau_{37}+\beta_{\ell_3}\tau_{87})} \widetilde{\mathscr{R}}^e_{k_7k_8,k_3k_4}(\alpha_{n_3},\beta_{\ell_3},\varepsilon_{\ell'}) \\
&= \quad \frac{1}{2}\sum_{k_5k_6k_7k_8}\int_{-1/T}^{1/T} d\tau_{31} e^{i\omega_n\tau_{31}} e^{i(\alpha_{n_1}\tau_1-\alpha_{n_3}\tau_3)} \\
&\times \quad T^7 \sum_{n_1,\ell_1'}\sum_{n_2,\ell_2,\ell_2'}\sum_{n_3,\ell_3}\int_0^{1/T} d\tau_5 e^{-i(\alpha_{n_1}+\gamma_{\ell_1'}-\alpha_{n_2}-\beta_{\ell_2})\tau_5} \\
&\times \quad \underbrace{\int_0^{1/T} d\tau_6 e^{-i(-\gamma_{\ell_1'}+\beta_{\ell_2})\tau_6}}_{=\frac{1}{T}\delta_{\gamma_{\ell_1'},\beta_{\ell_2}}} \int_0^{1/T} d\tau_7 e^{-i(\alpha_{n_2}+\gamma_{\ell_2'}-\alpha_{n_3}-\beta_{\ell_3})\tau_7} \underbrace{\int_0^{1/T} d\tau_8 e^{-(-\gamma_{\ell_2'}+\beta_{\ell_3})\tau_8}}_{=\frac{1}{T}\delta_{\gamma_{\ell_2'},\beta_{\ell_3}}} \\
&\times \quad \widetilde{\mathscr{D}}_{k_1k_2,k_5k_6}(\alpha_{n_1},\varepsilon_\ell,\gamma_{\ell_1'}) \mathscr{U}^e_{k_5k_6,k_7k_8}(\alpha_{n_2},\beta_{\ell_2},\gamma_{\ell_2'}) \widetilde{\mathscr{R}}^e_{k_7k_8,k_3k_4}(\alpha_{n_3},\beta_{\ell_3},\varepsilon_{\ell'}) \\
&= \quad \frac{T^5}{2}\sum_{k_5k_6k_7k_8}\int_{-1/T}^{1/T} d\tau_{31} e^{i\omega_n\tau_{31}} e^{i(\alpha_{n_1}\tau_1-\alpha_{n_3}\tau_3)} \sum_{n_1,n_3}\sum_{n_2,\ell_2,\ell_3} \underbrace{\int_0^{1/T} d\tau_5 e^{-i(\alpha_{n_1}-\alpha_{n_2})\tau_5}}_{=\frac{1}{T}\delta_{n_1,n_2}} \\
&\times \quad \underbrace{\int_0^{1/T} d\tau_7 e^{-i(\alpha_{n_2}-\alpha_{n_3})\tau_7}}_{=\frac{1}{T}\delta_{n_2,n_3}} \widetilde{\mathscr{D}}_{k_1k_2,k_5k_6}(\alpha_{n_1},\varepsilon_\ell,\beta_{\ell_2}) \mathscr{U}^e_{k_5k_6,k_7k_8}(\alpha_{n_2},\beta_{\ell_2},\beta_{\ell_3}) \\
&\times \quad \widetilde{\mathscr{R}}^e_{k_7k_8,k_3k_4}(\alpha_{n_3},\beta_{\ell_3},\varepsilon_{\ell'})
\end{aligned}
$$

$$
\begin{aligned}
&= \frac{T^3}{2}\sum_{k_5k_6k_7k_8}\int_{-1/T}^{1/T} d\tau_{31} e^{i\omega_n\tau_{31}} e^{i\alpha_{n_2}(\tau_1-\tau_3)} \sum_{n_2,\ell_2,\ell_3} \widetilde{\mathscr{D}}_{k_1k_2,k_5k_6}(\alpha_{n_2},\varepsilon_\ell,\beta_{\ell_2}) \\
&\times \mathscr{U}^e_{k_5k_6,k_7k_8}(\alpha_{n_2},\beta_{\ell_2},\beta_{\ell_3})\widetilde{\mathscr{R}}^e_{k_7k_8,k_3k_4}(\alpha_{n_3},\beta_{\ell_3},\varepsilon_{\ell'}) \\
I_2 &= T^2\sum_{k_5k_6k_7k_8}\sum_{\ell_2,\ell_3} \widetilde{\mathscr{D}}_{k_1k_2,k_5k_6}(\omega_n,\varepsilon_\ell,\beta_{\ell_2})\mathscr{U}^e_{k_5k_6,k_7k_8}(\omega_n,\beta_{\ell_2},\beta_{\ell_3})\widetilde{\mathscr{R}}^e_{k_7k_8,k_3k_4}(\omega_n,\beta_{\ell_3},\varepsilon_{\ell'}).
\end{aligned}
\tag{3.90}
$$

The similar calculation procedures can be applied to the integrals I_3 and I_4 to give

$$
\begin{aligned}
I_3 &= T\sum_{k_5k_6k_7k_8}\sum_{\ell_3} \sigma_{k_1}\delta_{\sigma_{k_1},-\sigma_{k_2}}\delta_{k_1k_5}\delta_{k_2k_6}\delta_{k_6k_8}(i\omega_n-\varepsilon_{k_1}+\varepsilon_{k_2})\widetilde{\mathscr{G}}_{k_1}(\varepsilon_\ell+\omega_n)\widetilde{\mathscr{G}}_{k_2}(\varepsilon_\ell) \\
&\times \widetilde{\mathscr{G}}_{k_5}(\varepsilon_{\ell_3}+\omega_n)\Sigma^e_{k_7k_5}(\omega_n+\varepsilon_{\ell_3})\widetilde{\mathscr{R}}^e_{k_7k_8,k_3k_4}(\omega_n,\varepsilon_{\ell_3},\varepsilon_{\ell'})
\end{aligned}
\tag{3.91}
$$

and

$$
\begin{aligned}
I_4 &= T\sum_{k_5k_6k_7k_8}\sum_{n_3} \sigma_{k_1}\delta_{\sigma_{k_1},-\sigma_{k_2}}\delta_{k_7k_5}\delta_{k_1k_5}\delta_{k_2k_6}(i\omega_n-\varepsilon_{k_1}+\varepsilon_{k_2})\widetilde{\mathscr{G}}_{k_1}(\varepsilon_\ell+\omega_n)\widetilde{\mathscr{G}}_{k_2}(\varepsilon_\ell) \\
&\times \widetilde{\mathscr{G}}_{k_6}(\omega_{n_3})\Sigma^e_{k_6k_8}(\omega_{n_3})\widetilde{\mathscr{R}}^e_{k_7k_8,k_3k_4}(\omega_n,\omega_{n_3},\varepsilon_{\ell'}).
\end{aligned}
\tag{3.92}
$$

Combining $\widetilde{\mathscr{R}}^0$ with the integrals I_2, I_3, and I_4 yields the correlated propagator $\widetilde{\mathscr{R}}^e$ in the spectral representation. After obtaining the analytical form of $\widetilde{\mathscr{R}}^e_{k_1k_2,k_3k_4}(\omega_n,\varepsilon_\ell,\varepsilon_{\ell'})$, we perform the summation over the Matsubara frequencies ω_ℓ and $\omega_{\ell'}$ according to Eq. (3.83) to obtain the BSE for one-variable correlated propagator $\widetilde{\mathscr{R}}^e_{k_1k_2,k_3k_4}(\omega_n)$ of the form

$$
\begin{aligned}
\widetilde{\mathscr{R}}^e_{k_1k_2,k_3k_4}(\omega_n) &= \widetilde{\mathscr{R}}^0_{k_1k_2,k_3k_4}(\omega_n) - \sum_{k_5k_6k_7k_8}\widetilde{\mathscr{R}}^0_{k_1k_2,k_5k_6}(\omega_n)\Big[\widetilde{\Phi}^{(1)}_{k_5k_6,k_7k_8}(\omega_n)+\widetilde{\Phi}^{(2)}_{k_5k_6,k_7k_8}(\omega_n) \\
&+ \widetilde{\Phi}^{(3)}_{k_5k_6,k_7k_8}(\omega_n)\Big]\widetilde{\mathscr{R}}^e_{k_7k_8,k_3k_4}(\omega_n).
\end{aligned}
\tag{3.93}
$$

The first term $\widetilde{\mathscr{R}}^0_{k_1k_2,k_3k_4}(\omega_n)$ of Eq. (3.93) is the uncorrelated propagator, which is given by

$$
\begin{aligned}
\widetilde{\mathscr{R}}^0_{k_1k_2,k_3k_4}(\omega_n) &= T^2\sum_\ell\sum_{\ell'}\widetilde{\mathscr{R}}^0_{k_1k_2,k_3k_4}(\omega_n,\varepsilon_\ell,\varepsilon_{\ell'}) \\
&= -\frac{1}{T}\delta_{k_1k_3}\delta_{k_2k_4}T^2\sum_\ell\sum_{\ell'}\delta_{\ell'\ell}\widetilde{\mathscr{G}}_{k_1}(\omega_n+\varepsilon_\ell)\widetilde{\mathscr{G}}_{k_2}(\varepsilon_\ell) \\
&= -\delta_{k_1k_3}\delta_{k_2k_4}T\sum_\ell\widetilde{\mathscr{G}}_{k_1}(\omega_n+\varepsilon_\ell)\widetilde{\mathscr{G}}_{k_2}(\varepsilon_\ell) \\
\widetilde{\mathscr{R}}^0_{k_1k_2,k_3k_4}(\omega_n) &= -\delta_{k_1k_3}\delta_{k_2k_4}T\sum_\ell\frac{1}{i(\omega_n+\varepsilon_\ell)-\varepsilon_{k_1}+\mu}\,\frac{1}{i\varepsilon_\ell-\varepsilon_{k_2}+\mu}.
\end{aligned}
\tag{3.94}
$$

The transformation of the summation over ℓ into a contour integral leads to

$$\widetilde{\mathscr{R}}^{0}_{k_1k_2,k_3k_4}(\omega_n) \;=\; -\delta_{k_1k_3}\delta_{k_2k_4}\frac{n(\varepsilon_{k_2},T)-n(\varepsilon_{k_1},T)}{i\omega_n-\varepsilon_{k_1}+\varepsilon_{k_2}}. \tag{3.95}$$

Before deriving the analytical form of the amplitude $\widetilde{\Phi}(\omega_n)$, it is convenient to express $\widetilde{\mathscr{R}}^{e}(12,34)$ as

$$\widetilde{\mathscr{R}}^{e}(12,34)=\sum_{56}^{\tau}\widetilde{\mathscr{D}}(12,56)T^{e}(56,34). \tag{3.96}$$

Its Fourier transform is given by

$$\begin{aligned}
\widetilde{\mathscr{R}}^{e}_{k_1k_2,k_3k_4}(\omega_n,\varepsilon_\ell,\varepsilon_{\ell'}) &= \frac{1}{8}\sum_{56}^{\tau}\int_{-1/T}^{1/T}d\tau_{31}e^{i\omega_n\tau_{31}}\int_{-1/T}^{1/T}d\tau_{21}e^{i\varepsilon_\ell\tau_{21}}\int_{-1/T}^{1/T}d\tau_{34}e^{i\varepsilon_{\ell'}\tau_{34}}\\
&\times\; \widetilde{\mathscr{D}}_{k_1k_2,k_5k_6}(\tau_{51},\tau_{21},\tau_{56})T^{e}_{k_5k_6,k_3k_4}(\tau_{35},\tau_{65},\tau_{34})\\
&= \sum_{k_5k_6}\delta_{\sigma_{k_1},-\sigma_{k_2}}\delta_{k_1k_5}\delta_{k_2k_6}\sigma_{k_1}(i\omega_n-\varepsilon_{k_1}+\varepsilon_{k_2})\\
&\times\; T\sum_{\ell_2}\widetilde{\mathscr{G}}_{k_1}(\omega_n+\varepsilon_\ell)\widetilde{\mathscr{G}}_{k_2}(\varepsilon_\ell)\widetilde{\mathscr{G}}_{k_5}(\omega_n+\varepsilon_{\ell_2})\widetilde{\mathscr{G}}_{k_6}(\varepsilon_{\ell_2})\\
&\times\; T^{e}_{k_5k_6,k_3k_4}(\omega_n,\varepsilon_{\ell_2},\varepsilon_{\ell'}).
\end{aligned} \tag{3.97}$$

Accordingly, $\widetilde{\mathscr{R}}^{e}_{k_1k_2,k_3k_4}(\omega_n)$ can be expressed as

$$\begin{aligned}
\widetilde{\mathscr{R}}^{e}_{k_1k_2,k_3k_4}(\omega_n) &= T^2\sum_{\varepsilon_\ell}\sum_{\varepsilon_{\ell'}}\widetilde{\mathscr{R}}^{e}_{k_1k_2,k_3k_4}(\omega_n,\varepsilon_\ell,\varepsilon_{\ell'})\\
&= \sum_{k_5k_6}\delta_{\sigma_{k_1},-\sigma_{k_2}}\delta_{k_1k_5}\delta_{k_2k_6}\sigma_1(i\omega_n-\varepsilon_{k_1}+\varepsilon_{k_2})T\sum_{\varepsilon_\ell}\widetilde{\mathscr{G}}_{k_1}(\omega_n+\varepsilon_\ell)\\
&\times\; \widetilde{\mathscr{G}}_{k_2}(\varepsilon_\ell)T^2\sum_{\ell_2}\sum_{\varepsilon_{\ell'}}\widetilde{\mathscr{G}}_{k_5}(\omega_n+\varepsilon_{\ell_2})\widetilde{\mathscr{G}}_{k_6}(\varepsilon_{\ell_2})T^{e}_{k_5k_6,k_3k_4}(\omega_n,\varepsilon_{\ell_2},\varepsilon_{\ell'})\\
&= \sum_{k_5k_6}\delta_{-\sigma_{k_1},\sigma_{k_2}}\delta_{k_1k_5}\delta_{k_2k_6}\sigma_{k_1}(i\omega_n-\varepsilon_{k_1}+\varepsilon_{k_2})\frac{n(\varepsilon_{k_2},T)-n(\varepsilon_{k_1},T)}{i\omega_n-\varepsilon_{k_1}+\varepsilon_{k_2}}\\
&\times\; T^2\sum_{\ell_2}\sum_{\varepsilon_{\ell'}}\widetilde{\mathscr{G}}_{k_5}(\omega_n+\varepsilon_{\ell_2})\widetilde{\mathscr{G}}_{k_6}(\varepsilon_{\ell_2})T^{e}_{k_5k_6,k_3k_4}(\omega_n,\varepsilon_{\ell_2},\varepsilon_{\ell'})\\
\widetilde{\mathscr{R}}^{e}_{k_1k_2,k_3k_4}(\omega_n) &= \delta_{\sigma_{k_1},-\sigma_{k_2}}\sigma_{k_1}[n(\varepsilon_{k_2},T)-n(\varepsilon_{k_1},T)]\\
&\times\; T^2\sum_{\varepsilon_\ell}\sum_{\varepsilon_{\ell'}}\widetilde{\mathscr{G}}_{k_1}(\omega_n+\varepsilon_\ell)\widetilde{\mathscr{G}}_{k_2}(\varepsilon_\ell)T^{e}_{k_5k_6,k_3k_4}(\omega_n,\varepsilon_\ell,\varepsilon_{\ell'}).
\end{aligned} \tag{3.98}$$

Inserting Eq. (3.97) into Eq. (3.90), one obtains

$$
\begin{aligned}
I_2 &= \sum_{k_5k_6k_7k_8} T^2 \sum_{\ell_2,\ell_3} \delta_{\sigma_{k_1},-\sigma_{k_2}} \delta_{k_1k_5}\delta_{k_2k_6}\sigma_{k_1}(i\omega_n - \varepsilon_{k_1} + \varepsilon_{k_2}) \widetilde{\mathscr{G}}_{k_1}(\omega_n + \varepsilon_\ell) \\
&\times \widetilde{\mathscr{G}}_{k_2}(\varepsilon_\ell) \widetilde{\mathscr{G}}_{k_5}(\omega_n + \beta_{\ell_2}) \widetilde{\mathscr{G}}_{k_6}(\beta_{\ell_2}) \mathscr{U}^e_{k_5k_6,k_7k_8}(\omega_n, \beta_{\ell_2}, \beta_{\ell_3}) \widetilde{\mathscr{R}}^e_{k_7k_8,k_3k_4}(\omega_n, \beta_{\ell_3}, \varepsilon_{\ell'}) \\
&= \sum_{k_5k_6k_7k_8} T^2 \sum_{\ell_2,\ell_3} \delta_{\sigma_{k_1},-\sigma_{k_2}} \delta_{k_1k_5}\delta_{k_2k_6}\sigma_{k_1}(i\omega_n - \varepsilon_{k_1} + \varepsilon_{k_2}) \widetilde{\mathscr{G}}_{k_1}(\omega_n + \varepsilon_\ell) \widetilde{\mathscr{G}}_{k_2}(\varepsilon_\ell) \\
&\times \widetilde{\mathscr{G}}_{k_5}(\omega_n + \beta_{\ell_2}) \widetilde{\mathscr{G}}_{k_6}(\beta_{\ell_2}) \mathscr{U}^e_{k_5k_6,k_7k_8}(\omega_n, \beta_{\ell_2}, \beta_{\ell_3}) \\
&\times \sum_{k_9k_{10}} \delta_{\sigma_{k_7},-\sigma_{k_8}} \delta_{k_7k_9}\delta_{k_8k_{10}}\sigma_{k_7}(i\omega_n - \varepsilon_{k_7} + \varepsilon_{k_8}) \\
&\times T \sum_{\ell_4} \widetilde{\mathscr{G}}_{k_7}(\omega_n + \beta_{\ell_3}) \widetilde{\mathscr{G}}_{k_8}(\beta_{\ell_3}) \widetilde{\mathscr{G}}_{k_9}(\omega_n + \beta_{\ell_4}) \widetilde{\mathscr{G}}_{k_{10}}(\beta_{\ell_4}) T^e_{k_9k_{10},k_3k_4}(\omega_n, \beta_{\ell_4}, \varepsilon_{\ell'}) \\
I_2 &= \sum_{k_5k_6k_7k_8} \delta_{\sigma_{k_1},-\sigma_{k_2}} \delta_{k_1k_5}\delta_{k_2k_6} \widetilde{\mathscr{G}}_{k_1}(\omega_n + \varepsilon_\ell) \widetilde{\mathscr{G}}_{k_2}(\varepsilon_\ell) \sigma_{k_5}(i\omega_n - \varepsilon_{k_5} + \varepsilon_{k_6}) \\
&\times T^2 \sum_{\ell_2,\ell_3} \widetilde{\mathscr{G}}_{k_5}(\omega_n + \beta_{\ell_2}) \widetilde{\mathscr{G}}_{k_6}(\beta_{\ell_2}) \mathscr{U}^e_{k_5k_6,k_7k_8}(\omega_n, \beta_{\ell_2}, \beta_{\ell_3}) \widetilde{\mathscr{G}}_{k_7}(\omega_n + \beta_{\ell_3}) \widetilde{\mathscr{G}}_{k_8}(\beta_{\ell_3}) \\
&\times \sigma_{k_7}(i\omega_n - \varepsilon_{k_7} + \varepsilon_{k_8}) \delta_{\sigma_{k_7},-\sigma_{k_8}} T \sum_{\ell_4} \widetilde{\mathscr{G}}_{k_7}(\omega_n + \beta_{\ell_4}) \widetilde{\mathscr{G}}_{k_8}(\beta_{\ell_4}) \\
&\times T^e_{k_7k_8,k_3k_4}(\omega_n, \beta_{\ell_4}, \varepsilon_{\ell'}). \qquad (3.99)
\end{aligned}
$$

Performing the summation over Matsubara frequencies ε_ℓ and $\varepsilon_{\ell'}$ for integral I_2 yields

$$
\begin{aligned}
T^2 \sum_{\varepsilon_\ell} \sum_{\varepsilon_{\ell'}} I_2 &= \sum_{k_5k_6k_7k_8} \delta_{k_1k_5}\delta_{k_2k_6} T \sum_{\varepsilon_\ell} \widetilde{\mathscr{G}}_{k_1}(\omega_n + \varepsilon_\ell) \widetilde{\mathscr{G}}_{k_2}(\varepsilon_\ell) \\
&\times \Bigg\{ - \delta_{\sigma_{k_5},-\sigma_{k_6}} \sigma_{k_5}(i\omega_n - \varepsilon_{k_5} + \varepsilon_{k_6}) \Bigg[- T^2 \sum_{\ell_2,\ell_3} \widetilde{\mathscr{G}}_{k_5}(\omega_n + \beta_{\ell_2}) \widetilde{\mathscr{G}}_{k_6}(\beta_{\ell_2}) \\
&\times \mathscr{U}^e_{k_5k_6,k_7k_8}(\omega_n, \beta_{\ell_2}, \beta_{\ell_3}) \widetilde{\mathscr{G}}_{k_7}(\omega_n + \beta_{\ell_3}) \widetilde{\mathscr{G}}_{k_8}(\beta_{\ell_3}) \Bigg] \sigma_{k_7}(i\omega_n - \varepsilon_{k_7} + \varepsilon_{k_8}) \Bigg\} \\
&\times \delta_{\sigma_{k_7},-\sigma_{k_8}} T^2 \sum_{\ell_4} \sum_{\varepsilon_{\ell'}} \widetilde{\mathscr{G}}_{k_7}(\omega_n + \beta_{\ell_4}) \widetilde{\mathscr{G}}_{k_8}(\beta_{\ell_4}) T^e_{k_7k_8,k_3k_4}(\omega_n, \beta_{\ell_4}, \varepsilon_{\ell'}) \\
&= - \sum_{k_5k_6k_7k_8} \left[-\delta_{k_1k_5}\delta_{k_2k_6} \frac{n(\varepsilon_{k_2}, T) - n(\varepsilon_{k_1}, T)}{i\omega_n - \varepsilon_{k_1} + \varepsilon_{k_2}} \right] \\
&\times \Bigg\{ - \delta_{\sigma_{k_5},-\sigma_{k_6}} \sigma_{k_5}(i\omega_n - \varepsilon_{k_5} + \varepsilon_{k_6}) \Bigg[- T^2 \sum_{\ell_2,\ell_3} \widetilde{\mathscr{G}}_{k_5}(\omega_n + \beta_{\ell_2}) \widetilde{\mathscr{G}}_{k_6}(\beta_{\ell_2}) \\
&\times \mathscr{U}^e_{k_5k_6,k_7k_8}(\omega_n, \beta_{\ell_2}, \beta_{\ell_3}) \widetilde{\mathscr{G}}_{k_7}(\omega_n + \beta_{\ell_3}) \widetilde{\mathscr{G}}_{k_8}(\beta_{\ell_3}) \Bigg] \sigma_{k_7}(i\omega_n - \varepsilon_{k_7} + \varepsilon_{k_8}) \Bigg\}
\end{aligned}
$$

$$
\begin{aligned}
&\times \quad \left[\delta_{\sigma_{k_7},-\sigma_{k_8}} T^2 \sum_{\ell_4} \sum_{\varepsilon_{\ell'}} \widetilde{\mathscr{G}}_{k_7}(\omega_n+\beta_{\ell_4}) \widetilde{\mathscr{G}}_{k_8}(\beta_{\ell_4}) T^e_{k_7k_8,k_3k_4}(\omega_n,\beta_{\ell_4},\varepsilon_{\ell'}) \right] \\
&= \quad -\sum_{k_5k_6k_7k_8} \left[-\delta_{k_1k_5}\delta_{k_2k_6} \frac{n(\varepsilon_{k_2},T)-n(\varepsilon_{k_1},T)}{i\omega_n-\varepsilon_{k_1}+\varepsilon_{k_2}} \right] \\
&\times \quad \left\{ -\delta_{\sigma_{k_5},-\sigma_{k_6}} \sigma_{k_5} (i\omega_n-\varepsilon_{k_5}+\varepsilon_{k_6} \left[-T^2 \sum_{\ell_2,\ell_3} \widetilde{\mathscr{G}}_{k_5}(\omega_n+\beta_{\ell_2}) \widetilde{\mathscr{G}}_{k_6}(\beta_{\ell_2}) \right.\right. \\
&\times \quad \left.\left. \mathscr{U}^e_{k_5k_6,k_7k_8}(\omega_n,\beta_{\ell_2},\beta_{\ell_3}) \widetilde{\mathscr{G}}_{k_7}(\omega_n+\beta_{\ell_3}) \widetilde{\mathscr{G}}_{k_8}(\beta_{\ell_3}) \right] \frac{\sigma_{k_7}(i\omega_n-\varepsilon_{k_7}+\varepsilon_{k_8})}{\sigma_{k_7}[n(\varepsilon_{k_8},T)-n(\varepsilon_{k_7},T)]} \right\} \\
&\times \quad \left[\delta_{\sigma_{k_7},-\sigma_{k_8}} \sigma_{k_7}[n(\varepsilon_{k_8},T)-n(\varepsilon_{k_7},T)] T^2 \sum_{\ell_4} \sum_{\varepsilon_{\ell'}} \widetilde{\mathscr{G}}_{k_7}(\omega_n+\beta_{\ell_4}) \widetilde{\mathscr{G}}_{k_8}(\beta_{\ell_4}) \right. \\
&\times \quad \left. T^e_{k_7k_8,k_3k_4}(\omega_n,\beta_{\ell_4},\varepsilon_{\ell'}) \right] \\
T^2 \sum_{\varepsilon_\ell} \sum_{\varepsilon_{\ell'}} I_2 &= -\sum_{k_5k_6k_7k_8} \widetilde{\mathscr{R}}^0_{k_1k_2,k_5k_6}(\omega_n) \Phi^{(1)}_{k_5k_6,k_7k_8}(\omega_n) \widetilde{\mathscr{R}}^e_{k_7k_8,k_3k_4}(\omega_n), \qquad (3.100)
\end{aligned}
$$

where we have used Eqs. (3.95) and (3.98), and defined the first term of the particle-phonon coupling amplitude $\widetilde{\Phi}_{k_1k_2,k_3k_4}(\omega_n)$ as

$$
\widetilde{\Phi}^{(1)}_{k_1k_2,k_3k_4}(\omega_n) = -\delta_{\sigma_{k_1},-\sigma_{k_2}} \sigma_{k_1} (i\omega_n-\varepsilon_{k_1}+\varepsilon_{k_2}) A^{[1](1)}_{k_1k_2,k_3k_4}(\omega_n) \sigma_{k_3} (i\omega_n-\varepsilon_{k_3}+\varepsilon_{k_4}), \qquad (3.101)
$$

where

$$
\begin{aligned}
A^{[1](1)}_{k_1k_2,k_3k_4}(\omega_n) &= -\frac{T^2}{\sigma_{k_3}[n(\varepsilon_{k_4},T)-n(\varepsilon_{k_3},T)]} \sum_{\ell_2,\ell_3} \widetilde{\mathscr{G}}_{k_1}(\omega_n+\beta_{\ell_2}) \widetilde{\mathscr{G}}_{k_2}(\beta_{\ell_2}) \\
&\times \quad \mathscr{U}^e_{k_1k_2,k_3k_4}(\omega_n,\beta_{\ell_2},\beta_{\ell_3}) \widetilde{\mathscr{G}}_{k_3}(\omega_n+\beta_{\ell_3}) \widetilde{\mathscr{G}}_{k_4}(\beta_{\ell_3}). \qquad (3.102)
\end{aligned}
$$

Inserting Eq. (3.97) into Eqs. (3.91) and (3.92), we obtain

$$
\begin{aligned}
I_3 &= \sum_{k_5k_6k_7k_8} \delta_{\sigma_{k_1},-\sigma_{k_2}} \delta_{k_1k_5}\delta_{k_2k_6} \widetilde{\mathscr{G}}_{k_1}(\omega_n+\varepsilon_\ell) \widetilde{\mathscr{G}}_{k_2}(\varepsilon_\ell) \left\{ -\sigma_{k_5}(i\omega_n-\varepsilon_{k_5}+\varepsilon_{k_6}) \right. \\
&\times \quad \left[-T \sum_{\ell_3} \widetilde{\mathscr{G}}_{k_5}(\omega_n+\varepsilon_{\ell_3}) \Sigma^e_{k_7k_5}(\omega_n+\varepsilon_{\ell_3}) \delta_{k_6k_8} \widetilde{\mathscr{G}}_{k_7}(\omega_n+\varepsilon_{\ell_3}) \widetilde{\mathscr{G}}_{k_8}(\varepsilon_{\ell_3}) \right] \\
&\times \quad \left. \sigma_{k_7}(i\omega_n-\varepsilon_{k_7}+\varepsilon_{k_8}) \right\} \delta_{\sigma_{k_7},-\sigma_{k_8}} T \sum_{\ell_4} \widetilde{\mathscr{G}}_{k_7}(\omega_n+\varepsilon_{\ell_4}) \widetilde{\mathscr{G}}_{k_8}(\varepsilon_{\ell_4}) \\
&\times \quad T^e_{k_7k_8,k_3k_4}(\omega_n,\varepsilon_{\ell_4},\varepsilon_{\ell'}) \qquad (3.103)
\end{aligned}
$$

and

$$
\begin{aligned}
I_4 &= \sum_{k_5k_6k_7k_8} \delta_{k_1k_5}\delta_{k_2k_6}\widetilde{\mathscr{G}}_{k_1}(\omega_n+\varepsilon_\ell)\widetilde{\mathscr{G}}_{k_2}(\varepsilon_\ell)\Big\{ -\delta_{\sigma_{k_5},-\sigma_{k_6}}\sigma_{k_5}(i\omega_n-\varepsilon_{k_5}+\varepsilon_{k_6}) \\
&\times \Big[-T\sum_{n_3}\widetilde{\mathscr{G}}_{k_6}(\omega_{n_3})\Sigma^e_{k_6k_8}(\omega_{n_3})\delta_{k_7k_5}\widetilde{\mathscr{G}}_{k_7}(\omega_n+\omega_{n_3})\widetilde{\mathscr{G}}_{k_8}(\omega_{n_3})\Big] \\
&\times \sigma_{k_7}(i\omega_n-\varepsilon_{k_7}+\varepsilon_{k_8})\Big\}\delta_{\sigma_{k_7},-\sigma_{k_8}} T\sum_{\ell_4}\widetilde{\mathscr{G}}_{k_7}(\omega_n+\varepsilon_{\ell_4})\widetilde{\mathscr{G}}_{k_8}(\varepsilon_{\ell_4}) \\
&\times T^e_{k_7k_8,k_3k_4}(\omega_n,\varepsilon_{\ell_4},\varepsilon_{\ell'}). \qquad (3.104)
\end{aligned}
$$

After performing the summation over Matsubara frequencies ε_ℓ and $\varepsilon_{\ell'}$ for integrals I_3 and I_4, one obtains

$$
T^2\sum_{\varepsilon_\ell}\sum_{\varepsilon_{\ell'}} I_3 = -\sum_{k_5k_6k_7k_8}\widetilde{\mathscr{R}}^0_{k_1k_2,k_5k_6}(\omega_n)\widetilde{\Phi}^{(2)}_{k_5k_6,k_7k_8}(\omega_n)\widetilde{\mathscr{R}}^e_{k_7k_8,k_3k_4}(\omega_n) \qquad (3.105)
$$

and

$$
T^2\sum_{\varepsilon_\ell}\sum_{\varepsilon_{\ell'}} I_4 = -\sum_{k_5k_6k_7k_8}\widetilde{\mathscr{R}}^0_{k_1k_2,k_5k_6}(\omega_n)\widetilde{\Phi}^{(3)}_{k_5k_6,k_7k_8}(\omega_n)\widetilde{\mathscr{R}}^e_{k_7k_8,k_3k_4}(\omega_n), \qquad (3.106)
$$

where the second and third terms of the particle-phonon coupling amplitude $\widetilde{\Phi}_{k_1k_2,k_3k_4}(\omega_n)$ are given as

$$
\widetilde{\Phi}^{(2)}_{k_1k_2,k_3k_4}(\omega_n) = -\delta_{\sigma_{k_1},-\sigma_{k_2}}\sigma_{k_1}(i\omega_n-\varepsilon_{k_1}+\varepsilon_{k_2})A^{[1](2)}_{k_1k_2,k_3k_4}(\omega_n)\sigma_{k_3}(i\omega_n-\varepsilon_{k_3}+\varepsilon_{k_4}) \qquad (3.107)
$$

and

$$
\widetilde{\Phi}^{(3)}_{k_1k_2,k_3k_4}(\omega_n) = -\delta_{\sigma_{k_1},-\sigma_{k_2}}\sigma_{k_1}(i\omega_n-\varepsilon_{k_1}+\varepsilon_{k_2})A^{[1](3)}_{k_1k_2,k_3k_4}(\omega_n)\sigma_{k_3}(i\omega_n-\varepsilon_{k_3}+\varepsilon_{k_4}). \qquad (3.108)
$$

Here we also have defined

$$
\begin{aligned}
A^{[1](2)}_{k_1k_2,k_3k_4}(\omega_n) &= -\frac{T}{\sigma_{k_3}[n(\varepsilon_{k_4},T)-n(\varepsilon_{k_3},T)]}\sum_{\ell_3}\widetilde{\mathscr{G}}_{k_1}(\omega_n+\varepsilon_{\ell_3})\Sigma^e_{k_3k_1}(\omega_n+\varepsilon_{\ell_3}) \\
&\times \delta_{k_2k_4}\widetilde{\mathscr{G}}_{k_3}(\omega_n+\varepsilon_{\ell_3})\widetilde{\mathscr{G}}_{k_4}(\varepsilon_{\ell_3}) \qquad (3.109)
\end{aligned}
$$

and

$$A^{[1](3)}_{k_1k_2,k_3k_4}(\omega_n) = -\frac{T}{\sigma_{k_3}[n(\varepsilon_{k_4},T)-n(\varepsilon_{k_3},T)]}\sum_{n_3}\widetilde{\mathscr{G}}_{k_2}(\omega_{n_3})\Sigma^e_{k_2k_4}(\omega_{n_3}) \times \delta_{k_3k_1}\widetilde{\mathscr{G}}_{k_3}(\omega_n+\omega_{n_3})\widetilde{\mathscr{G}}_{k_4}(\omega_{n_3}). \quad (3.110)$$

After performing the Matsubara summations in each term of $A^{[1]}_{k_1k_2,k_3k_4}(\omega_n)$, one obtains the analytical form of the particle-phonon coupling amplitude $\widetilde{\Phi}_{k_1k_2,k_3k_4}(\omega_n)$:

$$\widetilde{\Phi}_{k_1k_2,k_3k_4}(\omega_n) = \widetilde{\Phi}^{(1)}_{k_1k_2,k_3k_4}(\omega_n) + \widetilde{\Phi}^{(2)}_{k_1k_2,k_3k_4}(\omega_n) + \widetilde{\Phi}^{(3)}_{k_1k_2,k_3k_4}(\omega_n), \quad (3.111)$$

where

$$\begin{aligned}
\widetilde{\Phi}^{(1)}_{k_1k_2,k_3k_4}(\omega_n) &= \frac{\delta_{\sigma_{k_1},-\sigma_{k_2}}\sigma_{k_1}}{n(\varepsilon_{k_4},T)-n(\varepsilon_{k_3},T)}\Bigg\{\sum_m g^m_{k_4k_2}g^{m*}_{k_3k_1}\left[N(\omega_m,T)+n(\varepsilon_{k_4},T)\right] \\
&\times \frac{n(\varepsilon_{k_1},T)-n(\varepsilon_{k_4}-\omega_m,T)}{i\omega_n-\omega_m-\varepsilon_{k_1k_4}}+\sum_m g^m_{k_4k_2}g^{m*}_{k_3k_1}\left[N(\omega_m,T)+n(\varepsilon_{k_3},T)\right] \\
&\times \frac{n(\varepsilon_{k_3}-\omega_m,T)-n(\varepsilon_2,T)}{i\omega_n+\omega_m-\varepsilon_{k_3k_2}}+\sum_m g^m_{k_1k_3}g^{m*}_{k_2k_4}\left[N(\omega_m,T)+1-n(\varepsilon_{k_3},T)\right] \\
&\times \frac{n(\omega_m+\varepsilon_{k_3},T)-n(\varepsilon_{k_2},T)}{i\omega_n-\omega_m-\varepsilon_{k_3k_2}}+\sum_m g^m_{k_1k_3}g^{m*}_{k_2k_4}\left[N(\omega_m,T)+1-n(\varepsilon_4,T)\right] \\
&\times \frac{n(\varepsilon_{k_1},T)-n(\omega_m+\varepsilon_{k_4},T)}{i\omega_n+\omega_m-\varepsilon_{k_1k_4}}\Bigg\}, \quad (3.112)\\
\widetilde{\Phi}^{(2)}_{k_1k_2,k_3k_4}(\omega_n) &= \frac{\delta_{\sigma_{k_1},-\sigma_{k_2}}\sigma_{k_1}\delta_{k_2k_4}}{n(\varepsilon_{k_4},T)-n(\varepsilon_{k_3},T)}\Bigg\{\sum_{k_5,m} g^{m*}_{k_3k_5}g^m_{k_1k_5}[N(\omega_m,T)+1-n(\varepsilon_{k_5},T)] \\
&\times \frac{n(\varepsilon_{k_4},T)-n(\varepsilon_{k_5}+\omega_m,T)}{i\omega_n-\omega_m+\varepsilon_{k_4k_5}}+\sum_{k_5,m} g^m_{k_5k_3}g^{m*}_{k_5k_1}[N(\omega_m,T)+n(\varepsilon_{k_5},T)] \\
&\times \frac{n(\varepsilon_{k_4},T)-n(\varepsilon_{k_5}-\omega_m,T)}{i\omega_n+\omega_m+\varepsilon_{k_4k_5}}\Bigg\}, \quad (3.113)\\
\widetilde{\Phi}^{(3)}_{k_1k_2,k_3k_4}(\omega_n) &= \frac{\delta_{\sigma_{k_1},-\sigma_{k_2}}\sigma_{k_1}\delta_{k_3k_1}}{n(\varepsilon_{k_4},T)-n(\varepsilon_{k_3},T)}\sum_{k_6,m}\Bigg\{g^{m*}_{k_2k_6}g^m_{k_4k_6}[N(\omega_m,T)+1-n(\varepsilon_{k_6},T)] \\
&\times \frac{n(\omega_m+\varepsilon_{k_6},T)-n(\varepsilon_{k_3},T)}{i\omega_n+\omega_m-\varepsilon_{k_3k_6}}+g^m_{k_6k_2}g^{m*}_{k_6k_4}[N(\omega_m,T)+n(\varepsilon_{k_6},T)] \\
&\times \frac{n(\varepsilon_{k_6}-\omega_m,T)-n(\varepsilon_{k_3},T)}{i\omega_n-\omega_m-\varepsilon_{k_3k_6}}\Bigg\}, \quad (3.114)
\end{aligned}$$

and the energy differences $\varepsilon_{k_ik_j} \equiv \varepsilon_{k_i} - \varepsilon_{k_j}$. Introducing the phonon vertex matrices

$$\xi^{m\eta_m}_{k_1k_2,k_3k_4} = \delta_{k_1k_3} g^{m(\eta_m)}_{k_4k_2} - g^{m(\eta_m)}_{k_1k_3} \delta_{k_4k_2}, \tag{3.115}$$

the particle-phonon coupling amplitude $\widetilde{\Phi}_{k_1k_2,k_3k_4}(\omega_n)$ can be expressed concisely as

$$\begin{aligned} \widetilde{\Phi}_{k_1k_2,k_3k_4}(\omega_n) &= \frac{\delta_{\sigma_{k_1},-\sigma_{k_2}}\sigma_{k_1}}{n(\varepsilon_{k_4},T) - n(\varepsilon_{k_3},T)} \sum_{k_5,k_6,m} \sum_{\eta_m=\pm 1} \eta_m \xi^{m\eta_m}_{k_1k_2,k_5k_6} \xi^{m\eta_m *}_{k_3k_4,k_5k_6} \\ &\times \frac{[N(\eta_m\omega_m,T) + n(\varepsilon_{k_6},T)][n(\varepsilon_{k_6} - \eta_m\omega_m,T) - n(\varepsilon_{k_5},T)]}{i\omega_n - \varepsilon_{k_5} + \varepsilon_{k_6} - \eta_m\omega_m}. \end{aligned} \tag{3.116}$$

It can be verified that the hp components $\widetilde{\Phi}_{hp,h'p'}(\omega_n)$ of the particle-phonon coupling amplitude can be obtained from the ph components $\widetilde{\Phi}_{ph,p'h'}(\omega_n)$ via

$$\widetilde{\Phi}_{hp,h'p'}(\omega_n) = \widetilde{\Phi}^*_{ph,p'h'}(-\omega_n). \tag{3.117}$$

After the analytical continuation to the real frequencies, the BSE for the correlated ph propagator $\widetilde{\mathscr{R}}^e_{k_1k_2,k_3k_4}(\omega)$ takes the form:

$$\widetilde{\mathscr{R}}^e_{k_1k_2,k_3k_4}(\omega) = \widetilde{\mathscr{R}}^0_{k_1k_2,k_3k_4}(\omega) - \sum_{k_5k_6k_7k_8} \widetilde{\mathscr{R}}^0_{k_1k_2,k_5k_6}(\omega) \widetilde{\Phi}_{k_5k_6,k_7k_8}(\omega) \widetilde{\mathscr{R}}^e_{k_7k_8,k_3k_4}(\omega), \tag{3.118}$$

where the spectral representation of the uncorrelated propagator and the particle-phonon coupling amplitude are respectively given by

$$\widetilde{\mathscr{R}}^0_{k_1k_2,k_3k_4}(\omega) = -\delta_{k_1k_3}\delta_{k_2k_4} \frac{n(\varepsilon_{k_2},T) - n(\varepsilon_{k_1},T)}{\omega - \varepsilon_{k_1} + \varepsilon_{k_2}} \tag{3.119}$$

and

$$\begin{aligned} \widetilde{\Phi}_{k_1k_2,k_3k_4}(\omega) &= \frac{\delta_{\sigma_{k_1},-\sigma_{k_2}}\sigma_{k_1}}{n(\varepsilon_{k_4},T) - n(\varepsilon_{k_3},T)} \sum_{k_5,k_6,m} \sum_{\eta_m=\pm 1} \eta_m \xi^{m\eta_m}_{k_1k_2,k_5k_6} \xi^{m\eta_m *}_{k_3k_4,k_5k_6} \\ &\times \frac{[N(\eta_m\omega_m,T) + n(\varepsilon_{k_6},T)][n(\varepsilon_{k_6} - \eta_m\omega_m,T) - n(\varepsilon_{k_5},T)]}{\omega - \varepsilon_{k_5} + \varepsilon_{k_6} - \eta_m\omega_m}. \end{aligned} \tag{3.120}$$

Comparing Eq. (3.44) to Eq. (3.118), one should be able to highlight the merit of the imaginary-time projection operator. As already mentioned before, one has to handle the three-imaginary-time or, after doing a three-dimensional Fourier transform, three-energy variable integrations to solve Eq. (3.44). Since the kernel $\mathscr{W}^e$ consists of the energy-dependent mass operator Σ^e and interaction amplitude $\mathscr{U}^e$, which are singular, these

integrations are simply impossible to be done numerically. In contrast to Eq. (3.44), Eq. (3.118) no longer contains any energy integration with singular kernels. Instead, Eq. (3.118) allows us to perform the summations over the mean-field single-particle states, which are numerically feasible.

The full finite-temperature response function $\mathscr{R}$ now satisfies the Bethe-Salpeter equation:

$$\begin{aligned}\mathscr{R}_{k_1k_2,k_3k_4}(\omega) &= \widetilde{\mathscr{R}}^0_{k_1k_2,k_3k_4}(\omega) \\ &- \sum_{k_5k_6k_7k_8} \widetilde{\mathscr{R}}^0_{k_1k_2,k_5k_6}(\omega)[\widetilde{\mathscr{U}}_{k_5k_6,k_7k_8} + \delta\widetilde{\Phi}_{k_5k_6,k_7k_8}(\omega)]\mathscr{R}_{k_7k_8,k_3k_4}(\omega),\end{aligned} \tag{3.121}$$

where the corrected particle-phonon coupling amplitude $\delta\widetilde{\Phi}(\omega)$ is obtained directly from the subtraction of itself at $\omega = 0$, viz.,

$$\delta\widetilde{\Phi}(\omega) = \widetilde{\Phi}(\omega) - \widetilde{\Phi}(0). \tag{3.122}$$

This subtraction procedure serves as a method to eliminate the double counting of the PVC effects, which appears inevitably in calculations based on the effective residual interaction. In the finite-temperature relativistic random phase approximation (FT-RRPA) response formalism, i.e., Eq. (3.121) without $\delta\widetilde{\Phi}(\omega)$, the residual interaction is the kernel of the corresponding BSE. In the FT-RTBA, in addition to the residual interaction $\widetilde{\mathscr{U}}$, the kernel of BSE (3.121) also contains the contribution from the PVC amplitude $\widetilde{\Phi}(\omega)$.However, there already exist the implicit static contribution $\widetilde{\Phi}(0)$ of the PVC amplitude to the residual interaction $\widetilde{\mathscr{U}}$, because it is adjusted to experimental data on finite nuclei. Therefore, the subtraction procedure is necessary for solving the double counting problem, which arises from the presence of static contribution $\widetilde{\Phi}(0)$ inside the residual interaction $\widetilde{\mathscr{U}}$ [71, 77]. In addition, the subtraction improves considerably the convergence of the PVC amplitude and, in the case of the dipole response, also helps eliminate the spurious translational mode [71].

3.5 Strength Function and Transition Density

In order to calculate the strength function $\widetilde{S}(E)$, one normally starts from the Bethe-Salpeter equation (3.121). After solving Eq. (3.121) for the finite-temperature response function $\mathscr{R}(\omega)$, one utilizes Eq. (3.12) to calculate the strength distribution. It is useful, however, to start from a single convolution of Eq. (3.121) with external field $\hat{V}^0$. In fact, a single convolution of the finite-temperature response function $\mathscr{R}$ with external field $\hat{V}^0$

defines the density matrix variation $\delta\rho$, viz.,

$$\delta\rho_{k_1k_2}(\omega) = -\sum_{k_3k_4} \mathscr{R}_{k_1k_2,k_3k_4}(\omega) V^0_{k_4k_3}. \tag{3.123}$$

A single convolution of the uncorrelated propagator $\widetilde{\mathscr{R}}^0$ with external field $\hat{V}^0$ yields the uncorrelated density matrix variation

$$\delta\rho^0_{k_1k_2}(\omega) = -\sum_{k_3k_4} \widetilde{\mathscr{R}}^0_{k_1k_2,k_3k_4}(\omega) V^0_{k_4k_3}. \tag{3.124}$$

Accordingly, one can rewrite Eq. (3.121) in terms of $\delta\rho(\omega)$ and $\delta\rho^0(\omega)$ as

$$\begin{aligned} \delta\rho_{k_1k_2}(\omega) &= \delta\rho^0_{k_1k_2}(\omega) \\ &- \sum_{k_5k_6k_7k_8} \widetilde{\mathscr{R}}^0_{k_1k_2,k_5k_6}(\omega)[\widetilde{\mathscr{U}}_{k_5k_6,k_7k_8} + \delta\widetilde{\Phi}_{k_5k_6,k_7k_8}(\omega)]\delta\rho_{k_7k_8}(\omega) \end{aligned} \tag{3.125}$$

and the spectral density $S(E)$ as

$$S(E) = -\frac{1}{\pi} \lim_{\Delta\to+0} \mathrm{Im} \sum_{k_1k_2} V^{0*}_{k_2k_1} \delta\rho_{k_1k_2}(E + i\Delta). \tag{3.126}$$

The advantage of expressing the spectral density $S(E)$ in terms of density matrix variation $\delta\rho$ is that the transition density

$$\rho^{fi}_{k_1k_2} = \langle f|\hat{a}^\dagger_{k_1}\hat{a}_{k_2}|i\rangle \tag{3.127}$$

from the initial state $|i\rangle$ to final state $|f\rangle$ is connected to the spectral density $S(E)$ at the energy $E = \omega_{fi}$. In the vicinity of ω_{fi}, the full response function is a simple pole of the form:

$$\mathscr{R}^{fi}_{k_1k_2,k_3k_4}(E)\Big|_{E\approx\omega_{fi}} \approx -\frac{\rho^{fi}_{k_1k_2}\rho^{fi*}_{k_3k_4}}{E - \omega_{fi}}. \tag{3.128}$$

Consequently, the imaginary part of the matrix element $\delta\rho_{k_1k_2}(E + i\Delta)$ in the vicinity of ω_{fi} is given by

$$\mathrm{Im}\delta\rho_{k_1k_2}(\omega_{fi} + i\Delta) = -\frac{1}{\Delta}\rho^{fi}_{k_1k_2} \sum_{k_3k_4} \rho^{fi*}_{k_3k_4} V^0_{k_4k_3} \tag{3.129}$$

and the spectral density $S(\omega_{fi})$ takes the form:

$$S(\omega_{fi}) = \frac{1}{\pi} \lim_{\Delta \to +0} \frac{1}{\Delta} \left| \sum_{k_3 k_4} \rho^{fi*}_{k_3 k_4} V^0_{k_4 k_3} \right|^2 . \tag{3.130}$$

Combining the last two equations yields

$$\rho^{fi}_{k_1 k_2} = \lim_{\Delta \to +0} \sqrt{\frac{\Delta}{\pi S(\omega_{fi})}} \mathrm{Im} \delta\rho_{k_1 k_2}(\omega_{fi} + i\Delta) \tag{3.131}$$

in analogy to the case of zero temperature [77]. This relation allows us to extract the transition densities from a continuous strength distribution. To derive the normalization of the transition densities, we start from Eq. (3.121) and rewrite it as an operator equation of the form:

$$[(\widetilde{\mathscr{R}}^0(\omega))^{-1} + \widetilde{\mathscr{U}} + \widetilde{\Phi}(\omega) - \widetilde{\Phi}(0)]\mathscr{R}(\omega) = 1. \tag{3.132}$$

The derivative of Eq. (3.132) with respect to ω leads to

$$\begin{aligned} -\frac{d\mathscr{R}_{k_1 k_2, k_3 k_4}(\omega)}{d\omega} &= \sum_{k_5 k_6 k_7 k_8} \mathscr{R}_{k_1 k_2, k_5 k_6}(\omega) \frac{d(\widetilde{\mathscr{R}}^0)^{-1}_{k_5 k_6, k_7 k_8}(\omega)}{d\omega} \mathscr{R}_{k_7 k_8, k_3 k_4}(\omega) \\ &+ \sum_{k_5 k_6 k_7 k_8} \mathscr{R}_{k_1 k_2, k_5 k_6}(\omega) \frac{d\widetilde{\Phi}_{k_5 k_6, k_7 k_8}(\omega)}{d\omega} \mathscr{R}_{k_7 k_8, k_3 k_4}(\omega). \end{aligned} \tag{3.133}$$

Inserting Eqs. (3.119) and (3.128) into Eq. (3.133) yields the generalized normalization condition

$$1 = \sum_{k_1 k_2 k_3 k_4} \rho^{fi*}_{k_1 k_2} \left[\mathscr{N}_{k_1 k_2, k_3 k_4} - \left. \frac{d\widetilde{\Phi}_{k_1 k_2, k_3 k_4}(\omega)}{d\omega} \right|_{\omega = \omega_{fi}} \right] \rho^{fi}_{k_3 k_4}, \tag{3.134}$$

where the matrix element $\mathscr{N}_{k_1 k_2, k_3 k_4}$ is the finite-temperature random phase approximation (FT-RPA) norm of the form:

$$\mathscr{N}_{k_1 k_2, k_3 k_4} = \frac{\delta_{k_1 k_3} \delta_{k_2 k_4}}{n(\varepsilon_{k_2}, T) - n(\varepsilon_{k_1}, T)}. \tag{3.135}$$

For the case where the the only interaction involved is the residual interaction $\widetilde{\mathscr{U}}$, the derivative of $\widetilde{\Phi}(\omega)$ with respect to ω vanishes and, hence, the generalized normalization

condition (3.134) reduces to the usual FT-RPA normalization condition:

$$\sum_{ph} \frac{|\rho_{ph}^{fi}|^2 - |\rho_{hp}^{fi}|^2}{n(\varepsilon_h, T) - n(\varepsilon_p, T)} = 1. \tag{3.136}$$

The generalized normalization condition can be employed to investigate the relative contributions of dominant ph and $\widetilde{\text{ph}}$ components that define the underlying structure, the degree of collectivity, and PVC for a particular excited state at a specific temperature.

Chapter 4

Numerical Results

4.1 Numerical Details

In this section, we present realistic numerical calculations making use of the finite-temperature relativistic time-blocking approximation (FT-RTBA) developed in Chapter 3. We calculated the multipole strengths for even-even spherical nuclei ^{48}Ca, ^{68}Ni, ^{100,120,132}Sn, and ^{208}Pb at various temperatures and investigated the evolution of these multipole strengths with temperature. The general scheme of the calculations is given as follows [98]:

(i) We simultaneously solve the closed set of the RMF equations, i.e., Eqs. (2.42), (2.51)-(2.54), with the densities of Eqs. (2.75)-(2.78) and the particle number constraint (2.73) in a self-consistent way using the NL3 parameter set [156] of the nonlinear σ model. We discussed the iterative procedures for solving the closed set of the RMF equations in Section 2.3. The solution of the closed set of the RMF equations is the temperature-dependent single-particle basis in terms of the Dirac spinors $\varphi_k(\mathbf{r})$ and the corresponding single-particle energies ε_k.

(ii) The obtained single-particle basis is utilized to solve the finite-temperature relativistic random phase approximation (FT-RRPA) equations to obtain the phonon vertices g^m and frequencies ω_m. Here the FT-RRPA equations are equivalent to Eq. (3.125) without the corrected particle-phonon coupling amplitude $\delta\widetilde{\Phi}(\omega)$. Together with the single-particle basis, the set of phonons forms the model space of 1p1h$\otimes$phonon configurations for the particle-phonon coupling amplitude $\widetilde{\Phi}(\omega)$.

(iii) Finally, we solve Eq. (3.125) and compute the strength function being given by Eq. (3.12) for the specific external field V^0_{LM}. For the electric isoscalar monopole (E0) and

quadrupole (E2) transitions, the external field V^0_{LM} takes the forms [157]:

$$V^0_{00} = e\sum_{i=1}^{A} r_i^2 Y_{00}(\mathbf{n}_i) \tag{4.1}$$

and

$$V^0_{2M} = e\sum_{i}^{A} r_i^2 Y_{2M}(\mathbf{n}_i), \tag{4.2}$$

respectively, where $\mathbf{n}$ is a unit vector in the spherical coordinates. The isovector electric dipole (E1) transitions are associated with the external field V^0_{LM} of the form [98, 157]:

$$V^0_{1M} = \frac{eN}{A}\sum_{i=1}^{Z} r_i Y_{1M}(\mathbf{n}_i) - \frac{eZ}{A}\sum_{i=1}^{N} r_i Y_{1M}(\mathbf{n}_i), \tag{4.3}$$

which contains the correction for the center-of-mass motion. This whole scheme of the calculations can be performed in the Dirac-space representation, which allows for direct extraction of the transition densities, according to Eq. (3.131). A faster algorithm is, however, to solve Eq. (3.118) in the basis of Dirac spinors and then the Bethe-Salpeter equation

$$\mathscr{R}(\omega) = \widetilde{\mathscr{R}}^e(\omega) - \widetilde{\mathscr{R}}^e(\omega)\widetilde{\mathscr{U}}\mathscr{R}(\omega) \tag{4.4}$$

in the momentum-channel representation [78]. The momentum-channel representation provides a more economical execution of the calculations that involve large masses and high temperatures. The alternative algorithm implies the solution of Eq. (3.125) in the Dirac basis. The coincidence of the two solutions in the different representations serves as a validity test of our results.

In both calculation schemes, the particle-phonon coupling amplitude $\widetilde{\Phi}(\omega)$ is computed within the particle-hole (ph) energy window of 25 and 30 MeV around the Fermi surface. It has been verified that a further increase of this window gives insignificant change to the strength functions at the energies below the value of this window. To eliminate the spurious translational mode completely, the particle-hole basis was fixed by the limits $\varepsilon_{\rm ph} \leq 300$ MeV and $\varepsilon_{\alpha{\rm h}} \geq -1800$ MeV with respect to the positive continuum. The values of smearing parameter were set to be 500 keV for ^{48}Ca and ^{68}Ni nuclei, and 200 keV for ^{100,120,132}Sn and ^{208}Pb to match approximately the typical continuum width of the peaks of the strength distributions. The collective vibrations with quantum numbers of spin and parity $J^\pi = 2^+,\ 3^-,\ 4^+,\ 5^-,\ 6^+$ below the energy cutoff, which amounts to 15 and 20 MeV for heavy and medium-mass nuclei, were included in the phonon space. An additional truncation

condition was applied according to the values of the reduced transition probabilities $B(EL)$ of the corresponding electromagnetic transitions. For each J^π, all modes with the values of $B(EL)$ less than 5% of the maximal one were neglected. It is assumed that keeping the same truncation criteria for all temperature regimes guarantees a fair comparison of the calculated strength distributions. At high temperatures, the number of phonons increases due to the effect of thermal unblocking. In particular, at $T \approx$ 5-6 MeV, the average number of phonons included in the phonon space becomes an order of magnitude larger than that at $T = 0$. Finally, another truncation condition was made on the absolute values of the numerator of Eq. (3.119): All particle-hole pairs with $|n(\varepsilon_{k_2}, T) - n(\varepsilon_{k_1}, T)| \leq 0.01$ do not contribute to the solution of the Bethe-Salpeter equation (3.121).

4.2 Thermal Mean-field Calculations for Compound Nuclei[1]

The thermal RMF calculations of the excitation energy E^* as a function of temperature T for compound nuclei ^{48}Ca, ^{68}Ni and ^{100,132}Sn are illustrated in Fig. 4.1. Technically, as it follows from Chapter 2, the effect of finite temperature on the total energy of a thermally excited nucleus is mainly induced by the change of the fermionic occupation numbers from the values of zero and one at $T = 0$ to the Fermi-Dirac distribution (2.72). The fermionic densities of Eqs. (2.75)-(2.78) change accordingly and, thus, affect the meson and photon fields being the sources for Eqs. (2.51)-(2.54). In turn, the changed meson fields give the feedback on the nucleons, so that the thermodynamical equilibrium is achieved through the self-consistent set of the thermal RMF equations. As the nucleons start to be promoted to higher-energy orbits with the temperature increase, the total energy should grow continuously and, in principle, the dependence $E^*(T)$ has to be parabolic, in accordance with the non-interacting Fermi gas behavior. However, the discrete shell structure and especially the presence of the large shell gaps right above the Fermi surface in the doubly magic nuclei cause a flat behavior of the excitation energy until the temperature values become sufficient to promote the nucleons over the shell gaps. This effect is clearly visible in Fig. 4.1 for the doubly magic nuclei ^{48}Ca and ^{100,132}Sn, while it is much smaller in ^{68}Ni which has an open shell in the neutron subsystem. Otherwise, at $T \geq 1$ MeV the thermal RMF $E^*(T)$ dependencies can be very well approximated by the parabolic fits providing the level density parameters which are close to the empirical Fermi gas values $a = A/k$, where $8 < k < 12$.

[1]Sections 4.2 is reprinted from Ref. [98], in accordance with American Physical Society (APS) copyright policies (`https://journals.aps.org/copyrightFAQ.html`)

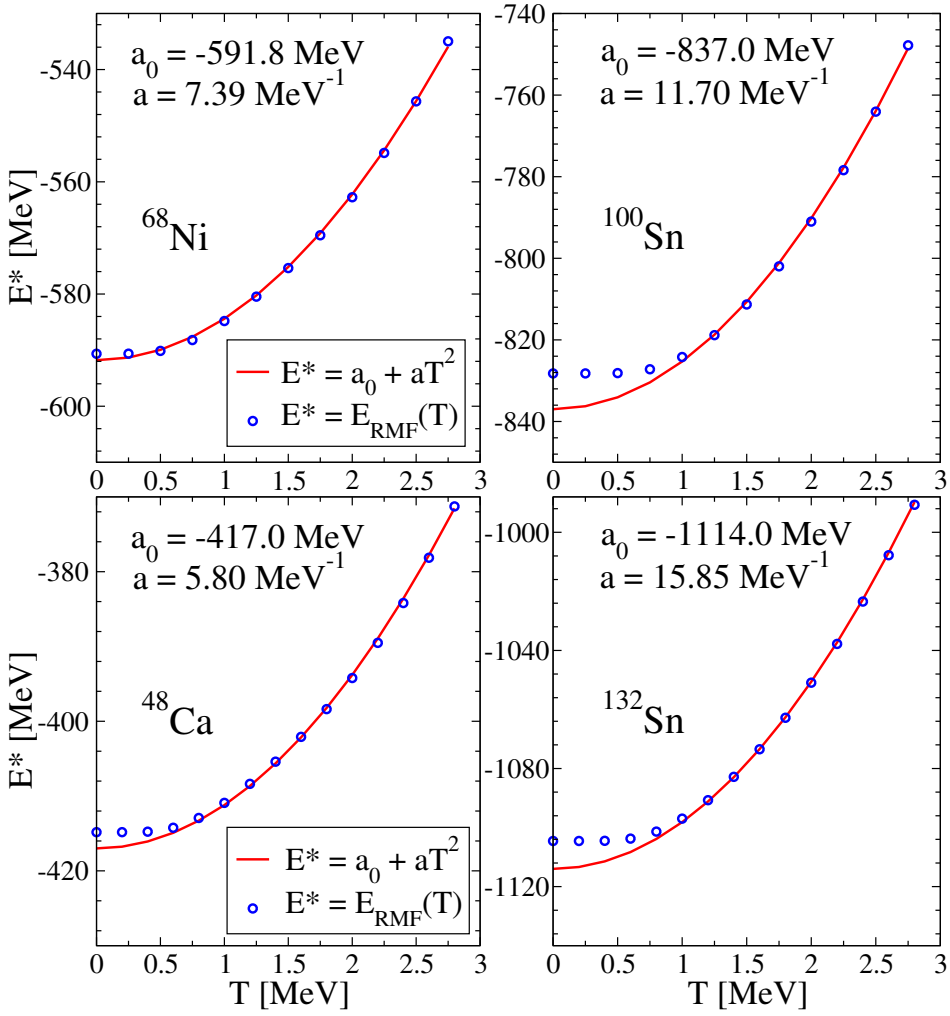

Figure 4.1: The energies of the thermally excited nuclei ^{48}Ca, ^{68}Ni and ^{100,132}Sn as functions of temperature: RMF (blue circles) and parabolic fits (red curves) [98].

4.3 Isovector Dipole Resonance in ^{48}Ca, ^{68}Ni, and ^{100,120,132}Sn[2]

The calculated temperature-dependent spectral densities $S(\omega)$ for ^{48}Ca, ^{68}Ni and ^{100,120,132}Sn nuclei at various temperatures are shown in Figs. 4.2 and 4.3, respectively, where we compare the evolution of the electric dipole spectral density within FT-RRPA (left panels) and FT-RTBA (right panels). As the temperature increases, we observe the following two major effects:

(i) The fragmentation of the dipole spectral density becomes stronger, so that the GDR

[2]Sections 4.3 is reprinted from Ref. [98], in accordance with American Physical Society (APS) copyright policies (`https://journals.aps.org/copyrightFAQ.html`)

undergoes a continuous broadening. The increased diffuseness of the Fermi surface enhances significantly the amount of thermally unblocked states, especially the ones above the Fermi energy ε_F, as shown schematically in Fig. 4.4. These states give rise to the new transitions within the thermal particle-hole pairs $\widetilde{\text{ph}}$, as follows from the form of the uncorrelated propagator (3.95). The increasing amount of these new pairs reinforces the Landau damping of the GDR. The spreading width of the GDR determined by the PVC amplitude of Eq. (3.116) also increases because of the increasing role of the new terms with $\eta_m = -1$, in addition to the terms with $\eta_m = +1$ which solely define the PVC at zero temperature. As these terms are associated with the new poles, they enhance the spreading effects with the temperature growth, in addition to the reinforced Landau damping. At high temperatures $T \approx 5 - 6$ MeV, when the low-energy phonons develop the new sort of collectivity, the coupling vertices increase accordingly, which leads to a reinforcement of the spreading width of the GDR. This is consistent with the experimental observations of the "disappearance" of the high-frequency GDR at temperatures $T \geq 6$ MeV reported in the Ref. [106], while these temperatures might be at the limits of existence of the considered atomic nuclei.

(ii) The formation and enhancement of the low-energy strength below the pygmy dipole resonance. This enhancement occurs due to the new transitions within thermal $\widetilde{\text{ph}}$ pairs with small energy differences. The number of these pairs increases with the temperature growth in such a way that at high temperature $T \approx$ 5-6 MeV the formation of new collective low-energy modes becomes possible. Within our model, these new low-energy modes are not strongly affected by PVC. The lack of fragmentation is due to the fact that for the thermal $\widetilde{\text{ph}}$ pairs with small energy differences the numerator of Eq. (3.116) contains the factors $n(\varepsilon_{k_6} - \eta_m\omega_m, T) - n(\varepsilon_{k_5}, T)$ which are considerably smaller than those for the regular $T = 0$ ph pairs of states located on the different sides with respect to the Fermi surface. Notice that the smallness of this factor for the $\widetilde{\text{ph}}$ pairs is not compensated by the denominator $n(\varepsilon_{k_4}, T) - n(\varepsilon_{k_3}, T)$ which is balanced by the numerator of Eq. (3.95). The inclusion of the finite-temperature ground state correlations (GSC) induced by the PVC in the particle-phonon coupling amplitude $\widetilde{\Phi}(\omega)$ may enforce the fragmentation of the low-energy peaks.

The trends are similar for the dipole strength in all considered nuclei shown in Figs. 4.2 and 4.3. The open-shell nuclei, such as ^{68}Ni and ^{120}Sn, are superfluid below the critical temperature, which is $T_c \approx 0.6\Delta_c$, where Δ_c is the superfluid pairing gap. It takes the values $\Delta_c = 1.6$ MeV and $\Delta_c = 1.1$ MeV for ^{68}Ni and ^{120}Sn, respectively, so that the superfluidity already vanishes at $T = 1$ MeV in these nuclei. As our approach does not

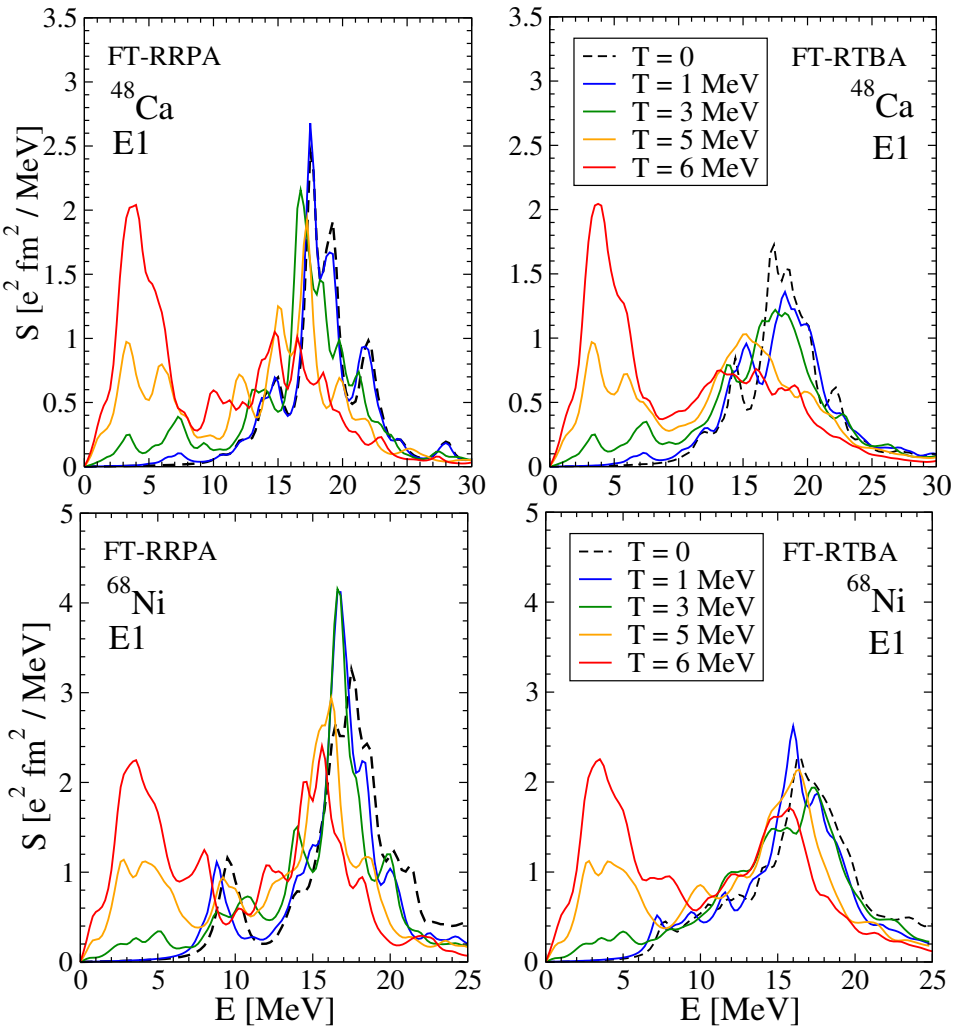

Figure 4.2: Electric dipole spectral density in ^{48}Ca and ^{68}Ni nuclei calculated within FT-RRPA (left panels) and FT-RTBA (right panels) at various temperatures. The value of smearing parameter $\Delta = 500$ keV was adopted in both calculations [98].

take the superfluid pairing into account at $T > 0$, we can not track this effect continuously; however, by comparing the strength distributions at $T = 0$ and $T = 1$ MeV for ^{68}Ni and ^{120}Sn we can see how the disappearance of superfluidity influences the strength. In the doubly magic nuclei the dipole strength shows almost no change when going from $T = 0$ to $T = 1$ MeV. This observation is consistent with the thermal RMF calculations displayed in Fig. 4.1. As already discussed above, the presence of the large shell gaps in both neutron and proton subsystems requires a certain value of temperature to promote the nucleons over the shell gap. One can see that this temperature is $T \approx 0.75 - 1$ MeV for the considered closed-shell nuclei.

Notice that until now we discussed the microscopic spectral density $S(E)$ without the

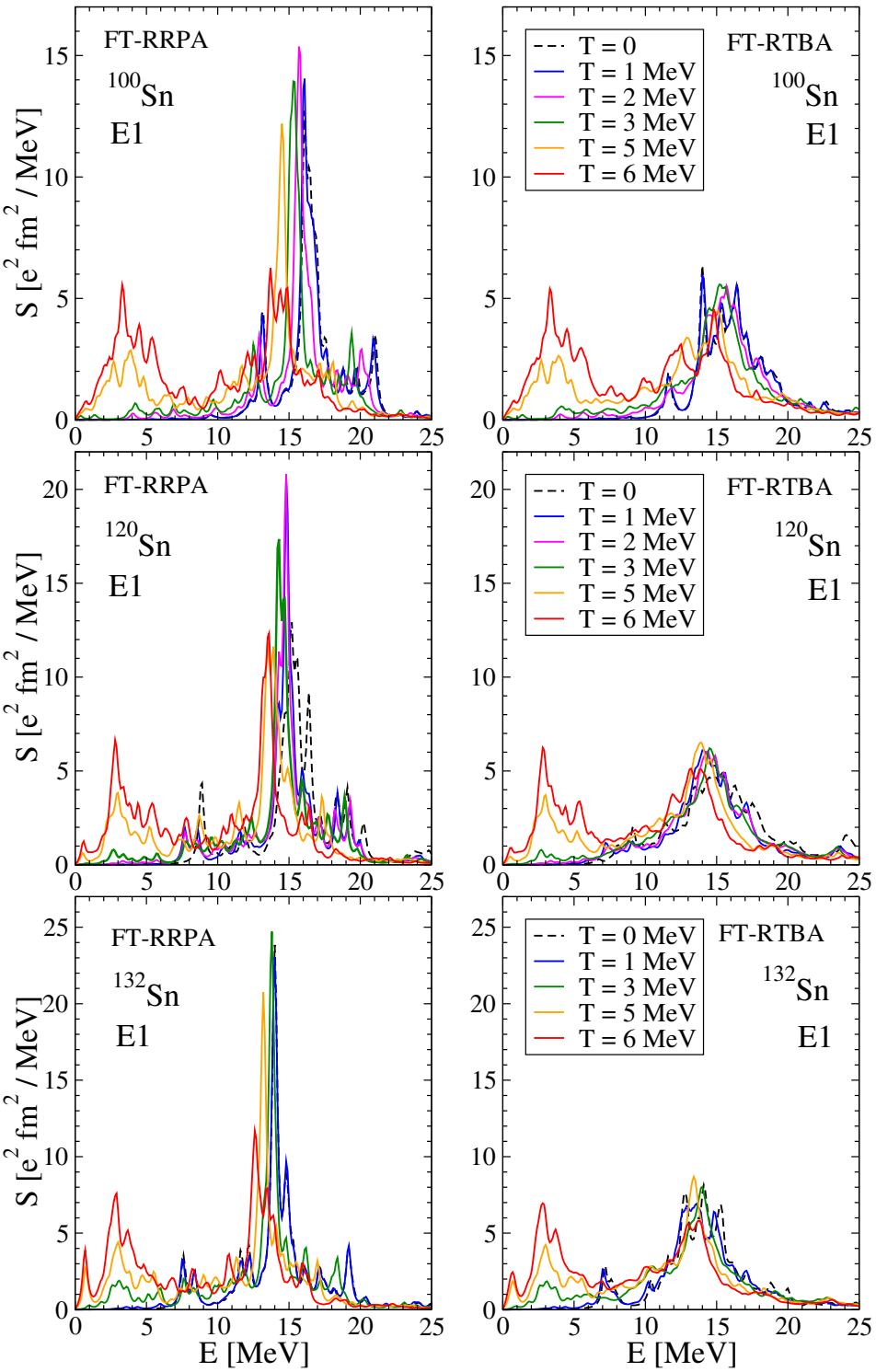

Figure 4.3: Same as in Fig. 4.2 but for ^{100,120,132}Sn nuclei with the smearing parameter $\Delta = 200$ keV [98].

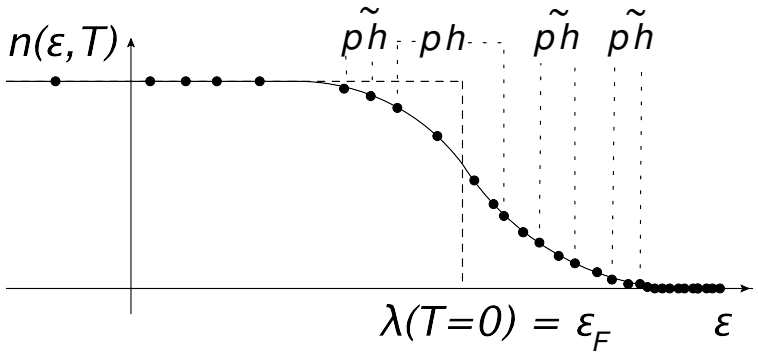

Figure 4.4: Emergence of thermally unblocked states below and above the Fermi energy ε_F. Here $\widetilde{\text{ph}}$ stands for the thermally unblocked hole-hole (hh) and particle-particle (pp) fermionic pairs with the non-zero values of the uncorrelated propagator (3.95) [98].

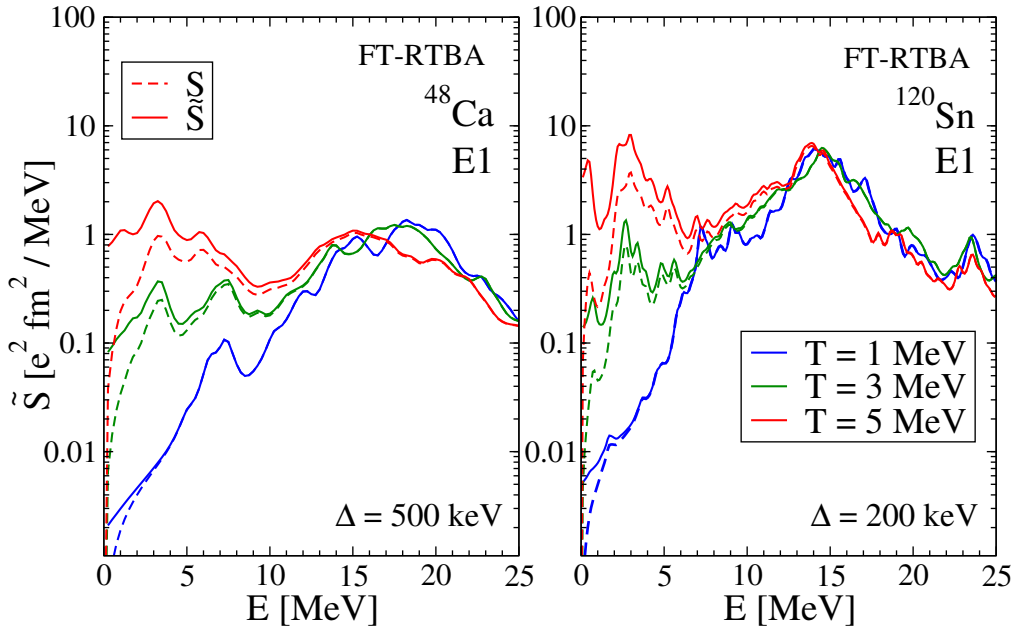

Figure 4.5: The role of the exponential factor: strength function $\tilde{S}(E)$ (solid curves) versus spectral density $S(E)$ (dashed curves) for the dipole strength in ^{48}Ca (left panel) and ^{120}Sn (right panel) [98].

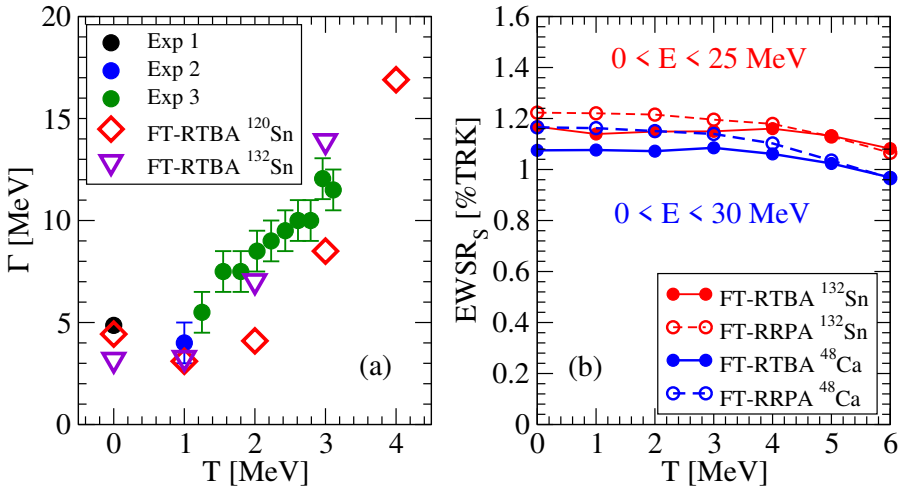

Figure 4.6: Width and energy-weighted sum rule (EWSR) of the giant dipole resonance. Left panel: Width of the giant dipole resonance in ^{120,132}Sn as a function of temperature. The experimental values from Refs. [158, 159, 160] are shown for ^{120}Sn. Right panel: The energy-weighted sum rule (EWSR) for ^{48}Ca and ^{132}Sn with respect to the TRK sum rule [98].

exponential factor $1/[1-\exp(-E/T)]$, which is present in the strength function $\tilde{S}(E)$ (3.12) due to the detailed balance. This factor does not affect the GDR region at all temperatures under study; however, at moderate to high temperatures it enhances noticeably the low-energy strength, as illustrated in Fig. 4.5 for the dipole response of ^{48}Ca and ^{120}Sn. At $E = 0$ this factor is singular while the spectral density is equal to zero, so that the total strength function has, thus, a nontrivial limit at $E \to 0$. As one can see from Fig. 4.5, this limit is finite except for the $T = 0$ case when the strength function coincides with the spectral density vanishing at $E \to 0$. In this work we focus mostly on the features of the spectral density, which is the zero-temperature analog of the strength function, in order to resolve clearly the details of the nuclear response at very low transition energies E without concealing its fine features by the exponential factor. It can be easily included, for instance, when experimental data on the low-energy response become available. The important features are, in particular, the absence of the spurious translational mode and the clear zero-energy limit of the spectral density.

The width and the energy weighted sum rules are the most important integral characteristics of the GDR which are usually addressed in theoretical and experimental studies. In particular, they help benchmarking the theoretical approaches because of their almost model-independent character. The left panel of Fig. 4.6 illustrates the evolution of GDR's width $\Gamma(T)$ with temperature obtained in FT-RTBA for ^{120}Sn and ^{132}Sn nuclei

Table 4.1: Widths of the giant dipole resonance in ^{120}Sn calculated by fitting the FT-RRPA and FT-RTBA strengths with the Lorentz distribution within the energy interval $0 \leq E \leq 25$ MeV [98].

T [MeV]	0	1.0	2.0	3.0	4.0
Γ [MeV], FT-RRPA	2.70	2.26	3.09	6.94	14.46
Γ [MeV], FT-RTBA	4.43	3.08	4.07	8.46	16.92

together with experimental data which are available only for ^{120}Sn. The theoretical widths at $T = 0$ are taken from our previous calculations [77, 78], respectively. Because of the phase transition in ^{120}Sn at $T < 1$ MeV, $\Gamma(T)$ has a smaller value at $T = 1$ MeV than at $T = 0$ as the disappearance of the superfluid pairing reduces the width. As already mentioned, the thermal unblocking effects do not yet appear at $T = 1$ MeV in both ^{120}Sn and ^{132}Sn because of their specific shell structure. For the protons which form the $Z = 50$ closed shell and have the next available orbitals only in the next major shell, $T = 1$ MeV temperature is not yet sufficient to promote them over the shell gap with a noticeable occupancy. In the neutron subsystem, the situation in ^{132}Sn is similar while in ^{120}Sn the lowest available orbit is the intruder $1h_{11/2}$ state where particles get promoted relatively easily, but after this orbit there is another shell gap. As a consequence, at $T = 1$ MeV there is still no room for the $\widetilde{\text{ph}}$ pair formation and, hence, for a noticeable thermal unblocking. Thus, our result can explain the unexpectedly small GDR's width at $T = 1$ MeV reported in Ref. [159], in contrast to the thermal shape fluctuation calculations. After $T = 1$ MeV in ^{132}Sn and $T = 2$ MeV in ^{120}Sn we obtain a fast increase of $\Gamma(T)$ because of the formation of the low-energy shoulder by $\widetilde{\text{ph}}$ pairs and due to a slow increase of the fragmentation of the high-energy peak emerging from the finite-temperature effects in the PVC amplitude $\widetilde{\Phi}(\omega)$. As ^{132}Sn is more neutron-rich than ^{120}Sn, the respective strength in the low-energy shoulder of ^{132}Sn is larger, which leads to a larger overall width in ^{132}Sn at temperatures above 1 MeV. The GDR's widths for $T > 3$ MeV in ^{132}Sn and for $T > 4$ MeV in ^{120}Sn are not presented because the standard procedure based on the Lorentzian fit of the microscopic strength distribution fails in recognizing the distribution as a single peak structure.

The overall agreement of FT-RTBA calculations with data for the GDR's width in ^{120}Sn is found very reasonable except for the temperatures around 2 MeV, possibly due to deformation and shape fluctuation effects, which are not included in the present calculations. Our results are also consistent with those of microscopic approach of Ref. [161], which are available for the GDR energy region at $T \leq 3$ MeV, while in the entire range of temperatures under study $\Gamma_{GDR}(T)$ shows a nearly quadratic dependence agreeing with the Fermi liquid theory [162]. Table 4.1 shows a comparison of $\Gamma_{GDR}(T)$ in ^{120}Sn calculated within FT-

RRPA and FT-RTBA by fitting the corresponding strength distribution by the Lorentzian within the energy interval $0 \leq E \leq 25$ MeV. One can see that in both approaches, after passing the minimum at $T = 1$ MeV because of the transition to the non-superfluid phase, $\Gamma_{GDR}(T)$ grows quickly with temperature. The difference between the width computed in the two models is about $1.0 - 1.7$ MeV at low temperatures while it increases to ≈ 2.5 MeV at $T = 4$ MeV. It can be concluded that the PVC contribution to the width evolution is rather minor and the latter occurs mostly due to the reinforcement of the Landau damping with the temperature growth. Indeed, we could observe from varying the boundaries of the energy interval, where the fitting procedure is performed, that the amount of the low-energy strength is very important for the value of the width.

The right panel of Fig. 4.6 shows the evolution of the energy-weighted sum rule for ^{48}Ca and ^{132}Sn nuclei calculated within FT-RRPA and FT-RTBA in the percentage with respect to the Thomas-Reiche-Kuhn (TRK) sum rule. The EWSR at $T > 0$ can be calculated in full analogy with the case of $T = 0$ [132, 163]. In our approach, where the meson-exchange interaction is velocity-dependent, already in RRPA and relativistic quasiparticle random phase approximation (RQRPA) at $T = 0$ we observe up to 40% enhancement of the TRK sum rule within the energy regions which are typically studied in experiments [77, 78], in agreement with data. In the resonant time-blocking approximation without the GSC of the PVC type the EWSR should have exactly the same value as in RPA [69] with a little violation when the subtraction procedure is performed [69, 70]. Typically, at $T = 0$ in the subtraction-corrected RTBA we find a few percent less EWSR in finite energy intervals below 25-30 MeV than in RRPA, but this difference decreases if we take larger intervals. This is due to the fact that in RTBA the strength distributions are more spread and if cut, leaves more strength outside the finite interval. A similar situation takes place at $T > 0$. Fig. 4.6 (b) shows that the EWSR decreases slowly with the temperature growth because the entire strength distribution moves down in energy. In both nuclei, the FT-RRPA and FT-RTBA EWSR values practically meet at $T = 6$ MeV when their high-energy tails become less important.

To gain a better understanding of the formation and enhancement of the low-energy strength, we have performed a more detailed investigation of the dipole strength in the energy region $E < 10$ MeV. The dipole strength in ^{68}Ni calculated at different temperatures with a small value of the smearing parameter $\Delta = 20$ keV is displayed in Fig. 4.7. In the testing phase, these calculations were used to ensure positive definiteness of the spectral density as it reflects a very delicate balance between the self-energy and exchange terms in the PVC amplitude $\widetilde{\Phi}(\omega)$. In particular, we found that consistency between $\widetilde{\text{ph}}$ pairs involved in self-energy and exchange terms is very important.

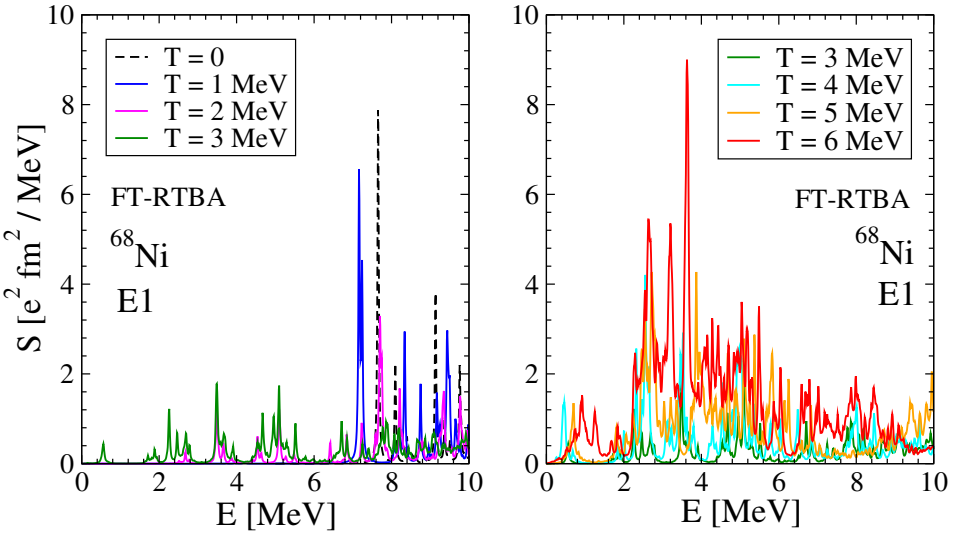

Figure 4.7: The temperature evolution of the low-energy dipole spectral density in ^{68}Ni calculated within FT-RTBA with the smearing parameter $\Delta = 20$ keV [98].

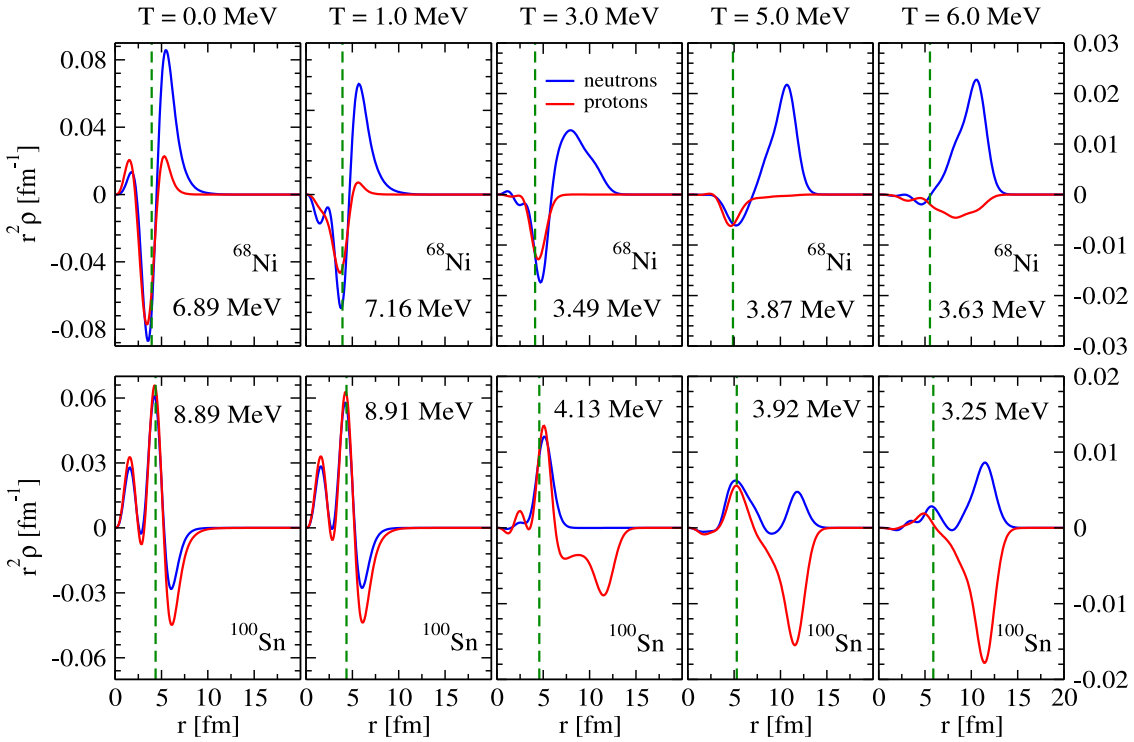

Figure 4.8: The evolution of the proton and neutron transition densities for the most prominent peaks below 10 MeV in ^{68}Ni and ^{100}Sn within FT-RTBA. The green dashed lines indicate the rms nuclear radius [98].

Table 4.2: Major contributions of neutron (n) and proton (p) ph and $\widetilde{\text{ph}}$ configurations to the strongest dipole states below 10 MeV in ^{68}Ni calculated within FT-RTBA for various temperatures [98].

$T = 0$; $E = 6.89$ MeV		$T = 1$ MeV; $E = 7.16$ MeV		$T = 2$ MeV; $E = 7.70$ MeV		$T = 3$ MeV; $E = 3.49$ MeV	
10.3%	$(2p_{3/2} \to 2d_{5/2})$ n	56.8%	$(2p_{1/2} \to 3s_{1/2})$ n	4.9%	$(1f_{5/2} \to 2d_{5/2})$ n	31.1%	$(3s_{1/2} \to 3p_{3/2})$ n
9.8%	$(2s_{1/2} \to 2p_{3/2})$ p	4.4%	$(1f_{7/2} \to 1g_{9/2})$ n	3.2%	$(1f_{7/2} \to 1g_{9/2})$ n	15.7%	$(2d_{5/2} \to 3p_{3/2})$ n
7.1%	$(1f_{7/2} \to 1g_{9/2})$ p	2.2%	$(1f_{5/2} \to 2d_{5/2})$ n	2.9%	$(2p_{3/2} \to 2d_{5/2})$ n	0.1%	$(3s_{1/2} \to 3p_{1/2})$ n
6.2%	$(1f_{5/2} \to 2d_{5/2})$ n	1.4%	$(1f_{7/2} \to 1g_{9/2})$ p	2.1%	$(1f_{5/2} \to 2d_{3/2})$ n	0.01%	$(1f_{7/2} \to 1g_{9/2})$ n
6.1%	$(1f_{7/2} \to 1g_{9/2})$ n	1.0%	$(1f_{5/2} \to 2d_{3/2})$ n	1.7%	$(1f_{7/2} \to 1g_{9/2})$ p	0.01%	$(1g_{9/2} \to 1h_{11/2})$ n
4.6%	$(1f_{5/2} \to 2d_{3/2})$ n	0.9%	$(2p_{3/2} \to 3s_{1/2})$ n	1.3%	$(2p_{1/2} \to 2d_{3/2})$ n		
1.0%	$(2p_{1/2} \to 2d_{3/2})$ n	0.9%	$(2p_{1/2} \to 2d_{3/2})$ n	1.1%	$(2s_{1/2} \to 2p_{3/2})$ p		
0.9%	$(1d_{3/2} \to 2p_{1/2})$ p	0.7%	$(2p_{1/2} \to 4s_{1/2})$ n	0.9%	$(2p_{3/2} \to 3s_{1/2})$ n		
0.9%	$(1d_{3/2} \to 2p_{3/2})$ p	0.5%	$(2p_{3/2} \to 2d_{5/2})$ n	0.2%	$(1d_{3/2} \to 2p_{1/2})$ p		
0.7%	$(2p_{3/2} \to 3s_{1/2})$ n	0.3%	$(1d_{3/2} \to 2p_{3/2})$ p	0.2%	$(1d_{3/2} \to 2p_{3/2})$ p		
0.4%	$(1f_{5/2} \to 3d_{3/2})$ n	0.2%	$(1d_{3/2} \to 2p_{1/2})$ p	0.1%	$(1f_{5/2} \to 3d_{3/2})$ n		
0.3%	$(2s_{1/2} \to 2p_{1/2})$ p	0.1%	$(2p_{1/2} \to 5s_{1/2})$ n				
0.2%	$(2p_{3/2} \to 3d_{5/2})$ n						
0.2%	$(1f_{5/2} \to 3d_{5/2})$ n						
0.2%	$(2p_{3/2} \to 2d_{3/2})$ n						
0.2%	$(1f_{7/2} \to 2d_{5/2})$ p						
0.1%	$(1f_{7/2} \to 2d_{5/2})$ n						
49.2%		69.4%		18.6%		46.92%	

$T = 4$ MeV; $E = 2.55$ MeV		$T = 5$ MeV; $E = 3.87$ MeV		$T = 6$ MeV; $E = 3.63$ MeV	
66.1%	$(2f_{7/2} \to 2g_{9/2})$ n	61.9%	$(2g_{9/2} \to 2h_{11/2})$ n	21.2%	$(1i_{11/2} \to 1j_{13/2})$ n
5.1%	$(3p_{1/2} \to 3d_{3/2})$ n	3.0%	$(3f_{7/2} \to 4d_{5/2})$ n	9.5%	$(2d_{5/2} \to 2f_{7/2})$ p
0.7%	$(2f_{5/2} \to 2g_{7/2})$ n	0.4%	$(2g_{7/2} \to 3f_{5/2})$ n	8.8%	$(1i_{13/2} \to 1j_{15/2})$ n
0.4%	$(2d_{3/2} \to 3p_{1/2})$ n	0.3%	$(2d_{3/2} \to 2f_{5/2})$ p	3.2%	$(2d_{3/2} \to 2f_{5/2})$ n
0.1%	$(1g_{7/2} \to 2f_{5/2})$ n	0.2%	$(1h_{11/2} \to 1i_{13/2})$ n	0.1%	$(2g_{9/2} \to 3f_{7/2})$ n
		0.1%	$(3d_{3/2} \to 2f_{5/2})$ n		
72.4%		65.9%		42.8%	

The FT-RTBA calculations presented in Fig. 4.7 resolve individual states in the low-energy region showing the details of the evolution of the thermally emergent dipole strength. In particular, one can trace how the major peak moves toward lower energies and its intensity increases. The proton and neutron transition densities for the most prominent peak below 10 MeV are displayed for different temperature values in Fig. 4.8 for the neutron-rich ^{68}Ni nucleus and for the neutron-deficient ^{100}Sn nucleus. In the neutron-rich ^{68}Ni nucleus proton and neutron transition densities show in-phase oscillations inside the nucleus while neutron oscillations become absolutely dominant outside for $0 \leq T \leq 5$ MeV. At the temperature $T = 6$ MeV protons and neutrons exhibit out of phase oscillation which resembles the well-recognized pattern of the collective giant resonance. Indeed, as it is shown in Table 4.2 discussed below, the low-energy peak at $T = 6$ MeV has some features of collective nature. The situation is quite similar in the neutron-deficient ^{100}Sn nucleus, which exhibits the in-phase oscillations of protons and neutrons inside the nucleus, but with the dominance of proton oscillations in the outer area. Analogously, at $T = 6$ MeV one starts to distinguish a GDR-like pattern of the out-of-phase oscillation in the low-lying state at $E = 3.25$ MeV. We also notice that at $3 \leq T \leq 6$ MeV the oscillations extend to far distances from the nuclear central region.

In order to have some more insights into the structure of the new low-energy states, we have extracted the $\widetilde{\text{ph}}$ compositions of the strongest low-energy states at various temperatures. The quantities

$$z_{\text{ph}}^{fi} = \frac{|\rho_{\text{ph}}^{fi}|^2 - |\rho_{\text{hp}}^{fi}|^2}{n_{\text{h}}(\varepsilon_{\text{h}}, T) - n_{\text{p}}(\varepsilon_{\text{p}}, T)} \tag{4.5}$$

are given in Table 4.2 in percentage with respect to the FT-RTBA generalized normalization condition of Eq. (3.134). In most of the cases, we omit contributions of less than 0.1%. The bottom line shows the total percentage of pure ph and $\widetilde{\text{ph}}$ configurations, so that the deviation of this number from 100% characterizes the degree of PVC, according to Eq. (3.134).

We start with the state at $E = 6.89$ MeV at $T = 0$ which shows up as a slightly neutron-dominant state with seven two-quasiparticle contributions bigger than 1%. This state can be classified as a relatively collective one. At $T = 1$ MeV the ^{68}Ni nucleus becomes nonsuperfluid and one can see that the strongest low-energy state has a dominant particle-hole configuration. For the $E = 7.70$ MeV state at $T = 2$ MeV the major contribution comes from the PVC as the particle-hole configurations sum up to 18.6% only. It is important to emphasize that the considered peaks at $T \leq 2$ MeV are dominated by the ph transitions of nucleons across the Fermi surface, while at $T \geq 3$ MeV they are mainly composed of the thermal $\widetilde{\text{ph}}$ transitions between the states above the Fermi energy. These states are mostly

located in the continuum, which is discretized in the present calculations. Although a more accurate continuum treatment is necessary to investigate the low-energy response at finite temperatures [137], as the large number of the basis harmonic oscillator shells are taken into account in this work, the discretized description of the continuum should be quite adequate. Thus, we notice that at $T \geq 2$ MeV the collectivity becomes destroyed by the thermal effects until it reappears again at $T = 6.0$ MeV. This temperature is, however, rather high and can be close to the limiting temperature which terminates existence of the nucleus [106].

4.4 Isoscalar Monopole and Quadrupole Resonances in ^{68}Ni

The study of the isoscalar monopole response (ISMR) is essential as the isoscalar giant monopole resonance (ISGMR), which dominates the ISMR, is related to the finite-nucleus incompressibility K_A. This relationship is described by the formula [108]

$$E^{\mathrm{ISGMR}} = \sqrt{\frac{\hbar^2 K_A}{m\langle r^2 \rangle}}, \tag{4.6}$$

where E^{ISGMR} is the centroid of ISGMR, m is the nucleon mass, and $\langle r^2 \rangle$ is the mean-square matter radius. The finite nucleus incompressibility K_A, in turn, can be related to the incompressibility of infinite symmetric nuclear matter K_0 via the leptodermous expansion [164]. The isoscalar monopole response in ^{68}Ni at various temperatures is shown in Fig. 4.9. At temperature $T = 2$ MeV both FT-RRPA and FT-RTBA spectral densities show the emergence of a new soft mode at $E \approx 5$ MeV and it strengthens as the temperature increases. At temperature $T = 3$ MeV one also observes the appearance of another new soft mode at $E \approx 9$ MeV. These two soft modes clearly manifests the effect of the thermal unblocking mechanism. The effect of PVC can be seen from the strong fragmentation of ISGMR for all temperatures. Another observation is the shift of the entire strength distribution toward lower energies with the temperature increase. Respectively, the centroid energy decreases as the temperature increases. According to Eq. (4.6), the decrease of the ISGMR centroid energy means the decrease of the finite-nucleus incompressibility K_A.

At zero temperature, the isoscalar quadrupole response (ISQR) comprises the two main structures of collective character: the pronounced low-energy 2^+ state and the broad collective isoscalar giant quadrupole resonance (ISGQR) at high energy. The ISGQR is closely related to the notion of the effective mass and, thus, provides a constraint on this quantity. It can serve for the determination of the nuclear symmetry energy and neutron skin

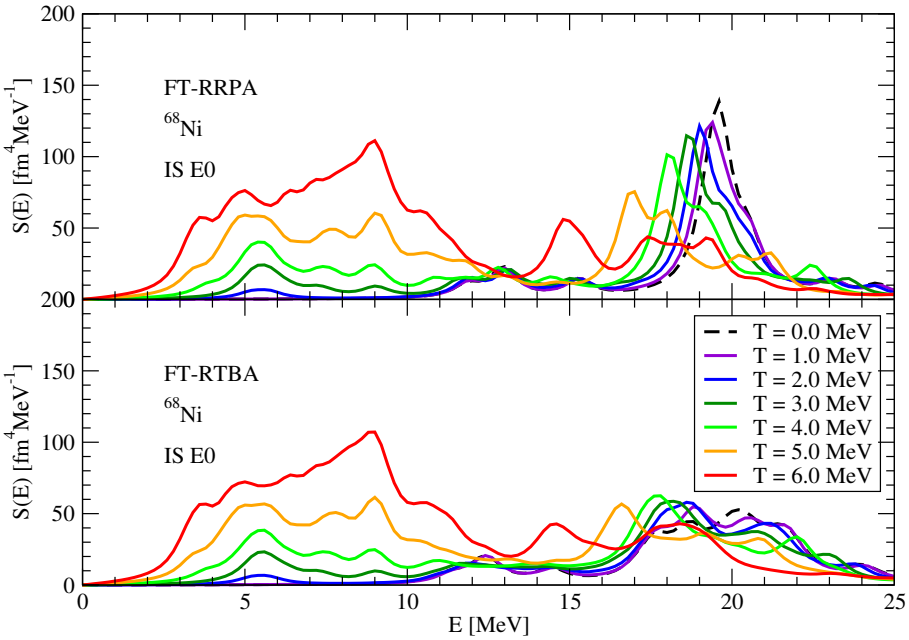

Figure 4.9: The isoscalar monopole response in ^{68}Ni as a function of temperature calculated within FT-RRPA (top panel) and FT-RTBA (bottom panel) with the smearing parameter $\Delta = 500$ keV

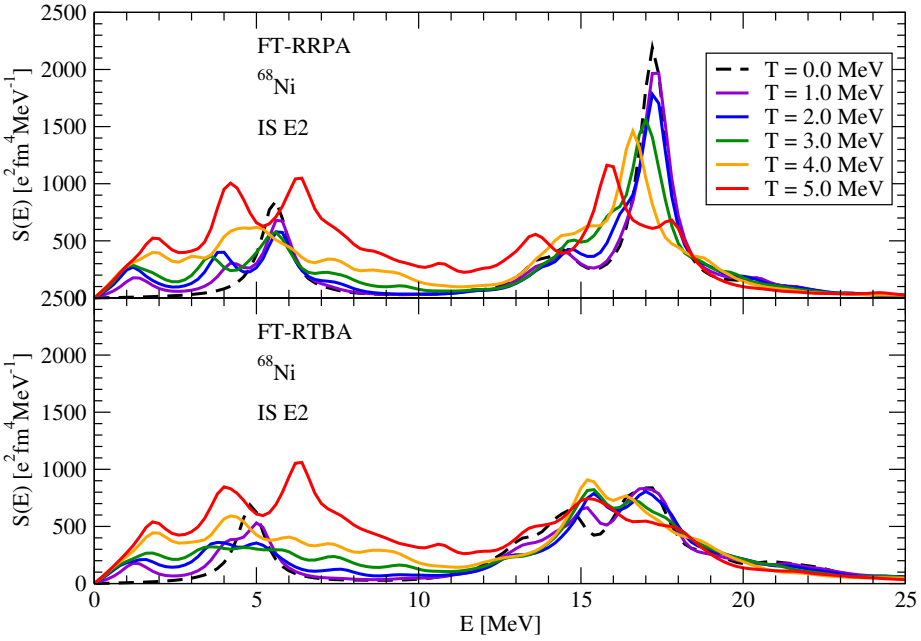

Figure 4.10: The isoscalar quadrupole response in ^{68}Ni as a function of temperature calculated within FT-RRPA (top panel) and FT-RTBA (bottom panel) with the smearing parameter $\Delta = 500$ keV.

thickness and, in addition, shows some sensitivity to the nuclear matter incompressibility [108]. The ISQR in ^{68}Ni at various temperatures is shown in Fig. 4.10, where FT-RRPA results (top panel) can be compared to those of FT-RTBA (bottom panel). At $T = 1$ MeV both FT-RRPA and FT-RTBA strength distributions already demonstrate the formation of new soft modes at the transition energies of $\sim$ 1 MeV and $\sim$ 4 MeV. As in the cases of the dipole and monopole response, the enhancement of the low-energy spectral density becomes stronger as the temperature increases due to the thermal unblocking mechanism. The FT-RTBA high-energy peak remains strongly fragmented at all temperatures. The vigorous enforcement of the PVC effects originates from the enhanced low-energy strengths of the phonons of all multipolarities (those with $J^\pi = 2^+,\ 3^-,\ 4^+,\ 5^-,\ 6^+$ are included in the calculations), as the new thermal phonon modes couple to the single-particle degrees of freedom forming the additional 1p1h $\otimes$ phonon configurations, which enter the $\widetilde{\Phi}(\omega)$ amplitude. The gradual fragmentation of the high-frequency peak and the enhancement of the low-energy spectral density again lead to nearly disappearance of the high-frequency ISGQR at high temperature, i.e., at $T = 5$ MeV.

Chapter 5

Nuclear Mean Field with Point Couplings and Pairing Correlations

5.1 Relativistic Mean-field Theory of Point Coupling

The relativistic mean-field (RMF) theory, which was discussed in Section 2.2, is a phenomenological theory, where the nucleons are treated as quantum mechanical Dirac particles moving independently in an average mean field produced by the exchange of several classical meson fields between the nucleons themselves. In such a phenomenological theory, the number of mesons is limited and the corresponding parameters−the meson masses and coupling constants, and the nonlinear coupling parameters−are adjusted to some bulk properties of a set of spherical nuclei [148]. This so-called RMF theory of finite range (RMFT-FR) is able to quantitatively describe the ground-state properties of spherical and deformed nuclei over the entire periodic table [31, 57]. As it was discussed in the previous chapters, RMFT-FR can also serve as a good starting point for the quantum field theory approaches, which go far beyond the mean-field approximation.

Alternatively to the finite-range interactions, for the low-energy nuclear phenomena, the exchange of heavy mesons can be approximated by contact interactions (point couplings) (see Fig. 5.1), that is the underlying assumption of the relativistic mean-field theory of point coupling (RMFT-PC). In the relativistic point-coupling theory, the isoscalar-scalar (σ-), isoscalar-vector (ω-), and isovector-vector (ρ-) meson exchange terms are replaced by the corresponding contact interactions between the nucleons. The gradient or derivative terms simulate the finite-range effects of the meson-exchange terms. The additional density-dependent interactions, which account for the medium effects, are taken into account by the density-dependent coupling constants in the two-body interactions (e.g., force DD-

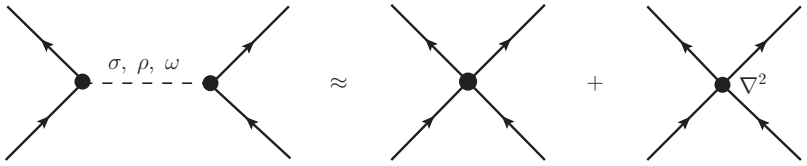

Figure 5.1: Diagrammatic representation of finite-range interactions and their corresponding approximate point-coupling interactions.

PC1), or by many-body contact terms (e.g., force PC-F1). The advantage of the RMFT-PC over the RMFT-FR is distinct. The numerical applications of RMFT-PC are more straightforward since one no longer solves the Klein-Gordon equations for the mesons, and the obtained particle-hole interaction has a channel structure and contains Dirac delta-function in coordinate space. The later summarizes the main reason one shifts from the RMFT-FR to the RMFT-PC when addressing the continuum effects. In the following section, we present the detailed theoretical framework of the relativistic point-coupling theory with DD-PC1 parametrizations. The interested reader can find our detailed review on the RMFT-PC with PC-F1 parameterizations in Appendix D.

5.1.1 DD-PC1 Force

We consider an effective Lagrangian of the form: [38]

$$\begin{aligned}\mathscr{L} &= \overline{\Psi}(i\gamma^{\mu}\partial_{\mu} - M)\Psi - \frac{1}{2}\alpha_S(\hat{\rho})(\overline{\Psi}\Psi)(\overline{\Psi}\Psi) - \frac{1}{2}\alpha_V(\hat{\rho})(\overline{\Psi}\gamma^{\mu}\Psi)(\overline{\Psi}\gamma_{\mu}\Psi) \\ &- \frac{1}{2}\alpha_{TV}(\hat{\rho})(\overline{\Psi}\vec{\tau}\gamma^{\mu}\Psi)\cdot(\overline{\Psi}\vec{\tau}\gamma_{\mu}\Psi) - \frac{1}{2}\delta_S(\partial_{\nu}\overline{\Psi}\Psi)(\partial^{\nu}\overline{\Psi}\Psi) - e\overline{\Psi}\gamma^{\mu}A_{\mu}\frac{1-\tau_3}{2}\Psi, \quad (5.1)\end{aligned}$$

which now includes the isoscalar-scalar, isoscalar-vector, and isovector-vector four-fermion interactions as well as the electromagnetic interaction. From the Euler-Lagrange equation

$$\frac{\partial\mathscr{L}}{\partial\overline{\Psi}} - \frac{\partial}{\partial x^{\mu}}\left[\frac{\partial\mathscr{L}}{\partial(\partial_{\mu}\overline{\Psi})}\right] = 0, \quad (5.2)$$

we obtain the equation of motion

$$[\gamma^{\mu}(i\partial_{\mu} - \Sigma^{\mu}_V - \vec{\tau}\cdot\vec{\Sigma}^{\mu}_{TV} - \Sigma^{\mu}_R) - (M + \Sigma_S)]\Psi = 0, \quad (5.3)$$

where isoscalar-scalar, isoscalar-vector, and isovector-vector mass operators are respectively given by

$$\begin{aligned}
\Sigma_S &= \alpha_S(\hat{\rho})(\overline{\Psi}\Psi) - \delta_S\Box(\overline{\Psi}\Psi), && (5.4)\\
\Sigma_V^\mu &= \alpha_V(\hat{\rho})j^\mu + eA^\mu\frac{1-\tau_3}{2}, && (5.5)\\
\vec{\Sigma}_{TV}^\mu &= \alpha_{TV}(\hat{\rho})(\overline{\Psi}\vec{\tau}\gamma^\mu\Psi), && (5.6)
\end{aligned}$$

and the rearrangement term Σ_R^μ is given as

$$\Sigma_R^\mu = \frac{1}{2}u^\mu\left\{\frac{\partial\alpha_S(\hat{\rho})}{\partial\hat{\rho}}(\overline{\Psi}\Psi)(\overline{\Psi}\Psi) + \frac{\partial\alpha_V(\hat{\rho})}{\partial\hat{\rho}}j^\alpha j_\alpha + \frac{\partial\alpha_{TV}(\hat{\rho})}{\partial\hat{\rho}}(\overline{\Psi}\vec{\tau}\gamma^\alpha\Psi)\cdot(\overline{\Psi}\vec{\tau}\gamma_\alpha\Psi)\right\}. \quad (5.7)$$

Here the nucleon four-current j^μ is defined as

$$j^\mu = \overline{\Psi}\gamma^\mu\Psi = \hat{\rho}u^\mu, \quad (5.8)$$

where the four-velocity u^μ is

$$u^\mu = \frac{(1,\mathbf{v})}{\sqrt{1-v^2}} \quad (5.9)$$

and the velocity $\mathbf{v}$ equals to zero in the rest-frame of the nuclear system. Accordingly, the strength parameters α_i ($i = S,\ V,\ TV$) depend on the density $\hat{\rho} = j^\mu u_\mu$. Multiplying Eq. (5.3) from the left by Dirac matrix γ^0, one obtains

$$\begin{aligned}
0 &= \Big\{i\partial_0 + i\boldsymbol{\alpha}\cdot\boldsymbol{\nabla} - \beta M - \frac{1}{2}\beta\frac{\partial\alpha_S(\hat{\rho})}{\partial\hat{\rho}}\gamma^\alpha u_\alpha(\overline{\Psi}\Psi)(\overline{\Psi}\Psi) - \beta\alpha_S(\hat{\rho})(\overline{\Psi}\Psi)\\
&- \frac{1}{2}\beta\frac{\partial\alpha_V(\hat{\rho})}{\partial\hat{\rho}}\gamma^\alpha u_\alpha j^\mu j_\mu - \beta\alpha_V(\hat{\rho})(\overline{\Psi}\gamma_\mu\Psi)\gamma^\mu - \frac{1}{2}\beta\frac{\partial\alpha_{TV}(\hat{\rho})}{\partial\hat{\rho}}\gamma^\alpha u_\alpha(\overline{\Psi}\vec{\tau}\gamma^\mu\Psi)\cdot(\overline{\Psi}\vec{\tau}\gamma_\mu\Psi)\\
&- \beta\alpha_{TV}(\hat{\rho})(\overline{\Psi}\vec{\tau}\gamma_\mu\Psi)\cdot\vec{\tau}\gamma^\mu - e\beta\gamma^\mu A_\mu\frac{1-\tau_3}{2} + \beta\delta_S\Box(\overline{\Psi}\Psi)\Big\}\Psi. \quad (5.10)
\end{aligned}$$

Making use of the stationary solution of the form

$$\Psi(\mathbf{r},t) = \sum_k \varphi_k(\mathbf{r})e^{-i\epsilon_k t}\hat{a}_k, \quad (5.11)$$

one arrives at

$$0 = \Big\{\epsilon_k - (\boldsymbol{\alpha}\cdot\mathbf{p} + \beta M) - \frac{1}{2}\beta\frac{\partial\alpha_S(\hat{\rho})}{\partial\hat{\rho}}\gamma^\alpha u_\alpha(\overline{\Psi}\Psi)(\overline{\Psi}\Psi) - \beta\alpha_S(\hat{\rho})(\overline{\Psi}\Psi)$$

$$
\begin{aligned}
- \quad & \frac{1}{2}\beta\frac{\partial\alpha_V(\hat{\rho})}{\partial\hat{\rho}}\gamma^\alpha u_\alpha j^\mu j_\mu - \beta\alpha_V(\hat{\rho})(\overline{\Psi}\gamma_\mu\Psi)\gamma^\mu - \frac{1}{2}\beta\frac{\partial\alpha_{TV}(\hat{\rho})}{\partial\hat{\rho}}\gamma^\alpha u_\alpha(\overline{\Psi}\vec{\tau}\gamma^\mu\Psi)\cdot(\overline{\Psi}\vec{\tau}\gamma_\mu\Psi) \\
- \quad & \beta\alpha_{TV}(\hat{\rho})(\overline{\Psi}\vec{\tau}\gamma_\mu\Psi)\cdot\vec{\tau}\gamma^\mu - e\beta\gamma^\mu A_\mu\frac{1-\tau_3}{2} + \beta\delta_S\Box(\overline{\Psi}\Psi)\Bigg\}\varphi_k(\mathbf{r}). \qquad (5.12)
\end{aligned}
$$

Taking the expectation value of this result with respect to the nuclear ground state $|\Phi\rangle$, one obtains

$$
\begin{aligned}
0 \;=\; & \Bigg\{\epsilon_k - (\boldsymbol{\alpha}\cdot\mathbf{p}+\beta M) - \frac{1}{2}\beta\frac{\partial\alpha_S(\rho_V)}{\partial\rho_V}\gamma^\alpha\frac{j_{\alpha V}(\mathbf{r})}{\rho_V}\rho_S^2(\mathbf{r}) - \beta\alpha_S(\rho_V)\rho_S(\mathbf{r}) \\
- \; & \frac{1}{2}\beta\frac{\partial\alpha_V(\rho_V)}{\partial\rho_V}\gamma^\alpha\frac{j_\alpha}{\rho_V}j_{\mu V}(\mathbf{r})j_V^\mu(\mathbf{r}) - \beta\alpha_V(\rho_V)j_{\mu V}(\mathbf{r})\gamma^\mu \\
- \; & \frac{1}{2}\beta\frac{\partial\alpha_{TV}(\rho_V)}{\partial\rho_V}\frac{j_{\alpha V}(\mathbf{r})}{\rho_V}\gamma^\alpha\vec{j}_{TV}^{\,\mu}(\mathbf{r})\cdot\vec{j}_{\mu TV}(\mathbf{r}) - \beta\alpha_{TV}(\rho_V)\vec{j}_{TV}^{\,\mu}\cdot\vec{\tau}\gamma_\mu \\
- \; & \beta e\gamma^\mu A_\mu\frac{1-\tau_3}{2} - \beta\delta_S\nabla^2\rho_S(\mathbf{r})\Bigg\}\varphi_k(\mathbf{r}), \qquad (5.13)
\end{aligned}
$$

where

$$
\begin{aligned}
\rho_S(\mathbf{r}) \;&=\; \langle\Phi|\overline{\Psi}\Psi|\Phi\rangle = \sum_{k\ell}\overline{\varphi}_k(\mathbf{r})\varphi_\ell(\mathbf{r})e^{i(\epsilon_k-\epsilon_\ell)t}\langle\Phi|\hat{a}_k^\dagger\hat{a}_\ell|\Phi\rangle \\
&=\; \sum_k n_k\overline{\varphi}_k(\mathbf{r})\varphi_k(\mathbf{r}), \qquad (5.14) \\
\rho \;&=\; \langle\Phi|\hat{\rho}|\Phi\rangle = \langle\Phi|\overline{\Psi}\gamma^\mu\Psi|\Phi\rangle u_\mu = u_\mu\sum_{k\ell}\overline{\varphi}_k(\mathbf{r})\gamma^\mu\varphi_\ell(\mathbf{r})e^{i(\epsilon_k-\epsilon_\ell)t}\langle\Phi|\hat{a}_k^\dagger\hat{a}_\ell|\Phi\rangle \\
&=\; u_\mu\sum_k n_k\overline{\varphi}_k(\mathbf{r})\gamma^\mu\varphi_k(\mathbf{r}) = u_\mu j_V^\mu(\mathbf{r}), \qquad (5.15) \\
\vec{j}_{\mu TV}(\mathbf{r}) \;&=\; \langle\Phi|\overline{\Psi}\vec{\tau}\gamma_\mu\Psi|\Phi\rangle = \sum_k n_k\overline{\varphi}_k(\mathbf{r})\vec{\tau}\gamma_\mu\varphi_k(\mathbf{r}). \qquad (5.16)
\end{aligned}
$$

In the rest frame of the nuclear system, where $\mathbf{v}=0$, only the time-like $u_0=1$ component of the velocity four-vector survives, so that we can substitute ρ with ρ_V of the form

$$
\rho_V = u_0 j_V^0(\mathbf{r}) = \sum_k n_k\varphi_k^\dagger(\mathbf{r})\varphi_k(\mathbf{r}). \qquad (5.17)
$$

The dependence of the strength parameters α_i ($i=S,\ V,\ TV$) on the density ρ_V is given by

$$
\alpha_i(\rho_V) = a_i + (b_i + c_i x)e^{-d_i x}, \qquad (5.18)
$$

where $x = \rho_V/\rho_{\rm sat}$. Here $\rho_{\rm sat}$ denotes the nucleonic saturation density of symmetric nuclear matter. The values of the parameters α_i are tabulated in Table 5.1.

Table 5.1: The density-dependent coupling constants in the DD-PC1 parameterization [38, 39]. The coupling constants a_{TV} and c_{TV} are zero.

Parameter	Value	Dimension
a_S	-10.0462	[fm^2]
b_S	-9.1504	[fm^2]
c_S	-6.4273	[fm^2]
d_S	1.3724	
a_V	5.9195	[fm^2]
b_V	8.8637	[fm^2]
d_V	0.6584	
b_{TV}	1.8360	[fm^2]
d_{TV}	0.6400	
δ_S	-0.815	[fm^4]

A further simplification can be made by considering: (1) the time-reversal symmetry of the mean field and (2) the isospin as a good quantum number. We thus obtain the Dirac Hamiltonian $\hat{h}^D$ of the form

$$\hat{h}^D = \boldsymbol{\alpha}\cdot\mathbf{p} + \beta[M + S(\mathbf{r})] + V(\mathbf{r}), \tag{5.19}$$

where

$$\begin{aligned}
S(\mathbf{r}) &= [\alpha_S(\rho_V) + \delta_S\nabla^2]\rho_S(\mathbf{r}), && (5.20)\\
V(\mathbf{r}) &= \Sigma_R(\mathbf{r}) + \Sigma_V(\mathbf{r}) + \tau_3\Sigma_{TV}(\mathbf{r}), && (5.21)\\
\Sigma_R(\mathbf{r}) &= \frac{1}{2}\frac{\partial\alpha_S(\rho_V)}{\partial\rho_V}\rho_S^2(\mathbf{r}) + \frac{1}{2}\frac{\partial\alpha_V(\rho_V)}{\partial\rho_V}\rho_V^2(\mathbf{r}) + \frac{1}{2}\frac{\partial\alpha_{TV}(\rho_V)}{\partial\rho_V}\rho_{TV}^2(\mathbf{r}), && (5.22)\\
\Sigma_V(\mathbf{r}) &= \alpha_V(\rho_V)\rho_V(\mathbf{r}) + eA_0\frac{1}{2}(1-\tau_3), && (5.23)\\
\Sigma_{TV}(\mathbf{r}) &= \alpha_{TV}(\rho_V)\rho_{TV}(\mathbf{r}). && (5.24)
\end{aligned}$$

The Hamiltonian $\hat{H}$ can be obtain from the Lagrangian (5.1) via

$$\hat{H} = \int d^3\mathbf{r}\left\{\frac{\partial\mathscr{L}}{\partial(\partial_0\Psi)}(\partial_0\Psi) + (\partial_0\overline{\Psi})\frac{\partial\mathscr{L}}{\partial(\partial_0\overline{\Psi})} + \frac{\partial\mathscr{L}}{\partial(\partial_0 A_\mu)}(\partial_0 A_\mu) - \mathscr{L}\right\}. \tag{5.25}$$

An insertion of the Lagrangian $\mathscr{L}$ into the Hamiltonian $\hat{H}$ leads to

$$\begin{aligned}
\hat{H} &= \int d^3\mathbf{r}\Bigg\{ \Psi^\dagger(\boldsymbol{\alpha}\cdot\mathbf{p}+\beta M)\Psi + \frac{1}{2}\alpha_S(\hat{\rho})(\overline{\Psi}\Psi)(\overline{\Psi}\Psi) \\
&+ \frac{1}{2}\alpha_V(\hat{\rho})(\overline{\Psi}\gamma^\mu\Psi)(\overline{\Psi}\gamma_\mu\Psi) + \frac{1}{2}\alpha_{TV}(\hat{\rho})(\overline{\Psi}\vec{\tau}\gamma^\mu\Psi)\cdot(\overline{\Psi}\vec{\tau}\gamma_\mu\Psi) \\
&- \frac{1}{2}\delta_S[(\partial_0\overline{\Psi}\Psi)(\partial^0\Psi\Psi) + (\boldsymbol{\nabla}\overline{\Psi}\Psi)\cdot(\boldsymbol{\nabla}\overline{\Psi}\Psi)] + e\overline{\Psi}\gamma^\mu A_\mu\frac{1-\tau_3}{2}\Psi\Bigg\}. \qquad (5.26)
\end{aligned}$$

Making use of the stationary solution of the form

$$\Psi(\mathbf{r},t) = \sum_k \varphi_k(\mathbf{r})e^{-i\epsilon_k t}\hat{a}_k \rightsquigarrow \Psi^\dagger(\mathbf{r},t) = \sum_\ell \varphi_\ell^\dagger(\mathbf{r})e^{i\epsilon_\ell t}\hat{a}_\ell^\dagger \qquad (5.27)$$

and taking the expectation value with respect to the nuclear ground state $|\Phi\rangle$, we obtain the covariant energy density functional (CEDF)

$$\begin{aligned}
E_{\rm RMF}[\hat{\rho},A] &\equiv \langle\Phi|\hat{H}|\Phi\rangle \\
&= \int d^3\mathbf{r}\sum_{k\ell}\varphi_k^\dagger(\mathbf{r},t)(\boldsymbol{\alpha}\cdot\mathbf{p}+\beta M)\varphi_\ell(\mathbf{r},t)\rho_{\ell k} \\
&+ \frac{1}{2}\int d^3\mathbf{r}\langle\Phi|\alpha_S(\hat{\rho})|\Phi\rangle\sum_{k\ell}\varphi_k^\dagger(\mathbf{r},t)\gamma^0\varphi_\ell(\mathbf{r},t)\rho_{\ell k} \\
&\times \sum_{mn}\varphi_m^\dagger(\mathbf{r},t)\gamma^0\varphi_n(\mathbf{r},t)\rho_{nm} \\
&+ \frac{1}{2}\int d^3\mathbf{r}\langle\Phi|\alpha_V(\hat{\rho})|\Phi\rangle\sum_{k\ell}\varphi_k^\dagger(\mathbf{r},t)\gamma^0\gamma^\mu\varphi_\ell(\mathbf{r},t)\rho_{\ell k} \\
&\times \sum_{mn}\varphi_m^\dagger(\mathbf{r},t)\gamma^0\gamma_\mu\varphi_n(\mathbf{r},t)\rho_{nm} \\
&+ \frac{1}{2}\int d^3\mathbf{r}\langle\Phi|\alpha_{TV}(\hat{\rho})|\Phi\rangle\sum_{k\ell}\varphi_k^\dagger(\mathbf{r},t)\gamma^0\vec{\tau}\gamma^\mu\varphi_\ell(\mathbf{r},t)\rho_{\ell k} \\
&\times \sum_{mn}\varphi_m^\dagger(\mathbf{r},t)\gamma^0\vec{\tau}\gamma_\mu\varphi_n(\mathbf{r},t)\rho_{nm} \\
&- \frac{1}{2}\delta_S\int d^3\mathbf{r}\sum_{k\ell}\partial_0\varphi_k^\dagger(\mathbf{r},t)\gamma^0\varphi_\ell(\mathbf{r},t)\rho_{\ell k} \\
&\times \sum_{mn}\partial^0\varphi_m^\dagger(\mathbf{r},t)\gamma_0\varphi_n(\mathbf{r},t)\rho_{nm} \\
&- \frac{1}{2}\delta_S\int d^3\mathbf{r}\sum_{k\ell}[\boldsymbol{\nabla}\varphi_k^\dagger(\mathbf{r},t)\gamma^0\varphi_\ell(\mathbf{r},t)]\rho_{\ell k}
\end{aligned}$$

$$
\begin{aligned}
&\times \quad \sum_{mn}[\boldsymbol{\nabla}\varphi_m^\dagger(\mathbf{r},t)\gamma^0\varphi_n(\mathbf{r},t)]\rho_{nm} \\
&+ \quad e\int d^3\mathbf{r}\sum_{k\ell}\varphi_k^\dagger(\mathbf{r},t)\gamma^0\gamma^\mu\frac{1-\tau_3}{2}A_\mu\varphi_\ell(\mathbf{r},t)\rho_{\ell k}. \qquad (5.28)
\end{aligned}
$$

Defining

$$
\mathrm{Tr}[\hat{\mathscr{O}}\hat{\rho}(\mathbf{r})] = \sum_k n_k\varphi_k^\dagger(\mathbf{r})\mathscr{O}\varphi_k(\mathbf{r}), \qquad (5.29)
$$

the CEDF (5.28) can be expressed as

$$
\begin{aligned}
E_{\mathrm{RMF}}[\hat{\rho},A] &= \int d^3\mathbf{r}\,\mathrm{Tr}[(\boldsymbol{\alpha}\cdot\mathbf{p}+\beta M)\hat{\rho}(\mathbf{r})] \\
&+ \int d^3\mathbf{r}\int d^3\mathbf{r}'\delta(\mathbf{r}-\mathbf{r}')\,\mathrm{Tr}[\gamma^0\hat{\rho}(\mathbf{r})]\frac{1}{2}\alpha_S[\mathrm{Tr}\,\hat{\rho}(\mathbf{r})]\,\mathrm{Tr}[\gamma^0\hat{\rho}(\mathbf{r}')] \\
&+ \int d^3\mathbf{r}\int d^3\mathbf{r}'\delta(\mathbf{r}-\mathbf{r}')\,\mathrm{Tr}\,\hat{\rho}(\mathbf{r})\frac{1}{2}\alpha_V[\mathrm{Tr}\,\hat{\rho}(\mathbf{r})]\,\mathrm{Tr}\,\hat{\rho}(\mathbf{r}') \\
&+ \int d^3\mathbf{r}\int d^3\mathbf{r}'\delta(\mathbf{r}-\mathbf{r}')\,\mathrm{Tr}[\gamma^0\gamma^i\hat{\rho}(\mathbf{r})]\frac{1}{2}\alpha_V[\mathrm{Tr}\,\hat{\rho}(\mathbf{r})]\,\mathrm{Tr}[\gamma^0\gamma_i\hat{\rho}(\mathbf{r}')] \\
&+ \int d^3\mathbf{r}\int d^3\mathbf{r}'\delta(\mathbf{r}-\mathbf{r}')\,\mathrm{Tr}[\vec{\tau}\hat{\rho}(\mathbf{r})]\frac{1}{2}\alpha_{TV}[\mathrm{Tr}\,\hat{\rho}(\mathbf{r})]\cdot\mathrm{Tr}[\vec{\tau}\hat{\rho}(\mathbf{r}')] \\
&+ \int d^3\mathbf{r}\int d^3\mathbf{r}'\delta(\mathbf{r}-\mathbf{r}')\,\mathrm{Tr}[\gamma^0\gamma^i\vec{\tau}\hat{\rho}(\mathbf{r})]\frac{1}{2}\alpha_{TV}[\mathrm{Tr}\,\hat{\rho}(\mathbf{r})]\cdot\mathrm{Tr}[\gamma^0\gamma_i\vec{\tau}\hat{\rho}(\mathbf{r}')] \\
&+ \int d^3\mathbf{r}\int d^3\mathbf{r}'\delta(\mathbf{r}-\mathbf{r}')\,\mathrm{Tr}[\gamma^0\hat{\rho}(\mathbf{r})]\frac{1}{2}\delta_S\nabla^2\,\mathrm{Tr}[\gamma^0\hat{\rho}(\mathbf{r}')] \\
&+ e\int d^3\mathbf{r}\,\mathrm{Tr}\left[\left(\gamma^0\gamma^\mu\frac{1-\tau_3}{2}A_\mu(\mathbf{r})\right)\hat{\rho}(\mathbf{r})\right]. \qquad (5.30)
\end{aligned}
$$

One considers (1) the time-reversal symmetry of the mean field and (2) isospin is a good quantum number. The CEDF $E_{\mathrm{RMF}}[\hat{\rho},A]$ thus becomes

$$
\begin{aligned}
E_{\mathrm{RMF}}[\hat{\rho},A] &= \int d^3\mathbf{r}\,\mathrm{Tr}[(\boldsymbol{\alpha}\cdot\mathbf{p}+\beta M)\hat{\rho}(\mathbf{r})] \\
&+ \int d^3\mathbf{r}\int d^3\mathbf{r}'\delta(\mathbf{r}-\mathbf{r}')\,\mathrm{Tr}[\gamma^0\hat{\rho}(\mathbf{r})]\frac{1}{2}\alpha_S[\mathrm{Tr}\,\hat{\rho}(\mathbf{r})]\,\mathrm{Tr}[\gamma^0\hat{\rho}(\mathbf{r}')] \\
&+ \int d^3\mathbf{r}\int d^3\mathbf{r}'\delta(\mathbf{r}-\mathbf{r}')\,\mathrm{Tr}\,\hat{\rho}(\mathbf{r})\frac{1}{2}\alpha_V[\mathrm{Tr}\,\hat{\rho}(\mathbf{r})]\,\mathrm{Tr}\,\hat{\rho}(\mathbf{r}') \\
&- \int d^3\mathbf{r}\int d^3\mathbf{r}'\delta(\mathbf{r}-\mathbf{r}')\,\mathrm{Tr}[\gamma^0\gamma^i\hat{\rho}(\mathbf{r})]\frac{1}{2}\alpha_V[\mathrm{Tr}\,\hat{\rho}(\mathbf{r})]\,\mathrm{Tr}[\gamma^0\gamma^i\hat{\rho}(\mathbf{r}')] \\
&+ \int d^3\mathbf{r}\int d^3\mathbf{r}'\delta(\mathbf{r}-\mathbf{r}')\,\mathrm{Tr}[\tau_3\hat{\rho}(\mathbf{r})]\frac{1}{2}\alpha_{TV}[\mathrm{Tr}\,\hat{\rho}(\mathbf{r})]\cdot\mathrm{Tr}[\tau_3\hat{\rho}(\mathbf{r}')] \\
&- \int d^3\mathbf{r}\int d^3\mathbf{r}'\delta(\mathbf{r}-\mathbf{r}')\,\mathrm{Tr}[\gamma^0\gamma^i\tau_3\hat{\rho}(\mathbf{r})]\frac{1}{2}\alpha_{TV}[\mathrm{Tr}\,\hat{\rho}(\mathbf{r})]\cdot\mathrm{Tr}[\gamma^0\gamma^i\tau_3\hat{\rho}(\mathbf{r}')]
\end{aligned}
$$

$$
\begin{aligned}
&+ \int d^3\mathbf{r} \int d^3\mathbf{r}' \delta(\mathbf{r}-\mathbf{r}') \,\mathrm{Tr}[\gamma^0 \hat{\rho}(\mathbf{r})] \frac{1}{2} \delta_S \nabla^2 \,\mathrm{Tr}[\gamma^0 \hat{\rho}(\mathbf{r}')] \\
&+ e \int d^3\mathbf{r} \,\mathrm{Tr}\left[\left(\frac{1-\tau_3}{2} A_0(\mathbf{r}) \right) \hat{\rho}(\mathbf{r}) \right], \qquad (5.31)
\end{aligned}
$$

where we have used the identity $\gamma_i = -\gamma^i$ $(i = 1, 2, 3)$. Using the identity

$$
\frac{\delta \,\mathrm{Tr}[\hat{\mathscr{O}} \hat{\rho}(\mathbf{r})]}{\delta \hat{\rho}(\mathbf{r}_1)} = \mathscr{O}(\mathbf{r}) \delta(\mathbf{r}-\mathbf{r}_1), \qquad (5.32)
$$

one obtains

$$
\begin{aligned}
\frac{\delta E_{\mathrm{RMF}}}{\delta \hat{\rho}(\mathbf{r}_1)} &= (\boldsymbol{\alpha}\cdot\mathbf{p} + \beta M)^{(1)} + \gamma^{0(1)} \frac{1}{2} \alpha_S(\rho_V(\mathbf{r}_1)) \,\mathrm{Tr}[\gamma^0 \hat{\rho}(\mathbf{r}_1)] \\
&+ \frac{1}{2} \frac{\partial \alpha_S(\rho_V(\mathbf{r}_1))}{\partial \rho_V(\mathbf{r}_1)} \,\mathrm{Tr}^2[\gamma^0 \hat{\rho}(\mathbf{r}_1)] \mathbf{1}^{(1)} + \mathrm{Tr}[\gamma^0 \hat{\rho}(\mathbf{r}_1)] \frac{1}{2} \alpha_S(\rho_V(\mathbf{r}_1)) \gamma^{0(1)} \\
&+ \mathbf{1}^{(1)} \frac{1}{2} \alpha_V(\rho_V(\mathbf{r}_1)) \,\mathrm{Tr}\,\hat{\rho}(\mathbf{r}_1) + \frac{1}{2} \frac{\partial \alpha_V(\rho_V(\mathbf{r}_1))}{\partial \rho_V(\mathbf{r}_1)} \,\mathrm{Tr}^2\,\hat{\rho}(\mathbf{r}_1) \mathbf{1}^{(1)} \\
&+ \mathrm{Tr}\,\hat{\rho}(\mathbf{r}_1) \frac{1}{2} \alpha_V(\rho_V(\mathbf{r}_1)) \mathbf{1}^{(1)} - \gamma^{0(1)} \gamma^{i(1)} \frac{1}{2} \alpha_V(\rho_V(\mathbf{r}_1)) \,\mathrm{Tr}[\gamma^0 \gamma^i \hat{\rho}(\mathbf{r}_1)] \\
&- \frac{1}{2} \frac{\partial \alpha_V(\rho_V(\mathbf{r}_1))}{\partial \rho_V(\mathbf{r}_1)} \,\mathrm{Tr}^2[\gamma^0 \gamma^i \hat{\rho}(\mathbf{r}_1)] \mathbf{1}^{(1)} - \mathrm{Tr}[\gamma^0 \gamma^i \hat{\rho}(\mathbf{r}_1)] \frac{1}{2} \alpha_V(\rho_V(\mathbf{r}_1)) \gamma^{0(1)} \gamma^{i(1)} \\
&+ \tau_3^{(1)} \frac{1}{2} \alpha_{TV}(\rho_V(\mathbf{r}_1)) \,\mathrm{Tr}[\tau_3 \hat{\rho}(\mathbf{r}_1)] + \frac{1}{2} \frac{\partial \alpha_{TV}(\rho_V(\mathbf{r}_1))}{\partial \rho_V(\mathbf{r}_1)} \,\mathrm{Tr}^2[\tau_3 \hat{\rho}(\mathbf{r}_1)] \mathbf{1}^{(1)} \\
&+ \mathrm{Tr}[\tau_3 \hat{\rho}(\mathbf{r}_1)] \frac{1}{2} \alpha_{TV}(\rho_V(\mathbf{r}_1)) \tau_3^{(1)} - \gamma^{0(1)} \gamma^{i(1)} \tau_3^{(1)} \frac{1}{2} \alpha_{TV}(\rho_V(\mathbf{r}_1)) \,\mathrm{Tr}[\gamma^0 \gamma^i \tau_3 \hat{\rho}(\mathbf{r}_1)] \\
&- \frac{1}{2} \frac{\partial \alpha_{TV}(\rho_V(\mathbf{r}_1))}{\partial \rho_V(\mathbf{r}_1)} \,\mathrm{Tr}^2[\gamma^0 \gamma^i \tau_3 \hat{\rho}(\mathbf{r}_1)] \mathbf{1}^{(1)} \\
&- \mathrm{Tr}[\gamma^0 \gamma^i \tau_3 \hat{\rho}(\mathbf{r}_1)] \frac{1}{2} \alpha_{TV}(\rho_V(\mathbf{r}_1)) \gamma^{0(1)} \gamma^{i(1)} \tau_3^{(1)} \\
&+ \gamma^{0(1)} \frac{1}{2} \delta_S \nabla_1^2 \,\mathrm{Tr}[\gamma^0 \hat{\rho}(\mathbf{r}_1)] + \mathrm{Tr}[\gamma^0 \hat{\rho}(\mathbf{r}_1)] \frac{1}{2} \delta_S \nabla_1^2 \gamma^{0(1)} \\
&+ \left[\frac{1-\tau_3}{2} \right]^{(1)} \frac{e^2}{4\pi} \int d^3\mathbf{r}' \frac{1}{|\mathbf{r}_1 - \mathbf{r}'|} \,\mathrm{Tr}\left[\left(\frac{1-\tau_3}{2} \right) \hat{\rho}(\mathbf{r}') \right], \qquad (5.33)
\end{aligned}
$$

where one has used the expression of the Coulomb field $A_0(\mathbf{r})$ of the form

$$
A^0(\mathbf{r}) = \frac{e}{4\pi} \int d^3\mathbf{r}' \frac{\rho_C(\mathbf{r}')}{|\mathbf{r}-\mathbf{r}'|}, \qquad \rho_C(\mathbf{r}) = \sum_k n_k \varphi_k^\dagger(\mathbf{r}) \frac{1-\tau_3}{2} \varphi_k(\mathbf{r}). \qquad (5.34)
$$

Second variational derivative of $E_{\mathrm{RMF}}[\hat{\rho}, A]$ with respect to $\hat{\rho}(\mathbf{r})$ results in the particle-hole

(ph) interaction $V^{\rm ph}(1,2)$ of the form

$$
\begin{aligned}
V^{\rm ph}(1,2) &= \frac{\delta^2 E_{\rm RMF}}{\delta\hat{\rho}(\mathbf{r}_1)\delta\hat{\rho}(\mathbf{r}_2)} \\
&= \gamma^{0(1)}[\alpha_S(\rho_V(\mathbf{r}_1)) + \delta_S\nabla_1^2]\delta(\mathbf{r}_1-\mathbf{r}_2)\gamma^{0(2)} \\
&+ \mathbf{1}^{(1)}\left[\frac{1}{2}\frac{\partial^2\alpha_S(\rho_V(\mathbf{r}_1))}{\partial\rho_V^2(\mathbf{r}_1)}\rho_S^2(\mathbf{r}_1) + 2\frac{\partial\alpha_V(\rho_V(\mathbf{r}_1))}{\partial\rho_V(\mathbf{r}_1)}\rho_V(\mathbf{r}_1) + \alpha_V(\rho_V(\mathbf{r}_1))\right. \\
&+ \left.\frac{1}{2}\frac{\partial^2\alpha_V(\rho_V(\mathbf{r}_1))}{\partial\rho_V^2(\mathbf{r}_1)}\rho_V^2(\mathbf{r}_1) + \frac{1}{2}\frac{\partial^2\alpha_{TV}(\rho_V(\mathbf{r}_1))}{\partial\rho_V^2(\mathbf{r}_1)}\rho_{TV}^2(\mathbf{r}_1)\right]\delta(\mathbf{r}_1-\mathbf{r}_2)\mathbf{1}^{(2)} \\
&+ \tau_3^{(1)}\alpha_{TV}(\rho_V(\mathbf{r}_1))\delta(\mathbf{r}_1-\mathbf{r}_2)\tau_3^{(2)} \\
&- \gamma^{0(1)}\gamma^{i(1)}\alpha_V(\rho_V(\mathbf{r}_1))\delta(\mathbf{r}_1-\mathbf{r}_2)\gamma^{0(2)}\gamma^{i(2)} \\
&- \gamma^{0(1)}\gamma^{i(1)}\tau_3^{(1)}\alpha_{TV}(\rho_V(\mathbf{r}_1))\delta(\mathbf{r}_1-\mathbf{r}_2)\gamma^{0(2)}\gamma^{i(2)}\tau_3^{(2)} \\
&+ \gamma^{0(1)}\frac{\partial\alpha_S(\rho_V(\mathbf{r}_1))}{\partial\rho_V(\mathbf{r}_1)}\rho_S(\mathbf{r}_1)\delta(\mathbf{r}_1-\mathbf{r}_2)\mathbf{1}^{(2)} \\
&+ \mathbf{1}^{(1)}\frac{\partial\alpha_S(\rho_V(\mathbf{r}_1))}{\partial\rho_V(\mathbf{r}_1)}\rho_S(\mathbf{r}_1)\delta(\mathbf{r}_1-\mathbf{r}_2)\gamma^{0(2)} \\
&+ \tau_3^{(1)}\frac{\partial\alpha_{TV}(\rho_V(\mathbf{r}_1))}{\partial\rho_V(\mathbf{r}_1)}\rho_{TV}(\mathbf{r}_1)\delta(\mathbf{r}_1-\mathbf{r}_2)\mathbf{1}^{(2)} \\
&+ \mathbf{1}^{(1)}\frac{\partial\alpha_{TV}(\rho_V(\mathbf{r}_1))}{\partial\rho_V(\mathbf{r}_1)}\rho_{TV}(\mathbf{r}_1)\delta(\mathbf{r}_1-\mathbf{r}_2)\tau_3^{(2)} \\
&+ \left[\frac{1-\tau_3}{2}\right]^{(1)}\frac{e^2}{4\pi}\frac{1}{|\mathbf{r}_1-\mathbf{r}_2|}\left[\frac{1-\tau_3}{2}\right]^{(2)}. \qquad (5.35)
\end{aligned}
$$

Analogous to the force PC-F1 (c.f. Appendix D), the particle-hole interaction $V^{\rm ph}(1,2)$ can be brought to the so-called channel form

$$
V^{\rm ph}(1,2) = \int_0^\infty r^2 dr \int_0^\infty r'^2 dr' \sum_{cc'} Q_c^{(1)}(r) v_{cc'}(r,r') Q_{c'}^{\dagger(2)}(r'), \qquad \text{(no Coulomb term)} \qquad (5.36)
$$

where the the effective interactions $v_{cc'}(r,r') = v_{cc'}(r)\delta(r-r')$ are now tabulated in Table 5.2.

Before continuing to the next subsection to discuss how the Coulomb interaction will be included in the channels, let us summarize the essential results from the current subsection. The single-particle basis $\{\varphi_k(\mathbf{r}), \epsilon_k\}$ is defined according to

$$
\hat{h}^D\varphi_k(\mathbf{r}) = \epsilon_k\varphi_k(\mathbf{r}),
$$

with the Dirac Hamiltonian $\hat{h}^D$,

$$\hat{h}^D = \boldsymbol{\alpha} \cdot \mathbf{p} + \beta[M + S(\mathbf{r})] + V(\mathbf{r}). \tag{5.37}$$

In the parametrization DD-PC1, the scalar potential $S(\mathbf{r})$ and vector potential $V(\mathbf{r})$ contains the strength parameters α_i ($i = S,\ V,\ TV$), which depends on the density ρ_V (Eq. (5.18) and Table 5.1). These potentials take the form

$$\begin{aligned} S(\mathbf{r}) &= [\alpha_S(\rho_V) + \delta_S \nabla^2]\rho_S(\mathbf{r}), \\ V(\mathbf{r}) &= \Sigma_R(\mathbf{r}) + \Sigma_V(\mathbf{r}) + \tau_3 \Sigma_{TV}(\mathbf{r}), \end{aligned}$$

with the self energies

$$\begin{aligned} \Sigma_R(\mathbf{r}) &= \frac{1}{2}\frac{\partial \alpha_S(\rho_V)}{\partial \rho_V}\rho_S^2(\mathbf{r}) + \frac{1}{2}\frac{\partial \alpha_V(\rho_V)}{\partial \rho_V}\rho_V^2(\mathbf{r}) + \frac{1}{2}\frac{\partial \alpha_{TV}(\rho_V)}{\partial \rho_V}\rho_{TV}^2(\mathbf{r}), \\ \Sigma_V(\mathbf{r}) &= \alpha_V(\rho_V)\rho_V(\mathbf{r}) + eA_0\frac{1}{2}(1-\tau_3), \\ \Sigma_{TV}(\mathbf{r}) &= \alpha_{TV}(\rho_V)\rho_{TV}(\mathbf{r}), \end{aligned}$$

and densities

$$\begin{aligned} \rho_S(\mathbf{r}) &= \sum_k n_k \overline{\varphi}_k(\mathbf{r})\varphi_k(\mathbf{r}), \\ \rho_V(\mathbf{r}) &= \sum_k n_k \varphi_k^\dagger(\mathbf{r})\varphi_k(\mathbf{r}), \end{aligned}$$

Table 5.2: The effective interactions $v_{cc'}(r)$ for the DD-PC1 parameterization. Here $F[\rho_V] = \alpha_V[\rho_V] + 2\alpha'_V[\rho_V]\rho_V + \frac{1}{2}\alpha''_V[\rho_V]\rho_V^2$ and $\alpha_i[\rho_V] \equiv \alpha_i(\rho_V(\mathbf{r}))$, where $i = S,\ V,\ TV$. The first and second derivative of $\alpha_i(\rho_V(\mathbf{r}))$ with respect to $\rho_V(\mathbf{r})$ are denoted as $\alpha'[\rho_V]$ and $\alpha''[\rho_V]$, respectively. The structure of channel c can be found in Table D.2 of Appendix D.

		Channel c'					
		1	2	3,4	5	6	7,8
Channel c	1	$\alpha_S[\rho_V] + \delta_S\nabla^2$	$\alpha'_S[\rho_V]\rho_S$	0	0	0	0
	2	$\alpha'_S[\rho_V]\rho_S$	$\frac{1}{2}\alpha''_S[\rho_V]\rho_S^2 + F[\rho_V]$ $+\frac{1}{2}\alpha''_{TV}[\rho_V]\rho_{TV}^2$	0	0	$\alpha'_{TV}[\rho_V]\rho_{TV}$	0
	3,4	0	0	$-\alpha_V[\rho_V]$	0	0	0
	5	0	0	0	0	0	0
	6	0	$\alpha'_{TV}[\rho_V]\rho_{TV}$	0	0	$\alpha_{TV}[\rho_V]$	0
	7,8	0	0	0	0	0	$-\alpha_{TV}[\rho_V]$

$$\rho_{TV}(\mathbf{r}) \;=\; \sum_k n_k \overline{\varphi}_k(\mathbf{r})\tau_3\gamma^0\varphi_k(\mathbf{r}).$$

The particle-hole interaction $V^{\rm ph}(1,2)$ is also given by

$$V^{\rm ph}(1,2) = \int_0^\infty r^2 dr \int_0^\infty r'^{\,2} dr' \sum_{cc'} Q_c^{(1)}(r) v_{cc'}(r,r') Q_{c'}^{\dagger(2)}(r'), \quad \text{(no Coulomb term)}$$

where the interaction $v_{cc'}(r,r')$ is not completely diagonal in the coordinate-channel representation, i.e., $v_{cc'}(r,r') = v_{cc'}(r)\delta(r-r')$. The multi-channel effective interactions $v_{cc'}(r)$ are tabulated in Table 5.2.

5.1.2 Treatment of the Coulomb Interaction in the Coordinate-channel Representation

We now turn our attention to the Coulomb term

$$\left[\frac{1}{2}(1+\tau_3)\right]^{(1)} v_C(\mathbf{r}_1,\mathbf{r}_2) \left[\frac{1}{2}(1+\tau_3)\right]^{(2)} \tag{5.38}$$

with the Coulomb potential

$$v_C(\mathbf{r}_1,\mathbf{r}_2) = \frac{e^2}{4\pi}\frac{1}{|\mathbf{r}_1-\mathbf{r}_2|} = \sum_{L=0}^{\infty}\sum_{M_L=-L}^{L} v_C^L(r_1,r_2) Y_{LM}^*(\mathbf{n}_2) Y_{LM}(\mathbf{n}_1), \tag{5.39}$$

where

$$v_C^L(r_1,r_2) = \frac{e^2}{2L+1}\frac{r_<^L}{r_>^{L+1}}. \tag{5.40}$$

Here $r_<$ and $r_>$ denote smaller (larger) of r_1 and r_2. The Coulomb term (5.38) breaks the isospin symmetry and can be decomposed according to

$$\left[\frac{1}{2}(1+\tau_3)\right]^{(1)} v_C(\mathbf{r}_1,\mathbf{r}_2) \left[\frac{1}{2}(1+\tau_3)\right]^{(2)} \;=\; \frac{1}{4} v_C(\mathbf{r}_1,\mathbf{r}_2)[\mathbf{1}^{(1)}\mathbf{1}^{(2)} + \mathbf{1}^{(1)}\tau_3^{(2)} + \tau_3^{(1)}\mathbf{1}^{(2)} + \tau_3^{(1)}\tau_3^{(2)}]. \tag{5.41}$$

Making use of the expansion of the Dirac delta-function (D.72), one can expand the Coulomb potential in the form

$$v_C(\mathbf{r}_1,\mathbf{r}_2) \;=\; \int d^3\mathbf{r} \int d^3\mathbf{r}'\; v_C(\mathbf{r},\mathbf{r}')\delta(\mathbf{r}_1-\mathbf{r})\delta(\mathbf{r}'-\mathbf{r}_2)$$

Table 5.3: The Coulomb interactions $v^C_{cc'}(r,r')$ for each channel.

		Channel c'					
		1	2	3,4	5	6	7,8
Channel c	1	0	0	0	0	0	0
	2	0	$\frac{1}{16}v^C_{L,L'}$	0	0	$\frac{1}{16}v^C_{L,L'}$	0
	3,4	0	0	$\frac{1}{16}v^C_{L,L'}$	0	0	$\frac{1}{16}v^C_{L,L'}$
	5	0	0	0	0	0	0
	6	0	$\frac{1}{16}v^C_{L,L'}$	0	0	$\frac{1}{16}v^C_{L,L'}$	0
	7,8	0	0	$\frac{1}{16}v^C_{L,L'}$	0	0	$\frac{1}{16}v^C_{L,L'}$

$$= \int r^2 dr \int r'^2 dr' \sum_{LM_L} v^L_C(r,r') Y_{LM_L}(\mathbf{n}_1) Y^*_{LM_L}(\mathbf{n}_2) \frac{\delta(r_1-r)}{rr_1} \frac{\delta(r'-r_2)}{r'r_2}. \tag{5.42}$$

Using this expansion and the identity

$$\frac{1}{4}\gamma^\mu\gamma_\mu = \mathbf{1}_{4\times 4}, \tag{5.43}$$

the Coulomb term (5.38) reads

$$\begin{aligned} & \left[\frac{1}{2}(1+\tau_3)\right]^{(1)} v_C(\mathbf{r}_1,\mathbf{r}_2) \left[\frac{1}{2}(1+\tau_3)\right]^{(2)} \\ = & \int r^2 dr \int r'^2 dr' \sum_{LM_L} \frac{1}{16} v^L_C(r,r') \frac{\delta(r_1-r)}{rr_1} \frac{\delta(r'-r_2)}{r'r_2} Y_{LM_L}(\mathbf{n}_1) Y^*_{LM_L}(\mathbf{n}_2) \\ \times & \ \gamma^\mu(1)\gamma_\mu(2) \otimes [\mathbf{1}^{(1)}\mathbf{1}^{(2)} + \mathbf{1}^{(1)}\tau_3^{(2)} + \tau_3^{(1)}\mathbf{1}^{(2)} + \tau_3^{(1)}\tau_3^{(2)}]. \end{aligned} \tag{5.44}$$

The last equation can be expressed in terms of the channels c defined in Table D.2, viz.

$$\left[\frac{1}{2}(1+\tau_3)\right]^{(1)} v_C(\mathbf{r}_1,\mathbf{r}_2) \left[\frac{1}{2}(1+\tau_3)\right]^{(2)} = \sum_{cc'} \int r^2 dr \int r'^2 dr' \; Q^{(1)}_c(r) v^C_{cc'}(r,r') Q^{(2)\dagger}_{c'}(r'), \tag{5.45}$$

where the Coulomb effective interactions $v^C_{cc'}(r,r') = \frac{1}{16}v^C_{LL'}(r,r')$ are now tabulated in Table 5.3.

Since the Coulomb term (5.38) has a similar channel structure as the non-Coulomb terms in the particle-hole interaction $V^{\rm ph}(1,2)$, the particle-hole interaction $V^{\rm ph}(1,2)$ can take a

generic form:

$$V^{\rm ph}(1,2) = \int_0^\infty r^2 dr \int_0^\infty r'^{\,2} dr' \sum_{cc'} Q_c^{(1)}(r) v_{cc'}^{\rm ph}(r,r') Q_{c'}^{\dagger(2)}(r'), \tag{5.46}$$

where the particle-hole effective interaction $v_{cc'}^{\rm ph}(r,r')$ now includes the Coulomb effective interaction $v_{cc'}^{C}(r,r')$ as well.

5.2 The BCS Theory

The inclusion of pairing correlations plays an essential role in giving a better description of structure phenomena in open-shell and deformed nuclei. The inclusion of the pairing correlations can be done in a self-consistent way in the framework of the relativistic Hartree-Fock-Bogoliubov (RHFB) theory [31, 41, 143]. For the case of not very loosely-bound nuclei with the Fermi level below the continuum, the treatment of pairing correlations using the Bardeen-Cooper-Schrieffer (BCS) approximation is considered sufficient. In this work, we will deal with the so-called like-particle pairing, i.e., either proton-proton (pp) or neutron-neutron (nn) pairing, and neglect the proton-neutron (pn) pairing. In the following we present the theoretical description of the BCS approximation to the superfluid pairing correlations.

5.2.1 The BCS Wave Function

Consider a pairing Hamiltonian $\hat{H}$ which contains the single-particle term and the pairing interaction term, viz.

$$\hat{H} = \sum_k \epsilon_k \hat{a}_k^\dagger \hat{a}_k - \sum_{kk'>0} G_{kk'} \hat{P}_k^\dagger \hat{P}_{k'}. \tag{5.47}$$

The pair-creation operator $\hat{P}_k^\dagger$,

$$\hat{P}_k^\dagger = \hat{a}_k^\dagger \hat{a}_{\bar{k}}^\dagger \coloneqq (-1)^{j-m} \hat{a}_{jm}^\dagger \hat{a}_{j-m}^\dagger, \tag{5.48}$$

creates a pair of nucleons, one in a single-particle state $|k\rangle = |jm\rangle$ and another in a time-reversed state $|\bar{k}\rangle = (-1)^{j-m}|j-m\rangle$. The corresponding pair-annihilation operator $\hat{P}_k$ is defined as

$$\hat{P}_k = \hat{a}_{\bar{k}} \hat{a}_k \coloneqq (-1)^{j-m} \hat{a}_{j-m} \hat{a}_{jm}. \tag{5.49}$$

The pairing strength $G_{kk'}$ determines the transition amplitude of a nucleon pair from the state $|k'\rangle$ and the time-reversed state $|\bar{k}'\rangle$ to the state $|k\rangle$ and the time-reversed state $|\bar{k}\rangle$. In

the simplest case one assumes the pairing strength $G_{kk'}$ is a constant G, and the Hamiltonian $\hat{H}$ becomes

$$\hat{H} = \sum_k \epsilon_k \hat{a}_k^\dagger \hat{a}_k - G \sum_{kk'>0} \hat{P}_k^\dagger \hat{P}_{k'}. \tag{5.50}$$

In the BCS model, the trial wave function is the ground state $|\mathrm{BCS}\rangle$ of the form:

$$|\mathrm{BCS}\rangle = \prod_{k>0}^{\infty} (u_k + v_k \hat{a}_k^\dagger \hat{a}_{\bar{k}}^\dagger)|-\rangle, \tag{5.51}$$

where $|-\rangle$ stands for the bare vacuum defined according to

$$\hat{a}_k|-\rangle = 0 \quad \text{and} \quad \hat{a}_{\bar{k}}|-\rangle = 0. \tag{5.52}$$

The parameters u_k and v_k are taken to be real and one also defines $u_{\bar{k}} = u_k$ and $v_{\bar{k}} = -v_k$. The normalization of the BCS state, $\langle \mathrm{BCS}|\mathrm{BCS}\rangle = 1$, leads to

$$u_k^2 + v_k^2 = 1. \tag{5.53}$$

The state $|\mathrm{BCS}\rangle$ is a vacuum state with respect to the quasi-particle operators $\hat{\alpha}_k$, i.e.,

$$\hat{\alpha}_k|\mathrm{BCS}\rangle = 0 \tag{5.54}$$

for all k. The quasi-particle creation (annihilation) operators $\hat{\alpha}_k^\dagger$ ($\hat{\alpha}_k$) are connected to the particle creation (annihilation) operators $\hat{a}_k^\dagger$ ($\hat{a}_k$) via the Bogoliubov-Valatin transformations:

$$\hat{\alpha}_k^\dagger = u_k \hat{a}_k^\dagger - v_k \hat{a}_{\bar{k}}, \tag{5.55}$$
$$\hat{\alpha}_{\bar{k}}^\dagger = u_k \hat{a}_{\bar{k}}^\dagger + v_k \hat{a}_k, \tag{5.56}$$
$$\hat{\alpha}_k = u_k \hat{a}_k - v_k \hat{a}_{\bar{k}}^\dagger, \tag{5.57}$$
$$\hat{\alpha}_{\bar{k}} = u_k \hat{a}_{\bar{k}} + v_k \hat{a}_k^\dagger. \tag{5.58}$$

The quasi-particle operators $\hat{\alpha}_k$, $\hat{\alpha}_k^\dagger$ satisfy the following commutation relations:

$$\{\hat{\alpha}_k, \hat{\alpha}_{k'}^\dagger\} = \delta_{kk'}; \quad \{\hat{\alpha}_k, \hat{\alpha}_{k'}\} = 0; \quad \{\hat{\alpha}_k^\dagger, \hat{\alpha}_{k'}^\dagger\} = 0 \tag{5.59}$$

for all k. The inverse Bogoliubov-Valatin transformations are then given by

$$\hat{a}_k^\dagger = u_k \hat{\alpha}_k^\dagger + v_k \hat{\alpha}_{\bar{k}}, \tag{5.60}$$

$$\hat{a}_k = u_k\hat{\alpha}_k + v_k\hat{\alpha}^\dagger_{\bar{k}}, \tag{5.61}$$

$$\hat{a}^\dagger_{\bar{k}} = u_k\hat{\alpha}^\dagger_{\bar{k}} - v_k\hat{\alpha}_k, \tag{5.62}$$

$$\hat{a}_{\bar{k}} = u_k\hat{\alpha}_{\bar{k}} - v_k\hat{\alpha}^\dagger_k. \tag{5.63}$$

The average particle number N serves as the constraint

$$N = \sum_{k>0}[v_k^2 + v_{\bar{k}}^2] = 2\sum_{k>0} v_k^2 \coloneqq \sum_k v_k^2. \tag{5.64}$$

From Eqs. (5.64) and (5.53), we can interpret v_k^2 as the probability of a pair state $(k, \bar{k})$ to be occupied, and, therefore, u_k^2 is the probability of the pair state $(k, \bar{k})$ to remain empty. The trial wave function $|\mathrm{BCS}\rangle$ does not conserve the particle number. This follows from the definition (5.51), where the wave function is a superposition of components with different numbers of fermionic pairs. Being a quantum mechanical operator, the particle number fluctuates around its average value, so that the mean square fluctuations of the particle number $(\Delta N)^2$ are quantified by

$$(\Delta N)^2 = \langle\mathrm{BCS}|\hat{N}^2|\mathrm{BCS}\rangle - \langle\mathrm{BCS}|\hat{N}|\mathrm{BCS}\rangle^2 = 4\sum_{k>0} u_k^2 v_k^2. \tag{5.65}$$

5.2.2 The BCS Equations

As the trial wave function $|\mathrm{BCS}\rangle$ does not conserve the particle number, the variational condition becomes

$$\delta\langle\mathrm{BCS}|(\hat{H} - \lambda\hat{N})|\mathrm{BCS}\rangle = 0, \tag{5.66}$$

where λ is the chemical potential. Using Eq. (5.53), the variational condition (5.66) can be rewritten as

$$0 = \left(\frac{\partial}{\partial v_k} + \frac{\partial u_k}{\partial v_k}\frac{\partial}{\partial u_k}\right)\langle\mathrm{BCS}|(\hat{H} - \lambda\hat{N})|\mathrm{BCS}\rangle. \tag{5.67}$$

The expectation value of $(\hat{H} - \lambda\hat{N})$ in the state $|\mathrm{BCS}\rangle$ is, therefore, given by

$$\begin{aligned}\langle\mathrm{BCS}|\hat{H} - \lambda\hat{N}|\mathrm{BCS}\rangle &= \sum_{k>0} 2\left(\epsilon_k - \lambda - \frac{G}{2}v_k^2\right)v_k^2 - G\left(\sum_{k>0} u_k v_k\right)^2 \\ &\approx \sum_{k>0} 2(\epsilon_k - \lambda)v_k^2 - G\left(\sum_{k>0} u_k v_k\right)^2,\end{aligned} \tag{5.68}$$

where the mean-field pairing contribution to the single-particle energy, i.e., $-Gv_k^2/2$, is neglected due to its smallness (see the discussion in Appendix G of Ref. [165]). Inserting Eq. (5.68) into Eq. (5.67), one obtains

$$0 = 4E_k^2 v_k^4 - 4E_k^2 v_k^2 + \Delta^2, \tag{5.69}$$

where the quasiparticle energy E_k is

$$\begin{aligned} E_k^2 &= (\epsilon_k - \lambda)^2 + \Delta^2 \\ E_k &= \sqrt{(\epsilon_k - \lambda)^2 + \Delta^2} > 0 \end{aligned} \tag{5.70}$$

and the gap parameter Δ is defined as

$$\Delta = G \sum_{k>0} u_k v_k. \tag{5.71}$$

Solving Eq. (5.69), one obtains

$$v_k^2 = \frac{1}{2} \pm \frac{1}{2} \frac{\epsilon_k - \lambda}{E_k}. \tag{5.72}$$

To determine the sign in v_k^2, one considers the case with no pairing, i.e., $\Delta = 0$. In this limit, one should have $E_k = |\epsilon_k - \lambda|$, $(\epsilon_k - \lambda) = -|\epsilon_k - \lambda|$, $v_k^2 = 1$, and $u_k^2 = 0$ for the occupied states below the Fermi energy. This limit can be achieved if one chooses

$$v_k^2 = \frac{1}{2} \left[1 - \frac{\epsilon_k - \lambda}{E_k} \right] \tag{5.73}$$

and, therefore, using Eq. (5.53), one also obtains

$$u_k^2 = 1 - v_k^2 = \frac{1}{2} \left[1 + \frac{\epsilon_k - \lambda}{E_k} \right]. \tag{5.74}$$

Inserting the explicit forms of u_k^2 and v_k^2 into Eq. (5.71) yields the famous gap equation:

$$1 = G \sum_{k>0} \frac{1}{2E_k}, \tag{5.75}$$

that allows finding the value of the pairing gap. The unrestricted sum over k in Eqs. (5.71) and (5.75) results in a divergence. This is an artifact of using a non-realistic constant pairing interaction strength. To avoid this situation, one has to introduce a cut-off energy or a fixed pairing window E_p around the Fermi surface, so that any state with energy higher than E_p

has the occupation probability $v_k^2 = 0$. In addition, one can also introduces an additional factor [166]:

$$f_k = \left[1 + \exp\left(\frac{\epsilon_k - \lambda - E_p}{\mu}\right)\right]^{-1}, \tag{5.76}$$

where the parameter μ here determines the smoothness of the cut-off. With the additional factor f_k, the gap equation (5.75) now reads:

$$1 = G\sum_{k>0} f_k \frac{1}{2E_k}. \tag{5.77}$$

Equations (5.70), (5.73), (5.74), and (5.77) constitute the BCS equations with the constraints related to the proton (neutron)-quasiparticle number N^π (N^ν):

$$N^{\pi,\nu} = \sum_k v_k^2. \tag{5.78}$$

These equations are valid for protons and neutrons separately. In the active pairing space (inside the pairing window), the BCS pairing correlations modify the four nucleonic densities $\rho_i(\mathbf{r})$ ($i = S,\ V,\ TS,\ TV$) by the replacement

$$\sum_k n_k \cdots \quad \Longrightarrow \quad \sum_k v_k^2 \cdots . \tag{5.79}$$

This modification will affect the scalar potential $S(\mathbf{r})$ and vector potential $V(\mathbf{r})$, and, in turn, the single-particle basis. Therefore, one solves the BCS equations with the constraint (5.78) together with the self-consistent mean-field equations to obtain the correct single-particle basis, chemical potential λ, quasiparticle energies E_k, the pairing strength G, the pairing gap Δ, and the BCS occupation numbers v_k^2. This is the general feature of the RMF+BCS model.

5.2.3 The Matrix Elements of One-body Operators

Consider a one-body operator $\hat{Q}$ in the second quantization representation:

$$\hat{Q} = \sum_{kk'} \langle k|\hat{Q}|k'\rangle \hat{a}_k^\dagger \hat{a}_{k'} = \sum_{kk'} Q_{kk'} \hat{a}_k^\dagger \hat{a}_{k'}. \tag{5.80}$$

Using the inverse Bogoliubov-Valatin transformations (5.60) and (5.61), the one-body operator $\hat{Q}$ can be expressed as

$$\hat{Q} = Q^0 + \sum_{kk'} Q^{11}_{kk'} \hat{\alpha}^\dagger_k \hat{\alpha}_{k'} + \frac{1}{2} \sum_{kk'} \left(Q^{20}_{kk'} \hat{\alpha}^\dagger_k \hat{\alpha}^\dagger_{k'} + Q^{02}_{k'k} \hat{\alpha}_{k'} \hat{\alpha}_k \right), \tag{5.81}$$

where

$$Q^0 = \sum_k Q_{kk} v_k^2 = \sum_{k>0} \{ Q_{kk} + Q_{\bar{k}\bar{k}} \} v_k^2, \tag{5.82}$$

$$Q^{11}_{kk'} = Q_{kk'} u_k u_{k'} - Q_{\bar{k}'\bar{k}} v_{k'} v_k, \tag{5.83}$$

$$Q^{20}_{kk'} = Q_{k\bar{k}'} u_k v_{k'} - Q_{k'\bar{k}} u_{k'} v_k, \tag{5.84}$$

$$Q^{02}_{k'k} = Q_{\bar{k}'k} v_{k'} u_k - Q_{\bar{k}k'} v_k u_{k'}. \tag{5.85}$$

In the case of time-reversal invariance $[\hat{\mathcal{T}}^{-1} \hat{F} \hat{\mathcal{T}}]^\dagger = (-1)^S \hat{F}$, where $S = 0$ for time-even operators, i.e., scalar and time-like components of vector fields, and $S = 1$ for time-odd operators, i.e., space-like components of the vector fields, one has (c.f. Appendix E)

$$\langle \bar{\mu} | \hat{F} | \bar{\nu} \rangle = (-1)^S \langle \nu | \hat{F} | \mu \rangle \quad \text{and} \quad \langle \bar{\mu} | \hat{F} | \nu \rangle = -(-1)^S \langle \bar{\nu} | \hat{F} | \mu \rangle. \tag{5.86}$$

Using these relations, one can rewrite Eqs. (5.82)-(5.85) in terms of the factors $\xi^S_{kk'}$ and $\eta^S_{kk'}$,

$$\xi^S_{kk'} = u_k u_{k'} - (-1)^S v_k v_{k'}, \tag{5.87}$$

$$\eta^S_{kk'} = u_k v_{k'} + (-1)^S v_k u_{k'}, \tag{5.88}$$

as follows:

$$Q^0 = \sum_{k>0} Q_{kk} \left[1 + (-1)^S \right] v_k^2, \tag{5.89}$$

$$Q^{11}_{kk'} = \xi^S_{kk'} Q_{kk'}, \tag{5.90}$$

$$Q^{20}_{kk'} = \eta^S_{kk'} Q_{k\bar{k}'}, \tag{5.91}$$

$$Q^{02}_{k'k} = \eta^S_{kk'} Q_{\bar{k}'k}. \tag{5.92}$$

This form of the one-body operators will be used in the following formalism.

Chapter 6

Continuum Relativistic Quasiparticle Random Phase Approximation

It is well-known that the phenomena of giant resonances (GRs) can be understood microscopically as a result of the collective nuclear excitations. The random phase approximation (RPA) is the simplest theory to describe the collective nuclear excitations. It starts by assuming the existence of a correlated ground state, and describes the collective excitations, which are caused by a weak external field, as a coherent superposition of particle-hole excitations from this correlated ground state. In the presence of pairing correlations, one has to extend the RPA formalism to the quasiparticle RPA (QRPA) formalism. In the QRPA formalism, it is the two-quasiparticle and two-quasi-hole pairs that form the transitions from the correlated ground state. The QRPA equations can be formulated in several ways. In the first section of this Chapter, we derive the QRPA equations in configuration space using the equation of motion method, following Ref. [21]. This formulation, however, does not include accurately the continuum effects, but instead, these effects are included implicitly via the so-called discretized continuum. In realistic calculations, however, because of the inevitable basis truncations, such a treatment of the continuum has limited accuracy and, thus, is not sufficient for the light and loosely-bound nuclear systems. To formulate the Bethe-Salpeter equation (BSE) for particle-hole response functions in the framework of the continuum relativistic QRPA, we employ the particle-hole $V^{\rm ph}(1,2)$ and particle-particle $\hat{V}^{\rm pp}$ interactions, which were defined in Section 5.1 and Section 5.2, respectively. We work out the detail procedures to obtain the BSE in the coordinate space representation for particle-hole and particle-particle channels in Section 6.2 and Section 6.3, respectively.

6.1 The Quasiparticle Random Phase Approximation (QRPA) Equations

Consider a set of exact eigenstates $|\nu\rangle$ of the nuclear Hamiltonian $\hat{H}$ satisfying the Schrödinger equation

$$\hat{H}|\nu\rangle = E_\nu|\nu\rangle \tag{6.1}$$

with the corresponding exact eigenvalues E_ν. The excitation operators $\hat{Q}^\dagger_\nu, \hat{Q}_\nu$ are defined in such a way that $\hat{Q}^\dagger_\nu$ creates the excited state $|\nu\rangle$, where $\nu > 0$, when acting on the nuclear ground state $|0\rangle$, whereas $\hat{Q}_\nu$ causes the state $|0\rangle$ to vanish, viz.

$$|\nu\rangle = \hat{Q}^\dagger_\nu|0\rangle \quad \text{and} \quad \hat{Q}_\nu|0\rangle = 0. \tag{6.2}$$

It is possible for the operator $\hat{Q}^\dagger_\nu$ to take the form

$$\hat{Q}^\dagger_\nu = |\nu\rangle\langle 0|. \tag{6.3}$$

Using the definition (6.3) of operator $\hat{Q}^\dagger_\nu$, the action of commutator $[\hat{H}, \hat{Q}^\dagger_\nu]$ on the state $|0\rangle$ gives the equation of motion

$$[\hat{H}, \hat{Q}^\dagger_\nu]|0\rangle = (E_\nu - E_0)|\nu\rangle, \tag{6.4}$$

where E_0 is the ground state energy. Multiplying Eq. (6.4) from the left with the variation $\delta\hat{Q}_\nu$ and closing it with the state $|0\rangle$, one obtains

$$\langle 0|[\delta\hat{Q}_\nu, [\hat{H}, \hat{Q}^\dagger_\nu]]|0\rangle = (E_\nu - E_0)\langle 0|[\delta\hat{Q}_\nu, \hat{Q}^\dagger_\nu]|0\rangle. \tag{6.5}$$

In the quasiparticle random phase approximation (QRPA), the operator $\hat{Q}^\dagger_\nu$ is the simplest phonon creation operator, which is built from the pairs quasiparticle operators, viz.

$$\hat{Q}^\dagger_\nu = \frac{1}{2}\sum_{p<p'}(X^\nu_{pp'}\hat{\alpha}^\dagger_p\hat{\alpha}^\dagger_{p'} - Y^\nu_{pp'}\hat{\alpha}_{p'}\hat{\alpha}_p). \tag{6.6}$$

The indices (p, q) and the prime indices (p', q') are used to label the quasiparticle basis. The interchange between p and p' in Eq. (6.6) gives

$$\hat{Q}^\dagger_\nu = \frac{1}{2}\sum_{p<p'}(X^\nu_{p'p}\hat{\alpha}^\dagger_{p'}\hat{\alpha}^\dagger_p - Y^\nu_{p'p}\hat{\alpha}_p\hat{\alpha}_{p'}) = \frac{1}{2}\sum_{p<p'}(-X^\nu_{p'p}\hat{\alpha}^\dagger_p\hat{\alpha}^\dagger_{p'} + Y^\nu_{p'p}\hat{\alpha}_{p'}\hat{\alpha}_p),$$

which implies the anti-symmetric property of the amplitudes $X^{\nu}_{pp'}$ and $Y^{\nu}_{pp'}$, i.e.,

$$X^{\nu}_{pp'} = -X^{\nu}_{p'p} \quad \text{and} \quad Y^{\nu}_{pp'} = -Y^{\nu}_{p'p}. \tag{6.7}$$

The QRPA ground state $|\text{QRPA}\rangle$ can be identified by the vacuum condition (6.2)

$$\hat{Q}_{\nu}|\text{QRPA}\rangle = 0. \tag{6.8}$$

Using the QRPA ground state $|\text{QRPA}\rangle$ as an approximation to the nuclear ground state $|0\rangle$ in Eq. (6.5), one obtains

$$\langle\text{QRPA}|[\delta\hat{Q}_{\nu}, [\hat{H}, \hat{Q}^{\dagger}_{\nu}]]|\text{QRPA}\rangle = \Omega_{\nu}\langle\text{QRPA}|[\delta\hat{Q}_{\nu}, \hat{Q}^{\dagger}_{\nu}]|\text{QRPA}\rangle, \tag{6.9}$$

where $\Omega_{\nu} = (E_{\nu} - E_0)$ is the phonon energy. Since the phonon creation operator consists of two amplitudes $X^{\nu}_{pp'}$ and $Y^{\nu}_{pp'}$, the corresponding variation $\delta\hat{Q}_{\nu}|\text{QRPA}\rangle$ has two terms, i.e., $\hat{\alpha}^{\dagger}_{p}\hat{\alpha}^{\dagger}_{p'}|\text{QRPA}\rangle\delta X^{\nu}_{pp'}$ and $\hat{\alpha}_{p'}\hat{\alpha}_{p}|\text{QRPA}\rangle\delta Y^{\nu}_{pp'}$. As they are associated with the independent variations, one obtains the two sets of equations for each amplitude, namely,

$$\langle\text{QRPA}|[\hat{\alpha}^{\dagger}_{p}\hat{\alpha}^{\dagger}_{p'}, [\hat{H}, \hat{Q}^{\dagger}_{\nu}]]|\text{QRPA}\rangle = \Omega_{\nu}\langle\text{QRPA}|[\hat{\alpha}^{\dagger}_{p}\hat{\alpha}^{\dagger}_{p'}, \hat{Q}^{\dagger}_{\nu}]|\text{QRPA}\rangle \tag{6.10}$$

and

$$\langle\text{QRPA}|[\hat{\alpha}_{p'}\hat{\alpha}_{p}, [\hat{H}, \hat{Q}^{\dagger}_{\nu}]]|\text{QRPA}\rangle = \Omega_{\nu}\langle\text{QRPA}|[\hat{\alpha}_{p'}\hat{\alpha}_{p}, \hat{Q}^{\dagger}_{\nu}]|\text{QRPA}\rangle. \tag{6.11}$$

To derive the QRPA equations from Eqs. (6.10) and (6.11), one applies the **quasi-boson approximation** by assuming that the correlated ground state $|\text{QRPA}\rangle$ does not differ very much from the Hartree-Fock-Bogoliubov (HFB) ground state $|\text{HFB}\rangle$. Here it is convenient to introduce two-quasiparticle creation operator $\hat{b}^{\dagger}_{pp'}$ and two-quasiparticle annihilation operator $\hat{b}_{pp'}$,

$$\hat{b}^{\dagger}_{pp'} = \hat{\alpha}^{\dagger}_{p}\hat{\alpha}^{\dagger}_{p'} \quad \text{and} \quad \hat{b}_{pp'} = \hat{\alpha}_{p'}\hat{\alpha}_{p}. \tag{6.12}$$

Applying the quasi-boson approximation, one obtains the three expectation values $\langle\text{QRPA}|[\hat{b}_{pp'}, \hat{b}^{\dagger}_{qq'}]|\text{QRPA}\rangle$, $\langle\text{QRPA}|[\hat{b}_{pp'}, \hat{b}_{qq'}]|\text{QRPA}\rangle$, and $\langle\text{QRPA}|[\hat{b}^{\dagger}_{pp'}, \hat{b}^{\dagger}_{qq'}]|\text{QRPA}\rangle$ as follows:

$$\langle\text{QRPA}|[\hat{b}_{pp'}, \hat{b}^{\dagger}_{qq'}]|\text{QRPA}\rangle \approx \langle\text{HFB}|[\hat{b}_{pp'}, \hat{b}^{\dagger}_{qq'}]|\text{HFB}\rangle = \delta_{qp}\delta_{q'p'} - \delta_{qp'}\delta_{q'p}, \tag{6.13}$$

$$\langle\text{QRPA}|[\hat{b}_{pp'}, \hat{b}_{qq'}]|\text{QRPA}\rangle \approx \langle\text{HFB}|[\hat{b}_{pp'}, \hat{b}_{qq'}]|\text{HFB}\rangle = 0, \tag{6.14}$$

$$\langle\text{QRPA}|[\hat{b}^{\dagger}_{pp'}, \hat{b}^{\dagger}_{qq'}]|\text{QRPA}\rangle \approx \langle\text{HFB}|[\hat{b}^{\dagger}_{pp'}, \hat{b}^{\dagger}_{qq'}]|\text{HFB}\rangle = 0. \tag{6.15}$$

With the aid of Eqs. (6.13), (6.14), and (6.15), Eqs. (6.10) and (6.11) become the so-called QRPA equations

$$\Omega_\nu X^\nu_{pp'} = \sum_{q<q'} A_{pp'qq'} X^\nu_{qq'} + \sum_{q<q'} B_{pp'qq'} Y^\nu_{qq'}, \tag{6.16}$$

$$\Omega_\nu Y^\nu_{pp'} = -\sum_{q<q'} B^*_{pp'qq'} X^\nu_{qq'} - \sum_{q<q'} A^*_{pp'qq'} Y^\nu_{qq'}, \tag{6.17}$$

where the matrix elements $A_{pp'qq'}$ and $B_{pp'qq'}$ are defined as

$$A_{pp'qq'} = \langle \mathrm{HFB} | [\hat{\alpha}_{p'}\hat{\alpha}_p, [\hat{H}, \hat{\alpha}^\dagger_q \hat{\alpha}^\dagger_{q'}]] | \mathrm{HFB} \rangle \tag{6.18}$$

and

$$B_{pp'qq'} = -\langle \mathrm{HFB} | [\hat{\alpha}_{p'}\hat{\alpha}_p, [\hat{H}, \hat{\alpha}_{q'} \hat{\alpha}_q]] | \mathrm{HFB} \rangle. \tag{6.19}$$

The complex conjugate of these two matrix elements are

$$A^*_{pp'qq'} = \langle \mathrm{HFB} | [\hat{\alpha}^\dagger_p \hat{\alpha}^\dagger_{p'}, [\hat{H}, \hat{\alpha}_{q'} \hat{\alpha}_q]] | \mathrm{HFB} \rangle \tag{6.20}$$

and

$$B^*_{pp'qq'} = -\langle \mathrm{HFB} | [\hat{\alpha}^\dagger_p \hat{\alpha}^\dagger_{p'}, [\hat{H}, \hat{\alpha}^\dagger_q \hat{\alpha}^\dagger_{q'}]] | \mathrm{HFB} \rangle. \tag{6.21}$$

In the quasiparticle representation, the Hamiltonian $\hat{H}$ can be expressed as

$$\begin{aligned}
\hat{H} &= H^0 + \sum_{p_1 p_2} H^{11}_{p_1 p_2} \hat{\alpha}^\dagger_{p_1} \hat{\alpha}_{p_2} + \frac{1}{2} \sum_{p_1 p_2} H^{20}_{p_1 p_2} \hat{\alpha}^\dagger_{p_1} \hat{\alpha}^\dagger_{p_2} + \frac{1}{2} \sum_{p_1 p_2} H^{20*}_{p_1 p_2} \hat{\alpha}_{p_2} \hat{\alpha}_{p_1} \\
&+ \sum_{p_1 p_2 p_3 p_4} H^{40}_{p_1 p_2 p_3 p_4} \hat{\alpha}^\dagger_{p_1} \hat{\alpha}^\dagger_{p_2} \hat{\alpha}^\dagger_{p_3} \hat{\alpha}^\dagger_{p_4} + \sum_{p_1 p_2 p_3 p_4} H^{40*}_{p_1 p_2 p_3 p_4} \hat{\alpha}_{p_4} \hat{\alpha}_{p_3} \hat{\alpha}_{p_2} \hat{\alpha}_{p_1} \\
&+ \sum_{p_1 p_2 p_3 p_4} H^{31}_{p_1 p_2 p_3 p_4} \hat{\alpha}^\dagger_{p_1} \hat{\alpha}^\dagger_{p_2} \hat{\alpha}^\dagger_{p_3} \hat{\alpha}_{p_4} + \sum_{p_1 p_2 p_3 p_4} H^{31*}_{p_1 p_2 p_3 p_4} \hat{\alpha}^\dagger_{p_4} \hat{\alpha}_{p_3} \hat{\alpha}_{p_2} \hat{\alpha}_{p_1} \\
&+ \frac{1}{4} \sum_{p_1 p_2 p_3 p_4} H^{22}_{p_1 p_2 p_3 p_4} \hat{\alpha}^\dagger_{p_1} \hat{\alpha}^\dagger_{p_2} \hat{\alpha}_{p_4} \hat{\alpha}_{p_3}.
\end{aligned} \tag{6.22}$$

Making use of the expression (6.22), one obtains

$$A_{pp'qq'} = (E_p + E_{p'}) \delta_{pq} \delta_{p'q'} + H^{22}_{pp'qq'}, \tag{6.23}$$

$$B_{pp'qq'} = 4! \cdot H^{40}_{pp'qq'}. \tag{6.24}$$

In the canonical basis, i.e., the basis that diagonalizes the normal one-body density matrix, the matrix elements of QRPA matrices **A** and **B** are given by

$$\begin{aligned} A_{kk'\ell\ell'} &= (E_k + E_{k'})\delta_{k\ell}\delta_{k'\ell'} + u_k u_{k'} u_\ell u_{\ell'} V^{\rm pp}_{kk'\ell\ell'} + v_k v_{k'} v_\ell v_{\ell'} V^{\rm pp}_{\bar{\ell}\bar{\ell}'\bar{k}\bar{k}'} \\ &+ u_k u_\ell v_{k'} v_{\ell'} V^{\rm ph}_{k\bar{\ell}'\bar{k}'\ell} + u_{k'} u_{\ell'} v_k v_\ell V^{\rm ph}_{k'\bar{\ell}\bar{k}\ell'} \\ &- u_k u_{\ell'} v_{k'} v_\ell V^{\rm ph}_{k\bar{\ell}\bar{k}'\ell'} - u_{k'} u_\ell v_k v_{\ell'} V^{\rm ph}_{k'\bar{\ell}'\bar{k}\ell}, \qquad (6.25) \\ B_{kk'\ell\ell'} &= -u_k u_{k'} v_\ell v_{\ell'} V^{\rm pp}_{kk'\bar{\ell}\bar{\ell}'} - v_k v_{k'} u_\ell u_{\ell'} V^{\rm pp}_{\ell\ell'\bar{k}\bar{k}'} + u_k v_{k'} u_\ell v_{\ell'} V^{\rm ph}_{k\ell\bar{k}'\bar{\ell}'} \\ &+ v_k u_{k'} v_\ell u_{\ell'} V^{\rm ph}_{k'\ell'\bar{k}\bar{\ell}} - u_k v_{k'} v_\ell u_{\ell'} V^{\rm ph}_{k\ell'\bar{k}'\bar{\ell}} - v_k u_{k'} u_\ell v_{\ell'} V^{\rm ph}_{k'\ell\bar{k}\bar{\ell}'}. \qquad (6.26) \end{aligned}$$

Accordingly, the QRPA equations in the canonical basis take the form

$$\begin{aligned} \Omega_\nu X^\nu_{kk'} &= \sum_{\ell<\ell'} A_{kk'\ell\ell'} X^\nu_{\ell\ell'} + \sum_{\ell<\ell'} B_{kk'\ell\ell'} Y^\nu_{\ell\ell'}, \qquad (6.27) \\ \Omega_\nu Y^\nu_{kk'} &= -\sum_{\ell<\ell'} B^*_{kk'\ell\ell'} X^\nu_{\ell\ell'} - \sum_{\ell<\ell'} A^*_{kk'\ell\ell'} Y^\nu_{\ell\ell'}. \qquad (6.28) \end{aligned}$$

The indices (k,ℓ) and the prime indices (k',ℓ') will be used to indicate the canonical basis throughout this chapter.

6.2 The Particle-hole Response Function Formalism for Continuum Relativistic QRPA

As discussed in Section 5.1, the particle-hole interaction $V^{\rm ph}(1,2)$ takes the form

$$V^{\rm ph}(x_1,x_2) = \int_0^\infty r^2 dr \int_0^\infty r'^{\,2} dr' \sum_{cc'} Q^{(1)}_c(r) v^{\rm ph}_{cc'}(r,r') Q^{\dagger(2)}_{c'}(r') \qquad (6.29)$$

in the coordinate representation. By means of the Dirac spinor

$$\varphi_k(\mathbf{r},\sigma,t) = \frac{1}{r}\begin{bmatrix} F_{\kappa_k}(r)\Omega_{j_k\ell_k m_k}(\mathbf{n},\sigma) \\ iG_{\kappa_k}(r)\Omega_{j_k\tilde{\ell}_k m_k}(\mathbf{n},\sigma) \end{bmatrix} \chi_{\frac{1}{2}\tau_k}(t), \qquad (6.30)$$

one defines the particle-hole interaction $V^{\rm ph}_{k\ell'k'\ell}$ in configuration space as

$$\begin{aligned} V^{\rm ph}_{k\ell'k'\ell} &= \int dx_1 \int dx_2\, \varphi^\dagger_k(x_1)\varphi^\dagger_{\ell'}(x_2) V^{\rm ph}(x_1,x_2)\varphi_{k'}(x_1)\varphi_\ell(x_2) \\ &= \sum_{cc'} \int dr\, r^2 \int dr'\, r'^2 Q^c_{kk'}(r) v^{\rm ph}_{cc'}(r,r') Q^{c'*}_{\ell\ell'}(r'), \qquad (6.31) \end{aligned}$$

where the matrix elements $Q^{c}_{kk'}(r)$ and $Q^{c'*}_{\ell\ell'}(r')$ are given by

$$\begin{aligned}
Q^{c}_{kk'}(r) &= \int dx_1\ \varphi^{\dagger}_{k}(x_1) Q^{(1)}_{c}(r) \varphi_{k'}(x_1) \\
&= \int d^3\mathbf{r}_1 \sum_{t_1 t'_1} \sum_{\sigma_1,\sigma'_1} \varphi^{\dagger}_{k}(\mathbf{r}_1,\sigma_1,t_1) \frac{\delta(r-r_1)}{r r_1} \gamma_D \otimes T_{JLSM}(\mathbf{n}_1)_{\sigma_1\sigma'_1} \otimes (\tau_{T0})_{t_1 t'_1} \\
&\times\ \varphi_{k'}(\mathbf{r}_1,\sigma'_1,t'_1) \\
&= \int r_1^2\, dr_1 \int d\mathbf{n}_1 \sum_{t_1 t'_1} \sum_{\sigma_1,\sigma'_1} \varphi^{\dagger}_{k}(\mathbf{r}_1,\sigma_1,t_1) \frac{\delta(r-r_1)}{r r_1} \gamma_D \otimes T_{JLSM}(\mathbf{n}_1)_{\sigma_1\sigma'_1} \\
&\otimes\ (\tau_{T0})_{t_1 t'_1}\ \varphi_{k'}(\mathbf{r}_1,\sigma'_1,t'_1) \\
&= \int d\mathbf{n}_1 \sum_{t_1 t'_1} \sum_{\sigma_1,\sigma'_1} \varphi^{\dagger}_{k}(r,\mathbf{n}_1,\sigma_1,t_1) \gamma_D \otimes T_{JLSM}(\mathbf{n}_1)_{\sigma_1\sigma'_1} \otimes (\tau_{T0})_{t_1 t'_1} \\
&\times\ \varphi_{k'}(r,\mathbf{n}_1,\sigma'_1,t'_1)
\end{aligned} \tag{6.32}$$

and

$$\begin{aligned}
Q^{c'*}_{\ell\ell'}(r') &= Q^{c'\dagger}_{\ell'\ell}(r') \\
&= \int dx_2\ \varphi^{\dagger}_{\ell'}(x_2) Q^{\dagger(2)}_{c'}(r') \varphi_{\ell}(x_2) \\
&= \int d^3\mathbf{r}_2 \sum_{t_2 t'_2} \sum_{\sigma_2,\sigma'_2} \varphi^{\dagger}_{\ell'}(\mathbf{r}_2,\sigma_2,t_2) \frac{\delta(r'-r_2)}{r' r_2} \gamma_{D'} \otimes T^{\dagger}_{J'L'S'M'}(\mathbf{n}_2)_{\sigma_2\sigma'_2} \otimes (\tau_{T'0})_{t_2 t'_2} \\
&\times\ \varphi_{\ell}(\mathbf{r}_2,\sigma'_2,t'_2) \\
&= \int r_2^2\, dr_2 \int d\mathbf{n}_2 \sum_{t_2 t'_2} \sum_{\sigma_2,\sigma'_2} \varphi^{\dagger}_{\ell'}(\mathbf{r}_2,\sigma_2,t_2) \frac{\delta(r'-r_2)}{r' r_2} \gamma_{D'} \otimes T^{\dagger}_{J'L'S'M'}(\mathbf{n}_2)_{\sigma_2\sigma'_2} \\
&\otimes\ (\tau_{T0})_{t_2 t'_2}\ \varphi_{\ell}(\mathbf{r}_2,\sigma'_2,t'_2) \\
&= \int d\mathbf{n}_2 \sum_{t_2 t'_2} \sum_{\sigma_2,\sigma'_2} \varphi^{\dagger}_{\ell'}(r',\mathbf{n}_2,\sigma_2,t_2) \gamma_{D'} \otimes T^{\dagger}_{J'L'S'M'}(\mathbf{n}_2)_{\sigma_2\sigma'_2} \otimes (\tau_{T0})_{t_2 t'_2} \\
&\times\ \varphi_{\ell}(r',\mathbf{n}_2,\sigma'_2,t'_2).
\end{aligned} \tag{6.33}$$

For computational convenience, one wants to avoid the denominator $1/r^2$ $(1/r'^2)$ in the matrix element $Q^{c}_{kk'}(r)$ $(Q^{c'*}_{\ell\ell'}(r'))$, which originates from the Dirac spinor $\varphi_k(\mathbf{r},\sigma,t)$. To achieve this purpose, one introduces the Dirac spinor

$$\Psi_k(\mathbf{r},\sigma,t) = \begin{bmatrix} F_{\kappa_k}(r)\Omega_{j_k\ell_k m_k}(\mathbf{n},\sigma) \\ iG_{\kappa_k}(r)\Omega_{j_k\tilde{\ell}_k m_k}(\mathbf{n},\sigma) \end{bmatrix} \chi_{\frac{1}{2}\tau_k}(t), \tag{6.34}$$

so that the particle-hole interaction $V^{\rm ph}_{k\ell' k'\ell}$ now reads

$$V^{\rm ph}_{k\ell' k'\ell} = \sum_{cc'} \int_0^\infty dr \int_0^\infty dr' \mathcal{Q}^c_{kk'}(r) v^{\rm ph}_{cc'}(r,r') \mathcal{Q}^{c'*}_{\ell\ell'}(r'), \tag{6.35}$$

where the matrix elements $\mathcal{Q}^c_{kk'}(r)$ and $\mathcal{Q}^{c'*}_{\ell\ell'}(r')$ are

$$\begin{aligned}
\mathcal{Q}^c_{kk'}(r) &= \int d\mathbf{n}_1 \sum_{t_1,t_1'} \sum_{\sigma_1,\sigma_1'} \Psi^\dagger_k(r,\mathbf{n}_1,\sigma_1,t_1) \gamma_D \otimes T_{JLSM}(\mathbf{n}_1)_{\sigma_1\sigma_1'} \otimes (\tau_{T0})_{t_1 t_1'} \\
&\times \Psi_{k'}(r,\mathbf{n}_1,\sigma_1',t_1'), \qquad (6.36) \\
\mathcal{Q}^{c'*}_{\ell\ell'}(r') &= \int d\mathbf{n}_2 \sum_{t_2,t_2'} \sum_{\sigma_2,\sigma_2'} \Psi^\dagger_{\ell'}(r',\mathbf{n}_2,\sigma_2,t_2) \gamma_{D'} \otimes T^\dagger_{J'L'S'M'}(\mathbf{n}_2)_{\sigma_2\sigma_2'} \otimes (\tau_{T0})_{t_2 t_2'} \\
&\times \Psi_\ell(r',\mathbf{n}_2,\sigma_2',t_2'). \qquad (6.37)
\end{aligned}$$

The use of symbol $\Psi_k(\mathbf{r},\sigma,t)$ to indicate the Dirac spinor without the denominator $1/r^2$ should not be confused with the fermionic field $\Psi(\mathbf{r},t)$. The radial functions $F_{\kappa_k}(r)$ and $G_{\kappa_k}(r)$ satisfy the normalization condition

$$\int_0^\infty dr [|F_{\kappa_k}(r)|^2 + |G_{\kappa_k}(r)|^2] = 1. \tag{6.38}$$

Making use of Eqs. (6.35) and (5.86), one obtains

$$\begin{aligned}
A_{kk'\ell\ell'} &= (E_k + E_{k'}) \delta_{k\ell} \delta_{k'\ell'} \\
&+ \sum_{cc'} \int_0^\infty dr \int_0^\infty dr' \, \eta^S_{kk'} \mathcal{Q}^c_{k\bar{k}'}(r) v^{\rm ph}_{cc'}(r,r') \eta^{S'}_{\ell\ell'} \mathcal{Q}^{c'*}_{\ell\bar{\ell}'}(r'), \qquad (6.39) \\
B_{kk'\ell\ell'} &= \sum_{cc'} \int_0^\infty dr \int_0^\infty dr' \, \eta^S_{kk'} \mathcal{Q}^c_{k\bar{k}'}(r) v^{\rm ph}_{cc'}(r,r') \eta^{S'}_{\ell\ell'} \mathcal{Q}^{c'*}_{\bar{\ell}'\ell}(r'). \qquad (6.40)
\end{aligned}$$

The corresponding complex conjugate of these matrix elements are

$$\begin{aligned}
A^*_{kk'\ell\ell'} &= (E_k + E_{k'}) \delta_{k\ell} \delta_{k'\ell'} \\
&+ \sum_{cc'} \int_0^\infty dr \int_0^\infty dr' \, \eta^S_{kk'} \mathcal{Q}^c_{\bar{k}'k}(r) v^{\rm ph}_{cc'}(r,r') \eta^{S'}_{\ell\ell'} \mathcal{Q}^{c'*}_{\bar{\ell}'\ell}(r'), \qquad (6.41) \\
B^*_{kk'\ell\ell'} &= \sum_{cc'} \int_0^\infty dr \int_0^\infty dr' \, \eta^S_{kk'} \mathcal{Q}^c_{\bar{k}'k}(r) v^{\rm ph}_{cc'}(r,r') \eta^{S'}_{\ell\ell'} \mathcal{Q}^{c'*}_{\ell\bar{\ell}'}(r'). \qquad (6.42)
\end{aligned}$$

Inserting Eqs. (6.39)-(6.42) into Eqs. (6.27) and (6.28) yields

$$\begin{aligned}[\omega - E_k - E_{k'}]X_{kk'} &= \sum_{\ell<\ell'}\sum_{cc'}\int_0^\infty dr\int_0^\infty dr'\ \mathcal{Q}^c_{k\bar{k}'}(r)\eta^S_{kk'}v^{\rm ph}_{cc'}(r,r') \\ &\times \left[\mathcal{Q}^{c'*}_{\ell\bar{\ell}'}(r')\eta^{S'}_{\ell\ell'}X_{\ell\ell'} + \mathcal{Q}^{c'*}_{\bar{\ell}'\ell}(r')\eta^{S'}_{\ell\ell'}Y_{\ell\ell'}\right] \end{aligned} \tag{6.43}$$

and

$$\begin{aligned}[\omega + E_k + E_{k'}]Y_{kk'} &= -\sum_{\ell<\ell'}\sum_{cc'}\int_0^\infty dr\int_0^\infty dr'\ \mathcal{Q}^c_{\bar{k}'k}(r)\eta^S_{kk'}v^{\rm ph}_{cc'}(r,r') \\ &\times \left[\mathcal{Q}^{c'*}_{\bar{\ell}'\ell}(r')\eta^{S'}_{\ell\ell'}Y_{\ell\ell'} + \mathcal{Q}^{c'*}_{\ell\bar{\ell}'}(r')\eta^{S'}_{\ell\ell'}X_{\ell\ell'}\right]. \end{aligned} \tag{6.44}$$

Defining

$$\mathscr{T}^{c'}(r') := \sum_{\ell<\ell'} T^{c'}_{\ell\ell'}(r') = \sum_{\ell<\ell'}\left[\mathcal{Q}^{c'*}_{\ell\bar{\ell}'}(r')\eta^{S'}_{\ell\ell'}X_{\ell\ell'} + \mathcal{Q}^{c'*}_{\bar{\ell}'\ell}\eta^{S'}_{\ell\ell'}Y_{\ell\ell'}\right], \tag{6.45}$$

one obtains

$$\begin{aligned} 0 &= [E_k + E_{k'} - \omega]X_{kk'} \\ &+ \sum_{\ell<\ell'}\sum_{cc'}\int_0^\infty dr\int_0^\infty dr'\ \mathcal{Q}^c_{k\bar{k}'}(r)\eta^S_{kk'}v^{\rm ph}_{cc'}(r,r')T^{c'}_{\ell\ell'}(r'), \end{aligned} \tag{6.46}$$

$$\begin{aligned} 0 &= [E_k + E_{k'} + \omega]Y_{kk'} \\ &+ \sum_{\ell<\ell'}\sum_{cc'}\int_0^\infty dr\int_0^\infty dr'\ \mathcal{Q}^c_{\bar{k}'k}(r)\eta^S_{kk'}v^{\rm ph}_{cc'}(r,r')T^{c'}_{\ell\ell'}(r'). \end{aligned} \tag{6.47}$$

These equations lead to the QRPA dispersion relation [167]

$$0 = \sum_{c'}\int_0^\infty dr'\left\{\delta(r''-r')\delta_{c''c'} - \sum_c\int_0^\infty dr\ \mathcal{R}^{0c''c}(r'',r,\omega)v^{\rm ph}_{cc'}(r,r')\right\}\mathscr{T}^{c'}(r'), \tag{6.48}$$

where the reduced free response function $\mathcal{R}^{0cc'}(r,r',\omega)$ is defined as

$$\mathcal{R}^{0cc'}(r,r',\omega) = \sum_{k<k'}\left\{\frac{\mathcal{Q}^{c*}_{k\bar{k}'}(r)\eta^S_{kk'}\mathcal{Q}^{c'}_{k\bar{k}'}(r')\eta^{S'}_{kk'}}{\omega - E_k - E_{k'}} - \frac{\mathcal{Q}^{c*}_{\bar{k}'k}(r)\eta^S_{kk'}\mathcal{Q}^{c'}_{\bar{k}'k}(r')\eta^{S'}_{kk'}}{\omega + E_k + E_{k'}}\right\}. \tag{6.49}$$

Defining

$$\mathcal{W}^{cc'}(r,r',\omega) = \delta(r-r')\delta_{cc'} - \sum_{c''}\int_0^\infty dr''\mathcal{R}^{0cc''}(r,r'',\omega)v^{\rm ph}_{c''c'}(r'',r'), \tag{6.50}$$

the reduced response function $\mathcal{R}^{cc'}(r,r',\omega)$ is determined via [167]

$$\mathcal{R}^{cc'}(r,r',\omega) = \int_0^\infty dr'' \sum_{c''} (\mathcal{W}^{cc''})^{-1}(r,r'',\omega)\mathcal{R}^{0c''c'}(r'',r',\omega), \tag{6.51}$$

which leads to the Bethe-Salpeter equation in the coordinate-channel representation:

$$\begin{aligned}\mathcal{R}^{cc'}(r,r',\omega) &= \mathcal{R}^{0cc'}(r,r',\omega) \\ &+ \sum_{c_1c_2}\int_0^\infty dr_1 \int_0^\infty dr_2\, \mathcal{R}^{0cc_1}(r,r_1,\omega)v^{\rm ph}_{c_1c_2}(r_1,r_2)\mathcal{R}^{c_2c'}(r_2,r',\omega).\end{aligned} \tag{6.52}$$

The reduced free response function $\mathcal{R}^{0cc'}(r,r',\omega)$ being given by Eq. (6.49) has the following spectral decomposition

$$\mathcal{R}^{0cc'}_{\rm 2qp}(r,r',\omega) = \sum_{k<k'}\left\{\frac{\mathcal{Q}^{c*}_{k\bar{k}'}(r)\eta^S_{kk'}\mathcal{Q}^{c'}_{k\bar{k}'}(r')\eta^{S'}_{kk'}}{\omega - E_k - E_{k'}} - \frac{\mathcal{Q}^{c*}_{\bar{k}'k}(r)\eta^S_{kk'}\mathcal{Q}^{c'}_{\bar{k}'k}(r')\eta^{S'}_{kk'}}{\omega + E_k + E_{k'}}\right\}. \tag{6.53}$$

Here the subscript 2qp indicates that the transitions occur between two quasiparticle states inside the pairing active space. In the present work, which applies the BCS approach for the pairing correlations, the pairing active space refers to the bound states with the single-particle energy $\epsilon_k < 0$. Under this assumption, the reduced free response function must include the excitations between the quasiparticle states and continuum states ($\epsilon_k > 0$), which are treated as pure particle states. Following Ref. [65], one starts with reduced free response function (6.49) but without the restriction $k < k'$, viz.

$$\begin{aligned}\mathcal{R}^{0cc'}(r,r',\omega) &= \sum_{kk'}\left\{\frac{\mathcal{Q}^{c*}_{k\bar{k}'}(r)\eta^S_{kk'}\mathcal{Q}^{c'}_{k\bar{k}'}(r')\eta^{S'}_{kk'}}{\omega - E_k - E_{k'}} - \frac{\mathcal{Q}^{c*}_{\bar{k}'k}(r)\eta^S_{kk'}\mathcal{Q}^{c'}_{\bar{k}'k}(r')\eta^{S'}_{kk'}}{\omega + E_k + E_{k'}}\right\} \\ &= \sum_{kk'}\left\{\frac{\mathcal{Q}^{c*}_{k\bar{k}'}(r)\eta^S_{kk'}\mathcal{Q}^{c'}_{k\bar{k}'}(r')\eta^{S'}_{kk'}}{\omega - E_k - E_{k'}} - (-1)^{S+S'}\frac{\mathcal{Q}^{c*}_{\bar{k}k'}(r)\eta^S_{kk'}\mathcal{Q}^{c'}_{\bar{k}k'}(r')\eta^{S'}_{kk'}}{\omega + E_k + E_{k'}}\right\}.\end{aligned} \tag{6.54}$$

Let k be the pure particle states, which are denoted by index i and have the BCS occupation number $v_i^2 = 0$. We also substitute the quasiparticle index k' with k. Accordingly, the multiplicative factor $\eta^S_{kk'}\eta^{S'}_{kk'}$ now reduces to the BCS occupation number $v_k^2 > 0$. Since there is no pairing interaction outside the pairing active space, the Bogoliubov energy E_i reduces

to $E_i = \epsilon_i - \lambda$. The reduced free response function (6.54) now becomes

$$\mathcal{R}^{0cc'}(r,r',\omega) = \sum_k v_k^2 \sum_i \left\{ \frac{\mathcal{Q}^{c\dagger}_{ki}(r)\mathcal{Q}^{c'}_{ik}(r')}{\omega - E_k + \lambda - \epsilon_i} + (-1)^{S+S'} \frac{\mathcal{Q}^{c\dagger}_{ki}(r)\mathcal{Q}^{c'}_{ik}(r')}{-\omega - E_k + \lambda - \epsilon_i} \right\} \tag{6.55}$$

or

$$\begin{aligned} \mathcal{R}^{0cc'}(r,r',\omega) &= \sum_k v_k^2 \Bigg\{ \langle k|\hat{\mathcal{Q}}^{c\dagger}(r) \frac{1}{\omega - E_k + \lambda - \hat{h}^D} \sum_i |i\rangle\langle i|\hat{\mathcal{Q}}^{c'}(r')|k\rangle \\ &+ (-1)^{S+S'} \langle k|\hat{\mathcal{Q}}^{c\dagger}(r) \frac{1}{-\omega - E_k + \lambda - \hat{h}^D} \sum_i |i\rangle\langle i|\hat{\mathcal{Q}}^{c'}(r')|k\rangle \Bigg\}, \end{aligned} \tag{6.56}$$

since the single-particle energies ϵ_i are the eigenvalues of the Dirac Hamiltonian $\hat{h}^D$. Using the completeness relation $\sum_i |i\rangle\langle i| = 1 - \sum_{k'} |k'\rangle\langle k'|$, one obtains

$$\begin{aligned} \mathcal{R}^{0cc'}(r,r',\omega) &= \sum_k v_k^2 \langle k|\hat{\mathcal{Q}}^{c\dagger}(r)[\hat{G}(\omega - E_k + \lambda) + (-1)^{S+S'}\hat{G}(-\omega - E_k + \lambda)]\hat{\mathcal{Q}}^{c'}(r')|k\rangle \\ &- \sum_{k<k'} \mathcal{Q}^{c*}_{k\bar{k}'}(r)\mathcal{Q}^{c'}_{k\bar{k}'}(r') \Bigg\{ v_k^2 \left[\frac{(-1)^{S+S'}}{\omega - (E_k + \epsilon_{k'} - \lambda)} - \frac{1}{\omega + (E_k + \epsilon_{k'} + \lambda)} \right] \\ &+ v_{k'}^2 \left[\frac{1}{\omega - (E_{k'} + \epsilon_k - \lambda)} - \frac{(-1)^{S+S'}}{\omega + (E_{k'} + \epsilon_k - \lambda)} \right] \Bigg\}, \end{aligned} \tag{6.57}$$

where the single-particle relativistic Green's function operators $\hat{G}(E)$ reads

$$\hat{G}(E) = \frac{1}{E - \hat{h}^D}. \tag{6.58}$$

The first term of Eq. (6.57) is the reduced non-spectral free response function,

$$\begin{aligned} \mathcal{R}^{0cc'}_{\rm cont}(r,r',\omega) &= \sum_k v_k^2 \langle k|\hat{\mathcal{Q}}^{c\dagger}(r)\Big\{\hat{G}(\omega - E_k + \lambda) + (-1)^{S+S'}\hat{G}(-\omega - E_k + \lambda)\Big\}\hat{\mathcal{Q}}^{c'}(r')|k\rangle \\ &= \sum_k v_k^2 \int dx_1 \int dx_2\ \Psi_k^\dagger(x_1)\mathcal{Q}_c^{(1)\dagger}(r)\Big\{G(x_1,x_2;\omega - E_k + \lambda) \\ &+ (-1)^{S+S'}G(x_1,x_2;-\omega - E_k + \lambda)\Big\}\mathcal{Q}^{(2)}_{c'}(r')\Psi_k(x_2). \end{aligned} \tag{6.59}$$

It includes the transitions from the quasiparticle states (bound states) to the pure particle states (both bound and continuum states). The second term of Eq. (6.57) is called the

correction term,

$$\mathcal{R}^{0cc'}_{\rm corr}(r,r',\omega) = \sum_{k<k'} \mathcal{Q}^{c*}_{k\bar{k}'}(r)\mathcal{Q}^{c'}_{k\bar{k}'}(r')\Bigg\{ v_k^2\left[\frac{(-1)^{S+S'}}{\omega-(E_k+\epsilon_{k'}-\lambda)}-\frac{1}{\omega+(E_k+\epsilon_{k'}+\lambda)}\right] + v_{k'}^2\left[\frac{1}{\omega-(E_{k'}+\epsilon_k-\lambda)}-\frac{(-1)^{S+S'}}{\omega+(E_{k'}+\epsilon_k-\lambda)}\right]\Bigg\} \tag{6.60}$$

This term emerges from the completeness relation and eliminates the double counting that occurs in the transitions between two bound states.

Following Ref. [168] the relativistic single-particle Green's function $G(x_1,x_2;E)$ takes the form

$$G(x_1,x_2;E) = \sum_k \frac{1}{W}\begin{pmatrix} \mathcal{F}_{\kappa_k}(r_1;E)\Omega_{j_k\ell_k m_k}(\mathbf{n}_1,\sigma_1) \\ i\mathcal{G}_{\kappa_k}(r_1;E)\Omega_{j_k\tilde{\ell}_k m_k}(\mathbf{n}_1,\sigma_1)\end{pmatrix}\chi_{\frac{1}{2}\tau_k}(t_1)\times \times \chi^*_{\frac{1}{2}\tau_k}(t_2)\begin{pmatrix} \Omega^*_{j_k\ell_k m_k}(\mathbf{n}_2,\sigma_2)\mathscr{P}^*_{\kappa_k}(r_2;E) & -i\Omega^*_{j_k\tilde{\ell}_k m_k}(\mathbf{n}_2,\sigma_2)\mathscr{Q}^*_{\kappa_k}(r_2;E)\end{pmatrix}, \tag{6.61}$$

for $r_1 < r_2$, and

$$G(x_1,x_2;E) = \sum_k \frac{1}{W}\begin{pmatrix} \mathscr{P}_{\kappa_k}(r_1;E)\Omega_{j_k\ell_k m_k}(\mathbf{n}_1,\sigma_1) \\ \mathscr{Q}_{\kappa_k}(r_1;E)\Omega_{j_k\tilde{\ell}_k m_k}(\mathbf{n}_1,\sigma_1)\end{pmatrix}\chi_{\frac{1}{2}\tau_k}(t_1)\times \times \chi^*_{\frac{1}{2}\tau_k}(t_2)\begin{pmatrix} \Omega^*_{j_k\ell_k m_k}(\mathbf{n}_2,\sigma_2)\mathcal{F}^*_{\kappa_k}(r_2;E) & -i\Omega^*_{j_k\tilde{\ell}_k m_k}(\mathbf{n}_2,\sigma_2)\mathcal{G}^*_{\kappa_k}(r_2;E)\end{pmatrix}, \tag{6.62}$$

for $r_1 > r_2$. The two radial functions $\mathcal{F}_{\kappa_k}(r;E)$ and $\mathcal{G}_{\kappa_k}(r;E)$ are the large and the small components of the radial Dirac spinor $|u_{\kappa_k}(r)\rangle$, viz.

$$|u_{\kappa_k}(r;E)\rangle = \begin{pmatrix} \mathcal{F}_{\kappa_k}(r;E) \\ i\mathcal{G}_{\kappa_k}(r;E)\end{pmatrix}, \tag{6.63}$$

so that the spinor $|u_{\kappa_k}(r;E)\rangle$ is the solution of the radial Dirac equation

$$(E-\hat{h}^D_{\kappa_k}(r))|u_{\kappa_k}(r;E)\rangle = 0, \tag{6.64}$$

where the radial Dirac Hamiltonian $\hat{h}^D_{\kappa_k}(r)$ is

$$\hat{h}^D_{\kappa_k}(r) = \begin{pmatrix} V(r)+S(r) & -i\left(-\frac{d}{dr}+\frac{\kappa_k}{r}\right) \\ i\left(\frac{d}{dr}+\frac{\kappa_k}{r}\right) & -2M+V(r)-S(r)\end{pmatrix}. \tag{6.65}$$

The solution $|u_{\kappa_k}(r;E)\rangle$ is regular at the origin. The radial Dirac spinor $|w_{\kappa_k}(r;E)\rangle$,

$$|w_{\kappa_k}(r;E)\rangle = \begin{pmatrix} \mathscr{P}_{\kappa_k}(r;E) \\ i\mathscr{Q}_{\kappa_k}(r;E) \end{pmatrix}, \tag{6.66}$$

is the irregular solution of the radial Dirac equation

$$(E - \hat{h}^D_{\kappa_k}(r))|w_{\kappa_k}(r;E)\rangle = 0. \tag{6.67}$$

At a large distance ($r \to \infty$), it represents an outgoing wave for $E > 0$ and, for $E < 0$, a wave function, which decreases exponentially. Multiplying Eq. (6.64) by $\langle w^*_{\kappa_k}(r;E)|$ and Eq. (6.67) by $\langle u^*_{\kappa_k}(r;E)|$ from the left, and taking the difference between the two, one obtains the expression for the Wronskian W, viz.

$$W = \begin{vmatrix} \mathscr{P}^*_{\kappa_k}(r;E) & \mathcal{F}_{\kappa_k}(r;E) \\ \mathscr{Q}^*_{\kappa_k}(r;E) & \mathcal{G}_{\kappa_k}(r;E) \end{vmatrix} = \mathscr{P}^*_{\kappa_k}(r;E)\mathcal{G}_{\kappa_k}(r;E) - \mathscr{Q}^*_{\kappa_k}(r;E)\mathcal{F}_{\kappa_k}(r;E) = \text{constant}, \tag{6.68}$$

where the constant is usually taken to be 1.

The potentials $V(r)+S(r)$ and $V(r)-S(r)$ can be considered as a constant, i.e., $V(r)+S(r) \approx V+S$ and $V(r)-S(r) \approx V-S$, near the origin. From the radial Dirac equation (6.64) one then obtains the following two coupled radial differential equations for $F_{\kappa_k}(r;E)$ and $G_{\kappa_k}(r;E)$:

$$0 = (E - V - S)F_{\kappa_k}(r) + \left(\frac{d}{dr} - \frac{\kappa_k}{r}\right) G_{\kappa_k}(r), \tag{6.69}$$

$$0 = (E + 2M - V + S)G_{\kappa_k}(r) - \left(\frac{d}{dr} + \frac{\kappa_k}{r}\right) F_{\kappa_k}(r). \tag{6.70}$$

Solving Eq. (6.70) for $G_{\kappa_k}(r)$, one obtains the relation between the upper and the lower components:

$$G_{\kappa_k}(r) = \frac{1}{E + 2M - V + S}\left(\frac{d}{dr} + \frac{\kappa_k}{r}\right) F_{\kappa_k}(r). \tag{6.71}$$

Inserting this result into Eq. (6.69) yields the equation for the upper component:

$$\frac{d^2}{dr^2}F_{\kappa_k}(r) - \frac{\kappa_k(\kappa_k+1)}{r}F_{\kappa_k}(r) + q^2 F_{\kappa_k}(r) = 0, \tag{6.72}$$

where $q^2 = (E - V - S)(E + 2M - V + S) > 0$ for $E > V + S$. The quantum number κ_k takes the values $\kappa_k = \mp(j_k + \frac{1}{2})$ for $j_k = \ell_k \pm \frac{1}{2}$. Since $\kappa_k(\kappa_k+1) = \ell_k(\ell_k+1)$ for each value

of κ_k, Eq. (6.72) can be written as

$$\frac{d^2F_{\ell_k}(r)}{dr^2} - \frac{\ell_k(\ell_k+1)}{r}F_{\ell_k}(r) + q^2F_{\ell_k}(r) = 0. \tag{6.73}$$

By substitution of the variable $x := qr$ and the ansatz $F_{\ell_k}(r) = r\tilde{F}_{\ell_k}(x)$, the radial equation (6.73) becomes

$$\frac{d^2\tilde{F}_{\ell_k}(x)}{dx^2} + \frac{2}{x}\frac{d\tilde{F}_{\ell_k}(x)}{dx} + \left[1 - \frac{\ell_k(\ell_k+1)}{x^2}\right]\tilde{F}_{\ell_k}(x) = 0, \tag{6.74}$$

which has four possible solutions: spherical Bessel functions $j_{\ell_k}(x)$, spherical Neumann functions $n_{\ell_k}(x)$, and the spherical Hankel functions $h^{(1)}_{\ell_k}(x) \equiv j_{\ell_k}(x) + in_{\ell_k}(x)$ and $h^{(2)}_{\ell_k}(x) \equiv h^{(1)*}_{\ell_k}(x)$ [169]. These four solutions ($f_{\ell_k}(x) = j_{\ell_k}(x),\ n_{\ell_k}(x),\ h^{(1,2)}_{\ell_k}(x)$) satisfy the recurrence relations: [170]

$$f_{\ell_k+1}(x) = \left(-\frac{d}{dx} + \frac{\ell_k}{x}\right)f_{\ell_k}(x), \tag{6.75}$$

$$f_{\ell_k-1}(x) = \left(\frac{d}{dx} + \frac{\ell_k+1}{x}\right)f_{\ell_k}(x). \tag{6.76}$$

Since the $n_{\ell_k}(x)$ are singular at the origin, the correct solution is $\tilde{F}_{\ell_k}(x) = j_{\ell_k}(x)$ and, hence, $F_{\ell_k}(r) = rj_{\ell_k}(qr)$. Inserting this result into Eq. (6.71) and making use of the recurrence relation (6.75), one obtains for the lower component

$$G_{\tilde{\ell}_k}(r) = -\frac{E-V-S}{q}rj_{\tilde{\ell}_k}(qr) \tag{6.77}$$

for $\kappa_k = -(\ell_k+1) = -\tilde{\ell}_k$. For the case of $\kappa_k = \ell_k = \tilde{\ell}_k + 1$, one obtains

$$G_{\tilde{\ell}_k}(r) = +\frac{E-V-S}{q}rj_{\tilde{\ell}_k}(qr). \tag{6.78}$$

Therefore, the analytical solution of Eq. (6.64) for $E > V + S$ is

$$|u_{\kappa_k}(r;E)\rangle = r\begin{pmatrix} j_{\ell_k}(qr) \\ \frac{\kappa_k}{|\kappa_k|}\frac{E-V-S}{q}j_{\tilde{\ell}_k}(qr) \end{pmatrix}. \tag{6.79}$$

In the limit of $r \to 0$ the spinor $|u_{\kappa_k}(r;E)\rangle$ reduces to [59]

$$|u_{\kappa_k}(r\to 0;E)\rangle = r\begin{pmatrix} \frac{(qr)^{\ell_k}}{(2\ell_k+1)!!} \\ \frac{\kappa_k}{|\kappa_k|}\frac{E-V-S}{q}\frac{(qr)^{\tilde{\ell}_k}}{(2\tilde{\ell}_k+1)!!} \end{pmatrix}. \tag{6.80}$$

To obtain the irregular solution of Eq. (6.67), one needs to consider two energy domains, i.e., $E<0$ and $E>0$. For $E>0$ two radial functions $\mathscr{P}_{\kappa_k}(r;E)$ and $\mathscr{Q}_{\kappa_k}(r;E)$ satisfy the two coupled radial differential equations:

$$0 = (E-V-S)\mathscr{P}_{\kappa_k}(r)+\left(\frac{d}{dr}-\frac{\kappa_k}{r}\right)\mathscr{Q}_{\kappa_k}(r), \tag{6.81}$$

$$0 = (E+2M-V+S)\mathscr{Q}_{\kappa_k}(r)-\left(\frac{d}{dr}+\frac{\kappa_k}{r}\right)\mathscr{P}_{\kappa_k}(r), \tag{6.82}$$

which are similar to Eqs. (6.69) and (6.70). The requirement that the solution of Eq. (6.67) for $E>0$ being an outgoing wave at large distance leads to

$$|w_{\kappa_k}(r;E>0)\rangle = qr\begin{pmatrix} h^{(1)}_{\ell_k}(qr) \\ \frac{|\kappa_k|}{\kappa_k}\frac{iq}{E+2M}h^{(1)}_{\tilde{\ell}_k}(qr)\end{pmatrix}, \tag{6.83}$$

where, in the limit of $r\to\infty$ it reduces to [59]

$$|w_{\kappa_k}(r\to\infty;E>0)\rangle = \begin{pmatrix} 1 \\ \frac{|\kappa_k|}{\kappa_k}\frac{iq}{E+M}\end{pmatrix}e^{iqr}. \tag{6.84}$$

Here one has also considered that the potentials $V(r)+S(r)$ and $V(r)-S(r)$ approach zero at a large distance to obtain the numerator of spinor $|w_{\kappa_k}(r;E>0)\rangle$. For $E<0$ Eqs. (6.81) and (6.82) yields

$$\frac{d^2\mathscr{P}_{\kappa_k}(r)}{dr^2}-\frac{\kappa_k(\kappa_k+1)}{r^2}\mathscr{P}_{\kappa_k}(r)-K^2\mathscr{P}_{\kappa_k}(r)=0, \tag{6.85}$$

together with

$$\mathscr{Q}_{\kappa_k}(r)=\frac{1}{E+2M}\left(\frac{d}{dr}+\frac{\kappa_k}{r}\right)\mathscr{P}_{\kappa_k}(r), \tag{6.86}$$

where $K=(V+S-E)(E-V+S+2M)>0$. The substitution $x=Kr$ and the ansatz $\mathscr{P}_{\kappa_k}(r)=x\tilde{\mathscr{P}}_{\kappa_k}(x)$ bring Eq. (6.85) to the form

$$\frac{d^2\tilde{\mathscr{P}}_{\ell_k}(x)}{dx^2}+\frac{2}{x}\frac{d\tilde{\mathscr{P}}_{\ell_k}(x)}{dx}-\left[1+\frac{\ell_k(\ell_k+1)}{x^2}\right]\tilde{\mathscr{P}}_{\ell_k}(x), \tag{6.87}$$

where one has used the relation $\kappa_k(\kappa_k+1)=\ell_k(\ell_k+1)$. The solution of this equation, which has the correct limit at a large distance, is given by

$$\tilde{\mathscr{P}}_{\ell_k}(x)=\sqrt{\frac{2}{\pi x}}K_{\ell_k+1/2}(x)\equiv k_{\ell_k}(x), \tag{6.88}$$

and, therefore, $P_{\ell_k}(r)=Kr\cdot k_{\ell_k}(Kr)$. Here $k_{\ell_k}(x)$ is the modified spherical Bessel function

and the function $K_\nu(x)$ is known as the modified Bessel function [169]. The modified spherical Bessel function $k_{\ell_k}(x)$ satisfy the following recurrence relations: [169]

$$k_{\ell_k+1}(x) = \left(-\frac{d}{dx}+\frac{\ell_k}{x}\right)k_{\ell_k}(x), \tag{6.89}$$

$$k_{\ell_k-1}(x) = -\left(\frac{d}{dx}+\frac{\ell_k+1}{x}\right)k_{\ell_k}(x). \tag{6.90}$$

For each value of κ_k Eq. (6.86) gives

$$\mathscr{Q}_{\tilde{\ell}_k}(r) = -\frac{K^2 r}{E+2M}k_{\tilde{\ell}_k}(x). \tag{6.91}$$

Therefore, one arrives at the spinor $|w_{\kappa_k}(r;E<0)\rangle$ of the form

$$|w_{\kappa_k}(r;E<0)\rangle = Kr\begin{pmatrix} k_{\ell_k}(Kr) \\ -\frac{K}{E+2M}k_{\tilde{\ell}_k}(Kr)\end{pmatrix}. \tag{6.92}$$

Finally, the spinor $|w_{\kappa_k}(r;E<0)\rangle$ reduces to [59]

$$|w_{\kappa_k}(r\to\infty;E<0)\rangle = \begin{pmatrix} 1 \\ -\frac{K}{E+2M}\end{pmatrix}e^{-Kr} \tag{6.93}$$

at a large distance ($r\to\infty$). The complete reduced free response function hence reads

$$\mathcal{R}^{0cc'}(r,r',\omega) = \mathcal{R}^{0cc'}_{\rm cont}(r,r',\omega)+\mathcal{R}^{0cc'}_{\rm 2qp}(r,r',\omega)-\mathcal{R}^{0cc'}_{\rm corr}(r,r',\omega). \tag{6.94}$$

The detailed calculation of the reduced matrix element of the free response $\mathcal{R}^{0cc'}(r,r',\omega)$ is given in Appendix G.

6.3 Pairing Interactions and Particle-particle Channels

As discussed in Section 5.2, the particle-particle interaction $\hat{V}^{\rm pp}$ can be approximated by the following Hamiltonian:

$$\hat{V}^{\rm pp} = -G\sum_{k_1,k_2>0}\hat{P}^\dagger_{k_1}\hat{P}_{k_2}, \tag{6.95}$$

where the pair-creation operator $\hat{P}^\dagger_{k_1}$ and the pair-annihilation operator $\hat{P}_{k_2}$ are defined as

$$\hat{P}^\dagger_{k_1} = \hat{a}^\dagger_{k_1}\hat{a}^\dagger_{\bar{k}_1} \tag{6.96}$$

and

$$\hat{P}_{k_2} = \hat{a}_{\bar{k}_2}\hat{a}_{k_2}. \tag{6.97}$$

With the aid of the inverse Bogoliubov transformations (5.60)-(5.63), the matrix element of $\hat{V}^{\rm pp}$ is given by

$$\begin{aligned} V^{\rm pp}_{kk'\ell\ell'} &= -G\sum_{k_1,k_2>0}\langle k|\hat{P}^\dagger_{k_1}|k'\rangle\langle\ell|\hat{P}_{k_2}|\ell'\rangle \\ &= -G\sum_{k_1,k_2>0}\langle {\rm BCS}|\hat{\alpha}_k\hat{P}^\dagger_{k_1}\hat{\alpha}^\dagger_{k'}|{\rm BCS}\rangle\langle {\rm BCS}|\hat{\alpha}_\ell\hat{P}_{k_2}\hat{\alpha}^\dagger_{\ell'}|{\rm BCS}\rangle \\ &= \chi\delta_{kk'}\delta_{\ell\ell'}, \end{aligned} \tag{6.98}$$

where the strength parameter χ is related to the gap parameter Δ and the pairing strength G via $\chi = -\Delta^2/G$. Retaining only the particle-particle channel, the matrix elements of QRPA matrices $\mathbf{A}$ and $\mathbf{B}$ now read

$$A_{kk'\ell\ell'} = (E_k + E_{k'})\delta_{k\ell}\delta_{k'\ell'} + \chi\sum_{d=\pm}\mathcal{S}^d_{kk'}\xi^d_{kk'}\mathcal{S}^d_{\ell\ell'}\xi^d_{\ell\ell'} \tag{6.99}$$

and

$$B_{kk'\ell\ell'} = \chi\sum_{d=\pm}\mathcal{S}^d_{kk'}\xi^d_{kk'}\mathcal{S}^d_{\ell\ell'}\xi^d_{\ell\ell'}, \tag{6.100}$$

where

$$\mathcal{S}^\pm_{kk'} = \frac{\delta_{kk'}}{\sqrt{2}} \quad \text{and} \quad \xi^\pm_{kk'} = u_k u_{k'} \mp v_k v_{k'}. \tag{6.101}$$

The QRPA eigenvalue equations now become

$$[\omega - E_k - E_{k'}]X_{kk'} = \chi\sum_{d=\pm}\mathcal{S}^d_{kk'}\xi^d_{kk'}\sum_{\ell<\ell'}\mathcal{S}^d_{\ell\ell'}\xi^d_{\ell\ell'}[X_{\ell\ell'} + Y_{\ell\ell'}], \tag{6.102}$$

$$-[\omega + E_k + E_{k'}]Y_{kk'} = \chi\sum_{d=\pm}\mathcal{S}^d_{kk'}\xi^d_{kk'}\sum_{\ell<\ell'}\mathcal{S}^d_{\ell\ell'}\xi^d_{\ell\ell'}[X_{\ell\ell'} + Y_{\ell\ell'}]. \tag{6.103}$$

Defining

$$T^d = \sum_{\ell<\ell'}\mathcal{S}^d_{\ell\ell'}\xi^d_{\ell\ell'}[X_{\ell\ell'} + Y_{\ell\ell'}], \tag{6.104}$$

one arrives at the dispersion relation

$$0 = \sum_{d=\pm}\left\{\delta_{dd'} - \mathcal{R}^{dd'}_0(\omega)\chi\right\}T^d, \tag{6.105}$$

where the free response function $\mathcal{R}_0^{dd'}(\omega)$ reads

$$\mathcal{R}_0^{dd'}(\omega) = \sum_{k<k'} \mathcal{S}^d_{kk'} \mathcal{S}^{d'}_{kk'} \xi^d_{kk'} \xi^{d'}_{kk'} \left[\frac{1}{\omega - E_k - E_{k'}} - \frac{1}{\omega + E_k + E_{k'}} \right]. \tag{6.106}$$

The particle-particle response function $\mathcal{R}^{dd'}(\omega)$ satisfies the Bethe-Salpeter equation

$$\mathcal{R}^{dd'}(\omega) = \mathcal{R}_0^{dd'}(\omega) + \sum_{d''=\pm} \mathcal{R}_0^{dd''}(\omega) \chi \mathcal{R}^{d''d'}(\omega). \tag{6.107}$$

Using the Wigner-Eckart theorem (see Appendix F), the particle-particle free response function reads

$$\mathcal{R}_0^{dd'}(\omega) = \sum_{(k\leq k')} \frac{1}{1+\delta_{(kk')}} \mathcal{S}^d_{(kk')} \mathcal{S}^{d'}_{(kk')} \xi^d_{(kk')} \xi^{d'}_{(kk')} \left[\frac{1}{\omega - E_{(k)} - E_{(k')}} - \frac{1}{\omega + E_{(k)} + E_{(k')}} \right], \tag{6.108}$$

where

$$\mathcal{S}^d_{(kk')} = \sqrt{j_k + \frac{1}{2}}\, \delta_{(kk')}. \tag{6.109}$$

Here the bracketed indices $(kk') \coloneqq \{j_k, \ell_k, j_{k'}, \ell_{k'}\}$ of a one-body operator refer to its corresponding reduced matrix element.

6.4 Strength Function

In the canonical basis, which coincides with the Dirac-BCS basis, the strength function $S(\omega)$ can be obtained from the particle-hole response function $R(\omega)$ via the well-known relation

$$S(\omega) \coloneqq -\frac{1}{\pi} \lim_{\Delta\to+0} \mathrm{Im} \sum_{kk'\ell\ell'} F^*_{kk'} R_{kk'\ell\ell'}(\omega + i\Delta) F_{\ell\ell'}, \tag{6.110}$$

where $F_{kk'}$ are the matrix elements of the one-body external field. The matrix elements $F_{kk'}$ can be expressed in terms of the matrix elements $\mathcal{Q}^c_{kk'}(r)$ as

$$F_{kk'} = \sum_c e_{cc_F} \int_0^\infty dr\ f^{c_F}(r) \mathcal{Q}^c_{kk'}(r), \tag{6.111}$$

where c_F is the channel index of the external field and e_{cc_F} is the corresponding effective charge. An external field for a specific mode of collective excitation is characterized by the channel index c_F, which comprises a set of quantum numbers: total angular momentum J, parity π, total orbital angular momentum L, spin S, and isospin T. The external field

Table 6.1: The list of channels c_F and their corresponding effective charges e_{cc_F}.

Channel c_F	J	π	L	T	$f^{c_F}(r)$	Channel c	e_{cc_F}
Isoscalar Monopole (ISM)	0	+	0	0	r^2	2	1
Isoscalar Quadrupole (ISQ)	2	+	2	0	r^2	2	1
Isovector Dipole (IVD)	1	−	1	1	r	2	$\frac{N-Z}{2A}$
						6	$\frac{1}{2}$

with channel c_F will act only on a certain channel c of the particle-hole interaction. The list of $S = 0$ channels $c_F \coloneqq (J,\ \pi,\ L,\ T)$ and their corresponding effective charges e_{cc_F} are tabulated in Table 6.1.

Let us now make a connection between the particle-hole response function $R_{kk'\ell\ell'}(\omega)$ and the particle-hole reduced response function $\mathcal{R}^{cc'}(r, r', \omega)$ in the coordinate-channel representation. The particle-hole response function $R_{kk'\ell\ell'}(\omega)$ satisfies the Bethe-Salpeter equation in the Dirac-BCS basis:

$$R_{kk'\ell\ell'}(\omega) = R^0_{kk'\ell\ell'}(\omega) + \sum_{k_1k_2\ell_1\ell_2} R^0_{kk'k_1\ell_1}(\omega) V^{\rm ph}_{k_1\ell_2\ell_1k_2} R_{k_2\ell_2\ell\ell'}(\omega). \tag{6.112}$$

Inserting Eq. (6.35) into the Bethe-Salpeter equation (6.112), we obtain

$$\begin{aligned} R_{kk'\ell\ell'}(\omega) &= R^0_{kk'\ell\ell'}(\omega) \\ &+ \sum_{c_1c_2} \int_0^\infty dr_1 \int_0^\infty dr_2 \sum_{k_1k_2\ell_1\ell_2} R^0_{kk'k_1\ell_1}(\omega) \mathcal{Q}^{c_1}_{k_1\ell_1}(r_1) v^{\rm ph}_{c_1c_2}(r_1, r_2) \mathcal{Q}^{c_2*}_{k_2\ell_2}(r_2) R_{k_2\ell_2\ell\ell'}(\omega). \end{aligned} \tag{6.113}$$

Multiplying the last equation with the matrix element $\mathcal{Q}^{c*}_{kk'}(r)$ from the left and $\mathcal{Q}^{c'}_{\ell\ell'}(r')$ from the right, and performing the summation over the indices $(kk'\ell\ell')$ lead to

$$\begin{aligned} &\sum_{kk'\ell\ell'} \mathcal{Q}^{c*}_{kk'}(r) R_{kk'\ell\ell'}(\omega) \mathcal{Q}^{c'}_{\ell\ell'}(r') \\ = &\sum_{kk'\ell\ell'} \mathcal{Q}^{c*}_{kk'}(r) R^0_{kk'\ell\ell'}(\omega) \mathcal{Q}^{c'}_{\ell\ell'}(r') + \sum_{c_1c_2} \int_0^\infty dr_1 \int_0^\infty dr_2 \sum_{kk'k_1\ell_1} \mathcal{Q}^{c*}_{kk'}(r) R^0_{kk'k_1\ell_1}(\omega) \mathcal{Q}^{c_1}_{k_1\ell_1}(r_1) \\ \times &\ v^{\rm ph}_{c_1c_2}(r_1, r_2) \sum_{k_2\ell_2\ell\ell'} \mathcal{Q}^{c_2*}_{k_2\ell_2}(r_2) R_{k_2\ell_2\ell\ell'}(\omega) \mathcal{Q}^{c'}_{\ell\ell'}(r'). \end{aligned} \tag{6.114}$$

Comparing the last equation and Eq. (6.52) one establishes the relationship between

the particle-hole response function $R_{kk'\ell\ell'}(\omega)$ in the Dirac-BCS basis and the particle-hole reduced response function $\mathcal{R}^{cc'}(r,r',\omega)$ in the coordinate-channel representation, viz.

$$\mathcal{R}^{cc'}(r,r',\omega) = \sum_{kk'\ell\ell'} \mathcal{Q}^{c*}_{kk'}(r) R_{kk'\ell\ell'}(\omega) \mathcal{Q}^{c'}_{\ell\ell'}(r'). \tag{6.115}$$

Similarly, one can also define the particle-hole reduced free response function $\mathcal{R}^{0cc'}(r,r',\omega)$ as

$$\mathcal{R}^{0cc'}(r,r',\omega) = \sum_{kk'\ell\ell'} \mathcal{Q}^{c*}_{kk'}(r) R^{0}_{kk'\ell\ell'}(\omega) \mathcal{Q}^{c'}_{\ell\ell'}(r'). \tag{6.116}$$

Using Eqs. (6.111) and (6.115), the strength function $S^{c_F}(\omega)$ for a specific excitation mode can be written as

$$\begin{aligned} S^{c_F}(\omega) &= -\frac{1}{\pi} \lim_{\Delta\to+0} \mathrm{Im} \sum_{cc'} e_{cc_F} e_{c'c_F} \int_0^\infty dr \int_0^\infty dr' f^{c_F}(r) \\ &\times \sum_{kk'\ell\ell'} \mathcal{Q}^{c*}_{kk'}(r) R_{kk'\ell\ell'}(\omega+i\Delta) \mathcal{Q}^{c'}_{\ell\ell'}(r') f^{c_F}(r') \\ &= -\frac{1}{\pi} \lim_{\Delta\to+0} \mathrm{Im} \sum_{cc'} e_{cc_F} e_{c'c_F} \int_0^\infty dr \int_0^\infty dr' f^{c_F}(r) \mathcal{R}^{cc'}(r,r',\omega+i\Delta) f^{c_F}(r'). \end{aligned} \tag{6.117}$$

Instead of solving Eq. (6.52), it is beneficial to solve the Bethe-Salpeter equation for the particle-hole response in terms of the density matrix variation $\delta\rho^{c}_{c_F}(r,\omega)$, which, in the coordinate-channel representation, has the form

$$\delta\rho^{c}_{c_F}(r,\omega) \coloneqq \int_0^\infty dr' \sum_{c'} e_{c'c_F} \mathcal{R}^{cc'}(r,r',\omega) f^{c_F}(r'). \tag{6.118}$$

The integral equation for this density matrix variation, as it follows from Eq. (6.52), becomes

$$\delta\rho^{c}_{c_F}(r,\omega) = \delta\rho^{0c}_{c_F}(r,\omega) + \sum_{c_1c_2} \int_0^\infty dr_1 \int_0^\infty dr_2 \; \mathcal{R}^{0cc_1}(r,r_1,\omega) v^{\mathrm{ph}}_{c_1c_2}(r_1,r_2) \delta\rho^{c_2}_{c_F}(r_2,\omega). \tag{6.119}$$

Accordingly, the strength function $S^{c_F}(\omega)$ is determined via the relation

$$S^{c_F}(\omega) = -\frac{1}{\pi} \lim_{\Delta\to+0} \mathrm{Im} \sum_{c} e_{cc_F} \int_0^\infty dr \; f^{c_F}(r) \; \delta\rho^{c}_{c_F}(r,\omega+i\Delta). \tag{6.120}$$

Thereby, the problem of solving the relativistic QRPA with the point-coupling interaction is formulated completely in the coordinate-channel representation. This allows for calculations

of nuclear response that take into account coupling to the single-particle continuum exactly. This is very important for calculating the nuclear multipole responses in light and loosely-bound nuclear systems. The numerical realization of the relativistic continuum QRPA has been done in Refs. [60, 144], where the results for the isoscalar giant monopole resonance and isovector giant dipole resonance for Sn isotopes were presented. The numerical calculations demonstrated reasonable agreement with the experimental data [171, 172, 173]. The continuum QRPA calculations also assessed the impact of the continuum effects on the low-lying pygmy dipole resonance (PDR) strengths in Tin isotopes. Now the task is to add the particle-vibration coupling to the relativistic continuum QRPA, as discussed in the first part of this dissertation, first at zero temperature, but eventually at $T > 0$. This will allow one to describe the spreading width of the high-frequency giant resonances and to resolve the fine structure of the PDR on equal footing with the continuum effects. The essential steps to perform this task are outlined in the next Chapter.

Chapter 7

Further Developments: The Inclusion of PVC Effects in the CRQRPA

The inclusion of the continuum effects in the relativistic QRPA has provided a better description of the strength distribution for spherical nuclei in both low-energy and high-energy domains. The continuum relativistic QRPA (CRQRPA) is designed to reproduce the escape width of the giant resonances (GRs) and to describe better the low-lying pygmy dipole resonance (PDR) in heavy spherical nuclei [59, 144]. However, one cannot describe the spreading width of GRs without taking into account the coupling between the correlated one-particle-one-hole (1p1h) excitations via the particle-vibration coupling mechanism. Here we outline the necessary steps to incorporate the PVC effects into the CRQRPA as follows:

1. Extract the phonon transition densities from the RCQRPA strength functions.
2. Verify the QRPA normalization condition numerically.
3. Calculate the particle-phonon coupling amplitude.
4. Construct the full response function in the coordinate space representation.

This program has been implemented in Ref. [70], however, relatively simple Woods-Saxon mean field and phenomenological Landau-Migdal effective interaction were used in the numerical implementation of this approach. The current developments are designed for implementations based on a more advanced relativistic self-consistent density-dependent forces. Because of the time constraints, only steps 1 and 2 were completed, and the remaining steps are to be done in the near future. We dedicate the next sections of this Chapter to explaining and introducing the essential formulas for steps 1 and 2.

7.1 Extraction of the Phonon Transition Densities

In what follows, we demonstrate how to extract the phonon transition densities of a specific multipolarity $c_F := J^\pi$. We start with Eq. (6.119) instead of (6.52). From the Eq. (6.119), one obtains the density matrix variation $\delta\rho^c_{c_F}(r,\omega)$. The density matrix variation $\delta\rho^c_{c_F}(r,\omega)$ relates to the phonon transition density $\rho^{\nu c}_{c_F}(r)$ via [77]

$$\rho^{\nu c}_{c_F}(r) = \lim_{\Delta\to+0}\sqrt{\frac{\Delta}{\pi S^{c_F}(\Omega^\nu)}}\mathrm{Im}\delta\rho^c_{c_F}(r,\Omega^\nu), \tag{7.1}$$

where Ω^ν is the energy of the excited state ν measured from the ground state energy E_0. We have investigated the accuracy of this formula at the pole $\omega = \Omega_\nu$ by performing numerical calculations. We first note that the transition probability can be calculated in the coordinate-channel representation as

$$B_{c_F}(\omega) = \left|\sum_c e_{cc_F}\int_0^\infty dr\ \rho^c_{c_F}(r,\omega)f^{c_F}(r)\right|^2 \tag{7.2}$$

for arbitrary ω. For arbitrary ω, we have defined

$$\rho^c_{c_F}(r,\omega) = \lim_{\Delta\to+0}\sqrt{\frac{\Delta}{\pi S^{c_F}(\omega)}}\mathrm{Im}\delta\rho^c_{c_F}(r,\omega). \tag{7.3}$$

Accordingly, the strength function $S^{c_F}(\omega)$ can be expressed in terms of the transition probability $B_{c_F}(\omega)$ as

$$S^{c_F}(\omega) \quad = \quad \lim_{\Delta\to+0}\frac{B_{c_F}(\omega)}{\pi\Delta}. \tag{7.4}$$

We have calculated the values of $S^{c_F}(\omega)$ numerically for a specific range of ω and compared

Table 7.1: Comparison between the isovector dipole (IVD) strengths $S^{(\mathrm{IVD})}(\omega)$ and $S^{(\mathrm{IVD})}_{\mathrm{ref}}(\omega)$ at the poles $\omega = \Omega_\nu$ for ^{16}O nucleus computed with the smearing parameter $\Delta = 200$ keV.

Ω [MeV]	$S^{(\mathrm{IVD})}_{\mathrm{ref}}(\Omega_\nu)$ [e^{2}fm^2/MeV]	$S^{(\mathrm{IVD})}(\Omega_\nu)$ [e^{2}fm^2/MeV], $\Delta = 200$ keV
16.70	6.5827898218804730	6.5827898218804712
18.50	0.68623455819759616	0.68623455819759593
19.90	0.20005132846979362	0.20005132846979365
23.10	0.17192296026764683	0.17192296026764683

the results to those of available code ($S^{c_F}_{\rm ref}(\omega)$) Ref. [60, 144]. We found that they are indeed the same at the pole $\omega = \Omega_\nu$ (see Table 7.1).

7.2 Numerical Verification of the QRPA Normalization Condition

We start with the QRPA equations written in the form

$$\begin{aligned}[\Omega_\nu - E_k - E_{k'}]X^\nu_{kk'} &= \sum_{\ell<\ell'}\sum_{cc'}\int_0^\infty dr\int_0^\infty dr'\ \mathcal{Q}^c_{k\bar{k}'}(r)\eta^S_{kk'}v^{\rm ph}_{cc'}(r,r') \\ &\times \left[\mathcal{Q}^{c'*}_{\ell\bar{\ell}'}(r')\eta^{S'}_{\ell\ell'}X^\nu_{\ell\ell'} + \mathcal{Q}^{c'*}_{\bar{\ell}'\ell}(r')\eta^{S'}_{\ell\ell'}Y^\nu_{\ell\ell'}\right] \end{aligned} \tag{7.5}$$

and

$$\begin{aligned}[\Omega_\nu + E_k + E_{k'}]Y^\nu_{kk'} &= -\sum_{\ell<\ell'}\sum_{cc'}\int_0^\infty dr\int_0^\infty dr'\ \mathcal{Q}^c_{\bar{k}'k}(r)\eta^S_{kk'}v^{\rm ph}_{cc'}(r,r') \\ &\times \left[\mathcal{Q}^{c'*}_{\bar{\ell}'\ell}(r')\eta^{S'}_{\ell\ell'}Y^\nu_{\ell\ell'} + \mathcal{Q}^{c'*}_{\ell\bar{\ell}'}(r')\eta^{S'}_{\ell\ell'}X^\nu_{\ell\ell'}\right] \end{aligned} \tag{7.6}$$

in the canonical basis. These are the equations (6.43) and (6.44) from the previous chapter with $\omega = \Omega_\nu$. Let us now define the radial components of the phonon transition densities $\rho^{c\nu}(r)$ as

$$\rho^{c\nu}(r) \coloneqq \sum_{\ell<\ell'}\left[\mathcal{Q}^{c*}_{\ell\bar{\ell}'}(r)\eta^S_{\ell\ell'}X^\nu_{\ell\ell'} + \mathcal{Q}^{c*}_{\bar{\ell}'\ell}(r)\eta^S_{\ell\ell'}Y^\nu_{\ell\ell'}\right]. \tag{7.7}$$

Using this definition, we can write the QRPA equations (7.5) and (7.6) as

$$X^\nu_{kk'} = \frac{1}{\Omega_\nu - E_k - E_{k'}}\sum_{cc'}\int_0^\infty dr\int_0^\infty dr'\ \mathcal{Q}^c_{k\bar{k}'}(r)\eta^S_{kk'}v^{\rm ph}_{cc'}(r,r')\rho^{c'\nu}(r'), \tag{7.8}$$

$$Y^\nu_{kk'} = -\frac{1}{\Omega_\nu + E_k + E_{k'}}\sum_{cc'}\int_0^\infty dr\int_0^\infty dr'\ \mathcal{Q}^c_{\bar{k}'k}(r)\eta^S_{kk'}v^{\rm ph}_{cc'}(r,r')\rho^{c'\nu}(r'). \tag{7.9}$$

The QRPA normalization condition reads

$$\frac{1}{4}\sum_{k<k'}\left[|X^\nu_{kk'}|^2 - |Y^\nu_{kk'}|^2\right] = 1, \tag{7.10}$$

where the factor $\frac{1}{4}$ originates from Eq. (6.6). Inserting Eqs. (7.8) and (7.9) into Eq. (7.10) and making use of Eqs. (G.22) and (G.23) (c.f. Appendix G) yields the reduced QRPA

normalization

$$\frac{1}{4}\sum_{(k\leq k')}\frac{1}{1+\delta_{(kk')}}[|X^{\nu}_{(kk')}|^2-|Y^{\nu}_{(kk')}|^2]=1, \tag{7.11}$$

where

$$\begin{aligned}
|X^{\nu}_{(kk')}|^2 &= \frac{1}{[\Omega^{\nu}-E_{(k)}-E_{(k')}]^2}\sum_{c_1c_2}\sum_{c_1'c_2'}\int_0^{\infty}dr_1\int_0^{\infty}dr_1'\int_0^{\infty}dr_2\int_0^{\infty}dr_2' \\
&\times \frac{\delta_{J_1J_1'}\delta_{M_1M_1'}}{2J_1+1}\left\{\mathcal{Q}^{c_1*}_{(kk')}(r_1)\eta^{S_1}_{(kk')}v^{\rm ph}_{c_1c_2}(r_1,r_2)\rho^{c_2\nu}(r_2)\right\} \\
&\times \left\{\mathcal{Q}^{c_1'*}_{(kk')}(r_1')\eta^{S_1'}_{(kk')}v^{\rm ph}_{c_1'c_2'}(r_1',r_2')\rho^{c_2'\nu}(r_2')\right\}, \qquad (7.12)\\
|Y^{\nu}_{(kk')}|^2 &= \frac{1}{[\Omega^{\nu}+E_{(k)}+E_{(k')}]^2}\sum_{c_1c_2}\sum_{c_1'c_2'}\int_0^{\infty}dr_1\int_0^{\infty}dr_1'\int_0^{\infty}dr_2\int_0^{\infty}dr_2' \\
&\times (-1)^{S_1+S_1'}\frac{\delta_{J_1J_1'}\delta_{M_1M_1'}}{2J_1+1}\left\{\mathcal{Q}^{c_1*}_{(kk')}(r_1)\eta^{S_1}_{(kk')}v^{\rm ph}_{c_1c_2}(r_1,r_2)\rho^{c_2\nu}(r_2)\right\} \\
&\times \left\{\mathcal{Q}^{c_1'*}_{(kk')}(r_1')\eta^{S_1'}_{(kk')}v^{\rm ph}_{c_1'c_2'}(r_1',r_2')\rho^{c_2'\nu}(r_2')\right\}. \qquad (7.13)
\end{aligned}$$

Since the phonon transition densities $\rho^{c\nu}(r)$ can be calculated numerically using Eq. (7.1), the numerical calculation of the reduced QRPA normalization is feasible.

Chapter 8

Conclusions and Outlook

The first part of this Ph.D. work focuses on a finite-temperature extension of the nuclear response theory beyond the relativistic RPA. Starting from the Lagrangian density of quantum hadrodynamics (QHD), the static residual interaction, which consists of the finite-range meson exchange between nucleons, is formulated. To calculate the dynamical, or induced, interaction, which contains coupling between nucleons and phonons, we generalized the time-blocking method developed previously for the zero-temperature case to the imaginary-time (Matsubara) formalism. In this generalization, we have shown that the temperature-dependent projection operator containing Fermi-Dirac occupation numbers gives rise to the soft blocking in the imaginary-time domain, replacing the sharp time blocking that occurs at zero temperature. The proposed soft-blocking technique, when applied to the Matsubara two-fermion propagators, results in the imaginary-time ordered diagrams. As a consequence, it reduces the Bethe-Salpeter equation for the nuclear response to a single frequency variable equation and well-defined analytical properties of the resulting response functions, such as locality and unitarity.

The method named finite-temperature relativistic time-blocking approximation (FT-RTBA) was implemented on the base of QHD using the NL3 parametrization. We investigated the temperature dependence of the dipole response in medium-light ^{48}Ca, ^{68}Ni, and medium-heavy ^{100,120,132}Sn nuclei. The obtained results are consistent with the existing experimental data on the GDR's width and with the result of Landau's theory for the temperature dependence of the GDR's width. The calculations extended to high temperatures explain the critical phenomenon of the disappearance of the GDR and suggest that the collective motion may reappear at low frequencies in the high-temperature regime. In addition to the dipole response, we also analyzed other multipoles, in particular, the isoscalar monopole and quadrupole responses in the ^{68}Ni nucleus. We found that the disappearance of the high-frequency collective motion at very high temperature and arising

prominent low-energy strength of thermal origin is a common phenomenon for all multipole responses. An accurate description of the low-lying strength, especially at the r-process temperature conditions, requires further improvement of the current version of FT-RTBA, such as the inclusion of the continuum effects and ground-state correlations associated with the PVC. The former is partly addressed in the second part of this dissertation, and the latter will be considered in the future work.

The first part of this Ph.D. work has resulted in four publications in peer-review journals: Physical Review Letters (PRL) [174], Physical Review C (PRC) [98], European Physical Journal A [157], and Physics Letters B [175]. The PRL paper briefly highlighted the essential formulas of the FT-RTBA and discussed the temperature dependence of dipole spectra in the even-even nuclei ^{48}Ca and $^{100,\,120,\,132}$Sn. A comprehensive analytical and numerical study within the FT-RTBA can be found in the PRC paper. In addition to the isovector dipole resonance in ^{48}Ca and $^{100,\,120,\,132}$Sn nuclei, the PRC paper discussed the temperature dependence of the isovector dipole response in ^{68}Ni nucleus. The temperature dependence of monopole and quadrupole response in ^{48}Ca nucleus was discussed in our publication in the European Physical Journal A. The PLB paper addressed the proton-neutron nuclear response in the framework of FT-RTBA. It discussed the temperature dependence of the Gamow-Teller and spin dipole resonances in the closed-shell nuclei ^{48}Ca, ^{78}Ni, and ^{132}Sn, as well as their broader impacts for the associated beta decay rates and lifetimes of ^{78}Ni and ^{132}Sn in hot astrophysical environments. Our results have also been disseminated in terms of oral presentations in two international conferences held by the American Physical Society (APS) Division of Nuclear Physics (DNP): 2017 Fall Meeting and 2019 April Meeting. In addition to the oral presentations, we presented our results in the form of a poster presentation in the Nuclear Structure 2018 conference.

In the second part of this Ph.D. work, we focus on the improvement of the continuum relativistic quasiparticle random phase approximation (CRQRPA) to incorporate the particle-vibration coupling effects. In an attempt to fully understand the CRQRPA, we work out in detail an alternative derivation of the CRQRPA equations starting from the non-relativistic QRPA equations in the canonical basis, in order to reconstruct and clarify the details of Ref. [60]. We demonstrated via numerical calculations that the phonon transition densities can be extracted directly from the phonon strength functions with high accuracy. We formulated a feasible formula to calculate the QRPA normalization condition numerically. The future work will address calculations of the particle-phonon coupling amplitude, and, in turn, the full response function in the coordinate space representation.

REFERENCES

[1] W. Nazarewicz, J. Phys. G: Nucl. Part. Phys. **43**, 044002 (2016).

[2] National Research Council, *Nuclear Physics: Exploring the Heart of Matter* (The National Academies Press, Washington, DC, 2013).

[3] T. Hamada and I. D. Johnston, Nucl. Phys. **34**, 382 (1962).

[4] R. V. Reid, Ann. Phys. **50**, 411 (1968).

[5] R. Machleidt, K. Holinde, and C. Elster, Phys. Rep. **149**, 1 (1987).

[6] R. B. Wiringa, V. G. Stoks, and R. Schiavilla, Phys. Rev. C **51**, 38 (1995).

[7] R. B. Wiringa, R. A. Smith, and T. L. Ainsworth, Phys. Rev. C **29**, 1207 (1984).

[8] M. Lacombe, B. Loiseau, J. M. Richard, R. V. Mau, J. Côté, P. Pirès, and R. de Tourreil, Phys. Rev. C **21**, 861 (1980).

[9] M. M. Nagels, T. A. Rijken, and J. J. De Swart, Phys. Rev. D **17**, 768 (1978).

[10] P. M. Maessen, T. A. Rijken, and J. J. De Swart, Phys. Rev. C **40**, 2226 (1989).

[11] V. G. Stoks, R. A. Klomp, C. P. Terheggen, and J. J. De Swart, Phys. Rev. C **49**, 2950 (1994).

[12] R. Machleidt, Q. MacPherson, E. Marji, R. Winzer, C. Zeoli, and D. R. Entem, Few-Body Systems **54**, 821 (2013).

[13] N. Ishii, S. Aoki, and T. Hatsuda, Phys. Rev. Lett. **99**, 022001 (2007).

[14] S. Aoki, T. Hatsuda, and N. Ishii, Prog. Theor. Phys **123**, 89 (2010).

[15] S. Aoki, T. Doi, T. Hatsuda, Y. Ikeda, T. Inoue, N. Ishii, K. Murano, H. Nemura, and K. Sasaki, Prog. Theor. Exp. Phys. **01A105** (2012).

[16] M. Naghdi, Phys. Part. Nucl. **45**, 924 (2014).

[17] B. S. Pudliner, V. R. Pandharipande, J. Carlson, S. C. Pieper, and R. B. Wiringa, Phys. Rev. C **56**, 1720 (1997).

[18] R. B. Wiringa, S. C. Pieper, J. Carlson, and V. R. Pandharipande, Phys. Rev. C **62**, 23 (2000).

[19] D. J. Dean and M. Hjorth-Jensen, Phys. Rev. C **69**, 054320 (2004).

[20] G. Hagen, T. Papenbrock, M. Hjorth-Jensen, and D. J. Dean, Rep. Prog. Phys. **77**, 096302 (2014).

[21] P. Ring and P. Schuck, *The Nuclear Many-Body Problem* (Springer-Verlag Berlin Heidelberg, Germany, 1980), 1st ed.

[22] T. H. R. Skyrme, Nucl. Phys. **9**, 615 (1958).

[23] M. Beiner, H. Flocard, N. Van Giai, and P. Quentin, Nucl. Phys. A **238**, 29 (1975).

[24] J. Bartel, P. Quentin, M. Brack, C. Guet, and H. B. Håkansson, Nucl. Phys. A **386**, 79 (1982).

[25] E. Chabanat, P. Bonche, P. Haensel, J. Meyer, and R. Schaeffer, Nucl. Phys. A **627**, 710 (1997).

[26] E. Chabanat, P. Bonche, P. Haensel, J. Meyer, and R. Schaeffer, Nucl. Phys. A **635**, 231 (1998).

[27] D. Gogny, in *Proceedings of the International Conference on Nuclear Selfconsistent Fields*, edited by G. Ripka and M. Porneuf (North Holland, Amsterdam, 1975), p. 333.

[28] L. M. Robledo, T. R. Rodriguez, and R. R. Rodriguez-Guzmán, J. Phys. G: Nucl. Part. Phys. **46**, 013001 (2019).

[29] D. Vautherin and D. M. Brink, Phys. Rev. C **5**, 626 (1972).

[30] J. Dechargé and D. Gogny, Phys. Rev. C **21**, 1568 (1980).

[31] P. Ring, Prog. Part. Nucl. Phys. **37**, 193 (1996).

[32] P. Ring, in *Proceedings of the NATO Advanced Research Workshop on The Nuclear Many-Body Problem 2001*, edited by W. Nazarewicz and D. Vretenar (Kluwer Academic Publishers, Dordrecht, The Netherlands, 2002).

[33] P. Ring, *Covariant Density Functional Theory and Applications to Finite Nuclei*, vol. 641 of *Lecture Notes in Physics* (Springer Berlin Heidelberg, Berlin, Heidelberg, 2004).

[34] J. N. Ginocchio, Phys. Rev. Lett. **78**, 436 (1997).

[35] P. Manakos and T. Mannel, Z. Phys. A **330**, 223 (1988).

[36] P. Manakos and T. Mannel, Z. Phys. A **334**, 481 (1989).

[37] T. Bürvenich, D. G. Madland, J. A. Maruhn, and P. G. Reinhard, Phys. Rev. C **65**, 044308 (2002).

[38] T. Nikšić, D. Vretenar, and P. Ring, Phys. Rev. C **78**, 034318 (2008).

[39] J. Meng, P. Ring, and P. Zhao, *Relativistic mean-field theory*, vol. 10 of *International Review of Nuclear Physics* (World Scientific, Singapore, 2016).

[40] P. G. Reinhard, M. Rufa, J. Maruhn, W. Greiner, and J. Friedrich, Z. Phys. A **323**, 13 (1986).

[41] H. Kucharek and P. Ring, Z. Phys. A **339**, 23 (1991).

[42] M. Serra and P. Ring, Phys. Rev. C **65**, 064324 (2002).

[43] M. Serra, A. Rummel, and P. Ring, Phys. Rev. C **65**, 014304 (2001).

[44] H. Kucharek, P. Ring, P. Schuk, R. Bengtsson, and M. Girod, Phys. Lett. B **216**, 249 (1989).

[45] T. Gonzalez-Llarena, J. L. Egido, G. A. Lalazissis, and P. Ring, Phys. Lett. B **379**, 13 (1996).

[46] M. N. Harakeh and A. van der Woude, *Giant Resonances: Fundamental High-Frequency Modes of Nuclear Excitation* (Oxford University Press, 2001).

[47] D. Vretenar, H. Berghammer, and P. Ring, Nucl. Phys. A **581**, 679 (1995).

[48] B. Podobnik, D. Vretenar, and P. Ring, Z. Phys. A **354**, 375 (1996).

[49] D. Vretenar, G. A. Lalazissis, R. Behnsch, W. Pöschl, and P. Ring, Nucl. Phys. A **621**, 853 (1997).

[50] J. M. Arias and M. Lozano, eds., *An Advanced Course in Modern Nuclear Physics*, vol. 581 of *Lecture Notes in Physics* (Springer Berlin Heidelberg, Berlin, Heidelberg, 2001).

[51] P. Ring, Z. Y. Ma, N. V. Giai, D. Vretenar, A. Wandelt, and L.-g. Cao, Nucl. Phys. A **694**, 249 (2001).

[52] Z. Ma, N. Van Giai, H. Toki, and M. L'Huillier, Phys. Rev. C **55**, 2385 (1997).

[53] J. F. Dawson and R. J. Furnstahl, Phys. Rev. C **42**, 2009 (1990).

[54] Z. Y. Ma, N. Van Giai, A. Wandelt, D. Vretenar, and P. Ring, Nucl. Phys. A **686**, 173 (2001).

[55] Z. Ma, H. Toki, and N. Van Giai, Nucl. Phys. A **627**, 1 (1997).

[56] N. Paar, P. Ring, T. Nikšić, and D. Vretenar, Phys. Rev. C **67**, 034312 (2003).

[57] Y. K. Gambhir, P. Ring, and A. Thimet, Ann. Phys. **198**, 132 (1990).

[58] S. G. Zhou, J. Meng, and P. Ring, Phys. Rev. C **68**, 034323 (2003).

[59] I. Daoutidis and P. Ring, Phys. Rev. C **80**, 24309 (2009).

[60] I. Daoutidis and P. Ring, Phys. Rev. C **83**, 044303 (2011).

[61] D. Yang, L. G. Cao, and Z. Y. Ma, Commun. Theor. Phys. **53**, 716 (2010).

[62] D. Yang, L. G. Cao, and Z. Y. Ma, Commun. Theor. Phys. **53**, 723 (2010).

[63] S. Shlomo and G. Bertsch, Nucl. Phys. A **243**, 507 (1975).

[64] S. Kamerdzhiev, R. J. Liotta, E. Litvinova, and V. Tselyaev, Phys. Rev. C **58**, 172 (1998).

[65] K. Hagino and H. Sagawa, Nucl. Phys. A **695**, 82 (2001).

[66] M. Matsuo, Nucl. Phys. A **696**, 371 (2001).

[67] V. Tselyaev, Sov. J. Nucl. Phys. **50**, 780 (1989).

[68] S. P. Kamerdzhiev, G. Y. Tertychny, and V. I. Tselyaev, Phys. Part. Nucl. **28**, 134 (1997).

[69] V. I. Tselyaev, Phys. Rev. C **75**, 024306 (2007).

[70] E. V. Litvinova and V. I. Tselyaev, Phys. Rev. C **75**, 054318 (2007).

[71] V. I. Tselyaev, Phys. Rev. C **88**, 1 (2013).

[72] N. Lyutorovich, J. Speth, A. Avdeenkov, F. Grümmer, S. Kamerdzhiev, S. Krewald, and V. I. Tselyaev, Eur. Phys. J. A **37**, 381 (2008).

[73] N. Lyutorovich, V. Tselyaev, J. Speth, S. Krewald, F. Grümmer, and P. G. Reinhard, Phys. Lett. B **749**, 292 (2015).

[74] V. Tselyaev, N. Lyutorovich, J. Speth, S. Krewald, and P. G. Reinhard, Phys. Rev. C **94**, 034306 (2016).

[75] N. Lyutorovich, V. Tselyaev, J. Speth, and P.-G. Reinhard, Phys. Rev. C **98**, 054304 (2018).

[76] N. A. Lyutorovich, V. I. Tselyaev, O. I. Achakovskiy, and S. P. Kamerdzhiev, JETP Lett. **107**, 659 (2018).

[77] E. Litvinova, P. Ring, and V. I. Tselyaev, Phys. Rev. C **75**, 064308 (2007).

[78] E. Litvinova, P. Ring, and V. Tselyaev, Phys. Rev. C **78**, 014312 (2008).

[79] E. Litvinova, P. Ring, and V. Tselyaev, Phys. Rev. Lett. **105**, 022502 (2010).

[80] E. Litvinova, P. Ring, and V. Tselyaev, Phys. Rev. C **88**, 044320 (2013).

[81] C. Robin and E. Litvinova, Eur. Phys. J. A **52**, 205 (2016).

[82] C. Robin and E. Litvinova, Phys. Rev. C **98**, 051301(R) (2018).

[83] C. Robin and E. Litvinova, Phys. Rev. Lett. **123**, 202501 (2019).

[84] E. Litvinova, Phys. Rev. C **91**, 034332 (2015).

[85] D. Savran, T. Aumann, and A. Zilges, Prog. Part. Nucl. Phys. **70**, 210 (2013).

[86] E. Litvinova, P. Ring, V. Tselyaev, and K. Langanke, Phys. Rev. C **79**, 054312 (2009).

[87] E. Litvinova, H. P. Loens, K. Langanke, G. Martínez-Pinedo, T. Rauscher, P. Ring, F. K. Thielemann, and V. Tselyaev, Nucl. Phys. A **823**, 26 (2009).

[88] J. Endres, E. Litvinova, D. Savran, P. A. Butler, M. N. Harakeh, S. Harissopulos, R. D. Herzberg, R. Krücken, A. Lagoyannis, N. Pietralla, et al., Phys. Rev. C **105**, 212503 (2010).

[89] A. Tamii, I. Poltoratska, P. Von Neumann-Cosel, Y. Fujita, T. Adachi, C. A. Bertulani, J. Carter, M. Dozono, H. Fujita, K. Fujita, et al., Phys. Rev. Lett. **107**, 062502 (2011).

[90] R. Massarczyk, R. Schwengner, F. Dönau, E. Litvinova, G. Rusev, R. Beyer, R. Hannaske, A. R. Junghans, M. Kempe, J. H. Kelley, et al., Phys. Rev. C **86**, 014319 (2012).

[91] E. G. Lanza, A. Vitturi, E. Litvinova, and D. Savran, Phys. Rev. C **89**, 041601(R) (2014).

[92] I. Poltoratska, R. W. Fearick, A. M. Krumbholz, E. Litvinova, H. Matsubara, P. Von Neumann-Cosel, V. Y. Ponomarev, A. Richter, and A. Tamii, Phys. Rev. C **89**, 054322 (2014).

[93] B. Özel-Tashenov, J. Enders, H. Lenske, A. M. Krumbholz, E. Litvinova, P. Von Neumann-Cosel, I. Poltoratska, A. Richter, G. Rusev, D. Savran, et al., Phys. Rev. C **90**, 024304 (2014).

[94] I. A. Egorova and E. Litvinova, Phys. Rev. C **94**, 034322 (2016).

[95] T. Marketin, E. Litvinova, D. Vretenar, and P. Ring, Phys. Lett. B **706**, 477 (2012).

[96] E. Litvinova, B. A. Brown, D. L. Fang, T. Marketin, and R. G. Zegers, Phys. Lett. B **730**, 307 (2014).

[97] E. Litvinova, C. Robin, and I. A. Egorova, Phys. Lett. B **776**, 72 (2018).

[98] H. Wibowo and E. Litvinova, Phys. Rev. C **100**, 024307 (2019).

[99] P. F. Bortignon, A. Bracco, and R. A. Broglia, *Giant Resonances: Nuclear Structure at Finite Temperature*, vol. 10 of *Contemporary Concepts in Physics* (CRC Press, 1998).

[100] J. J. Gaardhøje, C. Ellegaard, B. Herskind, and S. G. Steadman, Phys. Rev. Lett. **53**, 148 (1984), ISSN 0031-9007.

[101] J. J. Gaardhøje, C. Ellegaard, B. Herskind, R. M. Diamond, M. A. Deleplanque, G. Dines, A. O. Macchiavelli, and F. S. Stephens, Phys. Rev. Lett. **56**, 1783 (1986).

[102] A. Bracco, J. J. Gaardhøje, A. M. Bruce, J. D. Garrett, B. Herskind, M. Pignanelli, D. Barnéoud, H. Nifenecker, J. A. Pinston, C. Ristori, et al., Phys. Rev. Lett. **62**, 2080 (1989).

[103] E. Ramakrishnan, T. Baumann, A. Azhari, R. A. Kryger, R. Pfaff, M. Thoennessen, S. Yokoyama, J. R. Beene, M. L. Halbert, P. E. Mueller, et al., Phys. Rev. Lett. **76**, 2025 (1996).

[104] M. Mattiuzzi, A. Bracco, F. Camera, W. Ormand, J. Gaardhøje, A. Maj, B. Million, M. Pignanelli, and T. Tveter, Nucl. Phys. A **612**, 262 (1997).

[105] P. Heckman, D. Bazin, J. R. Beene, Y. Blumenfeld, M. J. Chromik, M. L. Halbert, J. F. Liang, E. Mohrmann, T. Nakamura, A. Navin, et al., Phys. Lett. B **555**, 43 (2003).

[106] D. Santonocito and Y. Blumenfeld, *Dynamics and Thermodynamics with Nuclear Degrees of Freedom* (Springer, 2006).

[107] N. Paar, D. Vretenar, E. Khan, and G. Colò, Rep. Prog. Phys. **70**, 691 (2007).

[108] X. Roca-Maza and N. Paar, Prog. Part. Nucl. Phys. **101**, 96 (2018).

[109] S. Goriely and E. Khan, Nucl. Phys. **A706**, 217 (2002).

[110] S. Goriely, E. Khan, and M. Samyn, Nuclear Physics A **739**, 331 (2004).

[111] A. C. Larsen and S. Goriely, Phys. Rev. C **82**, 14318 (2010).

[112] M. Arnould, S. Goriely, and K. Takahashi, Phys. Rep. **450**, 97 (2007).

[113] A. L. Goodman, Nucl. Phys. A **352**, 45 (1981), ISSN 03759474.

[114] O. Civitarese, R. Broglia, and C. Dasso, Ann. Phys. **156**, 142 (1984), ISSN 00034916.

[115] D. Vautherin and N. Vinh Mau, Phys. Lett. B **120**, 261 (1983).

[116] D. Vautherin and N. V. Mau, Nucl. Phys. A **422**, 140 (1984).

[117] W. Besold, P.-G. Reinhard, and C. Toepffer, Nucl. Phys. A **431**, 1 (1984).

[118] N. D. Dang and F. Sakata, Phys. Rev. C **55**, 6 (1997).

[119] M. Faber, J. Egido, and P. Ring, Phys. Lett. B **127**, 5 (1983).

[120] M. Gallardo, M. Diebel, T. Døssing, and R. A. Broglia, Nucl. Phys. A **443**, 415 (1985).

[121] P. Bortignon, R. Broglia, G. Bertsch, and J. Pacheco, Nucl. Phys. A **460**, 149 (1986).

[122] E. C. Seva and H. M. Sofia, Phys. Rev. C **56**, 3107 (1997).

[123] D. Lacroix, P. Chomaz, and S. Ayik, Phys. Rev. C **58**, 2154 (1998).

[124] D. Lacroix, P. Chomaz, and S. Ayik, Phys. Lett. B **489**, 137 (2000).

[125] A. N. Storozhenko, A. I. Vdovin, A. Ventura, and A. I. Blokhin, Phys. Rev. C **69**, 64320 (2004).

[126] Y. Alhassid, B. Bush, and S. Levit, Phys. Rev. Lett. **61**, 1926 (1988).

[127] Y. Alhassid and B. Bush, Nucl. Phys. A **509**, 461 (1990).

[128] Y. Alhassid and B. Bush, Phys. Rev. Lett. **65**, 2527 (1990), URL `https://link.aps.org/doi/10.1103/PhysRevLett.65.2527`.

[129] W. E. Ormand, P. F. Bortignon, and R. A. Broglia, Phys. Rev. Lett. **77**, 607 (1996).

[130] D. Kusnezov, Y. Alhassid, and K. A. Snover, Phys. Rev. Lett. **81**, 542 (1998).

[131] A. L. Goodman, Nucl. Phys. A **352**, 30 (1981).

[132] H. M. Sommermann, Ann. Phys. **151**, 163 (1983).

[133] P. Ring, L. M. Robledo, J. L. Egido, and M. Faber, Nucl. Phys. **A419**, 261 (1984).

[134] H. Sagawa and G. F. Bertsch, Phys. Lett. B **146**, 138 (1984).

[135] E. V. Litvinova, S. P. Kamerdziev, and V. I. Tselyaev, Phys. At. Nucl. **66**, 558 (2003).

[136] E. Khan, N. Van Giai, and M. Grasso, Nucl. Phys. A **731**, 311 (2004).

[137] E. Litvinova and N. Belov, Phys. Rev. C **88**, 031302(R) (2013).

[138] A. Voinov, E. Algin, U. Agvaanluvsan, T. Belgya, R. Chankova, M. Guttormsen, G. E. Mitchell, J. Rekstad, A. Schiller, and S. Siem, Phys. Rev. Lett. **93**, 142504 (2004).

[139] H. K. Toft, A. C. Larsen, A. Bürger, M. Guttormsen, A. Görgen, H. T. Nyhus, T. Renstrøm, S. Siem, G. M. Tveten, and A. Voinov, Phys. Rev. C **83**, 1 (2011).

[140] A. Simon, M. Guttormsen, A. C. Larsen, C. W. Beausang, P. Humby, J. T. Burke, R. J. Casperson, R. O. Hughes, T. J. Ross, J. M. Allmond, et al., Phys. Rev. C **93**, 034303 (2016).

[141] Y. F. Niu, N. Paar, D. Vretenar, and J. Meng, Phys. Lett. B **681**, 315 (2009).

[142] E. Yüksel, G. Colò, E. Khan, Y. F. Niu, and K. Bozkurt, Phys. Rev. C **96**, 024303 (2017).

[143] D. Vretenar, A. V. Afanasjev, G. A. Lalazissis, and P. Ring, Phys. Rep. **409**, 101 (2005).

[144] I. Daoutidis, Ph.D. thesis, Technische Universität München (2009).

[145] M. L. Bellac, F. Mortessagne, and G. G. Batrouni, *Equilibrium and Non-equilibrium Statistical Thermodynamics* (Cambridge University Press, Cambridge, 2004).

[146] B. D. Serot and J. D. Walecka, *Advances in Nuclear Physics Volume 16* (Plenum Press, New York, 1986).

[147] J. Boguta and A. R. Bodmer, Nucl. Phys. A **292**, 413 (1977).

[148] P.-G. Reinhard, Rep. Prog. Phys. **52**, 439 (1989).

[149] T. Matsubara, Prog. Theor. Phys **14**, 351 (1955).

[150] A. A. Abrikosov, L. P. Gorkov, and I. E. Dzyaloshinski, *Methods of Quantum Field Theory in Statistical Physics* (Dover Publications, New York, 1975).

[151] A. Zagoskin, *Quantum Theory of Many-Body Systems*, Graduate Texts in Physics (Springer International Publishing, Cham, 2014).

[152] S. Adachi and P. Schuck, Nucl. Phys. A **496**, 485 (1989).

[153] J. Dukelsky, G. Röpke, and P. Schuck, Nucl. Phys. A **628**, 17 (1998).

[154] E. Litvinova and P. Schuck, Phys. Rev. C **100**, 064320 (2019).

[155] S. Kamerdzhiev, J. Speth, and G. Tertychny, Phys. Rep. **393**, 1 (2004).

[156] G. A. Lalazissis, J. König, and P. Ring, Phys. Rev. C **55**, 540 (1997).

[157] E. Litvinova and H. Wibowo, Eur. Phys. J. A **55**, 223 (2019).

[158] S. C. Fultz, B. L. Berman, J. T. Caldwell, R. L. Bramblett, and M. A. Kelly, Phys. Rev. **186**, 1255 (1969).

[159] P. Heckman, D. Bazin, J. R. Beene, Y. Blumenfeld, M. J. Chromik, M. L. Halbert, J. F. Liang, E. Mohrmann, T. Nakamura, A. Navin, et al., Phys. Lett. B **555**, 43 (2003).

[160] E. Ramakrishnan, T. Baumann, A. Azhari, R. A. Kryger, R. Pfaff, M. Thoennessen, S. Yokoyama, J. R. Beene, M. L. Halbert, P. E. Mueller, et al., Phys. Rev. Lett. **76**, 2025 (1996).

[161] P. F. Bortignon, R. A. Broglia, G. F. Bertsch, and J. Pacheco, Nucl. Phys. A **460**, 149 (1986).

[162] L. D. Landau, Sov. Phys. JETP **5**, 101 (1957).

[163] M. Barranco, A. Polls, and J. Martorell, Nucl. Phys. A **444**, 445 (1985).

[164] J. R. Stone, N. J. Stone, and S. A. Moszkowski, Phys. Rev. C **89**, 044316 (2014).

[165] D. M. Brink and R. A. Broglia, *Nuclear Superfluidity* (Cambridge University Press, 2005).

[166] P. Bonche, H. Flocard, P. H. Heenen, S. J. Krieger, and M. S. Weiss, Nucl. Phys. A **443**, 39 (1985).

[167] K. Hagino, N. V. Giai, and H. Sagawa, Nucl. Phys. A **731**, 264 (2004).

[168] E. Tamura, Phys. Rev. B **45**, 3271 (1992).

[169] G. B. Arfken, H. J. Weber, and F. E. Harris, *Mathematical Methods for Physicists* (Elsevier, 2013), 7th ed.

[170] A. Wachter, *Relativistic Quantum Mechanics*, Theoretical and Mathematical Physics (Springer Netherlands, Dordrecht, 2011).

[171] T. Li, U. Garg, Y. Liu, R. Marks, B. K. Nayak, P. V. Rao, M. Fujiwara, H. Hashimoto, K. Kawase, K. Nakanishi, et al., Phys. Rev. Lett. **99**, 162503 (2007).

[172] A. Leprêtre, H. Beil, R. Bergère, P. Carlos, A. De Miniac, A. Veyssière, and K. Kernbach, Nucl. Phys. A **219**, 39 (1974).

[173] S. C. Fultz, B. L. Berman, J. T. Caldwell, R. L. Bramblett, and M. A. Kelly, Phys. Rev. **186**, 1255 (1969).

[174] E. Litvinova and H. Wibowo, Phys. Rev. Lett. **121**, 082501 (2018).

[175] E. Litvinova, C. Robin, and H. Wibowo, Phys. Lett. B **800**, 135134 (2020).

[176] F. Scheck, *Quantum Physics* (Springer Berlin Heidelberg, Berlin, Heidelberg, 2007).

Appendix A

Summation Over the Matsubara Frequencies

In this Appendix, we evaluate the first summation over ℓ' of Eq. (3.47), i.e.,

$$T\sum_{\ell'}\frac{1}{i\varepsilon_{\ell'}-\varepsilon_{k_3}+\mu}\frac{1}{i\varepsilon_{\ell}-i\varepsilon_{\ell'}+\omega_m}. \tag{A.1}$$

The fermion occupation number

$$n(\xi',T)=\frac{1}{e^{(\xi'-\mu)/T}+1} \tag{A.2}$$

has poles along the line of $\mathrm{Re}[\xi']=\mu$ given by

$$\xi_{\ell'}=i\varepsilon_{\ell'}+\mu, \tag{A.3}$$

where $\varepsilon_{\ell'}=(2\ell'+1)\pi T$ and $\ell'=0,\pm1,\pm2,....$ We expand the exponential term in the denominator of (A.2) in the vicinity of $\xi_{\ell'}$ and obtain

$$n(\xi',T)=-\frac{T}{\xi'-\xi_{\ell'}}. \tag{A.4}$$

Let us consider the contour integral

$$\oint_C\frac{d\xi'}{2\pi i}\frac{1}{\xi'-\varepsilon_{k_3}}\frac{1}{i\varepsilon_{\ell}-\xi'+\omega_m+\mu}n(\xi',T), \tag{A.5}$$

where the contour C is defined according to Figure A.1. Inserting Eq. (A.4) into Eq. (A.5) and using the residue theorem, it can be shown that Eq. (A.1) can be converted into the

contour integral (A.5), viz.,

$$T\sum_{\ell'}\frac{1}{i\varepsilon_{\ell'}-\varepsilon_{k_3}+\mu}\frac{1}{i\varepsilon_\ell-i\varepsilon_{\ell'}+\omega_m}=-\oint_C\frac{d\xi'}{2\pi i}\frac{1}{\xi'-\varepsilon_{k_3}}\frac{1}{i\varepsilon_\ell-\xi'+\omega_m+\mu}n(\xi',T). \quad \text{(A.6)}$$

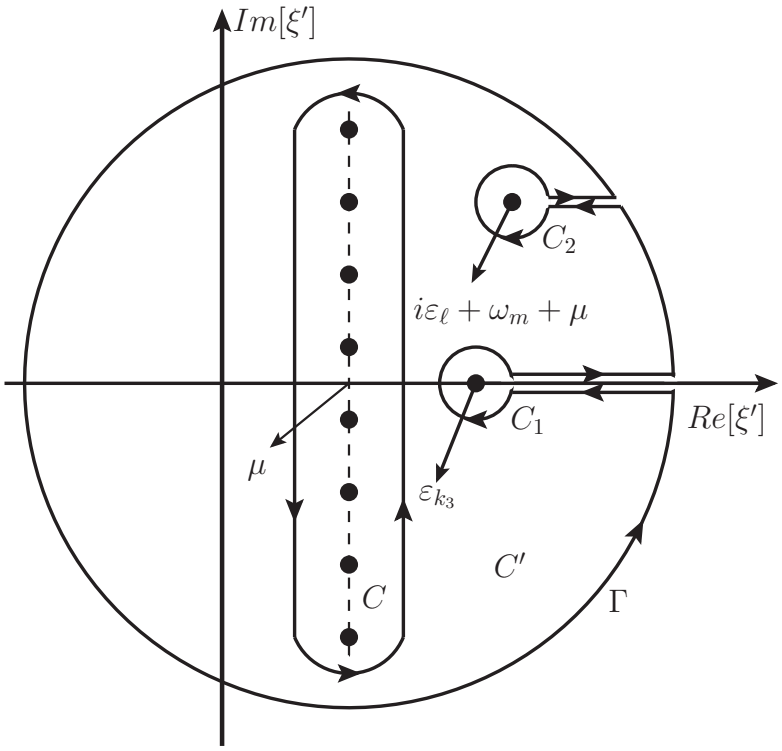

Figure A.1: Integration contours C and C' in the complex ξ'-plane.

Contour C now deforms into contour C', which consists of contours C_1, C_2, and Γ. The contours C_1 and C_2 enclose the poles ε_{k_3} and $i\varepsilon_\ell+\omega_m+\mu$, respectively (see Figure A.1). Accordingly, Eq. (A.6) then consists of three integrals:

$$\begin{aligned}
T\sum_{\ell'}\frac{1}{i\varepsilon_{\ell'}-\varepsilon_{k_3}+\mu}\frac{1}{i\varepsilon_\ell-i\varepsilon_{\ell'}+\omega_m} &= \oint_{C'}\frac{d\xi'}{2\pi i}\frac{1}{\xi'-\varepsilon_{k_3}}\frac{n(\xi',T)}{\xi'-i\varepsilon_\ell-\omega_m-\mu}\\
&= \int_\Gamma\frac{d\xi'}{2\pi i}\frac{1}{\xi'-\varepsilon_{k_3}}\frac{n(\xi',T)}{\xi'-i\varepsilon_\ell-\omega_m-\mu}\\
&+ \int_{C_1}\frac{d\xi'}{2\pi i}\frac{1}{\xi'-\varepsilon_{k_3}}\frac{n(\xi',T)}{\xi'-i\varepsilon_\ell-\omega_m-\mu}\\
&+ \int_{C_2}\frac{d\xi'}{2\pi i}\frac{1}{\xi'-\varepsilon_{k_3}}\frac{n(\xi',T)}{\xi'-i\varepsilon_\ell-\omega_m-\mu}. \quad \text{(A.7)}
\end{aligned}$$

The first integration along the contour Γ approaches zero as Γ goes to infinity. Using the residue theorem for the second and the third integrals, we thus obtain

$$T\sum_{\ell'}\frac{1}{i\varepsilon_{\ell'}-\varepsilon_{k_3}+\mu}\frac{1}{i\varepsilon_{\ell}-i\varepsilon_{\ell'}+\omega_m}=-\left[\frac{n(\varepsilon_{k_3},T)}{\varepsilon_{k_3}-i\varepsilon_{\ell}-\omega_m-\mu}+\frac{n(i\varepsilon_{\ell}+\omega_m+\mu,T)}{i\varepsilon_{\ell}+\omega_m+\mu-\varepsilon_{k_3}}\right]. \quad \text{(A.8)}$$

The numerator $n(i\varepsilon_{\ell}+\omega_m+\mu,T)$ can be identified as

$$n(i\varepsilon_{\ell}+\omega_m+\mu,T)=\frac{1}{1+e^{(i\varepsilon_{\ell}+\omega_m+\mu-\mu)/T}}=\frac{1}{1-e^{\omega_m/T}}=-N(\omega_m,T), \quad \text{(A.9)}$$

where $N(\omega_m,T)$ is phonon occupation number with energy ω_m. Therefore, (A.8) becomes

$$T\sum_{\ell'}\frac{1}{i\varepsilon_{\ell'}-\varepsilon_{k_3}+\mu}\frac{1}{i\varepsilon_{\ell}-i\varepsilon_{\ell'}+\omega_m}=\frac{n(\varepsilon_{k_3},T)+N(\omega_m,T)}{i\varepsilon_{\ell}-\varepsilon_{k_3}+\mu+\omega_m}. \quad \text{(A.10)}$$

Appendix B

Imaginary-time Projection Operator for Particle-hole Channel

In the τ representation, the $\widetilde{\mathscr{D}}$-operator for particle-hole channel, $\widetilde{\mathscr{D}}^{ph}(12,34)$, is given by

$$\begin{aligned}\widetilde{\mathscr{D}}^{ph}(12,34) &= -\delta_{k_1k_3}\delta_{k_2k_4}(1-n_{k_1})n_{k_2}[n_{k_2}\theta(\tau_{41})\theta(\tau_{31})\theta(\tau_{12}) \\ &+ (1-n_{k_1})\theta(\tau_{42})\theta(\tau_{32})\theta(\tau_{21})]e^{-[(\varepsilon_{k_1}-\mu)\tau_{31}+(\varepsilon_{k_2}-\mu)\tau_{24}]}. \qquad \text{(B.1)}\end{aligned}$$

Introducing the τ-difference variables $\tau_{31} = \tau_3 - \tau_1$, $\tau_{21} = \tau_2 - \tau_1$, and $\tau_{34} = \tau_3 - \tau_4$, the Fourier transformation of $\widetilde{\mathscr{D}}^{ph}(12,34) \equiv \widetilde{\mathscr{D}}^{ph}_{k_1k_2,k_3k_4}(\tau_{31},\tau_{21},\tau_{34})$ reads:

$$\begin{aligned}\widetilde{\mathscr{D}}^{ph}_{k_1k_2,k_3k_4}(\omega_n,\varepsilon_\ell,\varepsilon_{\ell'}) &= \int_{-1/T}^{1/T}\int_{-1/T}^{1/T}\int_{-1/T}^{1/T} d\tau_{31}d\tau_{21}d\tau_{34}\widetilde{\mathscr{D}}^{ph}_{k_1k_2,k_3k_4}(\tau_{31},\tau_{21},\tau_{34}) \\ &\times e^{i(\omega_n\tau_{31}+\varepsilon_\ell\tau_{21}+\varepsilon_{\ell'}\tau_{34})} \\ &= I_1 + I_2, \qquad \text{(B.2)}\end{aligned}$$

where

$$\begin{aligned}I_1 &= -\delta_{k_1k_3}\delta_{k_2k_4}[1-n_{k_1}]n_{k_2}^2\int d\tau_{31}d\tau_{21}d\tau_{34}e^{(i\omega_n-\varepsilon_{k_1}+\varepsilon_{k_2})\tau_{31}}e^{(i\varepsilon_\ell-\varepsilon_{k_2}+\mu)\tau_{21}} \\ &\times e^{(i\varepsilon_{\ell'}-\varepsilon_{k_2}+\mu)\tau_{34}}\theta(\tau_{31})\theta(\tau_{31}-\tau_{34})\theta(\tau_{12}), \qquad \text{(B.3)} \\ I_2 &= -\delta_{k_1k_3}\delta_{k_2k_4}[1-n_{k_1}]^2n_{k_2}\int d\tau_{31}d\tau_{21}d\tau_{34}e^{(i\omega_n-\varepsilon_{k_1}+\varepsilon_{k_2})\tau_{31}}e^{(i\varepsilon_\ell-\varepsilon_{k_2}+\mu)\tau_{21}} \\ &\times e^{(i\varepsilon_{\ell'}-\varepsilon_{k_2}+\mu)\tau_{34}}\theta(\tau_{21})\theta(\tau_{31}-\tau_{21}-\tau_{34})\theta(\tau_{31}-\tau_{21}). \qquad \text{(B.4)}\end{aligned}$$

We start by evaluating the term I_1. Normally, τ_{31} has range $-1/T \le \tau_{31} \le 1/T$. Because there is a theta function $\theta(\tau_{31})$, the limit of integration with respect to τ_{31} is $0 \le \tau_{31} \le 1/T$.

Similarly, the theta function $\theta(\tau_{12}) = \theta(-\tau_{21})$ constraints the limit of integration with respect to τ_{21} to be $-1/T \leq \tau_{21} \leq 0$. To determine the limit of integration with respect to τ_{34}, we consider the theta function $\theta(\tau_{31} - \tau_{34})$. The theta function $\theta(\tau_{31} - \tau_{34})$ constraints the limit of integration with respect to τ_{34} to be $-1/T \leq \tau_{34} - \tau_{31} \leq 0$ or $-1/T + \tau_{31} \leq \tau_{34} \leq \tau_{31}$. The theta functions $\theta(\tau_{31})$, $\theta(\tau_{12})$, and $\theta(\tau_{31} - \tau_{34})$ are expressed as

$$\begin{aligned}
\theta(\tau_{31}) &= -\lim_{\eta\to 0^+} \int_{-\infty}^{\infty} \frac{d\alpha}{2\pi i} \frac{e^{-i\alpha\tau_{31}}}{\alpha + i\eta}, && \text{(B.5)} \\
\theta(\tau_{12}) &= \theta(-\tau_{21}) = -\lim_{\xi\to 0^+} \int_{-\infty}^{\infty} \frac{d\beta}{2\pi i} \frac{e^{i\beta\tau_{21}}}{\beta + i\xi}, && \text{(B.6)} \\
\theta(\tau_{31} - \tau_{34}) &= -\lim_{\delta\to 0^+} \int_{-\infty}^{\infty} \frac{d\gamma}{2\pi i} \frac{e^{-i\gamma(\tau_{31}-\tau_{34})}}{\gamma + i\delta}. && \text{(B.7)}
\end{aligned}$$

Using these expressions and the consideration pertaining to the integral limits, I_1 becomes

$$\begin{aligned}
I_1 &= \delta_{k_1k_3}\delta_{k_2k_4}[1 - n_{k_1}]n_{k_2}^2 \lim_{\eta\to 0^+}\lim_{\xi\to 0^+}\lim_{\delta\to 0^+} \int_{-\infty}^{\infty} \frac{d\alpha}{2\pi i}\frac{1}{\alpha + i\eta} \int_{-\infty}^{\infty} \frac{d\beta}{2\pi i}\frac{1}{\beta + i\xi} \\
&\times \int_{-\infty}^{\infty} \frac{d\gamma}{2\pi i}\frac{1}{\gamma + i\delta} \int_{-1/T}^{0} d\tau_{21} e^{(i\varepsilon_\ell + i\beta - \varepsilon_{k_2} + \mu)\tau_{21}} \int_{0}^{1/T} d\tau_{31} e^{(i\omega_n - i\alpha - i\gamma - \varepsilon_{k_1} + \varepsilon_{k_2})\tau_{31}} \\
&\times \int_{-1/T+\tau_{31}}^{\tau_{31}} d\tau_{34} e^{(i\varepsilon_{\ell'} + i\gamma - \varepsilon_{k_2} + \mu)\tau_{34}}. && \text{(B.8)}
\end{aligned}$$

The result of the integration with respect to τ_{34} is

$$\int_{-1/T+\tau_{31}}^{\tau_{31}} d\tau_{34} e^{(i\varepsilon_{\ell'} + i\gamma - \varepsilon_{k_2} + \mu)\tau_{34}} = \frac{1}{i\varepsilon_{\ell'} + i\gamma - \varepsilon_{k_2} + \mu} e^{(i\varepsilon_{\ell'} + i\gamma - \varepsilon_{k_2} + \mu)\tau_{31}} \left[1 + e^{-(i\gamma - \varepsilon_{k_2} + \mu)/T}\right]. \quad \text{(B.9)}$$

The next integration with respect to τ_{31} gives

$$\begin{aligned}
&\int_{0}^{1/T} d\tau_{31} e^{(i\omega_n - i\alpha - i\gamma - \varepsilon_{k_1} + \varepsilon_{k_2})\tau_{31}} \int_{-1/T+\tau_{31}}^{\tau_{31}} d\tau_{34} e^{(i\varepsilon_{\ell'} + i\gamma - \varepsilon_{k_2} + \mu)\tau_{34}} \\
&= -\frac{1}{i\varepsilon_{\ell'} + i\gamma - \varepsilon_{k_2} + \mu} \frac{1}{i\omega_n + i\varepsilon_{\ell'} - i\alpha - \varepsilon_{k_1} + \mu} \left[1 + e^{-(i\gamma - \varepsilon_{k_2} + \mu)/T}\right] \\
&\times \left[e^{-(i\alpha + \varepsilon_{k_1} - \mu)/T} + 1\right]. && \text{(B.10)}
\end{aligned}$$

The last integration with respect to τ_{21} gives

$$\int_{-1/T}^{0} d\tau_{21} e^{(i\varepsilon_\ell + i\beta - \varepsilon_{k_2} + \mu)\tau_{21}} = \frac{1}{i\varepsilon_\ell + i\beta - \varepsilon_{k_2} + \mu} \left[1 + e^{-(i\beta - \varepsilon_{k_2} + \mu)/T}\right]. \quad \text{(B.11)}$$

Inserting these results into the term I_1, we obtain

$$\begin{aligned} I_1 &= -\delta_{k_1k_3}\delta_{k_2k_4}[1-n_{k_1}]n_{k_2}^2 \lim_{\eta\to 0^+}\int_{-\infty}^{\infty}\frac{d\alpha}{2\pi i}\frac{1}{\alpha+i\eta}\frac{1}{i\omega_n+i\varepsilon_{\ell'}-i\alpha-\varepsilon_{k_1}+\mu} \\ &\times \left[e^{-(i\alpha+\varepsilon_{k_1}-\mu)/T}+1\right]\lim_{\xi\to 0^+}\int_{-\infty}^{\infty}\frac{d\beta}{2\pi i}\frac{1}{\beta+i\xi}\frac{1}{i\varepsilon_\ell+i\beta-\varepsilon_{k_2}+\mu}\left[1+e^{-(i\beta-\varepsilon_{k_2}+\mu)/T}\right] \\ &\times \lim_{\delta\to 0^+}\int_{-\infty}^{\infty}\frac{d\gamma}{2\pi i}\frac{1}{\gamma+i\delta}\frac{1}{i\varepsilon_{\ell'}+i\gamma-\varepsilon_{k_2}+\mu}\left[1+e^{-(i\gamma-\varepsilon_{k_2}+\mu)/T}\right] \\ &= i\delta_{k_1k_3}\delta_{k_2k_4}[1-n_{k_1}]n_{k_2}^2 \lim_{\eta\to 0^+}\int_{-\infty}^{\infty}\frac{d\alpha}{2\pi i}\frac{1}{\alpha+i\eta}\frac{1}{\alpha-\omega_n-\varepsilon_{\ell'}-i(\varepsilon_{k_1}-\mu)} \\ &\times \left[e^{-(i\alpha+\varepsilon_{k_1}-\mu)/T}+1\right]\lim_{\xi\to 0^+}\int_{-\infty}^{\infty}\frac{d\beta}{2\pi i}\frac{1}{\beta+i\xi}\frac{1}{\beta+\varepsilon_\ell+i(\varepsilon_{k_2}-\mu)}\left[1+e^{-(i\beta-\varepsilon_{k_2}+\mu)/T}\right] \\ &\times \lim_{\delta\to 0^+}\int_{-\infty}^{\infty}\frac{d\gamma}{2\pi i}\frac{1}{\gamma+i\delta}\frac{1}{\gamma+\varepsilon_{\ell'}+i(\varepsilon_{k_2}-\mu)}\left[1+e^{-(i\gamma-\varepsilon_{k_2}+\mu)/T}\right]. \end{aligned} \tag{B.12}$$

The integration with respect to β is given by

$$\lim_{\xi\to 0^+}\int_{-\infty}^{\infty}\frac{d\beta}{2\pi i}\frac{1}{\beta+i\xi}\frac{1}{\beta+\varepsilon_\ell+i(\varepsilon_{k_2}-\mu)}\left[1+e^{-(i\beta-\varepsilon_{k_2}+\mu)/T}\right] = -\frac{i}{i\varepsilon_\ell-\varepsilon_{k_2}+\mu}\frac{1}{n_{k_2}}. \tag{B.13}$$

The integration with respect to γ is given by

$$\lim_{\delta\to 0^+}\int_{-\infty}^{\infty}\frac{d\gamma}{2\pi i}\frac{1}{\gamma+i\delta}\frac{1}{\gamma+\varepsilon_{\ell'}+i(\varepsilon_{k_2}-\mu)}\left[1+e^{-(i\gamma-\varepsilon_{k_2}+\mu)/T}\right] = -\frac{i}{i\varepsilon_{\ell'}-\varepsilon_{k_2}+\mu}\frac{1}{n_{k_2}}. \tag{B.14}$$

The integration with respect to α is given by

$$\begin{aligned} &\lim_{\eta\to 0^+}\int_{-\infty}^{\infty}\frac{d\alpha}{2\pi i}\frac{1}{\alpha+i\eta}\frac{1}{\alpha-\omega_n-\varepsilon_{\ell'}-i(\varepsilon_{k_1}-\mu)}\left[e^{-(i\alpha+\varepsilon_{k_1}-\mu)/T}+1\right] \\ &= \frac{i}{i(\varepsilon_{\ell'}+\omega_n)-\varepsilon_{k_1}+\mu}\frac{1}{1-n_{k_1}}. \end{aligned} \tag{B.15}$$

Inserting Eqs. (B.13), (B.14), and (B.15) into Eq. (B.12), we obtain

$$I_1 = \delta_{k_1k_3}\delta_{k_2k_4}\frac{1}{(i\varepsilon_\ell-\varepsilon_{k_2}+\mu)[i(\varepsilon_{\ell'}+\omega_n)-\varepsilon_{k_1}+\mu](i\varepsilon_{\ell'}-\varepsilon_{k_2}+\mu)}. \tag{B.16}$$

After evaluating the term I_1, we continue to evaluate the term I_2. The theta function $\theta(\tau_{21})$ constraints the integration limit of τ_{21} to be $0 \le \tau_{21} \le 1/T$. The theta function $\theta(\tau_{31}-\tau_{21})$ determines the integration limit of τ_{31} to be $0 \le \tau_{31}-\tau_{21} \le 1/T$ or $\tau_{21} \le \tau_{31} \le$

$\tau_{21} + 1/T$. The last theta function, i.e., $\theta(\tau_{31} - \tau_{21} - \tau_{34})$, gives the integration limit of τ_{34} as $-1/T \leq \tau_{34} - (\tau_{31} - \tau_{21}) \leq 0$ or $-1/T + (\tau_{31} - \tau_{21}) \leq \tau_{34} \leq \tau_{31} - \tau_{21}$. Similarly, we also express each of theta function as

$$\begin{aligned}
\theta(\tau_{21}) &= -\lim_{\eta\to 0^+} \int_{-\infty}^{\infty} \frac{d\alpha}{2\pi i} \frac{e^{-i\alpha\tau_{21}}}{\alpha + i\eta}, && \text{(B.17)} \\
\theta(\tau_{31} - \tau_{21}) &= -\lim_{\xi\to 0^+} \int_{-\infty}^{\infty} \frac{d\beta}{2\pi i} \frac{e^{-i\beta(\tau_{31}-\tau_{21})}}{\beta + i\xi}, && \text{(B.18)} \\
\theta(\tau_{31} - \tau_{21} - \tau_{34}) &= -\lim_{\delta\to 0^+} \int_{-\infty}^{\infty} \frac{d\gamma}{2\pi i} \frac{e^{-i\gamma(\tau_{31}-\tau_{21}-\tau_{34})}}{\gamma + i\delta}. && \text{(B.19)}
\end{aligned}$$

Using these expressions and the integral limits discussion above, the term I_2 can be written as

$$\begin{aligned}
I_2 &= \delta_{k_1k_3}\delta_{k_2k_4}[1 - n_{k_1}]^2 n_{k_2} \lim_{\eta\to 0^+} \lim_{\xi\to 0^+} \lim_{\delta\to 0^+} \int_{-\infty}^{\infty} \frac{d\alpha}{2\pi i} \frac{1}{\alpha + i\eta} \int_{-\infty}^{\infty} \frac{d\beta}{2\pi i} \frac{1}{\beta + i\xi} \\
&\times \int_{-\infty}^{\infty} \frac{d\gamma}{2\pi i} \frac{1}{\gamma + i\delta} \int_0^{1/T} d\tau_{21} e^{(i\varepsilon_\ell - i\alpha + i\beta + i\gamma - \varepsilon_{k_2} + \mu)\tau_{21}} \\
&\times \int_{\tau_{21}}^{\tau_{21}+1/T} d\tau_{31} e^{(i\omega_n - i\beta - i\gamma - \varepsilon_{k_1} + \varepsilon_{k_2})\tau_{31}} \int_{-1/T+(\tau_{31}-\tau_{21})}^{\tau_{31}-\tau_{21}} d\tau_{34} e^{(i\varepsilon_{\ell'} + i\gamma - \varepsilon_{k_2} + \mu)\tau_{34}}. \qquad \text{(B.20)}
\end{aligned}$$

The integration with respect to τ_{34} gives

$$\begin{aligned}
\int_{-1/T+(\tau_{31}-\tau_{21})}^{\tau_{31}-\tau_{21}} d\tau_{34} e^{(i\varepsilon_{\ell'} + i\gamma - \varepsilon_{k_2} + \mu)\tau_{34}} &= \frac{1}{i\varepsilon_{\ell'} + i\gamma - \varepsilon_{k_2} + \mu} e^{(i\varepsilon_{\ell'} + i\gamma - \varepsilon_{k_2} + \mu)(\tau_{31}-\tau_{21})} \\
&\times \left[1 + e^{-(i\gamma - \varepsilon_{k_2} + \mu)/T}\right]. \qquad \text{(B.21)}
\end{aligned}$$

Inserting this result into the term I_2, we obtain

$$\begin{aligned}
I_2 &= \delta_{k_1k_3}\delta_{k_2k_4}[1 - n_{k_1}]^2 n_{k_2} \lim_{\eta\to 0^+} \lim_{\xi\to 0^+} \lim_{\delta\to 0^+} \int_{-\infty}^{\infty} \frac{d\alpha}{2\pi i} \frac{1}{\alpha + i\eta} \int_{-\infty}^{\infty} \frac{d\beta}{2\pi i} \frac{1}{\beta + i\xi} \\
&\times \int_{-\infty}^{\infty} \frac{d\gamma}{2\pi i} \frac{1}{\gamma + i\delta} \frac{1}{i\varepsilon_{\ell'} + i\gamma - \varepsilon_{k_2} + \mu} \left[1 + e^{-(i\gamma - \varepsilon_{k_2} + \mu)/T}\right] \\
&\times \int_0^{1/T} d\tau_{21} e^{(i\varepsilon_\ell - i\varepsilon_{\ell'} - i\alpha + i\beta)\tau_{21}} \int_{\tau_{21}}^{\tau_{21}+1/T} d\tau_{31} e^{(i\omega_n + i\varepsilon_{\ell'} - i\beta - \varepsilon_{k_1} + \mu)\tau_{31}}. \qquad \text{(B.22)}
\end{aligned}$$

Now integration with respect to τ_{31} gives

$$\begin{aligned}
\int_{\tau_{21}}^{\tau_{21}+1/T} d\tau_{31} e^{(i\omega_n + i\varepsilon_{\ell'} - i\beta - \varepsilon_{k_1} + \mu)\tau_{31}} &= -\frac{1}{i\omega_n + i\varepsilon_{\ell'} - i\beta - \varepsilon_{k_1} + \mu} e^{(i\omega_n + i\varepsilon_{\ell'} - i\beta - \varepsilon_{k_1} + \mu)\tau_{21}} \\
&\times \left[1 + e^{-(i\beta + \varepsilon_{k_1} - \mu)/T}\right] \qquad \text{(B.23)}
\end{aligned}$$

and integration with respect to τ_{21} gives

$$\begin{aligned}
&\int_0^{1/T} d\tau_{21} e^{(i\varepsilon_\ell - i\varepsilon_{\ell'} - i\alpha + i\beta)\tau_{21}} \int_{\tau_{21}}^{\tau_{21}+1/T} d\tau_{31} e^{(i\omega_n + i\varepsilon_{\ell'} - i\beta - \varepsilon_{k_1} + \mu)\tau_{31}} \\
= &\frac{1}{i\omega_n + i\varepsilon_{\ell'} - i\beta - \varepsilon_{k_1} + \mu} \frac{1}{i\omega_n + i\varepsilon_\ell - i\alpha - \varepsilon_{k_1} + \mu} \left[1 + e^{-(i\alpha + \varepsilon_{k_1} - \mu)/T}\right] \\
\times &\left[1 + e^{-(i\beta + \varepsilon_{k_1} - \mu)/T}\right]. \qquad \text{(B.24)}
\end{aligned}$$

Using the results of the integration, the term I_2 can be written as

$$\begin{aligned}
I_2 = &\; i\delta_{k_1 k_3}\delta_{k_2 k_4}[1 - n_{k_1}]^2 n_{k_2} \\
&\times \lim_{\eta \to 0^+} \int_{-\infty}^{\infty} \frac{d\alpha}{2\pi i} \frac{1}{\alpha + i\eta} \frac{1}{\alpha - \omega_n - \varepsilon_\ell - i(\varepsilon_{k_1} - \mu)} \left[1 + e^{-(i\alpha + \varepsilon_{k_1} - \mu)/T}\right] \\
&\times \lim_{\xi \to 0^+} \int_{-\infty}^{\infty} \frac{d\beta}{2\pi i} \frac{1}{\beta + i\xi} \frac{1}{\beta - \omega_n - \varepsilon_{\ell'} - i(\varepsilon_{k_1} - \mu)} \left[1 + e^{-(i\beta + \varepsilon_{k_1} - \mu)/T}\right] \\
&\times \lim_{\delta \to 0^+} \int_{-\infty}^{\infty} \frac{d\gamma}{2\pi i} \frac{1}{\gamma + i\delta} \frac{1}{\gamma + \varepsilon_{\ell'} + i(\varepsilon_{k_2} - \mu)} \left[1 + e^{-(i\gamma - \varepsilon_{k_2} + \mu)/T}\right]. \qquad \text{(B.25)}
\end{aligned}$$

The integration with respect to γ gives

$$\lim_{\delta \to 0^+} \int_{-\infty}^{\infty} \frac{d\gamma}{2\pi i} \frac{1}{\gamma + i\delta} \frac{1}{\gamma + \varepsilon_{\ell'} + i(\varepsilon_{k_2} - \mu)} \left[1 + e^{-(i\gamma - \varepsilon_{k_2} + \mu)/T}\right] = -\frac{i}{i\varepsilon_{\ell'} - \varepsilon_{k_2} + \mu} \frac{1}{n_{k_2}}. \qquad \text{(B.26)}$$

The integration with respect to β gives

$$\begin{aligned}
&\lim_{\xi \to 0^+} \int_{-\infty}^{\infty} \frac{d\beta}{2\pi i} \frac{1}{\beta + i\xi} \frac{1}{\beta - \omega_n - \varepsilon_{\ell'} - i(\varepsilon_{k_1} - \mu)} \left[1 + e^{-(i\beta + \varepsilon_{k_1} - \mu)/T}\right] \\
= &\frac{i}{i(\omega_n + \varepsilon_{\ell'}) - \varepsilon_{k_1} + \mu} \frac{1}{1 - n_{k_1}}. \qquad \text{(B.27)}
\end{aligned}$$

The last integral with respect to α gives

$$\begin{aligned}
&\lim_{\eta \to 0^+} \int_{-\infty}^{\infty} \frac{d\alpha}{2\pi i} \frac{1}{\alpha + i\eta} \frac{1}{\alpha - \omega_n - \varepsilon_\ell - i(\varepsilon_{k_1} - \mu)} \left[1 + e^{-(i\alpha + \varepsilon_{k_1} - \mu)/T}\right] \\
= &\frac{i}{i(\varepsilon_\ell + \omega_n) - \varepsilon_{k_1} + \mu} \frac{1}{1 - n_{k_1}}. \qquad \text{(B.28)}
\end{aligned}$$

Inserting Eqs. (B.26), (B.27), and (B.28) into Eq. (B.25), we obtain

$$I_2 = -\delta_{k_1 k_3}\delta_{k_2 k_4} \frac{1}{(i\varepsilon_{\ell'} - \varepsilon_{k_2} + \mu)[i(\omega_n + \varepsilon_{\ell'}) - \varepsilon_{k_1} + \mu][i(\varepsilon_\ell + \omega_n) - \varepsilon_{k_1} + \mu]}. \qquad \text{(B.29)}$$

Inserting the terms I_1 and I_2 into the expression of $\widetilde{\mathscr{D}}^{ph}_{12,34}(\omega_n, \varepsilon_\ell, \varepsilon_{\ell'})$, we obtain

$$\widetilde{\mathscr{D}}^{ph}_{12,34}(\omega_n, \varepsilon_\ell, \varepsilon_{\ell'}) \;=\; \delta_{k_1 k_3}\delta_{k_2 k_4}(i\omega_n - \varepsilon_{k_1} + \varepsilon_{k_2})\widetilde{\mathcal{G}}_{k_1}(\varepsilon_\ell + \omega_n)\widetilde{\mathcal{G}}_{k_2}(\varepsilon_\ell)\widetilde{\mathcal{G}}_{k_3}(\varepsilon_{\ell'} + \omega_n)\widetilde{\mathcal{G}}_{k_4}(\varepsilon_{\ell'}). \quad \blacksquare$$

Appendix C

Derivation of Finite-temperature Free Response Function

In the τ representation, the finite-temperature free response function $\widetilde{\mathscr{R}}^0(12,34)$ is defined as

$$\widetilde{\mathscr{R}}^0(12,34) = \sum_{\sigma_1,\sigma_2} \widetilde{\mathscr{R}}^{0(\sigma_1,\sigma_2)}(12,34), \tag{C.1}$$

where

$$\widetilde{\mathscr{R}}^{0(\sigma_1,\sigma_2)}(12,34) = -\widetilde{\mathscr{G}}^{\sigma_1}(3,1)\widetilde{\mathscr{G}}^{\sigma_2}(2,4), \qquad \sigma_{1,2} = +1,-1. \tag{C.2}$$

The Matsubara's Green functions $\widetilde{\mathscr{G}}^{\sigma_1}(3,1)$ and $\widetilde{\mathscr{G}}^{\sigma_2}(2,4)$ are defined as

$$\begin{aligned}
\widetilde{\mathscr{G}}^{(+1)}(3,1) &= -\delta_{k_1k_3}[1-n(\varepsilon_{k_1}-\mu,T)]e^{-(\varepsilon_{k_1}-\mu)\tau_{31}}\theta(\tau_{31}) \\
&= -\delta_{k_1k_3}[1-n_{k_1}]e^{-(\varepsilon_{k_1}-\mu)\tau_{31}}\theta(\tau_{31}), &\text{(C.3)} \\
\widetilde{\mathscr{G}}^{(-1)}(3,1) &= \delta_{k_1k_3}n(\varepsilon_{k_1}-\mu,T)e^{-(\varepsilon_{k_1}-\mu)\tau_{31}}\theta(-\tau_{31}) \\
&= \delta_{k_1k_3}n_{k_1}e^{-(\varepsilon_{k_1}-\mu)\tau_{31}}\theta(-\tau_{31}), &\text{(C.4)} \\
\widetilde{\mathscr{G}}^{(+1)}(2,4) &= -\delta_{k_2k_4}[1-n(\varepsilon_{k_2}-\mu,T)]e^{-(\varepsilon_{k_2}-\mu)\tau_{24}}\theta(\tau_{24}) \\
&= -\delta_{k_2k_4}[1-n_{k_2}]e^{-(\varepsilon_{k_2}-\mu)\tau_{24}}\theta(\tau_{24}), &\text{(C.5)} \\
\widetilde{\mathscr{G}}^{(-1)}(2,4) &= \delta_{k_2k_4}n(\varepsilon_{k_2}-\mu,T)e^{-(\varepsilon_{k_2}-\mu)\tau_{24}}\theta(-\tau_{24}) \\
&= \delta_{k_2k_4}n_{k_2}e^{-(\varepsilon_{k_2}-\mu)\tau_{24}}\theta(-\tau_{24}). &\text{(C.6)}
\end{aligned}$$

The notion of particle (hole) is given for $\sigma = +1(-1)$. Each time τ_i, where $i = 1,2,3,4$, is defined to have an interval $0 \le \tau_i \le 1/T$, where $T > 0$ is temperature. Therefore, each time difference $\tau_{ij} \equiv \tau_i - \tau_j$ has an interval $-1/T \le \tau_{ij} \le 1/T$. The spectral representation of

$\widetilde{\mathscr{R}}^{0(\sigma_1,\sigma_2)}(12,34) \equiv \widetilde{\mathscr{R}}^{0(\sigma_1,\sigma_2)}_{k_1k_2,k_3k_4}(\tau_{31},\tau_{21},\tau_{34})$ is defined via the Fourier transformation:

$$\begin{aligned}\widetilde{\mathscr{R}}^{0(\sigma_1,\sigma_2)}_{k_1k_2,k_3k_4}(\omega_n,\varepsilon_\ell,\varepsilon_{\ell'}) &= \frac{1}{8}\int_{-1/T}^{1/T} d\tau_{31} e^{i\omega_n\tau_{31}} \int_{-1/T}^{1/T} d\tau_{21} e^{i\varepsilon_\ell\tau_{21}} \int_{-1/T}^{1/T} d\tau_{34} e^{i\varepsilon_{\ell'}\tau_{34}} \\ &\times \widetilde{\mathscr{R}}^{0(\sigma_1,\sigma_2)}_{k_1k_2,k_3k_4}(\tau_{31},\tau_{21},\tau_{34}), \end{aligned} \tag{C.7}$$

where $\omega_n = 2n\pi T$, $\varepsilon_\ell = (2\ell+1)\pi T$, $\varepsilon_{\ell'} = (2\ell'+1)\pi T$, and $n = \ell = \ell' = \cdots, -2, -1, 0, 1, 2, \cdots$. Inserting Eq.(C.2) into Eq.(C.7), one obtains

$$\widetilde{\mathscr{R}}^{0pp}_{12,34}(\omega_n,\varepsilon_\ell,\varepsilon_{\ell'}) = -\frac{1}{8}\int_{-1/T}^{1/T} d\tau_{31}d\tau_{21}d\tau_{34} e^{i(\omega_n\tau_{31}+\varepsilon_\ell\tau_{21}+\varepsilon_{\ell'}\tau_{34})} \widetilde{\mathscr{G}}^{(+1)}(3,1)\widetilde{\mathscr{G}}^{(+1)}(2,4), \tag{C.8}$$

$$\widetilde{\mathscr{R}}^{0ph}_{12,34}(\omega_n,\varepsilon_\ell,\varepsilon_{\ell'}) = -\frac{1}{8}\int_{-1/T}^{1/T} d\tau_{31}d\tau_{21}d\tau_{34} e^{i(\omega_n\tau_{31}+\varepsilon_\ell\tau_{21}+\varepsilon_{\ell'}\tau_{34})} \widetilde{\mathscr{G}}^{(+1)}(3,1)\widetilde{\mathscr{G}}^{(-1)}(2,4), \tag{C.9}$$

$$\widetilde{\mathscr{R}}^{0hp}_{12,34}(\omega_n,\varepsilon_\ell,\varepsilon_{\ell'}) = -\frac{1}{8}\int_{-1/T}^{1/T} d\tau_{31}d\tau_{21}d\tau_{34} e^{i(\omega_n\tau_{31}+\varepsilon_\ell\tau_{21}+\varepsilon_{\ell'}\tau_{34})} \widetilde{\mathscr{G}}^{(-1)}(3,1)\widetilde{\mathscr{G}}^{(+1)}(2,4), \tag{C.10}$$

$$\widetilde{\mathscr{R}}^{0hh}_{12,34}(\omega_n,\varepsilon_\ell,\varepsilon_{\ell'}) = -\frac{1}{8}\int_{-1/T}^{1/T} d\tau_{31}d\tau_{21}d\tau_{34} e^{i(\omega_n\tau_{31}+\varepsilon_\ell\tau_{21}+\varepsilon_{\ell'}\tau_{34})} \widetilde{\mathscr{G}}^{(-1)}(3,1)\widetilde{\mathscr{G}}^{(-1)}(2,4). \tag{C.11}$$

Inserting Eq.(C.3) and Eq.(C.5) into Eq.(C.8), we obtain

$$\begin{aligned}\widetilde{\mathscr{R}}^{0pp}_{k_1k_2,k_3k_4}(\omega_n,\varepsilon_\ell,\varepsilon_{\ell'}) &= -\frac{1}{8}\delta_{k_1k_3}\delta_{k_2k_4}[1-n_{k_1}][1-n_{k_2}] \int_{-1/T}^{1/T} d\tau_{31} e^{i\omega_n\tau_{31}} \\ &\times \int_{-1/T}^{1/T} d\tau_{21} e^{i\varepsilon_\ell\tau_{21}} \int_{-1/T}^{1/T} d\tau_{34} e^{i\varepsilon_{\ell'}\tau_{34}} e^{-(\varepsilon_{k_1}-\mu)\tau_{31}} \\ &\times e^{-(\varepsilon_{k_2}-\mu)(\tau_{21}+\tau_{34}-\tau_{31})}\theta(\tau_{31})\theta(\tau_{21}+\tau_{34}-\tau_{31}). \end{aligned} \tag{C.12}$$

$\widetilde{\mathscr{R}}^{0pp}_{k_1k_2,k_3k_4}(\omega_n,\varepsilon_\ell,\varepsilon_{\ell'})$ contains two theta functions, i.e., $\theta(\tau_{31})$ and $\theta(\tau_{24}) = \theta(\tau_{21}+\tau_{34}-\tau_{31})$. The theta function $\theta(\tau_{31})$ constrains the interval of τ_{31} to be $0 \le \tau_{31} \le 1/T$. Due to the presence of $\theta(\tau_{24})$, τ_{24} and, hence, the linear combination $\tau_{21}+\tau_{34}-\tau_{31}$ have an interval from 0 to $1/T$. We choose τ_{21} to have an interval $\tau_{31}-\tau_{34} \le \tau_{21} \le \tau_{31}-\tau_{34}+1/T$ and determine the interval of τ_{34} to be $-1/T \le \tau_{34} \le 1/T$. Under these considerations, Eq.(C.12) becomes

$$\widetilde{\mathscr{R}}^{0pp}_{k_1k_2,k_3k_4}(\omega_n,\varepsilon_\ell,\varepsilon_{\ell'}) = -\frac{1}{8}\delta_{k_1k_3}\delta_{k_2k_4}[1-n_{k_1}][1-n_{k_2}] \int_{0}^{1/T} d\tau_{31} e^{i\omega_n\tau_{31}}$$

$$
\begin{aligned}
&\times \int_{\tau_{31}-\tau_{34}}^{\tau_{31}-\tau_{34}+1/T} d\tau_{21} e^{i\varepsilon_\ell \tau_{21}} \int_{-1/T}^{1/T} d\tau_{34} e^{i\varepsilon_{\ell'}\tau_{34}} e^{-(\varepsilon_{k_1}-\mu)\tau_{31}} \\
&\times \quad e^{-(\varepsilon_{k_2}-\mu)(\tau_{21}+\tau_{34}-\tau_{31})} \theta(\tau_{31})\theta(\tau_{21}+\tau_{34}-\tau_{31}). \qquad \text{(C.13)}
\end{aligned}
$$

Next, we apply the integration representations of $\theta(\tau_{31})$ and $\theta(\tau_{21}+\tau_{34}-\tau_{31})$:

$$
\begin{aligned}
\theta(\tau_{31}) &= -\lim_{\eta\to 0^+} \int_{-\infty}^{\infty} \frac{d\alpha}{2\pi i} \frac{e^{-i\alpha\tau_{31}}}{\alpha+i\eta} \\
\theta(\tau_{21}+\tau_{34}-\tau_{31}) &= -\lim_{\xi\to 0^+} \int_{-\infty}^{\infty} \frac{d\beta}{2\pi i} \frac{e^{-i\beta(\tau_{21}+\tau_{34}-\tau_{31})}}{\beta+i\xi}
\end{aligned}
$$

to Eq.(C.13) and obtain

$$
\begin{aligned}
\widetilde{\mathscr{R}}^{0pp}_{k_1k_2,k_3k_4}(\omega_n,\varepsilon_\ell,\varepsilon_{\ell'}) &= -\frac{1}{8}\delta_{k_1k_3}\delta_{k_2k_4}[1-n_{k_1}][1-n_{k_2}] \lim_{\eta\to 0^+}\lim_{\xi\to 0^+} \int_{-\infty}^{\infty} \frac{d\alpha}{2\pi i}\frac{1}{\alpha+i\eta} \\
&\times \int_{-\infty}^{\infty} \frac{d\beta}{2\pi i}\frac{1}{\beta+i\xi} \int_0^{1/T} d\tau_{31} e^{(i\omega_n - i\alpha + i\beta - \varepsilon_{k_1}+\varepsilon_{k_2})\tau_{31}} \\
&\times \int_{-1/T}^{1/T} d\tau_{34} e^{(i\varepsilon_{\ell'} - i\beta - \varepsilon_{k_2}+\mu)\tau_{34}} \int_{\tau_{31}-\tau_{34}}^{\tau_{31}-\tau_{34}+1/T} d\tau_{21} e^{(i\varepsilon_\ell - i\beta - \varepsilon_{k_2}+\mu)\tau_{21}}.
\end{aligned} \qquad \text{(C.14)}
$$

We first evaluate the integration with respect to τ_{21} as follows:

$$
\begin{aligned}
\int_{\tau_{31}-\tau_{34}}^{\tau_{31}-\tau_{34}+1/T} d\tau_{21} e^{(i\varepsilon_\ell - i\beta - \varepsilon_{k_2}+\mu)\tau_{21}} &= \frac{1}{i\varepsilon_\ell - i\beta - \varepsilon_{k_2}+\mu} e^{(i\varepsilon_\ell - i\beta - \varepsilon_{k_2}+\mu)\tau_{21}} \Big|_{\tau_{31}-\tau_{34}}^{\tau_{31}-\tau_{34}+1/T} \\
&= \frac{1}{i\varepsilon_\ell - i\beta - \varepsilon_{k_2}+\mu} e^{(i\varepsilon_\ell - i\beta - \varepsilon_{k_2}+\mu)(\tau_{31}-\tau_{34})} \\
&\times \left[-e^{-(i\beta+\varepsilon_{k_2}-\mu)/T} - 1\right] \\
\int_{\tau_{31}-\tau_{34}}^{\tau_{31}-\tau_{34}+1/T} d\tau_{21} e^{(i\varepsilon_\ell - i\beta - \varepsilon_{k_2}+\mu)\tau_{21}} &= -\frac{1}{i\varepsilon_\ell - i\beta - \varepsilon_{k_2}+\mu} e^{(i\varepsilon_\ell - i\beta - \varepsilon_{k_2}+\mu)(\tau_{31}-\tau_{34})} \\
&\times \left[e^{-(i\beta+\varepsilon_{k_2}-\mu)/T} + 1\right].
\end{aligned} \qquad \text{(C.15)}
$$

Inserting this into Eq.(C.14), we obtain

$$
\begin{aligned}
\widetilde{\mathscr{R}}^{0pp}_{k_1k_2,k_3k_4}(\omega_n,\varepsilon_\ell,\varepsilon_{\ell'}) &= \frac{1}{8}\delta_{k_1k_3}\delta_{k_2k_4}[1-n_{k_1}][1-n_{k_2}] \lim_{\eta\to 0^+}\lim_{\xi\to 0^+} \int_{-\infty}^{\infty} \frac{d\alpha}{2\pi i}\frac{1}{\alpha+i\eta} \\
&\times \int_{-\infty}^{\infty} \frac{d\beta}{2\pi i}\frac{1}{\beta+i\xi} \frac{1}{i\varepsilon_\ell - i\beta - \varepsilon_{k_2}+\mu} \left[e^{-(i\beta+\varepsilon_{k_2}-\mu)/T} + 1\right] \\
&\times \int_0^{1/T} d\tau_{31} e^{(i\omega_n + i\varepsilon_\ell - i\alpha - \varepsilon_{k_1}+\mu)\tau_{31}} \int_{-1/T}^{1/T} d\tau_{34} e^{i(\varepsilon_{\ell'}-\varepsilon_\ell)\tau_{34}}.
\end{aligned} \qquad \text{(C.16)}
$$

The integration with respect to τ_{34} gives

$$\int_{-1/T}^{1/T} d\tau_{34} e^{i(\varepsilon_{\ell'}-\varepsilon_{\ell})\tau_{34}} = \frac{2}{T}\delta_{\ell\ell'} \tag{C.17}$$

and the integration with respect to τ_{31} gives

$$\int_{0}^{1/T} d\tau_{31} e^{(i\omega_n+i\varepsilon_{\ell}-i\alpha-\varepsilon_{k_1}+\mu)\tau_{31}} = -\frac{1}{i\omega_n+i\varepsilon_{\ell}-i\alpha-\varepsilon_{k_1}+\mu}\left[e^{-(i\alpha+\varepsilon_{k_1}-\mu)/T}+1\right]. \tag{C.18}$$

Inserting these results into Eq.(C.16), we obtain

$$\begin{aligned}
\widetilde{\mathscr{R}}^{0pp}_{12,34}(\omega_n,\varepsilon_{\ell},\varepsilon_{\ell'}) &= -\frac{1}{4T}\delta_{\ell\ell'}\delta_{k_1k_3}\delta_{k_2k_4}[1-n_{k_1}][1-n_{k_2}]\lim_{\eta\to 0^+}\int_{-\infty}^{\infty}\frac{d\alpha}{2\pi i}\frac{1}{\alpha+i\eta} \\
&\times \frac{1}{i\omega_n+i\varepsilon_{\ell}-i\alpha-\varepsilon_{k_1}+\mu}\left[e^{-(i\alpha+\varepsilon_{k_1}-\mu)/T}+1\right] \\
&\times \lim_{\xi\to 0^+}\int_{-\infty}^{\infty}\frac{d\beta}{2\pi i}\frac{1}{\beta+i\xi}\frac{1}{i\varepsilon_{\ell}-i\beta-\varepsilon_{k_2}+\mu} \\
&\times \left[e^{-(i\beta+\varepsilon_{k_2}-\mu)/T}+1\right].
\end{aligned} \tag{C.19}$$

The integration with respect to α gives

$$\begin{aligned}
I_{\alpha} &= \lim_{\eta\to 0^+}\int_{-\infty}^{\infty}\frac{d\alpha}{2\pi i}\frac{1}{\alpha+i\eta}\frac{1}{i\omega_n+i\varepsilon_{\ell}-i\alpha-\varepsilon_{k_1}+\mu}\left[e^{-(i\alpha+\varepsilon_{k_1}-\mu)/T}+1\right] \\
&= -\frac{1}{i(\omega_n+\varepsilon_{\ell})-\varepsilon_{k_1}+\mu}\frac{1}{1-n_{k_1}}
\end{aligned} \tag{C.20}$$

and the integration with respect to β gives

$$\begin{aligned}
I_{\beta} &= \lim_{\xi\to 0^+}\int_{-\infty}^{\infty}\frac{d\beta}{2\pi i}\frac{1}{\beta+i\xi}\frac{1}{i\varepsilon_{\ell}-i\beta-\varepsilon_{k_2}+\mu}\left[e^{-(i\beta+\varepsilon_{k_2}-\mu)/T}+1\right] \\
&= -\frac{1}{i\varepsilon_{\ell}-\varepsilon_{k_2}+\mu}\frac{1}{1-n_{k_2}}.
\end{aligned} \tag{C.21}$$

Inserting these results into Eq.(C.19), we obtain

$$\widetilde{\mathscr{R}}^{0pp}_{12,34}(\omega_n,\varepsilon_{\ell},\varepsilon_{\ell'}) = -\frac{1}{4T}\delta_{\ell\ell'}\delta_{k_1k_3}\delta_{k_2k_4}\widetilde{\mathscr{G}}_{k_1}(\omega_n+\varepsilon_{\ell})\widetilde{\mathscr{G}}_{k_2}(\varepsilon_{\ell}). \tag{C.22}$$

Inserting Eq.(C.3) and Eq.(C.6) into Eq.(C.9), we obtain

$$\begin{aligned}\widetilde{\mathscr{R}}^{0ph}_{k_1k_2,k_3k_4}(\omega_n,\varepsilon_\ell,\varepsilon_{\ell'}) &= \frac{1}{8}\delta_{k_1k_3}\delta_{k_2k_4}[1-n_{k_1}]n_{k_2}\int_{-1/T}^{1/T}d\tau_{31}e^{i\omega_n\tau_{31}}\int_{-1/T}^{1/T}d\tau_{21}e^{i\varepsilon_\ell\tau_{21}} \\ &\times \int_{-1/T}^{1/T}d\tau_{34}e^{i\varepsilon_{\ell'}\tau_{34}}e^{-(\varepsilon_{k_1}-\mu)\tau_{31}}e^{-(\varepsilon_{k_2}-\mu)(\tau_{21}+\tau_{34}-\tau_{31})} \\ &\times \theta(\tau_{31})\theta(\tau_{31}-\tau_{21}-\tau_{34}). \end{aligned} \tag{C.23}$$

$\widetilde{\mathscr{R}}^{0ph}_{k_1k_2,k_3k_4}(\omega_n,\varepsilon_\ell,\varepsilon_{\ell'})$ contains two theta functions, i.e., $\theta(\tau_{31})$ and $\theta(-\tau_{24})=\theta[-(\tau_{21}+\tau_{34}-\tau_{31})]$. The theta function $\theta(\tau_{31})$ constrains the interval of τ_{31} to be $0\le\tau_{31}\le 1/T$. Due to the presence of $\theta(-\tau_{24})$, τ_{24} and, hence, the linear combination $\tau_{21}+\tau_{34}-\tau_{31}$ have an interval from $-1/T$ to 0. We choose τ_{21} to have an interval $\tau_{31}-\tau_{34}-1/T\le\tau_{21}\le\tau_{31}-\tau_{34}$ and determine the interval of τ_{34} to be $-1/T$ to $1/T$. Under these considerations, Eq.(C.23) becomes

$$\begin{aligned}\widetilde{\mathscr{R}}^{0ph}_{k_1k_2,k_3k_4}(\omega_n,\varepsilon_\ell,\varepsilon_{\ell'}) &= \frac{1}{8}\delta_{k_1k_3}\delta_{k_2k_4}[1-n_{k_1}]n_{k_2}\int_{0}^{1/T}d\tau_{31}e^{i\omega_n\tau_{31}}\int_{\tau_{31}-\tau_{34}-1/T}^{\tau_{31}-\tau_{34}}d\tau_{21}e^{i\varepsilon_\ell\tau_{21}} \\ &\times \int_{-1/T}^{1/T}d\tau_{34}e^{i\varepsilon_{\ell'}\tau_{34}}e^{-(\varepsilon_{k_1}-\mu)\tau_{31}}e^{-(\varepsilon_{k_2}-\mu)(\tau_{21}+\tau_{34}-\tau_{31})} \\ &\times \theta(\tau_{31})\theta(\tau_{31}-\tau_{21}-\tau_{34}). \end{aligned} \tag{C.24}$$

Next, we apply the integration representations of $\theta(\tau_{31})$ and $\theta(\tau_{31}-\tau_{21}-\tau_{34})$:

$$\begin{aligned}\theta(\tau_{31}) &= -\lim_{\eta\to0^+}\int_{-\infty}^{\infty}\frac{d\alpha}{2\pi i}\frac{e^{-i\alpha\tau_{31}}}{\alpha+i\eta} \\ \theta(\tau_{31}-\tau_{21}-\tau_{34}) &= -\lim_{\xi\to0^+}\int_{-\infty}^{\infty}\frac{d\beta}{2\pi i}\frac{e^{-i\beta(\tau_{31}-\tau_{21}-\tau_{34})}}{\beta+i\xi}\end{aligned}$$

to Eq.(C.24) and obtain

$$\begin{aligned}\widetilde{\mathscr{R}}^{0ph}_{k_1k_2,k_3k_4}(\omega_n,\varepsilon_\ell,\varepsilon_{\ell'}) &= \frac{1}{8}\delta_{k_1k_3}\delta_{k_2k_4}[1-n_{k_1}]n_{k_2}\lim_{\eta\to0^+}\lim_{\xi\to0^+}\int_{-\infty}^{\infty}\frac{d\alpha}{2\pi i}\frac{1}{\alpha+i\eta} \\ &\times \int_{-\infty}^{\infty}\frac{d\beta}{2\pi i}\frac{1}{\beta+i\xi}\int_{0}^{1/T}d\tau_{31}e^{(i\omega_n-i\alpha-i\beta-\varepsilon_{k_1}+\varepsilon_{k_2})\tau_{31}} \\ &\times \int_{-1/T}^{1/T}d\tau_{34}e^{(i\varepsilon_{\ell'}+i\beta-\varepsilon_{k_2}+\mu)\tau_{34}}\int_{\tau_{31}-\tau_{34}-1/T}^{\tau_{31}-\tau_{34}}d\tau_{21}e^{(i\varepsilon_\ell+i\beta-\varepsilon_{k_2}+\mu)\tau_{21}}. \end{aligned} \tag{C.25}$$

We first evaluate the integration with respect to τ_{21} as follows:

$$\begin{aligned}\int_{\tau_{31}-\tau_{34}-1/T}^{\tau_{31}-\tau_{34}} d\tau_{21} e^{(i\varepsilon_\ell+i\beta-\varepsilon_{k_2}+\mu)\tau_{21}} &= \frac{1}{i\varepsilon_\ell+i\beta-\varepsilon_{k_2}+\mu} e^{(i\varepsilon_\ell+i\beta-\varepsilon_{k_2}+\mu)\tau_{21}}\Big|_{\tau_{31}-\tau_{34}-1/T}^{\tau_{31}-\tau_{34}} \\ &= \frac{1}{i\varepsilon_\ell+i\beta-\varepsilon_{k_2}+\mu} e^{(i\varepsilon_\ell+i\beta-\varepsilon_{k_2}+\mu)(\tau_{31}-\tau_{34})} \\ &\times \left[1+e^{-(i\beta-\varepsilon_{k_2}+\mu)/T}\right]. \end{aligned} \tag{C.26}$$

Inserting this into Eq.(C.25), we obtain

$$\begin{aligned}\widetilde{\mathscr{R}}^{0ph}_{k_1k_2,k_3k_4}(\omega_n,\varepsilon_\ell,\varepsilon_{\ell'}) &= \frac{1}{8}\delta_{k_1k_3}\delta_{k_2k_4}[1-n_{k_1}]n_{k_2} \lim_{\eta\to 0^+}\lim_{\xi\to 0^+}\int_{-\infty}^{\infty}\frac{d\alpha}{2\pi i}\frac{1}{\alpha+i\eta} \\ &\times \int_{-\infty}^{\infty}\frac{d\beta}{2\pi i}\frac{1}{\beta+i\xi}\frac{1}{i\varepsilon_\ell+i\beta-\varepsilon_{k_2}+\mu}\left[e^{-(i\beta-\varepsilon_{k_2}+\mu)/T}+1\right] \\ &\times \int_0^{1/T} d\tau_{31} e^{(i\omega_n+i\varepsilon_\ell-i\alpha-\varepsilon_{k_1}+\mu)\tau_{31}}\int_{-1/T}^{1/T} d\tau_{34} e^{i(\varepsilon_{\ell'}-\varepsilon_\ell)\tau_{34}}. \end{aligned} \tag{C.27}$$

The integration with respect to τ_{34} gives

$$\int_{-1/T}^{1/T} d\tau_{34} e^{i(\varepsilon_{\ell'}-\varepsilon_\ell)\tau_{34}} = \frac{2}{T}\delta_{\ell\ell'} \tag{C.28}$$

and the integration with respect to τ_{31} gives

$$\int_0^{1/T} d\tau_{31} e^{(i\omega_n+i\varepsilon_\ell-i\alpha-\varepsilon_{k_1}+\mu)\tau_{31}} = -\frac{1}{i\omega_n+i\varepsilon_\ell-i\alpha-\varepsilon_{k_1}+\mu}\left[e^{-(i\alpha+\varepsilon_{k_1}-\mu)/T}+1\right]. \tag{C.29}$$

Inserting these results into Eq.(C.27), we obtain

$$\begin{aligned}\widetilde{\mathscr{R}}^{0ph}_{k_1k_2,k_3k_4}(\omega_n,\varepsilon_\ell,\varepsilon_{\ell'}) &= -\frac{1}{4T}\delta_{\ell\ell'}\delta_{k_1k_3}\delta_{k_2k_4}[1-n_{k_1}]n_{k_2} \\ &\times \lim_{\eta\to 0^+}\int_{-\infty}^{\infty}\frac{d\alpha}{2\pi i}\frac{1}{\alpha+i\eta}\frac{1}{i\omega_n+i\varepsilon_\ell-i\alpha-\varepsilon_{k_1}+\mu} \\ &\times \left[e^{-(i\alpha+\varepsilon_{k_1}-\mu)/T}+1\right]\lim_{\xi\to 0^+}\int_{-\infty}^{\infty}\frac{d\beta}{2\pi i}\frac{1}{\beta+i\xi} \\ &\times \frac{1}{i\varepsilon_\ell+i\beta-\varepsilon_{k_2}+\mu}\left[e^{-(i\beta-\varepsilon_{k_2}+\mu)/T}+1\right]. \end{aligned} \tag{C.30}$$

The integration with respect to α gives

$$\begin{aligned} I_\alpha &= \lim_{\eta\to 0^+}\int_{-\infty}^{\infty}\frac{d\alpha}{2\pi i}\frac{1}{\alpha+i\eta}\frac{1}{i\omega_n+i\varepsilon_\ell-i\alpha-\varepsilon_{k_1}+\mu}\left[e^{-(i\alpha+\varepsilon_{k_1}-\mu)/T}+1\right] \\ &= -\frac{1}{i(\omega_n+\varepsilon_\ell)-\varepsilon_{k_1}+\mu}\frac{1}{1-n_{k_1}} \end{aligned} \tag{C.31}$$

and the integration with respect to β gives

$$\begin{aligned} I_\beta &= \lim_{\xi\to 0^+}\int_{-\infty}^{\infty}\frac{d\beta}{2\pi i}\frac{1}{\beta+i\xi}\frac{1}{i\varepsilon_\ell+i\beta-\varepsilon_{k_2}+\mu}\left[e^{-(i\beta-\varepsilon_{k_2}+\mu)/T}+1\right] \\ &= -\frac{1}{i\varepsilon_\ell-\varepsilon_{k_2}+\mu}\frac{1}{n_{k_2}}. \end{aligned} \tag{C.32}$$

Inserting these results into Eq.(C.30), we obtain

$$\widetilde{\mathscr{R}}^{0ph}_{k_1k_2,k_3k_4}(\omega_n,\varepsilon_\ell,\varepsilon_{\ell'}) = -\frac{1}{4T}\delta_{\ell\ell'}\delta_{k_1k_3}\delta_{k_2k_4}\widetilde{\mathscr{G}}_{k_1}(\omega_n+\varepsilon_\ell)\widetilde{\mathscr{G}}_{k_2}(\varepsilon_\ell). \tag{C.33}$$

Inserting Eq.(C.4) and Eq.(C.5) into Eq.(C.10), we obtain

$$\begin{aligned} \widetilde{\mathscr{R}}^{0hp}_{k_1k_2,k_3k_4}(\omega_n,\varepsilon_\ell,\varepsilon_{\ell'}) &= \frac{1}{8}\delta_{k_1k_3}\delta_{k_2k_4}n_{k_1}[1-n_{k_2}]\int_{-1/T}^{1/T}d\tau_{31}e^{i\omega_n\tau_{31}}\int_{-1/T}^{1/T}d\tau_{21}e^{i\varepsilon_\ell\tau_{21}} \\ &\times \int_{-1/T}^{1/T}d\tau_{34}e^{i\varepsilon_{\ell'}\tau_{34}}e^{-(\varepsilon_{k_1}-\mu)\tau_{31}}e^{-(\varepsilon_{k_2}-\mu)(\tau_{21}+\tau_{34}-\tau_{31})} \\ &\times \theta(-\tau_{31})\theta(\tau_{21}+\tau_{34}-\tau_{31}). \end{aligned} \tag{C.34}$$

$\widetilde{\mathscr{R}}^{0hp}_{k_1k_2,k_3k_4}(\omega_n,\varepsilon_\ell,\varepsilon_{\ell'})$ contains two theta functions, i.e., $\theta(-\tau_{31})$ and $\theta(\tau_{24})=\theta(\tau_{21}+\tau_{34}-\tau_{31})$. The theta function $\theta(-\tau_{31})$ constrains the interval of τ_{31} to be $-1/T\le\tau_{31}\le 0$. Due to the presence of $\theta(\tau_{24})$, τ_{24} and, hence, the linear combination $\tau_{21}+\tau_{34}-\tau_{31}$ have an interval from 0 to $1/T$. We choose τ_{21} to have an interval $\tau_{31}-\tau_{34}\le\tau_{21}\le\tau_{31}-\tau_{34}+1/T$ and determine the interval of τ_{34} to be $-1/T$ to $1/T$. Under these considerations, Eq.(C.34) becomes

$$\begin{aligned} \widetilde{\mathscr{R}}^{0hp}_{k_1k_2,k_3k_4}(\omega_n,\varepsilon_\ell,\varepsilon_{\ell'}) &= \frac{1}{8}\delta_{k_1k_3}\delta_{k_2k_4}n_{k_1}[1-n_{k_2}]\int_{-1/T}^{0}d\tau_{31}e^{i\omega_n\tau_{31}}\int_{\tau_{31}-\tau_{34}}^{\tau_{31}-\tau_{34}+1/T}d\tau_{21}e^{i\varepsilon_\ell\tau_{21}} \\ &\times \int_{-1/T}^{1/T}d\tau_{34}e^{i\varepsilon_{\ell'}\tau_{34}}e^{-(\varepsilon_{k_1}-\mu)\tau_{31}}e^{-(\varepsilon_{k_2}-\mu)(\tau_{21}+\tau_{34}-\tau_{31})} \\ &\times \theta(-\tau_{31})\theta(\tau_{21}+\tau_{34}-\tau_{31}). \end{aligned} \tag{C.35}$$

Next, we apply the integration representations of $\theta(-\tau_{31})$ and $\theta(\tau_{21}+\tau_{34}-\tau_{31})$:

$$\begin{aligned}\theta(-\tau_{31}) &= -\lim_{\eta\to 0^+}\int_{-\infty}^{\infty}\frac{d\alpha}{2\pi i}\frac{e^{i\alpha\tau_{31}}}{\alpha+i\eta}\\ \theta(\tau_{21}+\tau_{34}-\tau_{31}) &= -\lim_{\xi\to 0^+}\int_{-\infty}^{\infty}\frac{d\beta}{2\pi i}\frac{e^{-i\beta(\tau_{21}+\tau_{34}-\tau_{31})}}{\beta+i\xi}\end{aligned}$$

to Eq.(C.35) and obtain

$$\begin{aligned}\widetilde{\mathscr{R}}^{0hp}_{k_1k_2,k_3k_4}(\omega_n,\varepsilon_\ell,\varepsilon_{\ell'}) &= \frac{1}{8}\delta_{k_1k_3}\delta_{k_2k_4}n_{k_1}[1-n_{k_2}]\lim_{\eta\to 0^+}\lim_{\xi\to 0^+}\int_{-\infty}^{\infty}\frac{d\alpha}{2\pi i}\frac{1}{\alpha+i\eta}\\ &\times \int_{-\infty}^{\infty}\frac{d\beta}{2\pi i}\frac{1}{\beta+i\xi}\int_{-1/T}^{0}d\tau_{31}e^{(i\omega_n+i\alpha+i\beta-\varepsilon_{k_1}+\varepsilon_{k_2})\tau_{31}}\\ &\times \int_{-1/T}^{1/T}d\tau_{34}e^{(i\varepsilon_{\ell'}-i\beta-\varepsilon_{k_2}+\mu)\tau_{34}}\int_{\tau_{31}-\tau_{34}}^{\tau_{31}-\tau_{34}+1/T}d\tau_{21}e^{(i\varepsilon_\ell-i\beta-\varepsilon_{k_2}+\mu)\tau_{21}}.\end{aligned} \tag{C.36}$$

We first evaluate the integration with respect to τ_{21} as follows:

$$\begin{aligned}\int_{\tau_{31}-\tau_{34}}^{\tau_{31}-\tau_{34}+1/T}d\tau_{21}e^{(i\varepsilon_\ell-i\beta-\varepsilon_{k_2}+\mu)\tau_{21}} &= \frac{1}{i\varepsilon_\ell-i\beta-\varepsilon_{k_2}+\mu}e^{(i\varepsilon_\ell-i\beta-\varepsilon_{k_2}+\mu)\tau_{21}}\Big|_{\tau_{31}-\tau_{34}}^{\tau_{31}-\tau_{34}+1/T}\\ &= \frac{1}{i\varepsilon_\ell-i\beta-\varepsilon_{k_2}+\mu}e^{(i\varepsilon_\ell-i\beta-\varepsilon_{k_2}+\mu)(\tau_{31}-\tau_{34})}\\ &\times \left[-e^{-(i\beta+\varepsilon_{k_2}-\mu)/T}-1\right]\\ &= -\frac{1}{i\varepsilon_\ell-i\beta-\varepsilon_{k_2}+\mu}e^{(i\varepsilon_\ell-i\beta-\varepsilon_{k_2}+\mu)(\tau_{31}-\tau_{34})}\\ &\times \left[e^{-(i\beta+\varepsilon_{k_2}-\mu)/T}+1\right].\end{aligned} \tag{C.37}$$

Inserting this into Eq.(C.36), we obtain

$$\begin{aligned}\widetilde{\mathscr{R}}^{0hp}_{k_1k_2,k_3k_4}(\omega_n,\varepsilon_\ell,\varepsilon_{\ell'}) &= -\frac{1}{8}\delta_{k_1k_3}\delta_{k_2k_4}n_{k_1}[1-n_{k_2}]\lim_{\eta\to 0^+}\lim_{\xi\to 0^+}\int_{-\infty}^{\infty}\frac{d\alpha}{2\pi i}\frac{1}{\alpha+i\eta}\\ &\times \int_{-\infty}^{\infty}\frac{d\beta}{2\pi i}\frac{1}{\beta+i\xi}\frac{1}{i\varepsilon_\ell-i\beta-\varepsilon_{k_2}+\mu}\left[e^{-(i\beta+\varepsilon_{k_2}-\mu)/T}+1\right]\\ &\times \int_{-1/T}^{0}d\tau_{31}e^{(i\omega_n+i\varepsilon_\ell+i\alpha-\varepsilon_{k_1}+\mu)\tau_{31}}\int_{-1/T}^{1/T}d\tau_{34}e^{i(\varepsilon_{\ell'}-\varepsilon_\ell)\tau_{34}}.\end{aligned} \tag{C.38}$$

The integration with respect to τ_{34} gives

$$\int_{-1/T}^{1/T}d\tau_{34}e^{i(\varepsilon_{\ell'}-\varepsilon_\ell)\tau_{34}}=\frac{2}{T}\delta_{\ell\ell'} \tag{C.39}$$

and the integration with respect to τ_{31} gives

$$\int_{-1/T}^{0} d\tau_{31} e^{(i\omega_n + i\varepsilon_\ell + i\alpha - \varepsilon_{k_1} + \mu)\tau_{31}} = \frac{1}{i\omega_n + i\varepsilon_\ell + i\alpha - \varepsilon_{k_1} + \mu} \left[e^{-(i\alpha - \varepsilon_{k_1} + \mu)/T} + 1 \right]. \tag{C.40}$$

Inserting these results into Eq.(C.38), we obtain

$$\begin{aligned} \widetilde{\mathscr{R}}^{0hp}_{12,34}(\omega_n, \varepsilon_\ell, \varepsilon_{\ell'}) &= -\frac{1}{4T} \delta_{\ell\ell'} \delta_{k_1 k_3} \delta_{k_2 k_4} n_{k_1} [1 - n_{k_2}] \lim_{\eta \to 0^+} \int_{-\infty}^{\infty} \frac{d\alpha}{2\pi i} \frac{1}{\alpha + i\eta} \\ &\times \frac{1}{i\omega_n + i\varepsilon_\ell + i\alpha - \varepsilon_{k_1} + \mu} \left[e^{-(i\alpha - \varepsilon_{k_1} + \mu)/T} + 1 \right] \\ &\times \lim_{\xi \to 0^+} \int_{-\infty}^{\infty} \frac{d\beta}{2\pi i} \frac{1}{\beta + i\xi} \frac{1}{i\varepsilon_\ell - i\beta - \varepsilon_{k_2} + \mu} \left[e^{-(i\beta + \varepsilon_{k_2} - \mu)/T} + 1 \right]. \end{aligned} \tag{C.41}$$

The integration with respect to α gives

$$\begin{aligned} I_\alpha &= \lim_{\eta \to 0^+} \int_{-\infty}^{\infty} \frac{d\alpha}{2\pi i} \frac{1}{\alpha + i\eta} \frac{1}{i\omega_n + i\varepsilon_\ell + i\alpha - \varepsilon_{k_1} + \mu} \left[e^{-(i\alpha - \varepsilon_{k_1} + \mu)/T} + 1 \right] \\ &= -\frac{1}{i(\omega_n + \varepsilon_\ell) - \varepsilon_1 + \mu} \frac{1}{n_{k_1}} \end{aligned} \tag{C.42}$$

and the integration with respect to β gives

$$\begin{aligned} I_\beta &= \lim_{\xi \to 0^+} \int_{-\infty}^{\infty} \frac{d\beta}{2\pi i} \frac{1}{\beta + i\xi} \frac{1}{i\varepsilon_\ell - i\beta - \varepsilon_{k_2} + \mu} \left[e^{-(i\beta + \varepsilon_{k_2} - \mu)/T} + 1 \right] \\ &= -\frac{1}{i\varepsilon_\ell - \varepsilon_{k_2} + \mu} \frac{1}{1 - n_{k_2}}. \end{aligned} \tag{C.43}$$

Inserting these results into Eq.(C.41), we obtain

$$\widetilde{\mathscr{R}}^{0hp}_{k_1 k_2, k_3 k_4}(\omega_n, \varepsilon_\ell, \varepsilon_{\ell'}) = -\frac{1}{4T} \delta_{\ell\ell'} \delta_{k_1 k_3} \delta_{k_2 k_4} \widetilde{\mathscr{G}}_{k_1}(\omega_n + \varepsilon_\ell) \widetilde{\mathscr{G}}_{k_2}(\varepsilon_\ell). \tag{C.44}$$

Inserting Eq.(C.4) and Eq.(C.6) into Eq.(C.11), we obtain

$$\begin{aligned} \widetilde{\mathscr{R}}^{0hh}_{k_1 k_2, k_3 k_4}(\omega_n, \varepsilon_\ell, \varepsilon_{\ell'}) &= -\frac{1}{8} \delta_{k_1 k_3} \delta_{k_2 k_4} n_{k_1} n_{k_2} \int_{-1/T}^{1/T} d\tau_{31} e^{i\omega_n \tau_{31}} \int_{-1/T}^{1/T} d\tau_{21} e^{i\varepsilon_\ell \tau_{21}} \\ &\times \int_{-1/T}^{1/T} d\tau_{34} e^{i\varepsilon_{\ell'} \tau_{34}} e^{-(\varepsilon_{k_1} - \mu)\tau_{31}} e^{-(\varepsilon_{k_2} - \mu)(\tau_{21} + \tau_{34} - \tau_{31})} \\ &\times \theta(-\tau_{31}) \theta(\tau_{31} - \tau_{21} - \tau_{34}). \end{aligned} \tag{C.45}$$

$\widetilde{\mathscr{R}}^{0hh}_{k_1k_2,k_3k_4}(\omega_n,\varepsilon_\ell,\varepsilon_{\ell'})$ contains two theta functions, i.e., $\theta(-\tau_{31})$ and $\theta(-\tau_{24})=\theta[-(\tau_{21}+\tau_{34}-\tau_{31})]$. The theta function $\theta(-\tau_{31})$ constrains the interval of τ_{31} to be $-1/T\le\tau_{31}\le 0$. Due to the presence of $\theta(-\tau_{24})$, τ_{24} and, hence, the linear combination $\tau_{21}+\tau_{34}-\tau_{31}$ have an interval from $-1/T$ to 0. We choose τ_{21} to have an interval $\tau_{31}-\tau_{34}-1/T\le\tau_{21}\le\tau_{31}-\tau_{34}$ and determine the interval of τ_{34} to be $-1/T$ to $1/T$. Under these considerations, Eq.(C.45) becomes

$$\begin{aligned}\widetilde{\mathscr{R}}^{0hh}_{k_1k_2,k_3k_4}(\omega_n,\varepsilon_\ell,\varepsilon_{\ell'}) &= -\frac{1}{8}\delta_{k_1k_3}\delta_{k_2k_4}n_{k_1}n_{k_2}\int_{-1/T}^{0}d\tau_{31}e^{i\omega_n\tau_{31}}\int_{\tau_{31}-\tau_{34}-1/T}^{\tau_{31}-\tau_{34}}d\tau_{21}e^{i\varepsilon_\ell\tau_{21}}\\ &\times\int_{-1/T}^{1/T}d\tau_{34}e^{i\varepsilon_{\ell'}\tau_{34}}e^{-(\varepsilon_{k_1}-\mu)\tau_{31}}e^{-(\varepsilon_{k_2}-\mu)(\tau_{21}+\tau_{34}-\tau_{31})}\\ &\times\theta(-\tau_{31})\theta(\tau_{31}-\tau_{21}-\tau_{34}).\end{aligned}\tag{C.46}$$

Next, we apply the integration representations of $\theta(-\tau_{31})$ and $\theta(\tau_{31}-\tau_{21}-\tau_{34})$:

$$\begin{aligned}\theta(-\tau_{31}) &= -\lim_{\eta\to0^+}\int_{-\infty}^{\infty}\frac{d\alpha}{2\pi i}\frac{e^{i\alpha\tau_{31}}}{\alpha+i\eta}\\ \theta(\tau_{31}-\tau_{21}+\tau_{34}) &= -\lim_{\xi\to0^+}\int_{-\infty}^{\infty}\frac{d\beta}{2\pi i}\frac{e^{-i\beta(\tau_{31}-\tau_{21}-\tau_{34})}}{\beta+i\xi}\end{aligned}$$

to Eq.(C.46) and obtain

$$\begin{aligned}\widetilde{\mathscr{R}}^{0hh}_{k_1k_2,k_3k_4}(\omega_n,\varepsilon_\ell,\varepsilon_{\ell'}) &= -\frac{1}{8}\delta_{k_1k_3}\delta_{k_2k_4}n_{k_1}n_{k_2}\lim_{\eta\to0^+}\lim_{\xi\to0^+}\int_{-\infty}^{\infty}\frac{d\alpha}{2\pi i}\frac{1}{\alpha+i\eta}\\ &\times\int_{-\infty}^{\infty}\frac{d\beta}{2\pi i}\frac{1}{\beta+i\xi}\int_{-1/T}^{0}d\tau_{31}e^{(i\omega_n+i\alpha-i\beta-\varepsilon_{k_1}+\varepsilon_{k_2})\tau_{31}}\\ &\times\int_{-1/T}^{1/T}d\tau_{34}e^{(i\varepsilon_{\ell'}+i\beta-\varepsilon_{k_2}+\mu)\tau_{34}}\int_{\tau_{31}-\tau_{34}-1/T}^{\tau_{31}-\tau_{34}}d\tau_{21}e^{(i\varepsilon_\ell+i\beta-\varepsilon_{k_2}+\mu)\tau_{21}}.\end{aligned}\tag{C.47}$$

We first evaluate the integration with respect to τ_{21} as follows:

$$\begin{aligned}\int_{\tau_{31}-\tau_{34}-1/T}^{\tau_{31}-\tau_{34}}d\tau_{21}e^{(i\varepsilon_\ell+i\beta-\varepsilon_{k_2}+\mu)\tau_{21}} &= \frac{1}{i\varepsilon_\ell+i\beta-\varepsilon_{k_2}+\mu}e^{(i\varepsilon_\ell+i\beta-\varepsilon_{k_2}+\mu)\tau_{21}}\Big|_{\tau_{31}-\tau_{34}-1/T}^{\tau_{31}-\tau_{34}}\\ &= \frac{1}{i\varepsilon_\ell+i\beta-\varepsilon_{k_2}+\mu}e^{(i\varepsilon_\ell+i\beta-\varepsilon_{k_2}+\mu)(\tau_{31}-\tau_{34})}\\ &\times\left[e^{-(i\beta-\varepsilon_{k_2}+\mu)/T}+1\right].\end{aligned}\tag{C.48}$$

Inserting this into Eq.(C.47), we obtain

$$\begin{aligned}\widetilde{\mathscr{R}}^{0hh}_{k_1k_2,k_3k_4}(\omega_n,\varepsilon_\ell,\varepsilon_{\ell'}) &= -\frac{1}{8}\delta_{k_1k_3}\delta_{k_2k_4}n_{k_1}n_{k_2}\lim_{\eta\to 0^+}\lim_{\xi\to 0^+}\int_{-\infty}^{\infty}\frac{d\alpha}{2\pi i}\frac{1}{\alpha+i\eta}\int_{-\infty}^{\infty}\frac{d\beta}{2\pi i}\frac{1}{\beta+i\xi} \\ &\times \frac{1}{i\varepsilon_\ell+i\beta-\varepsilon_{k_2}+\mu}\left[e^{-(i\beta-\varepsilon_{k_2}+\mu)/T}+1\right] \\ &\times \int_{-1/T}^{0}d\tau_{31}e^{(i\omega_n+i\varepsilon_\ell+i\alpha-\varepsilon_{k_1}+\mu)\tau_{31}}\int_{-1/T}^{1/T}d\tau_{34}e^{i(\varepsilon_{\ell'}-\varepsilon_\ell)\tau_{34}}. \end{aligned} \tag{C.49}$$

The integration with respect to τ_{34} gives

$$\int_{-1/T}^{1/T}d\tau_{34}e^{i(\varepsilon_{\ell'}-\varepsilon_\ell)\tau_{34}} = \frac{2}{T}\delta_{\ell\ell'} \tag{C.50}$$

and the integration with respect to τ_{31} gives

$$\int_{-1/T}^{0}d\tau_{31}e^{(i\omega_n+i\varepsilon_\ell+i\alpha-\varepsilon_{k_1}+\mu)\tau_{31}} = \frac{1}{i\omega_n+i\varepsilon_\ell+i\alpha-\varepsilon_{k_1}+\mu}\left[e^{-(i\alpha-\varepsilon_{k_1}+\mu)/T}+1\right]. \tag{C.51}$$

Inserting these results into Eq.(C.49), we obtain

$$\begin{aligned}\widetilde{\mathscr{R}}^{0hh}_{k_1k_2,k_3k_4}(\omega_n,\varepsilon_\ell,\varepsilon_{\ell'}) &= -\frac{1}{4T}\delta_{\ell\ell'}\delta_{k_1k_3}\delta_{k_2k_4}n_{k_1}n_{k_2}\lim_{\eta\to 0^+}\int_{-\infty}^{\infty}\frac{d\alpha}{2\pi i}\frac{1}{\alpha+i\eta} \\ &\times \frac{1}{i\omega_n+i\varepsilon_\ell+i\alpha-\varepsilon_{k_1}+\mu}\left[e^{-(i\alpha-\varepsilon_{k_1}+\mu)/T}+1\right] \\ &\times \lim_{\xi\to 0^+}\int_{-\infty}^{\infty}\frac{d\beta}{2\pi i}\frac{1}{\beta+i\xi}\frac{1}{i\varepsilon_\ell+i\beta-\varepsilon_{k_2}+\mu}\left[e^{-(i\beta-\varepsilon_{k_2}+\mu)/T}+1\right]. \end{aligned} \tag{C.52}$$

The integration with respect to α gives

$$\begin{aligned} I_\alpha &= \lim_{\eta\to 0^+}\int_{-\infty}^{\infty}\frac{d\alpha}{2\pi i}\frac{1}{\alpha+i\eta}\frac{1}{i\omega_n+i\varepsilon_\ell+i\alpha-\varepsilon_{k_1}+\mu}\left[e^{-(i\alpha-\varepsilon_{k_1}+\mu)/T}+1\right] \\ &= -\frac{1}{i(\omega_n+\varepsilon_\ell)-\varepsilon_{k_1}+\mu}\frac{1}{n_{k_1}} \end{aligned} \tag{C.53}$$

and the integration with respect to β gives

$$\begin{aligned} I_\beta &= \lim_{\xi\to 0^+}\int_{-\infty}^{\infty}\frac{d\beta}{2\pi i}\frac{1}{\beta+i\xi}\frac{1}{i\varepsilon_\ell+i\beta-\varepsilon_{k_2}+\mu}\left[e^{-(i\beta-\varepsilon_{k_2}+\mu)/T}+1\right] \\ &= -\frac{1}{i\varepsilon_\ell-\varepsilon_{k_2}+\mu}\frac{1}{n_{k_2}}. \end{aligned} \tag{C.54}$$

Inserting these results into Eq.(C.52), we obtain

$$\widetilde{\mathscr{R}}^{0hh}_{k_1k_2,k_3k_4}(\omega_n,\varepsilon_\ell,\varepsilon_{\ell'}) \;=\; -\frac{1}{4T}\delta_{\ell\ell'}\delta_{k_1k_3}\delta_{k_2k_4}\widetilde{\mathscr{G}}_{k_1}(\omega_n+\varepsilon_\ell)\widetilde{\mathscr{G}}_{k_2}(\varepsilon_\ell). \tag{C.55}$$

Finally, the Fourier transform of full finite temperature free response function $\widetilde{\mathscr{R}}^0(12,34)$ is given by

$$\widetilde{\mathscr{R}}^{0}_{k_1k_2,k_3k_4}(\omega_n,\varepsilon_\ell,\varepsilon_{\ell'}) = -\frac{1}{T}\delta_{\ell\ell'}\delta_{k_1k_3}\delta_{k_2k_4}\widetilde{\mathscr{G}}_{k_1}(\omega_n+\varepsilon_\ell)\widetilde{\mathscr{G}}_{k_2}(\varepsilon_\ell). \quad \blacksquare$$

Appendix D

PC-F1 Force

The relativistic point-coupling Lagrangian density $\mathscr{L}$ is built from the point couplings of the general type [37]

$$\left(\overline{\Psi}\mathscr{O}_\tau\Gamma\Psi\right), \qquad \mathscr{O}_\tau \in \{1,\tau_i\}, \qquad \Gamma \in \{1,\gamma_\mu,\gamma_5,\gamma_5\gamma_\mu,\sigma_{\mu\nu}\}, \tag{D.1}$$

where Ψ is the Dirac spinor field of the nucleon, τ_i $(i=1,2,3)$ are the isospin Pauli matrices, and Γ represents one of the 4×4 Dirac matrices. Following Ref. [37], we consider the following four-fermion vertices:

$$\begin{aligned}
&\text{isoscalar-scalar:} && (\overline{\Psi}\Psi)^2,\\
&\text{isoscalar-vector:} && (\overline{\Psi}\gamma_\mu\Psi)(\overline{\Psi}\gamma^\mu\Psi),\\
&\text{isovector-scalar:} && (\overline{\Psi}\vec{\tau}\Psi)\cdot(\overline{\Psi}\vec{\tau}\Psi),\\
&\text{isovector-vector:} && (\overline{\Psi}\vec{\tau}\gamma_\mu\Psi)\cdot(\overline{\Psi}\vec{\tau}\gamma^\mu\Psi),
\end{aligned}$$

and their corresponding gradient couplings $\partial_\nu(\cdots)\partial^\nu(\cdots)$. From these ingredients, we start with the Lagrangian density $\mathscr{L}$ of the form

$$\mathscr{L} = \mathscr{L}^{\text{free}} + \mathscr{L}^{\text{4f}} + \mathscr{L}^{\text{hot}} + \mathscr{L}^{\text{der}} + \mathscr{L}^{\text{em}}. \tag{D.2}$$

Here $\mathscr{L}^{\text{free}}$ is the Lagrangian density for free nucleons:

$$\mathscr{L}^{\text{free}} = \overline{\Psi}(i\gamma_\mu\partial^\mu - M)\Psi. \tag{D.3}$$

The interaction between nucleons is described by the four-fermion point-coupling terms:

$$\mathscr{L}^{\text{4f}} \;=\; -\frac{1}{2}\alpha_S(\overline{\Psi}\Psi)(\overline{\Psi}\Psi) - \frac{1}{2}\alpha_V(\overline{\Psi}\gamma_\mu\Psi)(\overline{\Psi}\gamma^\mu\Psi)$$

$$- \quad \frac{1}{2}\alpha_{TS}(\overline{\Psi}\vec{\tau}\Psi)\cdot(\overline{\Psi}\vec{\tau}\Psi) - \frac{1}{2}\alpha_{TV}(\overline{\Psi}\vec{\tau}\gamma_\mu\Psi)\cdot(\overline{\Psi}\vec{\tau}\gamma^\mu\Psi), \tag{D.4}$$

the higher order terms:

$$\mathscr{L}^{\rm hot} = -\frac{1}{3}\beta_S(\overline{\Psi}\Psi)^3 - \frac{1}{4}\gamma_S(\overline{\Psi}\Psi)^4 - \frac{1}{4}\gamma_V[(\overline{\Psi}\gamma_\mu\Psi)(\overline{\Psi}\gamma^\mu\Psi)]^2, \tag{D.5}$$

which is responsible for the medium effects, and the derivative terms:

$$\begin{aligned}\mathscr{L}^{\rm der} &= -\frac{1}{2}\delta_S(\partial_\nu\overline{\Psi}\Psi)(\partial^\nu\overline{\Psi}\Psi) - \frac{1}{2}\delta_V(\partial_\nu\overline{\Psi}\gamma_\mu\Psi)(\partial^\nu\overline{\Psi}\gamma^\mu\Psi) \\ &- \frac{1}{2}\delta_{TS}(\partial_\nu\overline{\Psi}\vec{\tau}\Psi)\cdot(\partial^\nu\overline{\Psi}\vec{\tau}\Psi) - \frac{1}{2}\delta_{TV}(\partial_\nu\overline{\Psi}\vec{\tau}\gamma_\mu\Psi)\cdot(\partial^\nu\overline{\Psi}\vec{\tau}\gamma^\mu\Psi)\end{aligned} \tag{D.6}$$

simulating the finite-range effects. The electromagnetic interaction between protons is described by

$$\mathscr{L}^{\rm em} = -eA_\mu\overline{\Psi}\frac{1}{2}(1+\tau_3)\gamma^\mu\Psi - \frac{1}{4}F_{\mu\nu}F^{\mu\nu}, \tag{D.7}$$

where A_μ is the four-vector potential and the electromagnetic field strength tensor $F^{\mu\nu}$ is defined as

$$F^{\mu\nu} = \partial^\mu A^\nu - \partial^\nu A^\mu. \tag{D.8}$$

The value of τ_3 is $+1(-1)$ for proton (neutron). The set of nine coupling constants for the nonlinear point-coupling effective interaction PC-F1 is shown in Table D.1. In the PC-F1 parameterization, the coupling constants α_{TS} and δ_{TS} are zero.

Table D.1: The set of coupling constants in the PC-F1 parameterization [37].

Coupling Constant	Value	Dimension
α_S	-3.83577×10^{-4}	$[\mathrm{MeV}^{-2}]$
β_S	7.68567×10^{-11}	$[\mathrm{MeV}^{-5}]$
γ_S	-2.90443×10^{-17}	$[\mathrm{MeV}^{-8}]$
δ_S	-4.18530×10^{-10}	$[\mathrm{MeV}^{-4}]$
α_V	2.59333×10^{-4}	$[\mathrm{MeV}^{-2}]$
γ_V	-3.87900×10^{-18}	$[\mathrm{MeV}^{-8}]$
δ_V	-1.19210×10^{-10}	$[\mathrm{MeV}^{-4}]$
α_{TV}	3.46770×10^{-5}	$[\mathrm{MeV}^{-2}]$
δ_{TV}	-4.20000×10^{-11}	$[\mathrm{MeV}^{-4}]$

From the Euler-Lagrange equation

$$\frac{\partial\mathscr{L}}{\partial\overline{\Psi}} - \frac{\partial}{\partial x^\mu}\left(\frac{\partial\mathscr{L}}{\partial(\partial_\mu\overline{\Psi})}\right) = 0, \tag{D.9}$$

we obtain the Dirac equation of motion for the nucleonic fields:

$$\begin{aligned} 0 &= \Big\{(i\gamma_\mu\partial^\mu - M) - \alpha_S(\overline{\Psi}\Psi) - \alpha_V(\overline{\Psi}\gamma^\mu\Psi)\gamma_\mu - \alpha_{TS}(\overline{\Psi}\vec{\tau}\Psi)\cdot\vec{\tau} - \alpha_{TV}(\overline{\Psi}\vec{\tau}\gamma^\mu\Psi)\cdot\vec{\tau}\gamma_\mu \\ &- \beta_S(\overline{\Psi}\Psi)^2 - \gamma_S(\overline{\Psi}\Psi)^3 - \gamma_V[(\overline{\Psi}\gamma_\alpha\Psi)(\overline{\Psi}\gamma^\alpha\Psi)](\overline{\Psi}\gamma^\mu\Psi)\gamma_\mu - eA_\mu\frac{1}{2}(1+\tau_3)\gamma^\mu \\ &+ \delta_S\Box(\overline{\Psi}\Psi) + \delta_V\Box(\overline{\Psi}\gamma^\alpha\Psi)\gamma_\alpha + \delta_{TS}\Box(\overline{\Psi}\vec{\tau}\Psi)\cdot\vec{\tau} + \delta_{TV}\Box(\overline{\Psi}\vec{\tau}\gamma^\alpha\Psi)\cdot\vec{\tau}\gamma_\alpha\Big\}\Psi. \end{aligned} \tag{D.10}$$

The multiplication of Eq.(D.10) with $\beta \equiv \gamma^0$, the application of the expansion

$$\Psi(\mathbf{r},t) = \sum_k \varphi_k(\mathbf{r})e^{-i\epsilon_k t}\hat{a}_k \tag{D.11}$$

to Eq. (D.10), and the mean-field approximation lead to

$$\begin{aligned} 0 &= \Big\{\epsilon_k - (\boldsymbol{\alpha}\cdot\mathbf{p} + \beta M) - \beta\alpha_S\langle\Phi|\overline{\Psi}\Psi|\Phi\rangle - \beta\alpha_V\langle\Phi|\overline{\Psi}\gamma^\mu\Psi|\Phi\rangle\gamma_\mu \\ &- \beta\alpha_{TS}\langle\Phi|\overline{\Psi}\vec{\tau}\Psi|\Phi\rangle\cdot\vec{\tau} - \beta\alpha_{TV}\langle\Phi|\overline{\Psi}\vec{\tau}\gamma^\mu\Psi|\Phi\rangle\cdot\vec{\tau}\gamma_\mu - \beta\beta_S\langle\Phi|(\overline{\Psi}\Psi)^2|\Phi\rangle \\ &- \beta\gamma_S\langle\Phi|(\overline{\Psi}\Psi)^3|\Phi\rangle - \gamma_V\beta\langle\Phi|\overline{\Psi}\gamma^\mu\Psi[(\overline{\Psi}\gamma_\alpha\Psi)(\overline{\Psi}\gamma^\alpha\Psi)]|\Phi\rangle\gamma_\mu \\ &- e\gamma^0A_\mu\frac{1}{2}(1+\tau_3)\gamma^\mu + \delta_S\beta\Box\langle\Phi|\overline{\Psi}\Psi|\Phi\rangle + \delta_V\beta\gamma_\alpha\Box\langle\Phi|\overline{\Psi}\gamma^\alpha\Psi|\Phi\rangle \\ &+ \delta_{TS}\beta\vec{\tau}\cdot\Box\langle\Phi|\overline{\Psi}\vec{\tau}\Psi|\Phi\rangle + \delta_{TV}\beta\vec{\tau}\gamma_\alpha\cdot\Box\langle\Phi|\overline{\Psi}\vec{\tau}\gamma^\alpha\Psi|\Phi\rangle\Big\}\varphi_k(\mathbf{r}). \end{aligned} \tag{D.12}$$

Introducing the following density and currents:

$$\rho_S(\mathbf{r}) = \sum_k n_k\bar{\varphi}_k(\mathbf{r})\varphi_k(\mathbf{r}) \equiv \langle\Phi|\overline{\Psi}\Psi|\Phi\rangle, \tag{D.13}$$

$$j_V^\mu(\mathbf{r}) = \sum_k n_k\bar{\varphi}_k(\mathbf{r})\gamma^\mu\varphi_k(\mathbf{r}) \equiv \langle\Phi|\overline{\Psi}\gamma^\mu\Psi|\Phi\rangle, \tag{D.14}$$

$$\vec{j}_{TS}(\mathbf{r}) = \sum_k n_k\bar{\varphi}_k(\mathbf{r})\vec{\tau}\varphi_k(\mathbf{r}) \equiv \langle\Phi|\overline{\Psi}\vec{\tau}\Psi|\Phi\rangle, \tag{D.15}$$

$$\vec{j}_{TV}^\mu(\mathbf{r}) = \sum_k n_k\bar{\varphi}_k(\mathbf{r})\vec{\tau}\gamma^\mu\varphi_k(\mathbf{r}) \equiv \langle\Phi|\overline{\Psi}\vec{\tau}\gamma^\mu\Psi|\Phi\rangle, \tag{D.16}$$

Eq.(D.12) becomes

$$\begin{aligned} \epsilon_k\varphi_k(\mathbf{r}) &= \Big\{\boldsymbol{\alpha}\cdot\mathbf{p} + \beta M + \beta[\alpha_S\rho_S(\mathbf{r}) + \beta_S\rho_S^2(\mathbf{r}) + \gamma_S\rho_S^3(\mathbf{r}) + \delta_S\nabla^2\rho_S(\mathbf{r}) \\ &+ \alpha_{TS}\vec{\tau}\cdot\vec{j}_{TS}(\mathbf{r}) + \delta_{TS}\vec{\tau}\cdot\nabla^2\vec{j}_{TS}(\mathbf{r})] + \beta[\alpha_V\gamma_\mu j_V^\mu(\mathbf{r}) \\ &+ \gamma_V\gamma_\mu j_V^\mu(\mathbf{r})j_{V\alpha}(\mathbf{r})j_V^\alpha(\mathbf{r}) + \delta_V\gamma_\mu\nabla^2 j_V^\mu(\mathbf{r}) + e\gamma_\mu A^\mu\tfrac{1}{2}(1+\tau_3) \\ &+ \alpha_{TV}\vec{\tau}\gamma_\mu\cdot\vec{j}_{TV}^\mu(\mathbf{r}) + \delta_{TV}\vec{\tau}\gamma_\mu\cdot\nabla^2\vec{j}_{TV}^\mu(\mathbf{r})]\Big\}\varphi_k(\mathbf{r}). \end{aligned} \tag{D.17}$$

Assuming the time-reversal symmetry of the mean field and the isospin τ_3 is a good quantum number, the currents $j_V^\mu(\mathbf{r})$, $\vec{j}_{TS}(\mathbf{r})$, and $\vec{j}_{TV}^\mu(\mathbf{r})$ respectively become local densities:

$$\begin{aligned}
\rho_V(\mathbf{r}) &= \sum_k n_k \bar{\varphi}_k(\mathbf{r})\gamma^0\varphi_k(\mathbf{r}) = \sum_k n_k \varphi_k^\dagger(\mathbf{r})\varphi_k(\mathbf{r}), && \text{(D.18)}\\
\rho_{TS}(\mathbf{r}) &= \sum_k n_k \bar{\varphi}_k(\mathbf{r})\tau_3\varphi_k(\mathbf{r}), && \text{(D.19)}\\
\rho_{TV}(\mathbf{r}) &= \sum_k n_k \bar{\varphi}_k(\mathbf{r})\tau_3\gamma^0\varphi_k. && \text{(D.20)}
\end{aligned}$$

Equation (D.17) then becomes the time-independent Dirac equation for nucleon:

$$\begin{aligned}
\epsilon_k\varphi_k(\mathbf{r}) &= \Big\{\boldsymbol{\alpha}\cdot\mathbf{p} + \beta M + \beta[\alpha_S\rho_S(\mathbf{r}) + \beta_S\rho_S^2(\mathbf{r}) + \gamma_S\rho_S^3(\mathbf{r}) + \delta_S\nabla^2\rho_S(\mathbf{r})\\
&+ \tau_3\alpha_{TS}\rho_{TS}(\mathbf{r}) + \tau_3\delta_{TS}\nabla^2\rho_{TS}(\mathbf{r})] + [\alpha_V\rho_V(\mathbf{r}) + \gamma_V\rho_V^3(\mathbf{r})\\
&+ \delta_V\nabla^2\rho_V(\mathbf{r}) + eA^0\tfrac{1}{2}(1+\tau_3) + \tau_3\alpha_{TV}\rho_{TV}(\mathbf{r}) + \tau_3\delta_{TV}\nabla^2\rho_{TV}(\mathbf{r})]\Big\}\varphi_k(\mathbf{r})\\
\epsilon_k\varphi_k(\mathbf{r}) &= \hat{h}^D\varphi_k(\mathbf{r}), && \text{(D.21)}
\end{aligned}$$

where the Dirac Hamiltonian $\hat{h}^D$ is

$$\hat{h}^D = \boldsymbol{\alpha}\cdot\mathbf{p} + \beta[M + S(\mathbf{r})] + V(\mathbf{r}). \qquad \text{(D.22)}$$

Here the scalar potential $S(\mathbf{r})$ consists of the isoscalar-scalar $\Sigma_S(\mathbf{r})$ and isovector-scalar $\Sigma_{TS}(\mathbf{r})$ self-energies, viz.

$$\begin{aligned}
S(\mathbf{r}) &= \Sigma_S(\mathbf{r}) + \tau_3\Sigma_{TS}(\mathbf{r}), && \text{(D.23)}\\
\Sigma_S(\mathbf{r}) &= \alpha_S\rho_S(\mathbf{r}) + \beta_S\rho_S^2(\mathbf{r}) + \gamma_S\rho_S^3(\mathbf{r}) + \delta_S\nabla^2\rho_S(\mathbf{r}), && \text{(D.24)}\\
\Sigma_{TS}(\mathbf{r}) &= (\alpha_{TS} + \delta_{TS}\nabla^2)\rho_{TS}(\mathbf{r}). && \text{(D.25)}
\end{aligned}$$

The vector potential $V(\mathbf{r})$ is also decomposed into two self-energy terms, viz.

$$V(\mathbf{r}) = \Sigma_V(\mathbf{r}) + \tau_3\Sigma_{TV}(\mathbf{r}), \qquad \text{(D.26)}$$

where the isoscalar-vector $\Sigma_V(\mathbf{r})$ and isovector-vector $\Sigma_{TV}(\mathbf{r})$ self-energies respectively are given by

$$\begin{aligned}
\Sigma_V(\mathbf{r}) &= \alpha_V\rho_V(\mathbf{r}) + \gamma_V\rho_V^3(\mathbf{r}) + \delta_V\nabla^2\rho_V(\mathbf{r}) + eA^0\tfrac{1}{2}(1+\tau_3), && \text{(D.27)}\\
\Sigma_{TV}(\mathbf{r}) &= (\alpha_{TV} + \delta_{TV}\nabla^2)\rho_{TV}(\mathbf{r}). && \text{(D.28)}
\end{aligned}$$

From the Lagrangian density, we can obtain the total Hamiltonian $\hat{H}$ via

$$\hat{H} = \int d^3\mathbf{r} \left\{ \frac{\partial \mathcal{L}}{\partial(\partial_0 \Psi)}(\partial_0 \Psi) + (\partial_0 \overline{\Psi}) \frac{\partial \mathcal{L}}{\partial(\partial_0 \overline{\Psi})} + \frac{\partial \mathcal{L}}{\partial(\partial_0 A_\mu)}(\partial_0 A_\mu) - \mathcal{L} \right\}. \tag{D.29}$$

Insertion of Eqs. (D.2)-(D.7) into the expression of total Hamiltonian $\hat{H}$ leads to

$$\begin{aligned}
\hat{H} &= \int d^3\mathbf{r} \Big\{ \Psi^\dagger(\boldsymbol{\alpha}\cdot\mathbf{p} + \beta M)\Psi + \frac{1}{2}\alpha_S(\overline{\Psi}\Psi)(\overline{\Psi}\Psi) + \frac{1}{2}\alpha_V(\overline{\Psi}\gamma_\mu\Psi)(\overline{\Psi}\gamma^\mu\Psi) \\
&+ \frac{1}{2}\alpha_{TS}(\overline{\Psi}\vec{\tau}\Psi)\cdot(\overline{\Psi}\vec{\tau}\Psi) + \frac{1}{2}\alpha_{TV}(\overline{\Psi}\vec{\tau}\gamma_\mu\Psi)\cdot(\overline{\Psi}\vec{\tau}\gamma^\mu\Psi) + \frac{1}{3}\beta_S(\overline{\Psi}\Psi)^3 \\
&+ \frac{1}{4}\gamma_S(\overline{\Psi}\Psi)^4 + \frac{1}{4}\gamma_V[(\overline{\Psi}\gamma_\mu\Psi)(\overline{\Psi}\gamma^\mu\Psi)]^2 \\
&- \frac{1}{2}\delta_S[(\partial_0\overline{\Psi}\Psi)(\partial^0\overline{\Psi}\Psi) + (\boldsymbol{\nabla}\overline{\Psi}\Psi)\cdot(\boldsymbol{\nabla}\overline{\Psi}\Psi)] \\
&- \frac{1}{2}\delta_V[(\partial_0\overline{\Psi}\gamma_\mu\Psi)(\partial^0\overline{\Psi}\gamma^\mu\Psi) + (\boldsymbol{\nabla}\overline{\Psi}\gamma_\mu\Psi)\cdot(\boldsymbol{\nabla}\overline{\Psi}\gamma^\mu\Psi)] \\
&- \frac{1}{2}\delta_{TS}[(\partial_0\overline{\Psi}\vec{\tau}\Psi)\cdot(\partial^0\overline{\Psi}\vec{\tau}\Psi) + (\boldsymbol{\nabla}\overline{\Psi}\vec{\tau}\Psi)\cdot(\boldsymbol{\nabla}\overline{\Psi}\vec{\tau}\Psi)] \\
&- \frac{1}{2}\delta_{TV}[(\partial_0\overline{\Psi}\vec{\tau}\gamma_\mu\Psi)\cdot(\partial^0\overline{\Psi}\vec{\tau}\gamma^\mu\Psi) + (\boldsymbol{\nabla}\overline{\Psi}\vec{\tau}\gamma_\mu\Psi)\cdot(\boldsymbol{\nabla}\overline{\Psi}\vec{\tau}\gamma^\mu\Psi)]\Big\} \\
&- \frac{1}{2}\int d^3\mathbf{r}\left[\dot{A}^j\dot{A}_j + (\boldsymbol{\nabla}A^\mu)\cdot(\boldsymbol{\nabla}A_\mu)\right] + \int d^3\mathbf{r}\overline{\Psi}\Gamma_e^\mu A_\mu\Psi.
\end{aligned} \tag{D.30}$$

Using the mean-field approximation, the energy density functional reads:

$$\begin{aligned}
E_{\rm RMF}[\hat{\rho}, A] &= \langle\Phi|\hat{H}|\Phi\rangle \\
&= \int d^3\mathbf{r}\Big\{ \sum_{k\ell}\psi_k^\dagger(\mathbf{r},t)(\boldsymbol{\alpha}\cdot\mathbf{p} + \beta M)\psi_\ell(\mathbf{r},t)\rho_{\ell k} \\
&+ \frac{1}{2}\alpha_S\sum_{k\ell}\psi_k^\dagger(\mathbf{r},t)\gamma^0\psi_\ell(\mathbf{r},t)\rho_{\ell k}\sum_{mn}\psi_m^\dagger(\mathbf{r},t)\gamma^0\psi_n(\mathbf{r},t)\rho_{nm} \\
&+ \frac{1}{2}\alpha_V\sum_{k\ell}\psi_k^\dagger(\mathbf{r},t)\gamma^0\gamma_\mu\psi_\ell(\mathbf{r},t)\rho_{\ell k}\sum_{mn}\psi_m^\dagger(\mathbf{r},t)\gamma^0\gamma^\mu\psi_n(\mathbf{r},t)\rho_{nm} \\
&+ \frac{1}{2}\alpha_{TS}\sum_{k\ell}\psi_k^\dagger(\mathbf{r},t)\gamma^0\vec{\tau}\psi_\ell(\mathbf{r},t)\rho_{\ell k}\cdot\sum_{mn}\psi_m^\dagger(\mathbf{r},t)\gamma^0\vec{\tau}\psi_n(\mathbf{r},t)\rho_{nm} \\
&+ \frac{1}{2}\alpha_{TV}\sum_{k\ell}\psi_k^\dagger(\mathbf{r},t)\gamma^0\vec{\tau}\gamma_\mu\psi_\ell(\mathbf{r},t)\rho_{\ell k}\cdot\sum_{mn}\psi_m^\dagger(\mathbf{r},t)\gamma^0\vec{\tau}\gamma^\mu\Psi_n(\mathbf{r},t)\rho_{nm} \\
&+ \frac{1}{3}\beta_S\sum_{k\ell}\psi_k^\dagger(\mathbf{r},t)\gamma^0\psi_\ell(\mathbf{r},t)\rho_{\ell k}\sum_{mn}\psi_m^\dagger(\mathbf{r},t)\gamma^0\psi_n(\mathbf{r},t)\rho_{nm} \\
&\times \sum_{pq}\psi_p^\dagger(\mathbf{r},t)\gamma^0\psi_q(\mathbf{r},t)\rho_{qp}
\end{aligned}$$

$$
\begin{aligned}
&+ \quad \frac{1}{4}\gamma_S \sum_{k\ell} \psi_k^\dagger(\mathbf{r},t)\gamma^0\psi_\ell(\mathbf{r},t)\rho_{\ell k} \sum_{mn} \psi_m^\dagger(\mathbf{r},t)\gamma^0\psi_n(\mathbf{r},t)\rho_{nm} \\
&\times \quad \sum_{pq} \psi_p^\dagger(\mathbf{r},t)\gamma^0\psi_q(\mathbf{r},t)\rho_{qp} \sum_{rs} \psi_r^\dagger(\mathbf{r},t)\gamma^0\psi_s(\mathbf{r},t)\rho_{sr} \\
&+ \quad \frac{1}{4}\gamma_V \sum_{k\ell} \psi_k^\dagger(\mathbf{r},t)\gamma^0\gamma_\mu\psi_\ell(\mathbf{r},t)\rho_{\ell k} \sum_{mn} \psi_m^\dagger(\mathbf{r},t)\gamma^0\gamma^\mu\psi_n(\mathbf{r},t)\rho_{nm} \\
&\times \quad \sum_{pq} \psi_p^\dagger(\mathbf{r},t)\gamma^0\gamma_\alpha\psi_q(\mathbf{r},t)\rho_{qp} \sum_{rs} \psi_r^\dagger(\mathbf{r},t)\gamma^0\gamma^\alpha\psi_s(\mathbf{r},t)\rho_{sr} \\
&- \quad \frac{1}{2}\delta_S \sum_{k\ell} \partial_0\psi_k^\dagger(\mathbf{r},t)\gamma^0\psi_\ell(\mathbf{r},t)\rho_{\ell k} \sum_{mn} \partial^0\psi_m^\dagger(\mathbf{r},t)\gamma_0\psi_n(\mathbf{r},t)\rho_{nm} \\
&- \quad \frac{1}{2}\delta_S \sum_{k\ell} [\boldsymbol{\nabla}\psi_k^\dagger(\mathbf{r},t)\gamma^0\psi_\ell(\mathbf{r},t)]\rho_{\ell k} \cdot \sum_{mn} [\boldsymbol{\nabla}\psi_m^\dagger(\mathbf{r},t)\gamma^0\psi_n(\mathbf{r},t)]\rho_{nm} \\
&- \quad \frac{1}{2}\delta_V \sum_{k\ell} \partial_0\psi_k^\dagger(\mathbf{r},t)\gamma^0\gamma_\mu\psi_\ell(\mathbf{r},t)\rho_{\ell k} \sum_{mn} \partial^0\psi_m^\dagger(\mathbf{r},t)\gamma_0\gamma^\mu\psi_n(\mathbf{r},t)\rho_{nm} \\
&- \quad \frac{1}{2}\delta_V \sum_{k\ell} [\boldsymbol{\nabla}\psi_k^\dagger(\mathbf{r},t)\gamma^0\gamma_\mu\psi_\ell(\mathbf{r},t)]\rho_{\ell k} \cdot \sum_{mn} [\boldsymbol{\nabla}\psi_m^\dagger(\mathbf{r},t)\gamma_0\gamma_\mu\psi_n(\mathbf{r},t)]\rho_{nm} \\
&- \quad \frac{1}{2}\delta_{TS} \sum_{k\ell} [\partial_0\psi_k^\dagger(\mathbf{r},t)\gamma^0\vec{\tau}\psi_\ell(\mathbf{r},t)]\rho_{\ell k} \cdot \sum_{mn} [\partial^0\psi_m^\dagger(\mathbf{r},t)\gamma_0\vec{\tau}\psi_n(\mathbf{r},t)]\rho_{nm} \\
&- \quad \frac{1}{2}\delta_{TS} \sum_{k\ell} [\boldsymbol{\nabla}\psi_k^\dagger(\mathbf{r},t)\gamma^0\vec{\tau}\psi_\ell(\mathbf{r},t)]\rho_{\ell k} \cdot \sum_{mn} [\boldsymbol{\nabla}\psi_m^\dagger(\mathbf{r},t)\gamma_0\vec{\tau}\psi_n(\mathbf{r},t)]\rho_{nm} \\
&- \quad \frac{1}{2}\delta_{TV} \sum_{k\ell} [\partial_0\psi_k^\dagger(\mathbf{r},t)\gamma^0\vec{\tau}\gamma_\mu\psi_\ell(\mathbf{r},t)]\rho_{\ell k} \cdot \sum_{mn} [\partial^0\psi_m^\dagger(\mathbf{r},t)\gamma_0\vec{\tau}\gamma^\mu\psi_n(\mathbf{r},t)]\rho_{nm} \\
&- \quad \frac{1}{2}\delta_{TV} \sum_{k\ell} [\boldsymbol{\nabla}\psi_k^\dagger(\mathbf{r},t)\gamma^0\vec{\tau}\gamma_\mu\psi_\ell(\mathbf{r},t)]\rho_{\ell k} \cdot \sum_{mn} [\boldsymbol{\nabla}\psi_m^\dagger(\mathbf{r},t)\gamma_0\vec{\tau}\gamma^\mu\psi_n(\mathbf{r},t)]\rho_{nm} \\
&+ \quad \sum_{k\ell} \psi_k^\dagger(\mathbf{r},t)\gamma^0\Gamma_e^\mu A_\mu\psi_\ell(\mathbf{r},t)\rho_{\ell k}\Big\} - \frac{1}{2}\int d^3\mathbf{r}\left[\dot{A}^j\dot{A}_j + (\boldsymbol{\nabla}A^\mu)\cdot(\boldsymbol{\nabla}A_\mu)\right].
\end{aligned}
\tag{D.31}
$$

The first variational derivative of $E_{\rm RMF}[\hat{\rho},A]$ with respect to $\hat{\rho}$ gives the matrix element

$$
\begin{aligned}
H_{ab}^D &= \frac{\delta E_{\rm RMF}[\hat{\rho},A]}{\delta\rho_{ba}} \\
&= \int d^3\mathbf{r}\Big\{\psi_a^\dagger(\mathbf{r},t)[\boldsymbol{\alpha}\cdot\mathbf{p}+\beta M]\psi_b(\mathbf{r},t) + \alpha_S\psi_a^\dagger(\mathbf{r},t)\gamma^0\rho_S(\mathbf{r},t)\psi_b(\mathbf{r},t) \\
&+ \alpha_V\psi_a^\dagger(\mathbf{r},t)\gamma^0\gamma_\mu j_V^\mu(\mathbf{r},t)\psi_b(\mathbf{r},t) + \alpha_{TS}\psi_a^\dagger(\mathbf{r},t)\gamma^0\vec{\tau}\cdot\vec{j}_{TS}(\mathbf{r},t)\psi_b(\mathbf{r},t) \\
&+ \alpha_{TV}\psi_a^\dagger(\mathbf{r},t)\gamma^0\vec{\tau}\cdot\gamma_\mu\vec{j}_{TV}^\mu(\mathbf{r},t)\psi_b(\mathbf{r},t) + \beta_S\psi_a^\dagger(\mathbf{r},t)\gamma^0\rho_S^2(\mathbf{r},t)\psi_b(\mathbf{r},t) \\
&+ \gamma_S\psi_a^\dagger(\mathbf{r},t)\gamma^0\rho_S^3(\mathbf{r},t)\psi_b(\mathbf{r},t) + \gamma_V\psi_a^\dagger(\mathbf{r},t)\gamma_0\gamma_\mu j_V^\mu(\mathbf{r},t)j_{V\alpha}(\mathbf{r},t)j_V^\alpha(\mathbf{r},t)\psi_b(\mathbf{r},t)
\end{aligned}
$$

$$
\begin{aligned}
&- \delta_S \partial_0 \overline{\psi}_a(\mathbf{r},t)\psi_b(\mathbf{r},t)\partial^0\rho_S(\mathbf{r},t) - \delta_S[\boldsymbol{\nabla}\overline{\psi}_a(\mathbf{r},t)\psi_b(\mathbf{r},t)]\cdot\boldsymbol{\nabla}\rho_S(\mathbf{r},t)\\
&- \delta_V \partial_0 \overline{\psi}_a(\mathbf{r},t)\gamma_\mu\psi_b(\mathbf{r},t)\partial^0 j_V^\mu(\mathbf{r},t) - \delta_V[\boldsymbol{\nabla}\overline{\psi}_a(\mathbf{r},t)\gamma_\mu\psi_b(\mathbf{r},t)]\cdot\boldsymbol{\nabla} j_V^\mu(\mathbf{r},t)\\
&- \delta_{TS} \partial_0 \overline{\psi}_a(\mathbf{r},t)\vec{\tau}\psi_b(\mathbf{r},t)\cdot\partial^0\vec{j}_{TS}(\mathbf{r},t) - \delta_{TS}[\boldsymbol{\nabla}\overline{\psi}_a(\mathbf{r},t)\vec{\tau}\psi_b(\mathbf{r},t)]\cdot\boldsymbol{\nabla}\vec{j}_{TS}(\mathbf{r},t)\\
&- \delta_{TV} \partial_0 \overline{\psi}_a(\mathbf{r},t)\vec{\tau}\gamma_\mu\psi_b(\mathbf{r},t)\cdot\partial^0\vec{j}^\mu_{TV}(\mathbf{r},t) - \delta_{TV}[\boldsymbol{\nabla}\overline{\psi}_a(\mathbf{r},t)\vec{\tau}\gamma_\mu\psi_b(\mathbf{r},t)]\cdot\boldsymbol{\nabla}\vec{j}^\mu_{TV}(\mathbf{r},t)\\
&+ \overline{\psi}_a(\mathbf{r},t)\Gamma^\mu_e A_\mu\psi_b(\mathbf{r},t)\Big\}, \qquad \text{(D.32)}
\end{aligned}
$$

where the charge density $\rho_S(\mathbf{r},t)$ and the current densities $j_V^\mu(\mathbf{r},t)$, $\vec{j}_{TS}(\mathbf{r},t)$, and $\vec{j}^\mu_{TV}(\mathbf{r},t)$ are

$$
\begin{aligned}
\rho_S(\mathbf{r},t) &= \sum_{mn}\overline{\psi}_m(\mathbf{r},t)\psi_n(\mathbf{r},t)\rho_{nm}; && \text{(D.33)}\\
j_V^\mu(\mathbf{r},t) &= \sum_{mn}\overline{\psi}_m(\mathbf{r},t)\gamma^\mu\psi_n(\mathbf{r},t)\rho_{nm}; && \text{(D.34)}\\
\vec{j}_{TS}(\mathbf{r},t) &= \sum_{mn}\overline{\psi}_m(\mathbf{r},t)\vec{\tau}\psi_n(\mathbf{r},t)\rho_{nm}; && \text{(D.35)}\\
\vec{j}^\mu_{TV}(\mathbf{r},t) &= \sum_{mn}\overline{\psi}_m(\mathbf{r},t)\vec{\tau}\gamma^\mu\psi_n(\mathbf{r},t)\rho_{nm}. && \text{(D.36)}
\end{aligned}
$$

The static approximation

$$
\psi_a(\mathbf{r},t) = \varphi_a(\mathbf{r})e^{-i\epsilon_a t} \qquad \text{(D.37)}
$$

and the single-particle density matrix

$$
\rho_{ab} = n_a\delta_{ab}, \qquad \text{(D.38)}
$$

where n_a is the single-particle occupation numbers, lead to the time-independent charge density and current densities:

$$
\begin{aligned}
\rho_S(\mathbf{r}) &= \sum_m n_m\varphi_m^\dagger(\mathbf{r})\gamma^0\varphi_m(\mathbf{r}), && \text{(D.39)}\\
j_V^\mu(\mathbf{r}) &= \sum_m n_m\overline{\varphi}_m(\mathbf{r})\gamma^\mu\varphi_m(\mathbf{r}), && \text{(D.40)}\\
\vec{j}_{TS}(\mathbf{r}) &= \sum_m n_m\overline{\varphi}_m(\mathbf{r})\vec{\tau}\varphi_m(\mathbf{r}), && \text{(D.41)}\\
\vec{j}^\mu_{TV}(\mathbf{r}) &= \sum_m n_m\overline{\varphi}_m(\mathbf{r})\vec{\tau}\gamma^\mu\varphi_m(\mathbf{r}). && \text{(D.42)}
\end{aligned}
$$

Accordingly, the matrix element H^D_{ab} reduces to the matrix element of the Dirac Hamiltonian

$\hat{h}^D$:

$$\begin{aligned}\int d^3\mathbf{r}\varphi_a^\dagger(\mathbf{r})\hat{h}^D\varphi_b(\mathbf{r}) &= \int d^3\mathbf{r}\Big\{\varphi_a^\dagger(\mathbf{r})[\boldsymbol{\alpha}\cdot\mathbf{p}+\beta M]\varphi_b(\mathbf{r})+\alpha_S\varphi_a^\dagger(\mathbf{r})\gamma^0\rho_S(\mathbf{r})\varphi_b(\mathbf{r})\\ &+ \alpha_V\varphi_a^\dagger(\mathbf{r})\gamma^0\gamma_\mu j_V^\mu(\mathbf{r})\varphi_b(\mathbf{r})+\alpha_{TS}\varphi_a^\dagger(\mathbf{r})\gamma^0\vec{\tau}\cdot\vec{j}_{TS}(\mathbf{r})\varphi_b(\mathbf{r})\\ &+ \alpha_{TV}\varphi_a^\dagger(\mathbf{r})\gamma^0\vec{\tau}\cdot\gamma_\mu\vec{j}_{TV}^\mu(\mathbf{r})\varphi_b(\mathbf{r})+\beta_S\varphi_a^\dagger(\mathbf{r})\gamma^0\rho_S^2(\mathbf{r})\varphi_b(\mathbf{r})\\ &+ \gamma_S\varphi_a^\dagger(\mathbf{r})\gamma^0\rho_S^3(\mathbf{r})\varphi_b(\mathbf{r})+\gamma_V\varphi_a^\dagger(\mathbf{r})\gamma_0\gamma_\mu j_V^\mu(\mathbf{r})j_{V\alpha}(\mathbf{r})j_V^\alpha(\mathbf{r})\varphi_b(\mathbf{r})\\ &- \delta_S[\boldsymbol{\nabla}\overline{\varphi}_a(\mathbf{r})\varphi_b(\mathbf{r})]\cdot\boldsymbol{\nabla}\rho_S(\mathbf{r})-\delta_V[\boldsymbol{\nabla}\overline{\varphi}_a(\mathbf{r})\gamma_\mu\varphi_b(\mathbf{r})]\cdot\boldsymbol{\nabla}j_V^\mu(\mathbf{r})\\ &- \delta_{TS}[\boldsymbol{\nabla}\overline{\varphi}_a(\mathbf{r})\vec{\tau}\varphi_b(\mathbf{r})]\cdot\boldsymbol{\nabla}\vec{j}_{TS}(\mathbf{r})-\delta_{TV}[\boldsymbol{\nabla}\overline{\varphi}_a(\mathbf{r})\vec{\tau}\gamma_\mu\varphi_b(\mathbf{r})]\cdot\boldsymbol{\nabla}\vec{j}_{TV}^\mu(\mathbf{r})\\ &+ \overline{\varphi}_a(\mathbf{r})\Gamma_e^\mu A_\mu\varphi_b(\mathbf{r})\Big\}. \end{aligned} \tag{D.43}$$

The integrals involving the $\boldsymbol{\nabla}$ can be transformed as follows:

$$\int d^3\mathbf{r}[\boldsymbol{\nabla}\overline{\varphi}(\mathbf{r})\varphi_b(\mathbf{r})]\cdot\boldsymbol{\nabla}\rho_S(\mathbf{r}) = -\int d^3\mathbf{r}\overline{\varphi}_a(\mathbf{r})\nabla^2\rho_S(\mathbf{r})\varphi_b(\mathbf{r}), \tag{D.44}$$

$$\int d^3\mathbf{r}[\boldsymbol{\nabla}\overline{\varphi}_a(\mathbf{r})\gamma_\mu\varphi_b(\mathbf{r})]\cdot\boldsymbol{\nabla}j_V^\mu(\mathbf{r}) = -\int d^3\mathbf{r}\overline{\varphi}_a(\mathbf{r})\gamma_\mu\nabla^2 j_V^\mu(\mathbf{r})\varphi_b(\mathbf{r}), \tag{D.45}$$

$$\int d^3\mathbf{r}[\boldsymbol{\nabla}\overline{\varphi}_a(\mathbf{r})\vec{\tau}\varphi_b(\mathbf{r})]\cdot\boldsymbol{\nabla}\vec{j}_{TS}(\mathbf{r}) = -\int d^3\mathbf{r}\overline{\varphi}_a(\mathbf{r})\vec{\tau}\cdot\nabla^2\vec{j}_{TS}(\mathbf{r})\varphi_b(\mathbf{r}), \tag{D.46}$$

$$\int d^3\mathbf{r}[\boldsymbol{\nabla}\overline{\varphi}_a(\mathbf{r})\vec{\tau}\gamma_\mu\varphi_b(\mathbf{r})]\cdot\boldsymbol{\nabla}\vec{j}_{TV}^\mu(\mathbf{r}) = -\int d^3\mathbf{r}\overline{\varphi}_a(\mathbf{r})\vec{\tau}\gamma_\mu\cdot\nabla^2\vec{j}_{TV}^\mu(\mathbf{r})\varphi_b(\mathbf{r}). \tag{D.47}$$

The matrix element of the operator $\hat{h}^D$ then becomes

$$\begin{aligned}\int d^3\mathbf{r}\varphi_a^\dagger(\mathbf{r})\hat{h}^D\varphi_b(\mathbf{r}) &= \int d^3\mathbf{r}\varphi_a^\dagger(\mathbf{r})\Big\{(\boldsymbol{\alpha}\cdot\mathbf{p}+\beta M)+\alpha_S\gamma^0\rho_S(\mathbf{r})+\alpha_V\gamma^0\gamma_\mu j_V^\mu(\mathbf{r})\\ &+ \alpha_{TS}\gamma^0\vec{\tau}\cdot\vec{j}_{TS}(\mathbf{r})+\alpha_{TV}\gamma^0\vec{\tau}\cdot\gamma_\mu\vec{j}_{TV}^\mu(\mathbf{r})+\beta_S\gamma^0\rho_S^2(\mathbf{r})\\ &+ \gamma_S\gamma^0\rho_S^3(\mathbf{r})+\gamma_V\gamma_0\gamma_\mu j_V^\mu(\mathbf{r})j_{V\alpha}(\mathbf{r})j_V^\alpha(\mathbf{r})+\delta_S\gamma^0\nabla^2\rho_S(\mathbf{r})\\ &+ \delta_V\gamma^0\gamma_\mu\nabla^2 j_V^\mu(\mathbf{r})+\delta_{TS}\gamma^0\vec{\tau}\cdot\nabla^2\vec{j}_{TS}(\mathbf{r})\\ &+ \delta_{TV}\gamma^0\vec{\tau}\gamma_\mu\cdot\nabla^2\vec{j}_{TV}^\mu(\mathbf{r})+\gamma^0\Gamma_e^\mu A_\mu\Big\}\varphi_b(\mathbf{r}) \end{aligned} \tag{D.48}$$

and the Dirac Hamiltonian $\hat{h}^D$ is given by

$$\hat{h}^D = (\boldsymbol{\alpha}\cdot\mathbf{p}+\beta M)+\gamma^0\Sigma_S(\mathbf{r})+\gamma^0\gamma_\mu\Sigma_V^\mu(\mathbf{r})+\gamma^0\vec{\tau}\cdot\vec{\Sigma}_{TS}(\mathbf{r})+\gamma^0\vec{\tau}\gamma_\mu\cdot\vec{\Sigma}_{TV}^\mu(\mathbf{r}), \tag{D.49}$$

where

$$\Sigma_S(\mathbf{r}) = \alpha_S\rho_S(\mathbf{r}) + \beta_S\rho_S^2(\mathbf{r}) + \gamma_S\rho_S^3(\mathbf{r}) + \delta_S\nabla^2\rho_S(\mathbf{r}), \tag{D.50}$$

$$\Sigma_V^\mu(\mathbf{r}) = \alpha_V j_V^\mu(\mathbf{r}) + \gamma_V j_V^\mu(\mathbf{r}) j_{V\alpha}(\mathbf{r}) j_V^\alpha(\mathbf{r}) + \delta_V\nabla^2 j_V^\mu(\mathbf{r}) + \Gamma_e^\mu A_\mu, \tag{D.51}$$

$$\vec{\Sigma}_{TS}(\mathbf{r}) = \alpha_{TS}\vec{j}_{TS}(\mathbf{r}) + \delta_{TS}\nabla^2\vec{j}_{TS}(\mathbf{r}), \tag{D.52}$$

$$\vec{\Sigma}_{TV}^\mu = \alpha_{TV}\vec{j}_{TV}^\mu(\mathbf{r}) + \delta_{TV}\nabla^2\vec{j}_{TV}^\mu(\mathbf{r}). \tag{D.53}$$

Assuming the time-reversal symmetry of the mean field and the nucleon single-particle states do not mix isospin, the current densities (D.40)-(D.42) reduce to local densities $\rho_V(\mathbf{r})$, $\rho_{TS}(\mathbf{r})$, and $\rho_{TV}(\mathbf{r})$. Under these assumptions, we, therefore, obtain the Dirac Hamiltonian $\hat{h}^D$ given by Eq. (D.22).

Using the static approximation and the single-particle density matrix $\rho_{\ell k} = n_k\delta_{\ell k}$, the energy density functional $E_{\rm RMF}[\hat{\rho}, A]$ becomes

$$\begin{aligned}
E_{\rm RMF}[\hat{\rho}, A] &= \int d^3\mathbf{r}\sum_k n_k\varphi_k^\dagger(\mathbf{r})(\boldsymbol{\alpha}\cdot\mathbf{p} + \beta M)\varphi_k(\mathbf{r}) \\
&+ \int d^3\mathbf{r}\int d^3\mathbf{r}'\sum_k n_k\varphi_k^\dagger(\mathbf{r})\gamma^0\varphi_k(\mathbf{r})\frac{\alpha_S}{2}\delta(\mathbf{r}-\mathbf{r}')\sum_m n_m\varphi_m^\dagger(\mathbf{r}')\gamma^0\varphi_m(\mathbf{r}') \\
&+ \int d^3\mathbf{r}\int d^3\mathbf{r}'\sum_k n_k\varphi_k^\dagger(\mathbf{r})\gamma^0\gamma_\mu\varphi_k(\mathbf{r})\frac{\alpha_V}{2}\delta(\mathbf{r}-\mathbf{r}')\sum_m n_m\varphi_m^\dagger(\mathbf{r}')\gamma^0\gamma^\mu\varphi_m(\mathbf{r}') \\
&+ \int d^3\mathbf{r}\int d^3\mathbf{r}'\sum_k n_k\varphi_k^\dagger(\mathbf{r})\gamma^0\tau_3\varphi_k(\mathbf{r})\frac{\alpha_{TS}}{2}\delta(\mathbf{r}-\mathbf{r}')\sum_m n_m\varphi_m^\dagger(\mathbf{r}')\gamma^0\tau_3\varphi_m(\mathbf{r}') \\
&+ \int d^3\mathbf{r}\int d^3\mathbf{r}'\sum_k n_k\varphi_k^\dagger(\mathbf{r})\gamma^0\tau_3\gamma_\mu\varphi_k(\mathbf{r})\frac{\alpha_{TV}}{2}\delta(\mathbf{r}-\mathbf{r}') \\
&\times \sum_m n_m\varphi_m^\dagger(\mathbf{r}')\gamma^0\tau_3\gamma^\mu\varphi_m(\mathbf{r}') \\
&+ \frac{1}{3}\beta_S\int d^3\mathbf{r}\int d^3\mathbf{r}'\int d^3\mathbf{r}''\sum_k n_k\varphi_k^\dagger(\mathbf{r})\gamma^0\varphi_k(\mathbf{r})\delta(\mathbf{r}-\mathbf{r}') \\
&\times \sum_m n_m\varphi_m^\dagger(\mathbf{r}')\gamma^0\varphi_m(\mathbf{r}')\delta(\mathbf{r}'-\mathbf{r}'')\sum_p n_p\varphi_p^\dagger(\mathbf{r}'')\gamma^0\varphi_p(\mathbf{r}'') \\
&+ \frac{1}{4}\gamma_S\int d^3\mathbf{r}\int d^3\mathbf{r}'\int d^3\mathbf{r}''\int d^3\mathbf{r}'''\sum_k n_k\varphi_k^\dagger(\mathbf{r})\gamma^0\varphi_k(\mathbf{r})\delta(\mathbf{r}-\mathbf{r}') \\
&\times \sum_m n_m\varphi_m^\dagger(\mathbf{r}')\gamma^0\varphi_m(\mathbf{r}')\delta(\mathbf{r}'-\mathbf{r}'')\sum_p n_p\varphi_p^\dagger(\mathbf{r}'')\gamma^0\varphi_p(\mathbf{r}'')\delta(\mathbf{r}''-\mathbf{r}''') \\
&\times \sum_s n_s\varphi_s^\dagger(\mathbf{r}''')\gamma^0\varphi_s(\mathbf{r}''')
\end{aligned}$$

$$
\begin{aligned}
&+ \frac{1}{4}\gamma_V \int d^3\mathbf{r} \int d^3\mathbf{r}' \int d^3\mathbf{r}'' \int d^3\mathbf{r}''' \sum_k n_k \varphi_k^\dagger(\mathbf{r})\gamma^0\gamma_\mu\varphi_k(\mathbf{r})\delta(\mathbf{r}-\mathbf{r}') \\
&\times \sum_m n_m \varphi_m^\dagger(\mathbf{r}')\gamma^0\gamma^\mu\varphi_m(\mathbf{r}')\delta(\mathbf{r}'-\mathbf{r}'') \sum_p n_p \varphi_p^\dagger(\mathbf{r}'')\gamma^0\gamma_\alpha\psi_p(\mathbf{r}'')\delta(\mathbf{r}''-\mathbf{r}''') \\
&\times \sum_s n_s \varphi_s^\dagger(\mathbf{r}''')\gamma^0\gamma^\alpha\varphi_s(\mathbf{r}''') \\
&+ \int d^3\mathbf{r} \int d^3\mathbf{r}' \sum_k n_k \overline{\varphi}_k(\mathbf{r})\varphi_k(\mathbf{r})\frac{1}{2}\delta_S\nabla^2\delta(\mathbf{r}-\mathbf{r}') \sum_m n_m \overline{\varphi}_m(\mathbf{r}')\varphi_m(\mathbf{r}') \\
&+ \int d^3\mathbf{r} \int d^3\mathbf{r}' \sum_k n_k \overline{\varphi}_k(\mathbf{r})\gamma_\mu\varphi_k(\mathbf{r})\frac{1}{2}\delta_V\nabla^2\delta(\mathbf{r}-\mathbf{r}') \sum_m n_m \overline{\varphi}_m(\mathbf{r}')\gamma^\mu\varphi_m(\mathbf{r}') \\
&+ \int d^3\mathbf{r} \int d^3\mathbf{r}' \sum_k n_k \overline{\varphi}_k(\mathbf{r})\tau_3\varphi_k(\mathbf{r})\frac{1}{2}\delta_{TS}\nabla^2\delta(\mathbf{r}-\mathbf{r}') \sum_m n_m \overline{\varphi}_m(\mathbf{r}')\tau_3\varphi_m(\mathbf{r}') \\
&+ \int d^3\mathbf{r} \int d^3\mathbf{r}' \sum_k n_k \overline{\varphi}_k(\mathbf{r})\tau_3\gamma_\mu\varphi_k(\mathbf{r})\frac{1}{2}\delta_{TV}\nabla^2\delta(\mathbf{r}-\mathbf{r}') \\
&\times \sum_m n_m \overline{\varphi}_m(\mathbf{r}')\tau_3\gamma^\mu\varphi_m(\mathbf{r}') + \int d^3\mathbf{r} \sum_k n_k \varphi_k^\dagger(\mathbf{r})\gamma^0\frac{1}{2}(1+\tau_3)e\gamma^0 A_0(\mathbf{r})\varphi_k(\mathbf{r}) \\
&- \frac{1}{2}\int d^3\mathbf{r}(\boldsymbol{\nabla}A^0)\cdot(\boldsymbol{\nabla}A_0). \qquad \text{(D.54)}
\end{aligned}
$$

The zeroth component $A^0(\mathbf{r})$ of electromagnetic field satisfies the Poison equation

$$
-\nabla^2 A^0(\mathbf{r}) = e\rho_c(\mathbf{r}), \qquad \text{(D.55)}
$$

where the electric charge density $\rho_c(\mathbf{r})$ is

$$
\rho_c(\mathbf{r}) = \sum_k n_k \varphi_k^\dagger(\mathbf{r})\frac{1}{2}(1+\tau_3)\varphi_k(\mathbf{r}) \qquad \text{(D.56)}
$$

and its solution is given by

$$
A^0(\mathbf{r}) = \frac{e}{4\pi}\int d^3\mathbf{r}'\frac{\rho_c(\mathbf{r}')}{|\mathbf{r}-\mathbf{r}'|}. \qquad \text{(D.57)}
$$

Accordingly, the last integral on Eq. (D.54) can be expressed as

$$
\begin{aligned}
-\frac{1}{2}\int d^3\mathbf{r}(\boldsymbol{\nabla}A^0)\cdot(\boldsymbol{\nabla}A_0) &= \underbrace{-\frac{1}{2}\int d^3\mathbf{r}\boldsymbol{\nabla}\cdot[A^0\boldsymbol{\nabla}A_0]}_{=0} + \frac{1}{2}\int d^3\mathbf{r}A^0\nabla^2 A_0 \\
&= -\frac{1}{2}\int d^3\mathbf{r}A^0 e\rho_c(\mathbf{r}) \\
&= -\frac{1}{2}\int d^3\mathbf{r}\int d^3\mathbf{r}'\rho_c(\mathbf{r}')\frac{e^2}{4\pi}\frac{1}{|\mathbf{r}-\mathbf{r}'|}\rho_c(\mathbf{r})
\end{aligned}
$$

$$
\begin{aligned}
&= -\frac{1}{2}\int d^3\mathbf{r}\int d^3\mathbf{r}'\sum_k n_k\varphi_k^\dagger(\mathbf{r})\frac{1}{2}(1+\tau_3)\varphi_k(\mathbf{r}) \\
&\times \frac{e^2}{4\pi}\frac{1}{|\mathbf{r}-\mathbf{r}'|}\sum_m n_m\varphi_m^\dagger(\mathbf{r}')\frac{1}{2}(1+\tau_3)\varphi_m(\mathbf{r}'). \qquad \text{(D.58)}
\end{aligned}
$$

The insertion of Eqs. (D.57) and (D.58) on Eq. (D.54) leads to

$$
\begin{aligned}
E_{\rm RMF}[\hat{\rho},A] &= \int d^3\mathbf{r}\sum_k n_k\varphi_k^\dagger(\mathbf{r})(\boldsymbol{\alpha}\cdot\mathbf{p}+\beta M)\varphi_k(\mathbf{r}) \\
&+ \int d^3\mathbf{r}\int d^3\mathbf{r}'\sum_k n_k\varphi_k^\dagger(\mathbf{r})\gamma^0\varphi_k(\mathbf{r})\frac{\alpha_S}{2}\delta(\mathbf{r}-\mathbf{r}')\sum_m n_m\varphi_m^\dagger(\mathbf{r}')\gamma^0\varphi_m(\mathbf{r}') \\
&+ \int d^3\mathbf{r}\int d^3\mathbf{r}'\sum_k n_k\varphi_k^\dagger(\mathbf{r})\gamma^0\gamma_\mu\varphi_k(\mathbf{r})\frac{\alpha_V}{2}\delta(\mathbf{r}-\mathbf{r}')\sum_m n_m\varphi_m^\dagger(\mathbf{r}')\gamma^0\gamma^\mu\varphi_m(\mathbf{r}') \\
&+ \int d^3\mathbf{r}\int d^3\mathbf{r}'\sum_k n_k\varphi_k^\dagger(\mathbf{r})\gamma^0\tau_3\varphi_k(\mathbf{r})\frac{\alpha_{TS}}{2}\delta(\mathbf{r}-\mathbf{r}')\sum_m n_m\varphi_m^\dagger(\mathbf{r}')\gamma^0\tau_3\varphi_m(\mathbf{r}') \\
&+ \int d^3\mathbf{r}\int d^3\mathbf{r}'\sum_k n_k\varphi_k^\dagger(\mathbf{r})\gamma^0\tau_3\gamma_\mu\varphi_k(\mathbf{r})\frac{\alpha_{TV}}{2}\delta(\mathbf{r}-\mathbf{r}') \\
&\times \sum_m n_m\varphi_m^\dagger(\mathbf{r}')\gamma^0\tau_3\gamma^\mu\varphi_m(\mathbf{r}') \\
&+ \frac{1}{3}\beta_S\int d^3\mathbf{r}\int d^3\mathbf{r}'\int d^3\mathbf{r}''\sum_k n_k\varphi_k^\dagger(\mathbf{r})\gamma^0\varphi_k(\mathbf{r})\delta(\mathbf{r}-\mathbf{r}') \\
&\times \sum_m n_m\varphi_m^\dagger(\mathbf{r}')\gamma^0\varphi_m(\mathbf{r}')\delta(\mathbf{r}'-\mathbf{r}'')\sum_p n_p\varphi_p^\dagger(\mathbf{r}'')\gamma^0\varphi_p(\mathbf{r}'') \\
&+ \frac{1}{4}\gamma_S\int d^3\mathbf{r}\int d^3\mathbf{r}'\int d^3\mathbf{r}''\int d^3\mathbf{r}'''\sum_k n_k\varphi_k^\dagger(\mathbf{r})\gamma^0\varphi_k(\mathbf{r})\delta(\mathbf{r}-\mathbf{r}') \\
&\times \sum_m n_m\varphi_m^\dagger(\mathbf{r}')\gamma^0\varphi_m(\mathbf{r}')\delta(\mathbf{r}'-\mathbf{r}'')\sum_p n_p\varphi_p^\dagger(\mathbf{r}'')\gamma^0\varphi_p(\mathbf{r}'')\delta(\mathbf{r}''-\mathbf{r}''') \\
&\times \sum_s n_s\varphi_s^\dagger(\mathbf{r}''')\gamma^0\varphi_s(\mathbf{r}''') \\
&+ \frac{1}{4}\gamma_V\int d^3\mathbf{r}\int d^3\mathbf{r}'\int d^3\mathbf{r}''\int d^3\mathbf{r}'''\sum_k n_k\varphi_k^\dagger(\mathbf{r})\gamma^0\gamma_\mu\varphi_k(\mathbf{r})\delta(\mathbf{r}-\mathbf{r}') \\
&\times \sum_m n_m\varphi_m^\dagger(\mathbf{r}')\gamma^0\gamma^\mu\varphi_m(\mathbf{r}')\delta(\mathbf{r}'-\mathbf{r}'')\sum_p n_p\varphi_p^\dagger(\mathbf{r}'')\gamma^0\gamma_\alpha\psi_p(\mathbf{r}'')\delta(\mathbf{r}''-\mathbf{r}''') \\
&\times \sum_s n_s\varphi_s^\dagger(\mathbf{r}''')\gamma^0\gamma^\alpha\varphi_s(\mathbf{r}''') \\
&+ \int d^3\mathbf{r}\int d^3\mathbf{r}'\sum_k n_k\overline{\varphi}_k(\mathbf{r})\varphi_k(\mathbf{r})\frac{1}{2}\delta_S\nabla^2\delta(\mathbf{r}-\mathbf{r}')\sum_m n_m\overline{\varphi}_m(\mathbf{r}')\varphi_m(\mathbf{r}')
\end{aligned}
$$

$$
\begin{aligned}
&+ \int d^3\mathbf{r} \int d^3\mathbf{r}' \sum_k n_k \overline{\varphi}_k(\mathbf{r}) \gamma_\mu \varphi_k(\mathbf{r}) \frac{1}{2} \delta_V \nabla^2 \delta(\mathbf{r}-\mathbf{r}') \sum_m n_m \overline{\varphi}_m(\mathbf{r}') \gamma^\mu \varphi_m(\mathbf{r}') \\
&+ \int d^3\mathbf{r} \int d^3\mathbf{r}' \sum_k n_k \overline{\varphi}_k(\mathbf{r}) \tau_3 \varphi_k(\mathbf{r}) \frac{1}{2} \delta_{TS} \nabla^2 \delta(\mathbf{r}-\mathbf{r}') \sum_m n_m \overline{\varphi}_m(\mathbf{r}') \tau_3 \varphi_m(\mathbf{r}') \\
&+ \int d^3\mathbf{r} \int d^3\mathbf{r}' \sum_k n_k \overline{\varphi}_k(\mathbf{r}) \tau_3 \gamma_\mu \varphi_k(\mathbf{r}) \frac{1}{2} \delta_{TV} \nabla^2 \delta(\mathbf{r}-\mathbf{r}') \\
&\times \sum_m n_m \overline{\varphi}_m(\mathbf{r}') \tau_3 \gamma^\mu \varphi_m(\mathbf{r}') + \frac{1}{2} \int d^3\mathbf{r} \int d^3\mathbf{r}' \sum_k n_k \varphi_k^\dagger(\mathbf{r}) \frac{1}{2}(1+\tau_3) \varphi_k(\mathbf{r}) \\
&\times \frac{e^2}{4\pi} \frac{1}{|\mathbf{r}-\mathbf{r}'|} \sum_m n_m \varphi_m^\dagger(\mathbf{r}') \frac{1}{2}(1+\tau_3) \varphi_m(\mathbf{r}'). \qquad \text{(D.59)}
\end{aligned}
$$

Let us define $\mathrm{Tr}[\hat{\mathscr{O}}\hat{\rho}(\mathbf{r})]$ as

$$
\mathrm{Tr}[\hat{\mathscr{O}}\hat{\rho}(\mathbf{r})] = \sum_k n_k \varphi_k^\dagger(\mathbf{r}) \hat{\mathscr{O}} \varphi_k(\mathbf{r}) \qquad \text{(D.60)}
$$

and its first functional derivative with respect to $\hat{\rho}(\mathbf{r})$ as

$$
\frac{\delta}{\delta \hat{\rho}(\mathbf{r}')} \mathrm{Tr}[\hat{\mathscr{O}}\hat{\rho}(\mathbf{r})] = \hat{\mathscr{O}} \delta(\mathbf{r}-\mathbf{r}'). \qquad \text{(D.61)}
$$

Using these definitions, the first functional derivative of E_{RMF} with respect to $\hat{\rho}(\mathbf{r})$ reads

$$
\begin{aligned}
\frac{\delta E_{\mathrm{RMF}}}{\delta \hat{\rho}(\mathbf{r}_1)} &= (\boldsymbol{\alpha}\cdot\mathbf{p} + \beta M)^{(1)} + \alpha_S \int d^3\mathbf{r} \gamma^{0(1)} \delta(\mathbf{r}_1-\mathbf{r}) \,\mathrm{Tr}[\gamma^0 \hat{\rho}(\mathbf{r})] \\
&+ \alpha_V \int d^3\mathbf{r} \gamma^{0(1)} \gamma_\mu^{(1)} \delta(\mathbf{r}_1-\mathbf{r}) \,\mathrm{Tr}[\gamma^0 \gamma^\mu \rho(\mathbf{r})] \\
&+ \alpha_{TS} \int d^3\mathbf{r} \gamma^{0(1)} \tau_3^{(1)} \delta(\mathbf{r}_1-\mathbf{r}) \,\mathrm{Tr}[\gamma^0 \tau_3 \hat{\rho}(\mathbf{r})] \\
&+ \alpha_{TV} \int d^3\mathbf{r} \gamma^{0(1)} \tau_3^{(1)} \gamma_\mu^{(1)} \delta(\mathbf{r}_1-\mathbf{r}) \,\mathrm{Tr}[\gamma^0 \tau_3 \gamma^\mu \hat{\rho}(\mathbf{r})] \\
&+ \beta_S \int d^3\mathbf{r} \int d^3\mathbf{r}' \gamma^{0(1)} \delta(\mathbf{r}_1-\mathbf{r}) \,\mathrm{Tr}[\gamma^0 \hat{\rho}(\mathbf{r})] \delta(\mathbf{r}-\mathbf{r}') \,\mathrm{Tr}[\gamma^0 \hat{\rho}(\mathbf{r}')] \\
&+ \gamma_S \int d^3\mathbf{r} \int d^3\mathbf{r}' \int d^3\mathbf{r}'' \gamma^{0(1)} \delta(\mathbf{r}_1-\mathbf{r}) \,\mathrm{Tr}[\gamma^0 \hat{\rho}(\mathbf{r})] \\
&\times \delta(\mathbf{r}-\mathbf{r}') \,\mathrm{Tr}[\gamma^0 \hat{\rho}(\mathbf{r}')] \delta(\mathbf{r}'-\mathbf{r}'') \,\mathrm{Tr}[\gamma^0 \hat{\rho}(\mathbf{r}'')] \\
&+ \gamma_V \int d^3\mathbf{r} \int d^3\mathbf{r}' \int d^3\mathbf{r}'' \gamma^{0(1)} \gamma_\mu^{(1)} \delta(\mathbf{r}_1-\mathbf{r}) \,\mathrm{Tr}[\gamma^0 \gamma^\mu \hat{\rho}(\mathbf{r})] \\
&\times \delta(\mathbf{r}-\mathbf{r}') \,\mathrm{Tr}[\gamma^0 \gamma_\alpha \hat{\rho}(\mathbf{r}')] \delta(\mathbf{r}'-\mathbf{r}'') \,\mathrm{Tr}[\gamma^0 \gamma^\alpha \hat{\rho}(\mathbf{r}'')] \\
&+ \int d^3\mathbf{r} \gamma^{0(1)} \frac{1}{2} \delta_S \nabla^2 \delta(\mathbf{r}_1-\mathbf{r}) \,\mathrm{Tr}[\gamma^0 \hat{\rho}(\mathbf{r})]
\end{aligned}
$$

$$
\begin{aligned}
&+ \int d^3\mathbf{r}\,\mathrm{Tr}[\gamma^0\hat{\rho}(\mathbf{r})]\frac{1}{2}\delta_S\nabla^2\delta(\mathbf{r}-\mathbf{r}_1)\gamma^{0(1)} \\
&+ \int d^3\mathbf{r}\gamma^{0(1)}\gamma_\mu^{(1)}\frac{1}{2}\delta_V\nabla^2\delta(\mathbf{r}_1-\mathbf{r})\,\mathrm{Tr}[\gamma^0\gamma^\mu\hat{\rho}(\mathbf{r})] \\
&+ \int d^3\mathbf{r}\,\mathrm{Tr}[\gamma^0\gamma_\mu\hat{\rho}(\mathbf{r})]\frac{1}{2}\delta_V\nabla^2\delta(\mathbf{r}-\mathbf{r}_1)\gamma^{0(1)}\gamma^{\mu(1)} \\
&+ \int d^3\mathbf{r}\gamma^{0(1)}\tau_3^{(1)}\frac{1}{2}\delta_{TS}\nabla^2\delta(\mathbf{r}_1-\mathbf{r})\,\mathrm{Tr}[\gamma^0\tau_3\hat{\rho}(\mathbf{r})] \\
&+ \int d^3\mathbf{r}\,\mathrm{Tr}[\gamma^0\tau_3\hat{\rho}(\mathbf{r})]\frac{1}{2}\delta_{TS}\nabla^2\delta(\mathbf{r}-\mathbf{r}_1)\gamma^{0(1)}\tau_3^{(1)} \\
&+ \int d^3\mathbf{r}\gamma^{0(1)}\tau_3^{(1)}\gamma_\mu^{(1)}\frac{1}{2}\delta_{TV}\nabla^2\delta(\mathbf{r}_1-\mathbf{r})\,\mathrm{Tr}[\gamma^0\tau_3\gamma^\mu\hat{\rho}(\mathbf{r})] \\
&+ \int d^3\mathbf{r}\,\mathrm{Tr}[\gamma^0\tau_3\gamma_\mu\hat{\rho}(\mathbf{r})]\frac{1}{2}\delta_{TV}\nabla^2\delta(\mathbf{r}-\mathbf{r}_1)\gamma^{0(1)}\tau_3^{(1)}\gamma^{\mu(1)} \\
&+ \frac{1}{2}\int d^3\mathbf{r}\left[\frac{1}{2}(1+\tau_3)\right]^{(1)}\frac{e^2}{4\pi}\frac{1}{|\mathbf{r}_1-\mathbf{r}|}\,\mathrm{Tr}\left[\frac{1}{2}(1+\tau_3)\hat{\rho}(\mathbf{r})\right] \\
&+ \frac{1}{2}\int d^3\mathbf{r}\,\mathrm{Tr}\left[\frac{1}{2}(1+\tau_3)\hat{\rho}(\mathbf{r})\right]\frac{e^2}{4\pi}\frac{1}{|\mathbf{r}-\mathbf{r}_1|}\left[\frac{1}{2}(1+\tau_3)\right]^{(1)}. \qquad \text{(D.62)}
\end{aligned}
$$

The second functional derivative of $E_{\mathrm{RMF}}[\hat{\rho},A]$ with respect to $\hat{\rho}(\mathbf{r})$ gives the particle-hole interaction:

$$
\begin{aligned}
V^{\mathrm{ph}}(1,2) &= \frac{\delta^2 E_{\mathrm{RMF}}}{\delta\hat{\rho}(\mathbf{r}_1)\delta\hat{\rho}(\mathbf{r}_2)} \\
&= \gamma^{0(1)}[\alpha_S+2\beta_S\rho_S(\mathbf{r}_1)+3\gamma_S\rho_S^2(\mathbf{r}_1)+\delta_S\nabla^2]\delta(\mathbf{r}_1-\mathbf{r}_2)\gamma^{0(2)} \\
&+ [\gamma^{0(1)}\gamma^{0(1)}][\alpha_V+3\gamma_V\rho_V^2(\mathbf{r}_1)+\delta_V\nabla^2]\delta(\mathbf{r}_1-\mathbf{r}_2)[\gamma^{0(2)}\gamma^{0(2)}] \\
&+ [\gamma^{0(1)}\gamma_i^{(1)}][\alpha_V+3\gamma_V\rho_V^2(\mathbf{r}_1)+\delta_V\nabla^2]\delta(\mathbf{r}_1-\mathbf{r}_2)[\gamma^{0(2)}\gamma^{i(2)}] \\
&+ [\gamma^{0(1)}\otimes\tau_3^{(1)}][\alpha_{TS}+\delta_{TS}\nabla^2]\delta(\mathbf{r}_1-\mathbf{r}_2)[\gamma^{0(2)}\otimes\tau_3^{(2)}] \\
&+ [\gamma^{0(1)}\otimes\tau_3^{(1)}\gamma^{0(1)}][\alpha_{TV}+\delta_{TV}\nabla^2]\delta(\mathbf{r}_1-\mathbf{r}_2)[\gamma^{0(2)}\otimes\tau_3^{(2)}\gamma^{0(2)}] \\
&+ [\gamma^{0(1)}\otimes\tau_3^{(1)}\gamma_i^{(1)}][\alpha_{TV}+\delta_{TV}\nabla^2]\delta(\mathbf{r}_1-\mathbf{r}_2)[\gamma^{0(2)}\otimes\tau_3(2)\gamma^{i(2)}] \\
&+ \left[\frac{1}{2}(1+\tau_3)\right]^{(1)}\frac{e^2}{4\pi}\frac{1}{|\mathbf{r}_1-\mathbf{r}_2|}\left[\frac{1}{2}(1+\tau_3)\right]^{(2)}. \qquad \text{(D.63)}
\end{aligned}
$$

Since

$$
\gamma^0\gamma^0 = \begin{pmatrix}\mathbf{1}&\mathbf{0}\\ \mathbf{0}&-\mathbf{1}\end{pmatrix}\begin{pmatrix}\mathbf{1}&\mathbf{0}\\ \mathbf{0}&-\mathbf{1}\end{pmatrix} = \begin{pmatrix}\mathbf{1}&\mathbf{0}\\ \mathbf{0}&\mathbf{1}\end{pmatrix} = \mathbf{1}\otimes\mathbf{1}, \qquad \text{(D.64)}
$$

$$
\gamma^0\gamma_i = \begin{pmatrix}\mathbf{1}&\mathbf{0}\\ \mathbf{0}&-\mathbf{1}\end{pmatrix}\begin{pmatrix}\mathbf{0}&\sigma_i\\ -\sigma_i&\mathbf{0}\end{pmatrix} = \begin{pmatrix}\mathbf{0}&\sigma_i\\ \sigma_i&\mathbf{0}\end{pmatrix} = \gamma_5\otimes\sigma_i, \qquad \text{(D.65)}
$$

$$\gamma^0\gamma^i = \begin{pmatrix} \mathbf{1} & \mathbf{0} \\ \mathbf{0} & -\mathbf{1} \end{pmatrix} \begin{pmatrix} \mathbf{0} & -\sigma_i \\ \sigma_i & \mathbf{0} \end{pmatrix} = \begin{pmatrix} \mathbf{0} & -\sigma_i \\ -\sigma_i & \mathbf{0} \end{pmatrix} = -\gamma_5 \otimes \sigma_i, \tag{D.66}$$

the particle-hole interaction $V^{\rm ph}(1,2)$ then becomes

$$\begin{aligned} V^{\rm ph}(1,2) &= \{\gamma^0 \otimes \mathbf{1} \otimes \mathbf{1}\}^{(1)}[\alpha_S + 2\beta_S\rho_S(\mathbf{r}_1) + 3\gamma_S\rho_S^2(\mathbf{r}_1) + \delta_S\nabla^2]\delta(\mathbf{r}_1 - \mathbf{r}_2) \\ &\times \{\gamma^0 \otimes \mathbf{1} \otimes \mathbf{1}\}^{(2)} \\ &+ \{\mathbf{1} \otimes \mathbf{1} \otimes \mathbf{1}\}^{(1)}[\alpha_V + 3\gamma_V\rho_V^2(\mathbf{r}_1) + \delta_V\nabla^2]\delta(\mathbf{r}_1 - \mathbf{r}_2)\{\mathbf{1} \otimes \mathbf{1} \otimes \mathbf{1}\}^{(2)} \\ &- \{\gamma_5 \otimes \sigma_i \otimes \mathbf{1}\}^{(1)}[\alpha_V + 3\gamma_V\rho_V^2(\mathbf{r}_1) + \delta_V\nabla^2]\delta(\mathbf{r}_1 - \mathbf{r}_2)\{\gamma_5 \otimes \sigma_i \otimes \mathbf{1}\}^{(2)} \\ &+ \{\gamma^0 \otimes \mathbf{1} \otimes \tau_3\}^{(1)}[\alpha_{TS} + \delta_{TS}\nabla^2]\delta(\mathbf{r}_1 - \mathbf{r}_2)\{\gamma^0 \otimes \mathbf{1} \otimes \tau_3\}^{(2)} \\ &+ \{\mathbf{1} \otimes \mathbf{1} \otimes \tau_3\}^{(1)}[\alpha_{TV} + \delta_{TV}\nabla^2]\delta(\mathbf{r}_1 - \mathbf{r}_2)\{\mathbf{1} \otimes \mathbf{1} \otimes \tau_3\}^{(2)} \\ &- \{\gamma_5 \otimes \sigma_i \otimes \tau_3\}^{(1)}[\alpha_{TV} + \delta_{TV}\nabla^2]\delta(\mathbf{r}_1 - \mathbf{r}_2)\{\gamma_5 \otimes \sigma_i \otimes \tau_3\}^{(2)} \\ &+ \left[\frac{1}{2}(1+\tau_3)\right]^{(1)} \frac{e^2}{4\pi}\frac{1}{|\mathbf{r}_1 - \mathbf{r}_2|}\left[\frac{1}{2}(1+\tau_3)\right]^{(2)}. \end{aligned} \tag{D.67}$$

The scalar product between two Pauli matrices, viz.

$$\sigma_i^{(1)}\sigma_i^{(2)} \equiv \sum_{i=x,y,z} \sigma_i^{(1)}\sigma_i^{(2)}, \tag{D.68}$$

can be expressed in terms of the spherical Pauli matrices σ_{SM_S}, i.e.,

$$\sigma_{00} = \mathbf{1}, \quad \sigma_{1(+1)} = -\frac{1}{\sqrt{2}}[\sigma_x + i\sigma_y], \quad \sigma_{10} = \sigma_z, \quad \sigma_{1(-1)} = \frac{1}{\sqrt{2}}[\sigma_x - i\sigma_y], \tag{D.69}$$

as

$$\sigma_i^{(1)}\sigma_i^{(2)} = \sum_{M_S}(-1)^{M_S}\sigma_{1M_S}^{(1)}\sigma_{1(-M_S)}^{(2)}. \tag{D.70}$$

Using the definition of the spherical Pauli matrices, we can rewrite the particle-hole interaction $V^{\rm ph}(1,2)$ as

$$\begin{aligned} V^{\rm ph}(1,2) &= \{\gamma^0 \otimes \sigma_{00} \otimes \mathbf{1}\}^{(1)}[\alpha_S + 2\beta_S\rho_S(\mathbf{r}_1) + 3\gamma_S\rho_S^2(\mathbf{r}_1) + \delta_S\nabla^2]\delta(\mathbf{r}_1 - \mathbf{r}_2) \\ &\times \{\gamma^0 \otimes \sigma_{00} \otimes \mathbf{1}\}^{(2)} \\ &+ \{\mathbf{1} \otimes \sigma_{00} \otimes \mathbf{1}\}^{(1)}[\alpha_V + 3\gamma_V\rho_V^2(\mathbf{r}_1) + \delta_V\nabla^2]\delta(\mathbf{r}_1 - \mathbf{r}_2)\{\mathbf{1} \otimes \sigma_{00} \otimes \mathbf{1}\}^{(2)} \\ &- \sum_{M_S}(-1)^{M_S}\{\gamma_5 \otimes \sigma_{1M_S} \otimes \mathbf{1}\}^{(1)}[\alpha_V + 3\gamma_V\rho_V^2(\mathbf{r}_1) + \delta_V\nabla^2]\delta(\mathbf{r}_1 - \mathbf{r}_2) \\ &\times \{\gamma_5 \otimes \sigma_{1(-M_S)} \otimes \mathbf{1}\}^{(2)} \\ &+ \{\gamma^0 \otimes \sigma_{00} \otimes \tau_3\}^{(1)}[\alpha_{TS} + \delta_{TS}\nabla^2]\delta(\mathbf{r}_1 - \mathbf{r}_2)\{\gamma^0 \otimes \sigma_{00} \otimes \tau_3\}^{(2)} \end{aligned}$$

$$
\begin{aligned}
&+ \quad \{\mathbf{1}\otimes\sigma_{00}\otimes\tau_3\}^{(1)}[\alpha_{TV}+\delta_{TV}\nabla^2]\delta(\mathbf{r}_1-\mathbf{r}_2)\{\mathbf{1}\otimes\sigma_{00}\otimes\tau_3\}^{(2)} \\
&- \quad \sum_{M_S}(-1)^{M_S}\{\gamma_5\otimes\sigma_{1M_S}\otimes\tau_3\}^{(1)}[\alpha_{TV}+\delta_{TV}\nabla^2]\delta(\mathbf{r}_1-\mathbf{r}_2) \\
&\times \quad \{\gamma_5\otimes\sigma_{1(-M_S)}\otimes\tau_3\}^{(2)}+\left[\frac{1}{2}(1+\tau_3)\right]^{(1)}\frac{e^2}{4\pi}\frac{1}{|\mathbf{r}_1-\mathbf{r}_2|}\left[\frac{1}{2}(1+\tau_3)\right]^{(2)}
\end{aligned}
\tag{D.71}
$$

The expansion of Dirac delta function

$$
\delta(\mathbf{r}_1-\mathbf{r}_2)=\frac{\delta(r_1-r_2)}{r_1r_2}\sum_{LM_L}Y_{LM_L}(\Omega_1)Y^*_{LM_L}(\Omega_2) \tag{D.72}
$$

results in the term

$$
\sum_{M_S}\sum_{LM_L}(-1)^{M_S}\sigma^{(1)}_{SM_S}Y^{(1)}_{LM_L}\cdot\sigma^{(2)}_{S(-M_S)}Y^{*(2)}_{LM_L} \tag{D.73}
$$

for $S=0$ and $S=1$. This term can be expressed in terms of the coupling between spherical spin and harmonics,

$$
[\sigma_S Y_L]_{JM}=\sum_{M_LM_S}\langle LM_LSM_S|JM\rangle Y_{LM_L}\sigma_{SM_S}, \tag{D.74}
$$

as

$$
\sum_{M_S}\sum_{LM_L}(-1)^{M_S}\sigma^{(1)}_{SM_S}Y^{(1)}_{LM_L}\cdot\sigma^{(2)}_{S(-M_S)}Y^{*(2)}_{LM_L}=\sum_{LJM}[\sigma_SY_L]^{(1)}_{JM}[\sigma_SY_L]^{\dagger(2)}_{JM}. \tag{D.75}
$$

The particle-hole interaction $V^{\rm ph}(1,2)$ now becomes

$$
\begin{aligned}
V^{\rm ph}(1,2) \quad = \quad & \frac{\delta(r_1-r_2)}{r_1r_2}\sum_{LJM}\{\gamma^0\otimes[\sigma_0Y_L]_{JM}\otimes\mathbf{1}\}^{(1)}[\alpha_S+2\beta_S\rho_S(\mathbf{r}_1)+3\gamma_S\rho_S^2(\mathbf{r}_1)+\delta_S\nabla^2] \\
\times \quad & \{\gamma^0\otimes[\sigma_0Y_L]_{JM}\otimes\mathbf{1}\}^{\dagger(2)} \\
+ \quad & \frac{\delta(r_1-r_2)}{r_1r_2}\sum_{LJM}\{\mathbf{1}\otimes[\sigma_0Y_L]_{JM}\otimes\mathbf{1}\}^{(1)}[\alpha_V+3\gamma_V\rho_V^2(\mathbf{r}_1)+\delta_V\nabla^2] \\
\times \quad & \{\mathbf{1}\otimes[\sigma_0Y_L]_{JM}\otimes\mathbf{1}\}^{\dagger(2)} \\
+ \quad & \frac{\delta(r_1-r_2)}{r_1r_2}\sum_{LJM}\{\gamma_5\otimes[\sigma_1Y_L]_{JM}\otimes\mathbf{1}\}^{(1)}[-\alpha_V-3\gamma_V\rho_V^2(\mathbf{r}_1)-\delta_V\nabla^2] \\
\times \quad & \{\gamma_5\otimes[\sigma_1Y_L]_{JM}\otimes\mathbf{1}\}^{\dagger(2)} \\
+ \quad & \frac{\delta(r_1-r_2)}{r_1r_2}\sum_{LJM}\{\gamma^0\otimes[\sigma_0Y_L]_{JM}\otimes\tau_3\}^{(1)}[\alpha_{TS}+\delta_{TS}\nabla^2]
\end{aligned}
$$

$$
\begin{aligned}
&\times \quad \{\gamma^0 \otimes [\sigma_0 Y_L]_{JM} \otimes \tau_3\}^{\dagger(2)} \\
&+ \quad \frac{\delta(r_1 - r_2)}{r_1 r_2} \sum_{LJM} \{\mathbf{1} \otimes [\sigma_0 Y_L]_{JM} \otimes \tau_3\}^{(1)} [\alpha_{TV} + \delta_{TV} \nabla^2] \\
&\times \quad \{\mathbf{1} \otimes [\sigma_0 Y_L]_{JM} \otimes \tau_3\}^{\dagger(2)} \\
&+ \quad \frac{\delta(r_1 - r_2)}{r_1 r_2} \sum_{LJM} \{\gamma_5 \otimes [\sigma_1 Y_L]_{JM} \otimes \tau_3\}^{(1)} [-\alpha_{TV} - \delta_{TV} \nabla^2] \\
&\times \quad \{\gamma_5 \otimes [\sigma_1 Y_L]_{JM} \otimes \tau_3\}^{\dagger(2)} + \left[\frac{1}{2}(1 + \tau_3)\right]^{(1)} \frac{e^2}{4\pi} \frac{1}{|\mathbf{r}_1 - \mathbf{r}_2|} \left[\frac{1}{2}(1 + \tau_3)\right]^{(2)} . \quad \text{(D.76)}
\end{aligned}
$$

For the case of spherical nuclei the total angular momentum $\mathbf{J} = \mathbf{L} + \mathbf{S}$ is a good quantum number. When $S = 0$, there is only a single value of $L = J$ for a specific value of J. On the other hand, there are three possible values of $L = J - 1, J, J + 1$ for $S = 1$. We assign $S = 0$ to a scalar and time-like vector and $S = 1$ to a space-like vector. Then the possible values of L for each value of S are

$$
L = \begin{cases} J, & \text{for } S = 0, \\ J \pm 1, & \text{for } S = 1. \end{cases} \quad \text{(D.77)}
$$

Together with two possible values of $T = 0, 1$, we end up with eight possible combinations (channels c) of quantum numbers $S,\ L,$ and T, which are listed in Table D.2.

Table D.2: The list of channels $c = (D,\ S,\ L,\ J,\ M, T)$.

c	D	S	L	T	$\gamma_D \otimes [\sigma_S Y_L]_{JM} \otimes \tau_{T0}$
1	S	0	J	0	$\gamma_0 \otimes [\sigma_0 Y_L]_{JM} \otimes \mathbf{1}$
2	V	0	J	0	$\mathbf{1} \otimes [\sigma_0 Y_L]_{JM} \otimes \mathbf{1}$
3	V	1	$J-1$	0	$\gamma_5 \otimes [\sigma_1 Y_L]_{JM} \otimes \mathbf{1}$
4	V	1	$J+1$	0	$\gamma_5 \otimes [\sigma_1 Y_L]_{JM} \otimes \mathbf{1}$
5	S	0	J	1	$\gamma_0 \otimes [\sigma_0 Y_L]_{JM} \otimes \tau_3$
6	V	0	J	1	$\mathbf{1} \otimes [\sigma_0 Y_L]_{JM} \otimes \tau_3$
7	V	1	$J-1$	1	$\gamma_5 \otimes [\sigma_1 Y_L]_{JM} \otimes \tau_3$
8	V	1	$J+1$	1	$\gamma_5 \otimes [\sigma_1 Y_L]_{JM} \otimes \tau_3$

Apart from the Coulomb interaction, the particle-hole interaction $V^{\rm ph}(1,2)$ takes the form:

$$
V^{\rm ph}(1,2) = \frac{\delta(r_1 - r_2)}{r_1 r_2} \sum_{cc'} \Gamma_c^{(1)} v_{cc'}(r_1) \Gamma_{c'}^{\dagger(2)} \quad \text{(no Coulomb term)}, \quad \text{(D.78)}
$$

where the vertices

$$
\Gamma_c = \gamma_D \otimes [\sigma_S Y_L]_{JM} \otimes \tau_{T0} \quad \text{(D.79)}
$$

consist of matrix γ_D of the types:

$$\gamma_0 = \begin{pmatrix} 1 & 0 \\ 0 & -1 \end{pmatrix}, \quad \mathbf{1} = \begin{pmatrix} 1 & 0 \\ 0 & 1 \end{pmatrix}, \quad \gamma_5 = \begin{pmatrix} 0 & 1 \\ 1 & 0 \end{pmatrix}, \tag{D.80}$$

the coupling $[\sigma_S Y_L]_{JM}$ between spin S and angular momentum L, and the isospin matrices τ_{T0} of the types:

$$\tau_{00} = \mathbf{1}, \quad \tau_{10} = \tau_3. \tag{D.81}$$

Using the identity

$$\int_0^\infty r^2 dr \frac{\delta(r-r_1)}{rr_1}\frac{\delta(r-r_2)}{rr_2} v_{cc'}(r) = \frac{\delta(r_1-r_2)}{r_1 r_2} v_{cc'}(r_1), \tag{D.82}$$

the particle-hole interaction (D.78) thus becomes

$$\begin{aligned} V^{\rm ph}(1,2) &= \int_0^\infty r^2 dr \sum_{cc'} \frac{\delta(r-r_1)}{rr_1}\Gamma_c^{(1)} v_{cc'}(r) \frac{\delta(r-r_2)}{rr_2}\Gamma_{c'}^{\dagger(2)} \\ &= \int_0^\infty r^2 dr \int_0^\infty r'^2 dr' \sum_{cc'} Q_c^{(1)}(r) v_{cc'}(r,r') Q_{c'}^{\dagger(2)}(r'), \end{aligned} \tag{D.83}$$

where $v_{cc'}(r,r') = v_c(r)\delta_{cc'}\delta(r-r')$ and the single-particle operator $Q_c^{(1)}(r)$ is defined as

$$Q_c^{(1)}(r) = \frac{\delta(r-r_1)}{rr_1}\Gamma_c^{(1)} = \frac{\delta(r-r_1)}{rr_1}\gamma_D^{(1)} \otimes [\sigma_S Y_L]_{JM}^{(1)} \otimes \tau_{T0}^{(1)}. \tag{D.84}$$

The effective interactions $v_c(r)$ are summarized in Table D.3 and the Laplacian operator ∇^2 takes the form:

$$\begin{aligned} \nabla^2 &= \frac{1}{r^2}\frac{\partial}{\partial r}\left\{r^2 \frac{\partial}{\partial r}\right\} - \frac{L(L+1)}{r^2} \\ &= -\frac{\overleftarrow{\partial}}{\partial r}\frac{\overrightarrow{\partial}}{\partial r} - \frac{L(L+1)}{r^2} \qquad \text{(D.85)} \\ &= -\frac{1}{r^2}\frac{\overleftarrow{\partial}}{\partial r} r^2 \frac{\overrightarrow{\partial}}{\partial r} - \frac{L(L+1)-2}{r^2}. \qquad \text{(D.86)} \end{aligned}$$

At this stage one can summarize the important results of this subsection as follows. Starting from the Lagrangian density $\mathscr{L}$ (Eq. (D.2)) with the nonlinear point-coupling interactions PC-F1 (see Table D.1), one can derive the time-independent Dirac equation for nucleon

$$\hat{h}^D \varphi_k(\mathbf{r}) = \epsilon_k \varphi_k(\mathbf{r}), \tag{D.87}$$

Table D.3: The effective interactions $v_c(r)$ for each channel.

Character	$v_c(r)$
Scalar	$\alpha_S + 2\beta_S\rho_S(r) + 3\gamma_S\rho_S^2(r) + \delta_S\nabla^2$
Timelike vector	$\alpha_V + 3\gamma_V\rho_V^2(r) + \delta_V\nabla^2$
Spacelike vector	$-\alpha_V - 3\gamma_V\rho_V^2(r) - \delta_V\nabla^2$
Isoscalar	$\alpha_{TS} + \delta_{TS}\nabla^2$
Timelike isovector	$\alpha_{TV} + \delta_{TV}\nabla^2$
Spacelike isovector	$-\alpha_{TV} - \delta_{TV}\nabla^2$

where the Dirac Hamiltonian $\hat{h}^D$ reads

$$\hat{h}^D = \boldsymbol{\alpha}\cdot\mathbf{p} + \beta[M + S(\mathbf{r})] + V(\mathbf{r}).$$

Here the scalar potential $S(\mathbf{r})$ and vector potential $V(\mathbf{r})$ are given by

$$S(\mathbf{r}) = \Sigma_S(\mathbf{r}) + \tau_3\Sigma_{TS}(\mathbf{r}), V(\mathbf{r}) = \Sigma_V(\mathbf{r}) + \tau_3\Sigma_{TV}(\mathbf{r}),$$

with the self-energies $\Sigma_i(\mathbf{r})$ $(i = S,\ V,\ TS,\ TV)$ are

$$\begin{aligned}
\Sigma_S(\mathbf{r}) &= \alpha_S\rho_S(\mathbf{r}) + \beta_S\rho_S^2(\mathbf{r}) + \gamma_S\rho_S^3(\mathbf{r}) + \delta_S\nabla^2\rho_S(\mathbf{r}),\\
\Sigma_{TS}(\mathbf{r}) &= (\alpha_{TS} + \delta_{TS}\nabla^2)\rho_{TS}(\mathbf{r}),\\
\Sigma_V(\mathbf{r}) &= \alpha_V\rho_V(\mathbf{r}) + \gamma_V\rho_V^3(\mathbf{r}) + \delta_V\nabla^2\rho_V(\mathbf{r}) + eA^0\tfrac{1}{2}(1+\tau_3),\\
\Sigma_{TV}(\mathbf{r}) &= (\alpha_{TV} + \delta_{TV}\nabla^2)\rho_{TV}(\mathbf{r}).
\end{aligned}$$

In obtaining the Dirac equation (D.87), one has made use of the mean-field approximation, and assumed the time-reversal symmetry of the mean field and the isospin τ_3 is a good quantum number. Together with the various densities $\rho_i(\mathbf{r})$ $(i = S,\ V,\ TS,\ TV)$:

$$\begin{aligned}
\rho_S(\mathbf{r}) &= \sum_k n_k\bar{\varphi}_k(\mathbf{r})\varphi_k(\mathbf{r}),\\
\rho_V(\mathbf{r}) &= \sum_k n_k\varphi_k^\dagger(\mathbf{r})\varphi_k(\mathbf{r}),\\
\rho_{TS}(\mathbf{r}) &= \sum_k n_k\bar{\varphi}_k(\mathbf{r})\tau_3\varphi_k(\mathbf{r}),\\
\rho_{TV}(\mathbf{r}) &= \sum_k n_k\bar{\varphi}_k(\mathbf{r})\tau_3\gamma^0\varphi_k(\mathbf{r}),
\end{aligned}$$

and the zeroth component $A^0(\mathbf{r})$ of electromagnetic field:

$$A^0(\mathbf{r}) = \frac{e}{4\pi}\int d^3\mathbf{r}'\frac{\rho_c(\mathbf{r}')}{|\mathbf{r}-\mathbf{r}'|}, \qquad \rho_c(\mathbf{r}) = \sum_k n_k \varphi_k^\dagger(\mathbf{r})\frac{1}{2}(1+\tau_3)\varphi_k(\mathbf{r}),$$

Dirac equation (D.87) can be solved in a self-consistent way to obtain the single-particle basis, which consists of the Dirac spinors $\varphi_k(\mathbf{r})$ and single-particle energies ϵ_k. Apart from the Coulomb interaction, the particle-hole interaction $V^{\rm ph}(1,2)$ has a multi-channel structure:

$$V^{\rm ph}(1,2) = \int_0^\infty r^2 dr \int_0^\infty r'^2 dr' \sum_{cc'} Q_c^{(1)}(r) v_{cc'}(r,r') Q_{c'}^{\dagger(2)}(r'),$$

where the single-particle operator $Q_c^{(1)}(r)$ is defined according to Eq. (D.84) and Table D.2. The interaction matrix elements $v_{cc'}(r,r')$ are diagonal in the channel and radial coordinate representations, i.e., $v_{cc'}(r,r') = v_c(r)\delta_{cc'}\delta(r-r')$, where the effective interactions $v_c(r)$ are given in Table D.3.

Appendix E

Time-reversal Transformation

The time-reversal operator $\hat{\mathcal{T}}$ is defined as [176]

$$\hat{\mathcal{T}} = \hat{\mathcal{U}}\hat{\mathcal{K}}, \tag{E.1}$$

where $\hat{\mathcal{K}}$ is a complex conjugate operator and $\hat{\mathcal{U}}$ is a unitary operator. The action of operator $\hat{\mathcal{T}}$ on a single-particle state $|jm\rangle$ with angular momentum quantum numbers (j, m) defines time-conjugate state $\overline{|jm\rangle}$ as

$$\overline{|jm\rangle} = \hat{\mathcal{T}}|jm\rangle = (-1)^{j-m}|j-m\rangle. \tag{E.2}$$

We summarize the properties of operator $\hat{\mathcal{T}}$ as follows:

A. The time-reversal operator $\hat{\mathcal{T}}$ is an anti-linear operator since the inner product of two time-conjugate states satisfies:

$$\langle\bar{\mu}|\bar{\nu}\rangle = \langle^*\mu|\underbrace{\hat{\mathcal{U}}^\dagger\hat{\mathcal{U}}}_{=1}|\nu^*\rangle = \langle^*\mu|\nu^*\rangle = \langle\mu|\nu\rangle^* = \langle\nu|\mu\rangle. \tag{E.3}$$

B. The Hermitian conjugate of operator $\hat{\mathcal{T}}$ is its own inverse:

$$\hat{\mathcal{T}}^\dagger\hat{\mathcal{T}} = \hat{\mathcal{K}}\hat{\mathcal{U}}^\dagger\hat{\mathcal{U}}\hat{\mathcal{K}} = \hat{\mathcal{K}}\hat{\mathcal{K}} = 1 \quad \text{or} \quad \hat{\mathcal{T}}^\dagger = \hat{\mathcal{T}}^{-1}. \tag{E.4}$$

C. For fermions (with half-integer j), operator $\hat{\mathcal{T}}$ satisfies:

$$\hat{\mathcal{T}}^2|jm\rangle = (-1)^{j-m}\hat{\mathcal{T}}|j-m\rangle = (-1)^{j-m}(-1)^{j+m}|jm\rangle = (-1)^{2j}|jm\rangle \quad \text{or} \quad \hat{\mathcal{T}}^2 = -1. \tag{E.5}$$

The time-reversal transformation of a one-body operator $\hat{F}$ is [165]

$$\left(\hat{\mathcal{T}}^{-1}\hat{F}\hat{\mathcal{T}}\right)^{\dagger} = (-1)^{S}\hat{F}, \tag{E.6}$$

where $S = 0$ for time-even operators, i.e., scalar and time-like parts of vectors, and $S = 1$ for time-odd operators, i.e., space-like components of the vector fields. Accordingly, the matrix element $\langle\bar{\mu}|\hat{F}|\bar{\nu}\rangle$ can be evaluated as follows:

$$\begin{aligned}
\langle\bar{\mu}|\hat{F}|\bar{\nu}\rangle &= \langle\bar{\gamma}|\bar{\nu}\rangle \quad \text{(by defining } \langle\bar{\mu}|\hat{F} = \langle\bar{\gamma}|\text{)} \\
&= \langle\gamma|\nu\rangle^{*} \quad \text{(by property A of operator } \hat{\mathcal{T}}\text{)} \\
&= \langle\nu|\gamma\rangle \\
&= \langle\nu|\hat{\mathcal{T}}^{-1}|\bar{\gamma}\rangle \\
&= \langle\nu|\hat{\mathcal{T}}^{-1}\hat{F}^{\dagger}|\bar{\mu}\rangle \\
&= \langle\nu|\hat{\mathcal{T}}^{-1}\hat{F}^{\dagger}\hat{\mathcal{T}}\hat{\mathcal{T}}^{-1}|\bar{\mu}\rangle \\
&= \langle\nu|\hat{\mathcal{T}}^{-1}\hat{F}^{\dagger}\hat{\mathcal{T}}|\mu\rangle \\
&= \langle\nu|\left(\hat{\mathcal{T}}^{-1}\hat{F}\hat{\mathcal{T}}\right)^{\dagger}|\mu\rangle \\
\langle\bar{\mu}|\hat{F}|\bar{\nu}\rangle &= (-1)^{S}\langle\nu|\hat{F}|\mu\rangle.
\end{aligned} \tag{E.7}$$

Similarly, one also obtains

$$\begin{aligned}
\langle\bar{\mu}|\hat{F}|\nu\rangle &= \langle\bar{\gamma}|\nu\rangle \\
&= \langle\nu|\bar{\gamma}\rangle^{*} \\
&= \langle\nu^{*}|\bar{\gamma}^{*}\rangle \\
&= \langle\hat{\mathcal{K}}\nu|\hat{\mathcal{K}}\bar{\gamma}\rangle \\
&= \langle\hat{\mathcal{U}}^{\dagger}\hat{\mathcal{U}}\hat{\mathcal{K}}\nu|\hat{\mathcal{K}}\hat{\mathcal{U}}\hat{\mathcal{K}}\gamma\rangle \\
&= \langle\hat{\mathcal{U}}\hat{\mathcal{K}}\nu|\hat{\mathcal{U}}\hat{\mathcal{K}}\hat{\mathcal{U}}\hat{\mathcal{K}}|\gamma\rangle \\
&= \langle\hat{\mathcal{T}}\nu|\hat{\mathcal{T}}^{2}|\gamma\rangle \quad \text{(by the definition of operator } \hat{\mathcal{T}}\text{)} \\
&= -\langle\bar{\nu}|\gamma\rangle \\
&= -\langle\bar{\nu}|\hat{\mathcal{T}}^{-1}|\bar{\gamma}\rangle \\
&= -\langle\bar{\nu}|\hat{\mathcal{T}}^{-1}\hat{F}^{\dagger}|\bar{\mu}\rangle \\
&= -\langle\bar{\nu}|\hat{\mathcal{T}}^{-1}\hat{F}^{\dagger}\hat{\mathcal{T}}|\mu\rangle \\
&= -\langle\bar{\nu}|\left(\hat{\mathcal{T}}^{-1}\hat{F}\hat{\mathcal{T}}\right)^{\dagger}|\mu\rangle \\
\langle\bar{\mu}|\hat{F}|\nu\rangle &= -(-1)^{S}\langle\bar{\nu}|\hat{F}|\mu\rangle.
\end{aligned} \tag{E.8}$$

Appendix F

Some Useful Formulas From The Quantum Theory of Angular Momentum

F.1 Clebsch-Gordan Coefficients

The state vectors $|\gamma j_1 j_2 j m\rangle$ are given in terms of the state vectors $|\gamma j_1 m_1 j_2 m_2\rangle$ by the unitary transformation

$$|\gamma j_1 j_2 j m\rangle = \sum_{m_1,(m_2)} |\gamma j_1 m_1 j_2 m_2\rangle \langle j_1 m_1 j_2 m_2 | j_1 j_2 j m\rangle. \tag{F.1}$$

The additional quantum numbers γ clearly are not included in the coefficients $\langle j_1 m_1 j_2 m_2 | j_1 j_2 j m\rangle$. These coefficients are known as **vector-coupling, Wigner, or Clebsch-Gordan (C-G) coefficients**. The pair j, m are determined by j_1 and j_2 according to the vector addition rules:

$$j = j_1 + j_2, j_1 + j_2 - 1, j_1 + j_2 - 2, \cdots, |j_1 - j_2| + 1, |j_1 - j_2| \tag{F.2}$$

$$m = -j, \cdots, j. \tag{F.3}$$

Since m is fixed by j and $m = m_1 + m_2$, m_2 is determined by m_1 and m. This is the reason m_2 is written in parentheses in the summation symbol. **The Clebsch-Gordan coefficients are zero unless the vector addition rules are satisfied**.

The inverse transformation is

$$|\gamma j_1 m_1 j_2 m_2\rangle = \sum_j |\gamma j_1 j_2 j m\rangle\langle j_1 j_2 j m|j_1 m_1 j_2 m_2\rangle, \tag{F.4}$$

where the coefficients $\langle j_1 j_2 j m|j_1 m_1 j_2 m_2\rangle$ are the complex conjugates of the corresponding coefficients $\langle j_1 m_1 j_2 m_2|j_1 j_2 j m\rangle$:

$$\langle j_1 j_2 j m|j_1 m_1 j_2 m_2\rangle \;\; = \;\; \langle j_1 m_1 j_2 m_2|j_1 j_2 j m\rangle^*. \tag{F.5}$$

The summation is over j only because m is fixed by the fixed values of m_1 and m_2. The Clebsch-Gordan coefficients are often abbreviated by $\langle j_1 m_1 j_2 m_2|jm\rangle$ and $\langle jm|j_1 m_1 j_2 m_2\rangle$. The Clebsch-Gordan coefficients are usually taken to be **real**:

$$\langle jm|j_1 m_1 j_2 m_2\rangle = \langle j_1 m_1 j_2 m_2|jm\rangle. \tag{F.6}$$

The orthogonality relations of the Clebsch-Gordan coefficients are

$$\sum_j \langle j_1 m_1' j_2 m_2'|jm\rangle\langle j_1 m_1 j_2 m_2|jm\rangle \;\; = \;\; \delta_{m_1' m_1}\delta_{m_2', m_2}, \tag{F.7}$$

$$\sum_{m_1,(m_2)} \langle j_1 m_1 j_2 m_2|j' m'\rangle\langle j_1 m_1 j_2 m_2|jm\rangle \;\; = \;\; \delta_{j' j}\delta_{m' m}. \tag{F.8}$$

Setting $j' = j$ and $m' = m$, the last equation gives orthonormality relation

$$\sum_{m_1,(m_2)} |\langle j_1 m_1 j_2 m_2|jm\rangle|^2 = 1. \tag{F.9}$$

The symmetry properties of Clebsch-Gordan coefficients are given as follows:

1. The cyclic exchange of the type $123 \to 213$ introduces the phase $(-1)^{j_1+j_2-j_3}$.

$$\langle j_1 m_1 j_2 m_2|j_3 m_3\rangle = (-1)^{j_1+j_2-j_3}\langle j_2 m_2 j_1 m_1|j_3 m_3\rangle. \tag{F.10}$$

2. The cyclic exchange of the type $123 \to 3(-2)1$ introduces the phase $(-1)^{j_1-j_3+m_2}$ and a multiplication factor.

$$\langle j_1 m_1 j_2 m_2|j_3 m_3\rangle = (-1)^{j_1-j_3+m_2}\sqrt{\frac{2j_3+1}{2j_1+1}}\langle j_3 m_3 j_2(-m_2)|j_1 m_1\rangle. \tag{F.11}$$

3. The cyclic exchange of the type $123 \to (-2)31$ gives the phase $(-1)^{j_2+m_2}$ and a

multiplication factor.

$$\langle j_1 m_1 j_2 m_2 | j_3 m_3 \rangle = (-1)^{j_2+m_2} \sqrt{\frac{2j_3+1}{2j_1+1}} \langle j_2(-m_2) j_3 m_3 | j_1 m_1 \rangle. \tag{F.12}$$

4. The reverse of the signs of all three m's gives the phase $(-1)^{j_1+j_2-j_3}$.

$$\langle j_1 m_1 j_2 m_2 | j_3 m_3 \rangle = (-1)^{j_1+j_2-j_3} \langle j_1(-m_1) j_2(-m_2) | j_3(-m_3) \rangle. \tag{F.13}$$

F.2 3-j Symbol and the Wigner-Eckart Theorem

The 3-j symbol of Wigner is defined as

$$\begin{pmatrix} j_1 & j_2 & j_3 \\ m_1 & m_2 & m_3 \end{pmatrix} = \frac{(-1)^{j_1-j_2-m_3}}{\sqrt{2j_3+1}} \langle j_1 m_1 j_2 m_2 | j_1 j_2 j_3(-m_3) \rangle. \tag{F.14}$$

The symmetry properties of 3-j symbol are given as follows:

1. The numerical value of a 3-j symbol remains unchanged under an **even** permutation.

$$\begin{pmatrix} j_1 & j_2 & j_3 \\ m_1 & m_2 & m_3 \end{pmatrix} = \begin{pmatrix} j_2 & j_3 & j_1 \\ m_2 & m_3 & m_1 \end{pmatrix} = \begin{pmatrix} j_3 & j_1 & j_2 \\ m_3 & m_1 & m_2 \end{pmatrix}. \tag{F.15}$$

2. The **odd** permutation gives multiplication factor of $(-1)^{j_1+j_2+j_3}$.

$$\begin{aligned} (-1)^{j_1+j_2+j_3} \begin{pmatrix} j_1 & j_2 & j_3 \\ m_1 & m_2 & m_3 \end{pmatrix} &= \begin{pmatrix} j_2 & j_1 & j_3 \\ m_2 & m_1 & m_3 \end{pmatrix} = \begin{pmatrix} j_1 & j_3 & j_2 \\ m_1 & m_3 & m_2 \end{pmatrix} \\ &= \begin{pmatrix} j_3 & j_2 & j_1 \\ m_3 & m_2 & m_1 \end{pmatrix}. \end{aligned} \tag{F.16}$$

3. The reverse of the signs of all three m's introduces multiplication factor of $(-1)^{j_1+j_2+j_3}$.

$$\begin{pmatrix} j_1 & j_2 & j_3 \\ m_1 & m_2 & m_3 \end{pmatrix} = (-1)^{j_1+j_2+j_3} \begin{pmatrix} j_1 & j_2 & j_3 \\ -m_1 & -m_2 & -m_3 \end{pmatrix}. \tag{F.17}$$

The orthogonality relations of 3-j symbol are

$$\sum_{j_3,m_3} (2j_3+1) \begin{pmatrix} j_1 & j_2 & j_3 \\ m_1 & m_2 & m_3 \end{pmatrix} \begin{pmatrix} j_1 & j_2 & j_3 \\ m_1' & m_2' & m_3 \end{pmatrix} = \delta_{m_1' m_1} \delta_{m_2' m_2}, \tag{F.18}$$

$$\sum_{m_1,(m_2)} \begin{pmatrix} j_1 & j_2 & j_3 \\ m_1 & m_2 & m_3 \end{pmatrix} \begin{pmatrix} j_1 & j_2 & j_3' \\ m_1 & m_2 & m_3' \end{pmatrix} = \frac{1}{2j_3+1}\delta_{j_3 j_3'}\delta_{m_3 m_3'}. \quad \text{(F.19)}$$

Some useful formula for calculating 3-j symbol are

$$\begin{pmatrix} J & J & 0 \\ M & -M & 0 \end{pmatrix} = \frac{(-1)^{J-M}}{\sqrt{2J+1}}, \quad \text{(F.20)}$$

$$\begin{pmatrix} J & J & 1 \\ M & -M & 0 \end{pmatrix} = (-1)^{J-M}\frac{M}{\sqrt{(2J+1)(J+1)J}}, \quad \text{(F.21)}$$

$$\begin{pmatrix} J & J & 1 \\ M & -M-1 & 1 \end{pmatrix} = (-1)^{J-M}\sqrt{\frac{2(J-M)(J+M+1)}{(2J+2)(2J+1)2J}} \quad \text{(F.22)}$$

$$\begin{pmatrix} j_1 & j_2 & j_3 \\ m_1 & m_2 & m_3 \end{pmatrix} = 0, \quad \text{if } m_1+m_2 \neq -m_3. \quad \text{(F.23)}$$

The Wigner-Eckart Theorem can be stated as follows:

Let $\hat{T}^k_q$ be a spherical tensor operator. The projection quantum numbers dependence of the matrix element $\langle \gamma' j' m' | \hat{T}^k_q | \gamma j m \rangle$ is solely contained in the Clebsch-Gordan coefficient.

$$\langle \gamma' j' m' | \hat{T}^k_q | \gamma j m \rangle = (-1)^{j-m}\frac{\langle j' m' j(-m) | j' j k q \rangle}{\sqrt{2k+1}} \langle \gamma' j' || \hat{T}^k || \gamma j \rangle. \quad \text{(F.24)}$$

Here, the matrix element $\langle \gamma' j' || \hat{T}^k || \gamma j \rangle$ is called the **"double-barred" or "reduced" matrix element**. Instead of Eq. (F.24), one often uses the following statement of the Wigner-Eckart theorem:

$$\langle \gamma' j' m' | \hat{T}^k_q | \gamma j m \rangle = (-1)^{j'-m'} \begin{pmatrix} j' & k & j \\ -m' & q & m \end{pmatrix} \langle \gamma' j' || \hat{T}^k || \gamma j \rangle. \quad \text{(F.25)}$$

F.3 Spin Angular Tensor Operator

The spin-angular tensor operator T_{JLSM} are defined as

$$T_{JLSM}(\mathbf{n})_{\sigma_1\sigma_2} = \sum_{m\mu} \langle LmS\mu | JM \rangle Y_{Lm}(\mathbf{n})(\sigma_{S\mu})_{\sigma_1\sigma_2}, \quad \text{(F.26)}$$

where $\mathbf{n} = \mathbf{r}/r$, $Y_{Lm}(\mathbf{n})$ are spherical harmonics functions, and $\sigma_{S\mu}$ are the spherical spin Pauli matrices. Here, m, μ, and M have values

$$m = -L, \cdots, L;$$

$$\begin{aligned} \mu &= -S, \cdots, S; \\ M &= m + \mu = -J, \cdots, J. \end{aligned} \tag{F.27}$$

For $S = 0$ and $S = 1$, the spherical spin Pauli matrices are given by

$$\sigma_{00} = \begin{pmatrix} 1 & 0 \\ 0 & 1 \end{pmatrix}, \tag{F.28}$$

$$\sigma_{10} = \sigma_z = \begin{pmatrix} 1 & 0 \\ 0 & -1 \end{pmatrix}, \tag{F.29}$$

$$\sigma_{1(+1)} = -\frac{1}{\sqrt{2}}(\sigma_x + i\sigma_y) = -\frac{1}{\sqrt{2}} \begin{pmatrix} 0 & 2 \\ 0 & 0 \end{pmatrix}, \tag{F.30}$$

$$\sigma_{1(-1)} = \frac{1}{\sqrt{2}}(\sigma_x - i\sigma_y) = \frac{1}{\sqrt{2}} \begin{pmatrix} 0 & 0 \\ 2 & 0 \end{pmatrix}. \tag{F.31}$$

The components of spherical spin Pauli matrices can be written compactly as

$$(\sigma_{S\mu})_{\sigma_1\sigma_2} = \sqrt{2(2S+1)}(-1)^{\frac{1}{2}-\sigma_1} \begin{pmatrix} \frac{1}{2} & \frac{1}{2} & S \\ \sigma_2 & -\sigma_1 & \mu \end{pmatrix}, \tag{F.32}$$

where $\sigma_1, \sigma_2 = \pm\frac{1}{2}$. Inserting $S = 0$ and $S = 1$, one can reproduce (F.28)-(F.31). Since the Clecbsch-Gordan coefficients are real, (F.32) suggests that the spherical spin Pauli matrices are also real. The spherical spin Pauli matrices satisfy orthogonality relation:

$$\frac{1}{2}\,\mathrm{Tr}(\sigma^\dagger_{S_1\mu_1}\sigma_{S_2\mu_2}) = \delta_{S_1S_2}\delta_{\mu_1\mu_2}. \tag{F.33}$$

The orthogonality relation of the spherical harmonics functions $Y_{Lm}(\mathbf{n})$ is

$$\int d\mathbf{n}\; Y^*_{Lm}(\mathbf{n})Y_{L'm'}(\mathbf{n}) = \delta_{LL'}\delta_{mm'}. \tag{F.34}$$

Applying (F.33) and (F.34), we obtain the orthogonality relation for the spin-angular tensor operator $T_{JLSM}(\mathbf{n})$:

$$\frac{1}{2}\,\mathrm{Tr}\int d\mathbf{n}\; T^\dagger_{J_1L_1S_1M_1}(\mathbf{n})T_{J_2L_2S_2M_2}(\mathbf{n}) = \delta_{J_1J_2}\delta_{M_1M_2}\delta_{L_1L_2}\delta_{S_1S_2}. \tag{F.35}$$

The completeness relations of the spin-angular tensor operator are

$$\sum_M T^\dagger_{JLSM}(\mathbf{n})T_{JLSM}(\mathbf{n}) = \frac{2J+1}{4\pi}, \tag{F.36}$$

$$\frac{1}{2}\sum_{JLSM} T^*_{JLSM}(\mathbf{n})_{\sigma_1\sigma_2} T_{JLSM}(\mathbf{n}')_{\sigma'_1\sigma'_2} = \delta(\mathbf{n}-\mathbf{n}')\delta_{\sigma_1\sigma'_1}\delta_{\sigma_2\sigma'_2}. \tag{F.37}$$

From (F.26), we obtain

$$\begin{aligned}
T^\dagger_{JLSM}(\mathbf{n})_{\sigma_1\sigma_2} &= \sum_{m\mu}\langle JM|LmS\mu\rangle Y^*_{Lm}(\mathbf{n})(\sigma^\dagger_{S\mu})_{\sigma_1\sigma_2} \\
T^\dagger_{JLS(-M)}(\mathbf{n})_{\sigma_1\sigma_2} &= \sum_{m\mu}\langle J(-M)|LmS\mu\rangle Y^*_{Lm}(\mathbf{n})(\sigma^\dagger_{S\mu})_{\sigma_1\sigma_2} \\
&= \sum_{m\mu}\langle LmS\mu|J(-M)\rangle Y^*_{Lm}(\mathbf{n})(\sigma^\dagger_{S\mu})_{\sigma_1\sigma_2} \qquad \text{(C-G coefficients are real)} \\
T^\dagger_{JLS(-M)}(\mathbf{n})_{\sigma_1\sigma_2} &= (-1)^{L+S-J}\sum_{m\mu}\langle L(-m)S(-\mu)|JM\rangle(-1)^{-m}Y_{L(-m)}(\mathbf{n})(\sigma^\dagger_{S\mu})_{\sigma_1\sigma_2},
\end{aligned} \tag{F.38}$$

where we have used the fourth symmetry property of the C-G coefficients and the symmetry property of the spherical harmonics functions:

$$Y_{L(-m)}(\mathbf{n}) = (-1)^m Y^*_{Lm}(\mathbf{n}). \tag{F.39}$$

We can evaluate $(\sigma^\dagger_{S\mu})_{\sigma_1\sigma_2}$ as follows:

$$\begin{aligned}
(\sigma^\dagger_{S\mu})_{\sigma_1\sigma_2} &= (\sigma_{S\mu})^*_{\sigma_2\sigma_1} \\
&= \sqrt{2(2S+1)}(-1)^{\frac{1}{2}-\sigma_2}\begin{pmatrix} \frac{1}{2} & \frac{1}{2} & S \\ \sigma_1 & -\sigma_2 & \mu \end{pmatrix}^* \\
&= \sqrt{2(2S+1)}(-1)^{\frac{1}{2}-\sigma_2}\begin{pmatrix} \frac{1}{2} & \frac{1}{2} & S \\ \sigma_1 & -\sigma_2 & \mu \end{pmatrix} \\
&= \sqrt{2(2S+1)}(-1)^{\frac{1}{2}-\sigma_2}(-1)^{\frac{1}{2}+\frac{1}{2}+S}\begin{pmatrix} \frac{1}{2} & \frac{1}{2} & S \\ -\sigma_1 & \sigma_2 & -\mu \end{pmatrix} \\
&= \sqrt{2(2S+1)}(-1)^{\frac{1}{2}-\sigma_2}(-1)^{\frac{1}{2}+\frac{1}{2}+S}(-1)^{\frac{1}{2}+\frac{1}{2}+S}\begin{pmatrix} \frac{1}{2} & \frac{1}{2} & S \\ \sigma_2 & -\sigma_1 & -\mu \end{pmatrix} \\
&= \sqrt{2(2S+1)}(-1)^{\frac{1}{2}-\sigma_2}\begin{pmatrix} \frac{1}{2} & \frac{1}{2} & S \\ \sigma_2 & -\sigma_1 & -\mu \end{pmatrix} \\
&= \sqrt{2(2S+1)}(-1)^{\frac{1}{2}-\sigma_1}(-1)^{-\mu}\begin{pmatrix} \frac{1}{2} & \frac{1}{2} & S \\ \sigma_2 & -\sigma_1 & -\mu \end{pmatrix} \\
(\sigma^\dagger_{S\mu})_{\sigma_1\sigma_2} &= (-1)^{-\mu}(\sigma_{S(-\mu)})_{\sigma_1\sigma_2}.
\end{aligned} \tag{F.40}$$

Introducing the notation $m' = -m = -L, \cdots, L$ and $\mu' = -\mu = -S, \cdots, S$, (F.38) becomes

$$\begin{aligned} T^{\dagger}_{JLSM}(\mathbf{n})_{\sigma_1\sigma_2} &= (-1)^{L+S-J}\sum_{m\mu}\langle L(-m)S(-\mu)|J(-M)\rangle(-1)^{-m-\mu}Y_{L(-m)}(\mathbf{n})(\sigma_{S(-\mu)})_{\sigma_1\sigma_2} \\ &= (-1)^{L+S-J}\sum_{m'\mu'}\langle Lm'S\mu'|J(-M)\rangle(-1)^{-M}Y_{Lm'}(\mathbf{n})(\sigma_{S\mu'})_{\sigma_1\sigma_2} \\ &= \underbrace{(-1)^{-2J}}_{=1}(-1)^{L+S+J-M}T_{JLS(-M)}(\mathbf{n})_{\sigma_1\sigma_2} \\ T^{\dagger}_{JLSM}(\mathbf{n})_{\sigma_1\sigma_2} &= (-1)^{L+S+J-M}T_{JLS(-M)}(\mathbf{n})_{\sigma_1\sigma_2}. \end{aligned} \tag{F.41}$$

This is one of the symmetry properties of spin angular tensor operators. Another symmetry property of $T_{JLSM}(\mathbf{n})$ is

$$T_{JLSM}(\mathbf{n})_{\sigma_1\sigma_2} = (-1)^{S+\frac{1}{2}-\sigma_1+\frac{1}{2}-\sigma_2}T_{JLSM}(\mathbf{n})_{(-\sigma_2)(-\sigma_1)}. \tag{F.42}$$

Introducing a tensor spherical harmonics

$$\Omega_{j_k\ell_k m_k}(\mathbf{n},\sigma) = \sum_{m_\ell, m_s}\langle \ell m_\ell \tfrac{1}{2} m_s|jm\rangle Y_{\ell m_\ell}(\mathbf{n})\chi_{\frac{1}{2}m_s}(\sigma), \tag{F.43}$$

the matrix element of spin angular tensor operator $T_{JLSM}(\mathbf{n})_{\sigma_1\sigma_2}$ is defined as

$$\langle j_k\ell_k m_k|T_{JLSM}|j_{k'}\ell_{k'}m_{k'}\rangle = \int d\mathbf{n}\sum_{\sigma_1\sigma_2}\Omega^*_{j_k\ell_k m_k}(\mathbf{n},\sigma_1)T_{JLSM}(\mathbf{n})_{\sigma_1\sigma_2}\Omega_{j_{k'}\ell_{k'}m_{k'}}(\mathbf{n},\sigma_2). \tag{F.44}$$

Using the Wigner-Eckart theorem, one obtains

$$\langle j_k\ell_k m_k|T_{JLSM}|j_{k'}\ell_{k'}m_{k'}\rangle = (-1)^{j_k-m_k}\begin{pmatrix} j_k & J & j_{k'} \\ -m_k & M & m_{k'}\end{pmatrix}\langle j_k\ell_k||T_{JLS}||j_{k'}\ell_{k'}\rangle, \tag{F.45}$$

where the reduced matrix element $\langle j_k\ell_k||T_{JLS}||j_{k'}\ell_{k'}\rangle$ reads

$$\begin{aligned} &\langle j_k\ell_k||T_{JLS}||j_{k'}\ell_{k'}\rangle \\ =\ & \frac{1}{2}[1+(-1)^{L+\ell_k+\ell_{k'}}](-1)^{S+j_{k'}-\frac{1}{2}}\sqrt{\frac{(2J+1)(2L+1)(2j_k+1)(2j_{k'}+1)}{4\pi}} \\ \times\ & \begin{pmatrix} j_k & j_{k'} & J \\ \frac{1}{2} & -\frac{1}{2} & 0\end{pmatrix}\left\{\begin{pmatrix} J & L & S \\ 0 & 0 & 0\end{pmatrix} + \sqrt{\frac{S(S+1)}{J(J+1)}}\begin{pmatrix} J & L & S \\ 1 & 0 & -1\end{pmatrix}\right. \end{aligned}$$

$$\times \quad [(\ell_k - j_k)(2j_k+1) + (-1)^{J+L+S}(\ell_{k'} - j_{k'})(2j_{k'}+1)] \Bigg\}. \tag{F.46}$$

Using the symmetry property (F.41) and the Wigner-Eckart theorem, the matrix element $\langle j_{k'}\ell_{k'}m_{k'}|T^{\dagger}_{JLSM}|j_k\ell_k m_k\rangle$ can be written as

$$\begin{aligned}
\langle j_{k'}\ell_{k'}m_{k'}|T^{\dagger}_{JLSM}|j_k\ell_k m_k\rangle &= (-1)^{L+S+J-M}\langle j_{k'}\ell_{k'}m_{k'}|T_{JLS(-M)}|j_k\ell_k m_k\rangle \\
&= (-1)^{L+S+J-M}(-1)^{j_{k'}-m_{k'}} \begin{pmatrix} j_{k'} & J & j_k \\ -m_{k'} & -M & m_k \end{pmatrix} \\
&\times \quad \langle j_{k'}\ell_{k'}||T_{JLS}||j_k\ell_k\rangle \\
&= (-1)^{L+S+J-M}(-1)^{j_{k'}-m_{k'}} \begin{pmatrix} j_k & J & j_{k'} \\ -m_k & M & m_{k'} \end{pmatrix} \\
&\times \quad \langle j_{k'}\ell_{k'}||T_{JLS}||j_k\ell_k\rangle.
\end{aligned} \tag{F.47}$$

Using the identity $\langle j_k\ell_k m_k|T_{JLSM}|j_{k'}\ell_{k'}m_{k'}\rangle = \langle j_{k'}\ell_{k'}m_{k'}|T^{\dagger}_{JLSM}|j_k\ell_k m_k\rangle^*$ and the fact that the reduced matrix element $\langle j_k\ell_k||T_{JLS}||j_{k'}\ell_{k'}\rangle$ is real, one can prove the following symmetry property:

$$\langle j_k\ell_k||T_{JLS}||j_{k'}\ell_{k'}\rangle = (-1)^{L+S+J}(-1)^{j_{k'}-j_k}\langle j_{k'}\ell_{k'}||T_{JLS}||j_k\ell_k\rangle. \tag{F.48}$$

Applying this result to Eq. (F.47), one obtains

$$\begin{aligned}
\langle j_{k'}\ell_{k'}m_{k'}|T^{\dagger}_{JLSM}|j_k\ell_k m_k\rangle &= (-1)^{j_{k'}-j_k}(-1)^{L+S+J}(-1)^{j_k-m_{k'}-M} \begin{pmatrix} j_k & J & j_{k'} \\ -m_k & M & m_{k'} \end{pmatrix} \\
&\times \quad \langle j_{k'}\ell_{k'}||T_{JLS}||j_k\ell_k\rangle \\
&= (-1)^{j_k-m_k} \begin{pmatrix} j_k & J & j_{k'} \\ -m_k & M & m_{k'} \end{pmatrix} \langle j_k\ell_k||T_{JLS}||j_{k'}\ell_{k'}\rangle.
\end{aligned} \tag{F.49}$$

Appendix G

Reduced Matrix Elements of the Particle-hole Free Response Function in the Continuum Relativistic QRPA

Using the definition of the Dirac spinor:

$$\Psi_k(\mathbf{r},\sigma,t) = \begin{bmatrix} F_{\kappa_k}(r)\Omega_{j_k\ell_k m_k}(\mathbf{n},\sigma) \\ iG_{\kappa_k}(r)\Omega_{j_k\tilde{\ell}_k m_k}(\mathbf{n},\sigma) \end{bmatrix} \chi_{\frac{1}{2}\tau_k}(t) \tag{G.1}$$

the matrix element $\mathcal{Q}^c_{kk'}(r)$ given by Eq. (6.36) now reads:

$$\begin{aligned}
\mathcal{Q}^c_{kk'}(r) &\equiv \langle k|\mathcal{Q}^c(r)|k'\rangle \\
&= \int d\mathbf{n}_1 \sum_{t_1 t_1'} \sum_{\sigma_1,\sigma_1'} \Psi^\dagger_k(r,\mathbf{n}_1,\sigma_1,t_1)\gamma_D \otimes T_{JLSM}(\mathbf{n}_1)_{\sigma_1\sigma_1'} \otimes (\tau_{T0})_{t_1 t_1'} \\
&\times \Psi_{k'}(r,\mathbf{n}_1,\sigma_1',t_1'), \\
&= \int d\mathbf{n}_1 \sum_{t_1 t_1'} \sum_{\sigma_1,\sigma_1'} \chi^*_{\frac{1}{2}\tau_k}(t_1) \begin{pmatrix} \Omega^*_{j_k\ell_k m_k}(\mathbf{n}_1,\sigma_1)F^*_{\kappa_k}(r) & -i\Omega^*_{j_k\tilde{\ell}_k m_k}(\mathbf{n}_1,\sigma_1)G^*_{\kappa_k}(r) \end{pmatrix} \\
&\times \gamma_D \otimes T_{JLSM}(\mathbf{n}_1)_{\sigma_1\sigma_1'} \otimes (\tau_{T0})_{t_1 t_1'} \begin{pmatrix} F_{\kappa_{k'}}(r)\Omega_{j_{k'}\ell_{k'}m_{k'}}(\mathbf{n}_1,\sigma_1') \\ iG_{\kappa_{k'}}(r)\Omega_{j_{k'}\tilde{\ell}_{k'}m_{k'}}(\mathbf{n}_1,\sigma_1') \end{pmatrix} \chi_{\frac{1}{2}\tau_{k'}}(t_1') \\
\mathcal{Q}^c_{kk'}(r) &= \sum_{t_1 t_1'} \chi^*_{\frac{1}{2}\tau_k}(t_1)(\tau_{T0})_{t_1 t_1'}\chi_{\frac{1}{2}\tau_{k'}}(t_1') \\
&\times \int d\mathbf{n}_1 \sum_{\sigma_1,\sigma_1'} \begin{pmatrix} \Omega^*_{j_k\ell_k m_k}(\mathbf{n}_1,\sigma_1)F^*_{\kappa_k}(r) & -i\Omega^*_{j_k\tilde{\ell}_k m_k}(\mathbf{n}_1,\sigma_1)G^*_{\kappa_k}(r) \end{pmatrix} \\
&\times \gamma_D \otimes T_{JLSM}(\mathbf{n}_1)_{\sigma_1\sigma_1'} \begin{pmatrix} F_{\kappa_{k'}}(r)\Omega_{j_{k'}\ell_{k'}m_{k'}}(\mathbf{n}_1,\sigma_1') \\ iG_{\kappa_{k'}}(r)\Omega_{j_{k'}\tilde{\ell}_{k'}m_{k'}}(\mathbf{n}_1,\sigma_1') \end{pmatrix}.
\end{aligned} \tag{G.2}$$

Let us define an isospin charge $q^T_{\rm isospin}$ as

$$q^T_{\rm isospin} = \sum_{t_1 t'_1} \chi^*_{\frac{1}{2}\tau_k}(t_1)(\tau_{T0})_{t_1 t'_1}\chi_{\frac{1}{2}\tau_{k'}}(t'_1). \tag{G.3}$$

There are two operators τ_{T0}, i.e., $\tau_{00} = \mathbf{1}$ and $\tau_{10} = \tau_3$, which are diagonal. Since

$$\chi_{\frac{1}{2}\tau_k}(t_1) = \delta_{t_1\tau_k}, \tag{G.4}$$

the isospin charge $q^T_{\rm isospin}$ takes the form

$$q^T_{\rm isospin} = \sum_{t_1 t'_1} \delta_{t_1\tau_k}(\tau_{T0})_{t_1 t'_1}\delta_{t'_1\tau_{k'}} = (\tau_{T0})_{\tau_k\tau_k}\delta_{\tau_k\tau_{k'}}, \tag{G.5}$$

which implies the condition $\tau_k = \tau_{k'}$. There are two values of τ_k, i.e., $+1/2$ for neutrons and -1/2 for protons. For the case of isoscalar ($\tau_{00} = \mathbf{1}$), we obtain

$$q^0_{\rm isospin} = (\tau_{00})_{+1/2,+1/2} = 1 \tag{G.6}$$

for neutron and

$$q^0_{\rm isospin} \;\; = \;\; (\tau_{00})_{-1/2,-1/2} = 1 \tag{G.7}$$

for proton. For the case of isovector ($\tau_{10} = \tau_3$), we obtain

$$q^1_{\rm isospin} = (\tau_{10})_{+1/2,+1/2} = 1 \tag{G.8}$$

for neutron and

$$q^1_{\rm isospin} = (\tau_{10})_{-1/2,-1/2} = -1 \tag{G.9}$$

for proton. Therefore, neutrons always have the isospin charge $+1$, whereas protons have the isospin charge $+1$ (-1) for isoscalar (isovector) case.

It is worthwhile to work out the matrix elements $\mathcal{Q}^c_{kk'}(r)$ for specific channels. Let us begin with channel $c = 1$. Channel $c = 1$ has the Dirac matrix $\gamma_D = \gamma^0$, spin angular tensor $T_{JLSM}(\mathbf{n})_{\sigma_1\sigma'_1} = ([\sigma_0 Y_J]_{JM})_{\sigma_1\sigma'_1}$, and $q^0_{\rm isospin} = 1$ for protons and neutrons. For $c = 1$, the matrix element $\mathcal{Q}^1_{kk'}(r)$ takes the form

$$\mathcal{Q}^1_{kk'}(r) \;\; = \;\; F^*_{\kappa_k}(r)F_{\kappa_{k'}}(r)\int d\mathbf{n}_1 \sum_{\sigma_1,\sigma'_1} \Omega^*_{j_k\ell_k m_k}(\mathbf{n}_1,\sigma_1)([\sigma_0 Y_J]_{JM})_{\sigma_1\sigma'_1}\Omega_{j_{k'}\ell_{k'}m_{k'}}(\mathbf{n}_1,\sigma'_1)$$

$$
\begin{aligned}
&- \quad G^*_{\kappa_k}(r)G_{\kappa_{k'}}(r)\int d\mathbf{n}_1 \sum_{\sigma_1,\sigma_1'} \Omega^*_{j_k\tilde{\ell}_k m_k}(\mathbf{n}_1,\sigma_1)([\sigma_0 Y_J]_{JM})_{\sigma_1\sigma_1'}\Omega_{j_{k'}\tilde{\ell}_{k'}m_{k'}}(\mathbf{n}_1,\sigma_1') \\
&= \quad F^*_{\kappa_k}(r)F_{\kappa_{k'}}(r)\langle j_k\ell_k m_k|[\sigma_0 Y_J]_{JM}|j_{k'}\ell_{k'}m_{k'}\rangle \\
&- \quad G^*_{\kappa_k}(r)G_{\kappa_{k'}}(r)\langle j_k\tilde{\ell}_k m_k|[\sigma_0 Y_J]_{JM}|j_{k'}\tilde{\ell}_{k'}m_{k'}\rangle. \qquad \text{(G.10)}
\end{aligned}
$$

By the Wigner-Eckart theorem, the matrix element $\mathcal{Q}^1_{kk'}(r)$ reads

$$
\mathcal{Q}^1_{kk'}(r) = (-1)^{j_k-m_k}\begin{pmatrix} j_k & J & j_{k'} \\ -m_k & M & m_{k'}\end{pmatrix}\mathcal{Q}^1_{(kk')}(r), \qquad \text{(G.11)}
$$

where the reduced matrix element $\mathcal{Q}^1_{(kk')}(r)$ is given by

$$
\begin{aligned}
\mathcal{Q}^1_{(kk')}(r) &= F^*_{\kappa_k}(r)F_{\kappa_{k'}}(r)\langle j_k\ell_k||[\sigma_0 Y_J]_J||j_{k'}\ell_{k'}\rangle \\
&- G^*_{\kappa_k}(r)G_{\kappa_{k'}}(r)\langle j_k\tilde{\ell}_k||[\sigma_0 Y_J]_J||j_{k'}\tilde{\ell}_{k'}\rangle. \qquad \text{(G.12)}
\end{aligned}
$$

For channel $c = 2$, one still has an isospin charge $q^0_{\text{isospin}} = 1$ and the spin angular tensor $T_{JLSM}(\mathbf{n})_{\sigma_1\sigma_1'} = ([\sigma_0 Y_J]_{JM})_{\sigma_1\sigma_1'}$, except that $\gamma_D = \mathbf{1}_{4\times4}$. For channel $c = 2$, one obtains

$$
\mathcal{Q}^2_{kk'}(r) = (-1)^{j_k-m_k}\begin{pmatrix} j_k & J & j_{k'} \\ -m_k & M & m_{k'}\end{pmatrix}\mathcal{Q}^2_{(kk')}(r), \qquad \text{(G.13)}
$$

where the reduced matrix element $\mathcal{Q}^2_{(kk')}(r)$ is given by

$$
\begin{aligned}
\mathcal{Q}^2_{(kk')}(r) &= F^*_{\kappa_k}(r)F_{\kappa_{k'}}(r)\langle j_k\ell_k||[\sigma_0 Y_J]_J||j_{k'}\ell_{k'}\rangle \\
&+ G^*_{\kappa_k}(r)G_{\kappa_{k'}}(r)\langle j_k\tilde{\ell}_k||[\sigma_0 Y_J]_J||j_{k'}\tilde{\ell}_{k'}\rangle. \qquad \text{(G.14)}
\end{aligned}
$$

For channel $c = 3$ with an isospin charge $q^0_{\text{isospin}} = 1$, the spin angular tensor $T_{JLSM}(\mathbf{n})_{\sigma_1\sigma_1'} = ([\sigma_1 Y_{J-1}]_{JM})_{\sigma_1\sigma_1'}$, and the Dirac matrix $\gamma_D = \gamma_5$, the matrix element $\mathcal{Q}^3_{kk'}(r)$ reads

$$
\mathcal{Q}^3_{kk'}(r) = (-1)^{j_k-m_k}\begin{pmatrix} j_k & J & j_{k'} \\ -m_k & M & m_{k'}\end{pmatrix}\mathcal{Q}^3_{(kk')}(r), \qquad \text{(G.15)}
$$

where the reduced matrix element $\mathcal{Q}^3_{(kk')}(r)$ takes the form

$$
\begin{aligned}
\mathcal{Q}^3_{(kk')}(r) &= -iG^*_{\kappa_k}(r)F_{\kappa_{k'}}(r)\langle j_k\tilde{\ell}_k||[\sigma_1 Y_{J-1}]_J||j_{k'}\ell_{k'}\rangle \\
&+ iF^*_{\kappa_k}(r)G_{\kappa_{k'}}(r)\langle j_k\ell_k||[\sigma_1 Y_{J-1}]_J||j_{k'}\tilde{\ell}_{k'}\rangle. \qquad \text{(G.16)}
\end{aligned}
$$

Therefore, a matrix element $\mathcal{Q}^{c}_{kk'}(r)$ for a specific channel c has a generic form:

$$\mathcal{Q}^{c}_{kk'}(r) = (-1)^{j_k - m_k} \begin{pmatrix} j_k & J & j_{k'} \\ -m_k & M & m_{k'} \end{pmatrix} \mathcal{Q}^{c}_{(kk')}(r), \tag{G.17}$$

where $\mathcal{Q}^{c}_{(kk')}(r)$ is the corresponding reduced matrix element, which has included the isospin charge $q^{T}_{\rm isospin}$ implicitly.
The matrix element $\mathcal{Q}^{c'*}_{kk'}(r')$ is given by

$$\begin{aligned} \mathcal{Q}^{c'*}_{kk'}(r') &= \int d\mathbf{n}_2 \sum_{t_2,t_2'} \sum_{\sigma_2,\sigma_2'} \Psi^{\dagger}_{k'}(r',\mathbf{n}_2,\sigma_2,t_2)\gamma_{D'} \otimes T^{\dagger}_{J'L'S'M'}(\mathbf{n}_2)_{\sigma_2\sigma_2'} \otimes (\tau_{T0})_{t_2t_2'} \\ &\times \Psi_k(r',\mathbf{n}_2,\sigma_2',t_2') \\ &= q^{T'}_{\rm isospin} \int d\mathbf{n}_2 \sum_{\sigma_2,\sigma_2'} \begin{pmatrix} \Omega^{*}_{j_{k'}\ell_{k'}m_{k'}}(\mathbf{n}_2,\sigma_2)F^{*}_{\kappa_{k'}}(r) & -i\Omega^{*}_{j_{k'}\tilde{\ell}_{k'}m_{k'}}(\mathbf{n}_2,\sigma_2)G^{*}_{\kappa_{k'}}(r') \end{pmatrix} \\ &\times \gamma_{D'} \otimes T^{\dagger}_{J'L'S'M'}(\mathbf{n}_1)_{\sigma_2\sigma_2'} \begin{pmatrix} F_{\kappa_k}(r')\Omega_{j_k\ell_k m_k}(\mathbf{n}_2,\sigma_2') \\ iG_{\kappa_k}(r')\Omega_{j_k\tilde{\ell}_k m_k}(\mathbf{n}_2,\sigma_2') \end{pmatrix}. \end{aligned} \tag{G.18}$$

With the aid of Eq. (F.49), one can deduce

$$\mathcal{Q}^{c'*}_{kk'}(r') = (-1)^{j_k - m_k} \begin{pmatrix} j_k & J' & j_{k'} \\ -m_k & M' & m_{k'} \end{pmatrix} \mathcal{Q}^{c'*}_{(kk')}(r'), \tag{G.19}$$

where, for example, the reduced matrix element $\mathcal{Q}^{c'*}_{(kk')}(r')$ takes the form

$$\begin{aligned} \mathcal{Q}^{1*}_{(kk')}(r') &= F^{*}_{\kappa_{k'}}(r')F_{\kappa_k}(r')\langle j_k\ell_k||[\sigma_0 Y_{J'}]_{J'}||j_{k'}\ell_{k'}\rangle \\ &- G^{*}_{\kappa_{k'}}(r')G_{\kappa_k}(r')\langle j_k\tilde{\ell}_k||[\sigma_0 Y_{J'}]_{J'}||j_{k'}\tilde{\ell}_{k'}\rangle. \end{aligned} \tag{G.20}$$

for channel $c' = 1$.

The reduced spectral free response function given by Eq. (6.53) reads

$$\mathcal{R}^{0cc'}_{\rm 2qp}(r,r',\omega) = \sum_{k<k'} \left\{ \frac{\mathcal{Q}^{c*}_{k\bar{k}'}(r)\eta^{S}_{kk'}\mathcal{Q}^{c'}_{k\bar{k}'}(r')\eta^{S'}_{kk'}}{\omega - E_k - E_{k'}} - \frac{\mathcal{Q}^{c*}_{\bar{k}'k}(r)\eta^{S}_{kk'}\mathcal{Q}^{c'}_{k'k}(r')\eta^{S'}_{kk'}}{\omega + E_k + E_{k'}} \right\}. \tag{G.21}$$

The numerator of the first term on the right-hand side can be evaluated using the Wigner-Eckart theorem and the definition of time-conjugate state (E.2) as follows:

$$\mathcal{Q}^{c*}_{k\bar{k}'}(r) = (-1)^{j_k - m_k}(-1)^{j_{k'} - m_{k'}} \begin{pmatrix} j_k & J & j_{k'} \\ -m_k & M & -m_{k'} \end{pmatrix} \mathcal{Q}^{c*}_{(kk')}(r)$$

$$
\begin{aligned}
\mathcal{Q}^{c'}_{k\bar{k}'}(r') &= (-1)^{j_k-m_k}(-1)^{j_{k'}-m_{k'}}\begin{pmatrix} j_k & J' & j_{k'} \\ -m_k & M' & -m_{k'} \end{pmatrix}\mathcal{Q}^{c'}_{(kk')}(r') \\
\sum_{m_k,m_{k'}}\mathcal{Q}^{c*}_{k\bar{k}'}(r)\mathcal{Q}^{c'}_{k\bar{k}'}(r') &= \sum_{m_k,m_{k'}}\underbrace{(-1)^{2j_k-2m_k}}_{=1}\underbrace{(-1)^{2j_{k'}-2m_{k'}}}_{=1}\mathcal{Q}^{c*}_{(kk')}(r)\mathcal{Q}^{c'}_{(kk')}(r') \\
&\quad\times\begin{pmatrix} j_k & J & j_{k'} \\ -m_k & M & -m_{k'} \end{pmatrix}\begin{pmatrix} j_k & J' & j_{k'} \\ -m_k & M' & -m_{k'} \end{pmatrix} \\
&= \sum_{m_k,m_{k'}}\begin{pmatrix} j_k & J & j_{k'} \\ -m_k & M & -m_{k'} \end{pmatrix}\begin{pmatrix} j_k & J' & j_{k'} \\ -m_k & M' & -m_{k'} \end{pmatrix} \\
&\quad\times\mathcal{Q}^{c*}_{(kk')}(r)\mathcal{Q}^{c'}_{(kk')}(r') \\
\sum_{m_k,m_{k'}}\mathcal{Q}^{c*}_{k\bar{k}'}(r)\mathcal{Q}^{c'}_{k\bar{k}'}(r') &= \frac{\delta_{JJ'}\delta_{MM'}}{2J+1}\mathcal{Q}^{c*}_{(kk')}(r)\mathcal{Q}^{c'}_{(kk')}(r'). \qquad \text{(G.22)}
\end{aligned}
$$

Similarly, the numerator of the second term on the right-hand side can be evaluated as follows:

$$
\begin{aligned}
\mathcal{Q}^{c*}_{\bar{k}'k}(r) &= -(-1)^S\mathcal{Q}^{c*}_{\bar{k}k'}(r) \quad \text{(by Eq. (E.8))} \\
&= -(-1)^S(-1)^{j_k+m_k}(-1)^{j_k-m_k}\begin{pmatrix} j_k & J & j_{k'} \\ m_k & M & m_{k'} \end{pmatrix}\mathcal{Q}^{c*}_{(kk')}(r) \\
\mathcal{Q}^{c*}_{\bar{k}'k}(r) &= -(-1)^S(-1)^{2j_k}\begin{pmatrix} j_k & J & j_{k'} \\ m_k & M & m_{k'} \end{pmatrix}\mathcal{Q}^{c*}_{(kk')}(r) \\
\mathcal{Q}^{c'}_{\bar{k}'k}(r) &= -(-1)^{S'}(-1)^{2j_k}\begin{pmatrix} j_k & J' & j_{k'} \\ m_k & M' & m_{k'} \end{pmatrix}\mathcal{Q}^{c'}_{(kk')}(r) \\
\sum_{m_k,m_{k'}}\mathcal{Q}^{c*}_{\bar{k}'k}(r)\mathcal{Q}^{c'}_{\bar{k}'k}(r') &= (-1)^{S+S'}\sum_{m_k,m_{k'}}\underbrace{(-1)^{4j_k}}_{=1}\begin{pmatrix} j_k & J & j_{k'} \\ m_k & M & m_{k'} \end{pmatrix}\begin{pmatrix} j_k & J' & j_{k'} \\ m_k & M' & m_{k'} \end{pmatrix} \\
&\quad\times\mathcal{Q}^{c*}_{(kk')}(r)\mathcal{Q}^{c'}_{(kk')}(r) \\
&= (-1)^{S+S'}\frac{\delta_{JJ'}\delta_{MM'}}{2J+1}\mathcal{Q}^{c*}_{(kk')}(r)\mathcal{Q}^{c'}_{(kk')}(r'). \qquad \text{(G.23)}
\end{aligned}
$$

Therefore, the reduced spectral free response function now can be written as

$$
\begin{aligned}
\mathcal{R}^{0cc'}_{2\mathrm{qp}}(r,r',\omega) &= \sum_{(k<k')}\sum_{m_k,m_{k'}}\left\{\frac{\mathcal{Q}^{c*}_{k\bar{k}'}(r)\eta^{S}_{(kk')}\mathcal{Q}^{c'}_{k\bar{k}'}(r')\eta^{S'}_{(kk')}}{\omega-E_{(k)}-E_{(k')}}-\frac{\mathcal{Q}^{c*}_{\bar{k}'k}(r)\eta^{S}_{(kk')}\mathcal{Q}^{c'}_{\bar{k}'k}(r')\eta^{S'}_{(kk')}}{\omega+E_{(k)}+E_{(k')}}\right\} \\
&= \frac{\delta_{JJ'}\delta_{MM'}}{2J+1}\sum_{(k\le k')}\frac{\mathcal{Q}^{c*}_{(kk')}(r)\eta^{S}_{(kk')}\mathcal{Q}^{c'}_{(kk')}(r')\eta^{S'}_{(kk')}}{1+\delta_{(kk')}}
\end{aligned}
$$

$$\times \quad \left\{ \frac{1}{\omega - E_{(k)} - E_{(k')}} - \frac{(-1)^{S+S'}}{\omega + E_{(k)} + E_{(k')}} \right\} \tag{G.24}$$

Analogous to the reduced spectral free response function $\mathcal{R}^{0cc'}_{\rm 2qp}(r,r',\omega)$, the reduced free response function $\mathcal{R}^{0cc'}_{\rm corr}(r,r',\omega)$ defined by Eq. (6.60) now reads

$$\begin{aligned}
\mathcal{R}^{0cc'}_{\rm corr}(r,r',\omega) &= \frac{\delta_{JJ'}\delta_{MM'}}{2J+1} \sum_{(k\le k')} \frac{\mathcal{Q}^{c*}_{(kk')}(r)\mathcal{Q}^{c'}_{(kk')}(r')}{1+\delta_{(kk')}} \\
&\times \left\{ v^2_{(k)} \left[\frac{(-1)^{S+S'}}{\omega - (E_{(k)} + \epsilon_{(k')} - \lambda)} - \frac{1}{\omega + (E_{(k)} + \epsilon_{(k')} + \lambda)} \right] \right. \\
&+ \left. v^2_{(k')} \left[\frac{1}{\omega - (E_{(k')} + \epsilon_{(k)} - \lambda)} - \frac{(-1)^{S+S'}}{\omega + (E_{(k')} + \epsilon_{(k)} - \lambda)} \right] \right\}.
\end{aligned} \tag{G.25}$$

To evaluate the reduced non-spectral free response function $\mathcal{R}^{0cc'}_{\rm cont}(r,r',\omega)$,

$$\begin{aligned}
\mathcal{R}^{0cc'}_{\rm cont}(r,r',\omega) &= \sum_k v^2_k \int dx_1 \int dx_2 \; \Psi^\dagger_k(x_1)\mathcal{Q}^{(1)\dagger}_c(r) \Big\{ G(x_1,x_2;\omega - E_k + \lambda) \\
&+ (-1)^{S+S'} G(x_1,x_2;-\omega - E_k + \lambda) \Big\} \mathcal{Q}^{(2)}_{c'}(r')\Psi_k(x_2),
\end{aligned} \tag{G.26}$$

one needs to evaluate the integral

$$\int dx_1 \int dx_2 \; \Psi^\dagger_k(x_1)\mathcal{Q}^{(1)\dagger}_c(r) G(x_1,x_2;E) \mathcal{Q}^{(2)}_{c'}(r')\Psi_k(x_2). \tag{G.27}$$

Here the relativistic single-particle Green's function $G(x_1,x_2;E)$ takes the form ($W=1$):

$$\begin{aligned}
G(x_1,x_2;E) &= \sum_{k'} \begin{pmatrix} \mathcal{F}_{\kappa_{k'}}(r_1;E)\Omega_{j_{k'}\ell_{k'}m_{k'}}(\mathbf{n}_1,\sigma_1) \\ i\mathcal{G}_{\kappa_{k'}}(r_1;E)\Omega_{j_{k'}\tilde{\ell}_{k'}m_{k'}}(\mathbf{n}_1,\sigma_1) \end{pmatrix} \chi_{\frac{1}{2}\tau_{k'}}(t_1) \\
&\times \chi^*_{\frac{1}{2}\tau_{k'}}(t_2) \begin{pmatrix} \Omega^*_{j_{k'}\ell_{k'}m_{k'}}(\mathbf{n}_2,\sigma_2)\mathscr{P}^*_{\kappa_{k'}}(r_2;E) & -i\Omega^*_{j_{k'}\tilde{\ell}_{k'}m_{k'}}(\mathbf{n}_2,\sigma_2)\mathscr{Q}^*_{\kappa_{k'}}(r_2;E) \end{pmatrix},
\end{aligned} \tag{G.28}$$

for $r_1 < r_2$, and

$$\begin{aligned}
G(x_1,x_2;E) &= \sum_{k'} \begin{pmatrix} \mathscr{P}_{\kappa_{k'}}(r_1;E)\Omega_{j_{k'}\ell_{k'}m_{k'}}(\mathbf{n}_1,\sigma_1) \\ i\mathscr{Q}_{\kappa_{k'}}(r_1;E)\Omega_{j_{k'}\tilde{\ell}_{k'}m_{k'}}(\mathbf{n}_1,\sigma_1) \end{pmatrix} \chi_{\frac{1}{2}\tau_{k'}}(t_1) \\
&\times \chi^*_{\frac{1}{2}\tau_{k'}}(t_2) \begin{pmatrix} \Omega^*_{j_{k'}\ell_{k'}m_{k'}}(\mathbf{n}_2,\sigma_2)\mathcal{F}^*_{\kappa_{k'}}(r_2;E) & -i\Omega^*_{j_{k'}\tilde{\ell}_{k'}m_{k'}}(\mathbf{n}_2,\sigma_2)\mathcal{G}^*_{\kappa_{k'}}(r_2;E) \end{pmatrix},
\end{aligned} \tag{G.29}$$

for $r_1 > r_2$. Let us evaluate the integral (G.27) for the case of $r_1 < r_2$. Inserting Eq. (G.28) into Eq. (G.27) yields

$$\int dx_1 \int dx_2 \; \Psi_k^\dagger(x_1) \mathcal{Q}_c^{(1)\dagger}(r) G(x_1, x_2; E) \mathcal{Q}_{c'}^{(2)}(r') \Psi_k(x_2) := \sum_{k'} \mathcal{M}_{kk'}^{c\dagger}(r; E) \mathcal{M}_{k'k}^{c'}(r'; E),$$

where the matrix elements $\mathcal{M}_{kk'}^{c\dagger}(r; E)$ and $\mathcal{M}_{k'k}^{c'}(r'; E)$ are respectively defined as

$$\begin{aligned} \mathcal{M}_{kk'}^{c\dagger}(r; E) &= \int d^3\mathbf{r}_1 \sum_{\sigma_1, \sigma_1'} \sum_{t_1, t_1'} \Psi_k^\dagger(\mathbf{r}_1, \sigma_1, t_1) \mathcal{Q}_c^{(1)\dagger}(r) \begin{pmatrix} \mathcal{F}_{\kappa_{k'}}(r_1; E) \Omega_{j_{k'} \ell_{k'} m_{k'}}(\mathbf{n}_1, \sigma_1') \\ i\mathcal{G}_{\kappa_{k'}}(r_1; E) \Omega_{j_{k'} \tilde{\ell}_{k'} m_{k'}}(\mathbf{n}_1, \sigma_1') \end{pmatrix} \\ &\times \chi_{\frac{1}{2}\tau_{k'}}(t_1') \end{aligned} \tag{G.30}$$

and

$$\begin{aligned} \mathcal{M}_{k'k}^{c'}(r'; E) &= \int d^3\mathbf{r}_2 \sum_{\sigma_2 \sigma_2'} \sum_{t_2, t_2'} \chi_{\frac{1}{2}\tau_{k'}}^*(t_2) \\ &\times \begin{pmatrix} \Omega_{j_{k'} \ell_{k'} m_{k'}}^*(\mathbf{n}_2, \sigma_2) \mathscr{P}_{\kappa_{k'}}^*(r_2; E) & -i\Omega_{j_{k'} \tilde{\ell}_{k'} m_{k'}}^*(\mathbf{n}_2, \sigma_2) \mathscr{Q}_{\kappa_{k'}}^*(r_2; E) \end{pmatrix} \\ &\times \mathcal{Q}_{c'}^{(2)}(r') \Psi_k(\mathbf{r}_2, \sigma_2', t_2'). \end{aligned} \tag{G.31}$$

Making use of Eq. (G.1) and the definition of the one-body operator $\mathcal{Q}_c^{(1)\dagger}(r)$,

$$\mathcal{Q}_c^{(1)\dagger}(r) = \frac{\delta(r - r_1)}{r r_1} \gamma_D^{(1)} \otimes T_{JLSM}^\dagger(\mathbf{n}_1)_{\sigma_1 \sigma_1'} (\tau_{T0})_{t_1 t_1'}, \tag{G.32}$$

one arrives at

$$\begin{aligned} \mathcal{M}_{kk'}^{c\dagger}(r; E) &= q_{\text{isospin}}^T \int d\mathbf{n}_1 \sum_{\sigma_1, \sigma_1'} \begin{pmatrix} \Omega_{j_k \ell_k m_k}^*(\mathbf{n}_1, \sigma_1) F_{\kappa_k}^*(r) & -i\Omega_{j_k \tilde{\ell}_k m_k}^*(\mathbf{n}_1, \sigma_1) G_{\kappa_k}^*(r) \end{pmatrix} \\ &\times \gamma_D^{(1)} \otimes T_{JLSM}^\dagger(\mathbf{n}_1)_{\sigma_1 \sigma_1'} \begin{pmatrix} \mathcal{F}_{\kappa_{k'}}(r_1; E) \Omega_{j_{k'} \ell_{k'} m_{k'}}(\mathbf{n}_1, \sigma_1') \\ i\mathcal{G}_{\kappa_{k'}}(r_1; E) \Omega_{j_{k'} \tilde{\ell}_{k'} m_{k'}}(\mathbf{n}_1, \sigma_1') \end{pmatrix} \chi_{\frac{1}{2}\tau_{k'}}(t_1'). \end{aligned} \tag{G.33}$$

As before, the Wigner-Eckart theorem suggests that one can write the matrix element $\mathcal{M}_{kk'}^{c\dagger}(r; E)$ in a generic form:

$$\mathcal{M}_{kk'}^{c\dagger}(r; E) = (-1)^{j_{k'} - m_{k'}} \begin{pmatrix} j_{k'} & J & j_k \\ -m_{k'} & M & m_k \end{pmatrix} \mathcal{M}_{(k'k)}^{c*}(r; E), \tag{G.34}$$

where, for example, the reduced matrix element $\mathcal{M}^{c*}_{(k'k)}(r;E)$ takes the form

$$\begin{aligned}\mathcal{M}^{1*}_{(k'k)}(r;E) &= F^*_{\kappa_k}(r)\mathcal{F}_{\kappa_{k'}}(r;E)\langle j_{k'}\ell_{k'}||[\sigma_0 Y_J]_J||j_k\ell_k\rangle \\ &- G^*_{\kappa_k}(r)\mathcal{G}_{\kappa_{k'}}(r;E)\langle j_{k'}\tilde{\ell}_{k'}||[\sigma_0 Y_J]_J||j_k\tilde{\ell}_k\rangle. \end{aligned} \tag{G.35}$$

for $c = 1$. Similarly, the application of the Wigner-Eckart theorem to the matrix element $\mathcal{M}^{c'}_{k'k}(r';E)$ results in

$$\mathcal{M}^{c'}_{k'k}(r';E) = (-1)^{j_{k'}-m_{k'}}\begin{pmatrix} j_{k'} & J' & j_k \\ -m_{k'} & M' & m_k \end{pmatrix}\mathcal{M}^{c'}_{(k'k)}(r';E), \tag{G.36}$$

where the reduced matrix element $\mathcal{M}^{c'}_{(k'k)}(r';E)$ reads

$$\begin{aligned}\mathcal{M}^{1}_{(k'k)}(r';E) &= \mathscr{P}^*_{\kappa_{k'}}(r';E)F_{\kappa_k}(r')\langle j_{k'}\ell_{k'}||[\sigma_0 Y_J]_J||j_k\ell_k\rangle \\ &- \mathscr{Q}^*_{\kappa_{k'}}(r';E)G_{\kappa_k}(r')\langle j_{k'}\tilde{\ell}_{k'}||[\sigma_0 Y_J]_J||j_k\ell_k\rangle \end{aligned} \tag{G.37}$$

for $c' = 1$. Therefore, the reduced non-spectral free response function $\mathcal{R}^{0cc'}_{\rm cont}(r,r',\omega)$ takes the form

$$\begin{aligned}\mathcal{R}^{0cc'}_{\rm cont}(r,r',\omega) &= \sum_{(k,k')} v^2_{(k)} \sum_{m_k,m_{k'}} \underbrace{(-1)^{2j_{k'}-2m_{k'}}}_{=1}\begin{pmatrix} j_{k'} & J & j_k \\ -m_{k'} & M & m_k \end{pmatrix}\begin{pmatrix} j_{k'} & J' & j_k \\ -m_{k'} & M' & m_k \end{pmatrix} \\ &\times \Big\{\mathcal{M}^{c*}_{(k'k)}(r;\omega - E_{(k)}+\lambda)\mathcal{M}^{c'}_{(k'k)}(r';\omega - E_{(k)}+\lambda) \\ &+ (-1)^{S+S'}\mathcal{M}^{c*}_{(k'k)}(r;-\omega - E_{(k)}+\lambda)\mathcal{M}^{c'}_{(k'k)}(r';-\omega - E_{(k)}+\lambda)\Big\} \\ &= \frac{\delta_{JJ'}\delta_{MM'}}{2J+1}\sum_{(k,k')} v^2_{(k)}\Big\{\mathcal{M}^{c*}_{(k'k)}(r;\omega - E_{(k)}+\lambda)\mathcal{M}^{c'}_{(k'k)}(r';\omega - E_{(k)}+\lambda) \\ &+ (-1)^{S+S'}\mathcal{M}^{c*}_{(k'k)}(r;-\omega - E_{(k)}+\lambda)\mathcal{M}^{c'}_{(k'k)}(r';-\omega - E_{(k)}+\lambda)\Big\} \end{aligned} \tag{G.38}$$

for $r < r'$. For $r > r'$, the response $\mathcal{R}^{0cc'}_{\rm cont}(r,r',\omega)$ reads

$$\begin{aligned}\mathcal{R}^{0cc'}_{\rm cont}(r,r',\omega) &= \frac{\delta_{JJ'}\delta_{MM'}}{2J+1}\sum_{(k,k')} v^2_{(k)}\Big\{\mathcal{N}^{c*}_{(k'k)}(r;\omega - E_{(k)}+\lambda)\mathcal{N}^{c'}_{(k'k)}(r';\omega - E_{(k)}+\lambda) \\ &+ (-1)^{S+S'}\mathcal{N}^{c*}_{(k'k)}(r;-\omega - E_{(k)}+\lambda)\mathcal{N}^{c'}_{(k'k)}(r';-\omega - E_{(k)}+\lambda)\Big\}, \end{aligned} \tag{G.39}$$

where the expression for the matrix elements $\mathcal{N}^{c*}_{(k'k)}(r;E)$ and $\mathcal{N}^{c'}_{(k'k)}(r';E)$ can be derived from Eqs. (G.30) and (G.31) by interchanging $(\mathcal{F},\mathcal{G})$ and $(\mathscr{P},\mathscr{Q})$.